Neuro-Fuzzy Control Modelling for Gas Metal Arc Welding process

by

Gholam Hossein Khalaf

A Doctoral Thesis

Submitted in partial fulfilment of the requirements

For the award of

Doctor of Philosophy

of Loughborough University

February 98

Department of Manufacturing Engineering

Loughborough University


بسم الله الرحمن الرحيم

IN THE NAME OF ALLAH, THE BENEFICENT, THE MERCIFULL

Dedication

To

My Father and my mother who have laid the foundation of my education and my wife for her warm encouragement and support, my children Shiva, Poya, and Aida for the constant joy they bring.

Abstract

Weld quality features are difficult or impossible to directly measure and control during welding, therefore indirect methods are necessary. Penetration is the most important geometric feature since in most applications it is the most significant factor affecting joint strength. Observation of penetration is only possible from the back face of the full penetration weld. In all other cases, since direct measurement of depth of penetration is not possible, real time control of penetration in the Gas Metal Arc Welding (GMAW) process by sensing conditions at the top surface of the joint is necessary. This continues to be a major area of interest for automation of the process.

The objective of this research has been to develop an on-line intelligent process control model for GMAW, which can monitor and control the welding process. The model uses measurement of the temperature at a point on the surface of the workpiece to predict the depth of penetration being achieved, and to provide feedback for corrective adjustment of welding variables. Neural Network and Fuzzy Logic technologies have been used to achieve a reliable Neuro–Fuzzy control model for GMAW of a typical closed butt joint having 60° Vee edge preparation.

The neural network model predicts the surface temperature expected for a set of fixed and adjustable welding variables when a prescribed level of penetration is achieved. This predicted temperature is compared with the actual surface temperature occurring during welding, as measured by an infrared sensor. If there is a difference between the measured temperature and the temperature predicted by the neural network, a fuzzy logic model will recommend changes to the adjustable welding variables necessary to achieve the desired weld penetration.

Large scale experiments to obtain data for modelling and for model validation, and various other modelling studies are described. The results are used to establish the relationships between the output surface temperature measurement, welding variables and the corresponding achieved weld quality criteria. The effectiveness of the

modelling methodology in dealing with fixed or variable root gap has also been tested.

The result shows that the Neuro-fuzzy models are capable of providing control of penetration to an acceptable degree of accuracy, and a potential control response time, using modestly powerful computing hardware, of the order of one hundred milliseconds. This is more than adequate for real time control of GMAW. The application potential for control using these models is significant since, unlike many other top surface monitoring methods, it does not require sensing of the highly transient weld pool shape or surface.

ACKNOWLEDGEMENTS

The author is very grateful to Ministry of Culture and Higher Education and Iranian Research Organisation for Science and Technology for their financial sponsorship and support.

The author wishes to express his sincere thanks to his supervisor Mr. John E. Middle, for his invaluable supervision, encouragement, suggestion and help throughout this research. Thanks must also be extended to those staff of department of manufacturing engineering who have been kind and helpful, especially R.G. Price, D. Hardwick, T. Smith, R. Temple, G.P. Charles, N.D. Carpenter and D. Walters.

The author wishes to thanks Dr. A.R. Rahimi, Dr. R. Naimi, Dr. A. Aghaie, Dr. A.Shahandeh, Mr. M. Hadian, Mr. H. Mahbobie, Mr. S. Al-Amoudi and Mr. R. Monfarad for their help, support and friendship.

Finally, the author is very grateful to his parents, wife and his children who preserved and offered their warm encouragement and help over the past years.

CONTENTS

Chapter one Introduction

1.1 Introduction

This chapter introduces the background to the development of a Neuro-Fuzzy Control Model (NFCM) for the Gas Metal Arc Welding process. It describes the scope and objectives of the research, and introduces the main areas of research reported in this thesis.

1.2 The research background

Welding is the most widely used metal joining technique in the fabrication industry today. Fusion welding by the arc welding process is the most important among the welding processes, and may be used for joining most types of ferrous and non-ferrous metals, including carbon, alloy and stainless steels, aluminium, and magnesium alloys, copper, and titanium, in all thicknesses.

The Gas Metal Arc Welding (GMAW) process has become widely used because of the following advantages when compared with other welding processes. As shown in table 1.1 (1,2).

- It is very versatile in application
- It has potential for increasing productivity and quality.
- It has good potential for both dedicated and flexible automation.

Characteristic		TIG	SMAW	GMAW	FCAW	SAW
All-position welding		Yes	Yes	Yes	Yes	No
Weldability	Mild, low-alloy steel	Yes	Yes	Yes	Yes	Yes
	Stainless steel	Yes	Yes	Yes	Yes	Yes
	Aluminium	Yes	Yes	Yes	No	No
Deposition rate, Kg./hr		4.5	9	11.25	18	45
Welding speed, mm/min (6mm fillet)		127	508	762	940	1220
Adaptable to automation	Gun control	Yes	N/A	Yes	Yes	Yes
	Total automation	Yes	No	Yes	Yes	Yes
	Robotics	Yes	No	Yes	Yes	No

Table 1.1 Comparison of arc welding processes (adapted from (1))

Welding procedures and control systems used for manual welding are not easily adapted to automatic welding. This is because most manual welding relies heavily upon the action of a welder to cope with variability. To achieve good welding quality, the welder must make difficult choices among welding variables, which are related to each other in non-linear modes. For example, welding current is nonlinearly dependent on wire feed rate, electrode size, and stickout. Arc voltage depends nonlinearly on welding current, electrode size, wire feed rate, shielding gas, and arc

length. The empirical nature of these interdependent variables further complicates system development for controlling welding variables. In addition to selecting and controlling welding parameters, the welder may introduce varying manipulation of the heat source in the joint, often learned only through experience in dealing with joint and process variability. However, adaptive control of arc welding variables such as arc length and voltage, electrode feed rate, travel speed, and arc manipulation is increasingly possible through the introduction of computers in arc welding, and the development of a wide variety of sensors that can, to some extent, emulate those of the human welder. For instance it is possible to measure, in process and in real time, the geometry and condition of the unwelded joint or the finished weld bead, and to monitor the sound or light emitted from the welding system, or the temperature distribution in the joint material during welding. Such sensing is discussed later. The development of Artificial Intelligence (AI) enables human knowledge and inferencing to be incorporated into control systems, and may provide for situations where knowledge is incomplete or where there is uncertainty.

The most important quality feature in welding is the depth of penetration, which largely dictates the mechanical properties of the welded joint. Unlike other weld bead features such as width, height, and toe angle which can be measured in process from the top face, the depth of penetration, or rather the achievement of full penetration, can only be measured directly from the back face. This is often difficult or impossible. Nadew (4) monitored visible light through the root gap to measure the penetration in an open butt joint, however, this was only applicable to the first welding pass. Bentley (5) developed feedback control of penetration by measuring the amount of visible and near-infrared light emitted from the backside of the weld. This method is only suitable for flat plate welding. Song and Hardt (6) developed a mathematical model to estimate the depth of penetration in real time by measuring the temperature of the under side of the workpiece.

Several techniques for estimating depth of penetration by sensing features of the top face have been investigated. Hardt and Katz (3) measured the penetration depth by

using an ultrasonic sensor, but it was difficult to couple the transducers to the workpiece and synchronise their movement with the welding torch. Zhang et al (79) used a high shutter speed camera to measure the topside pool width in GMAW processes, and then estimated the backside bead width and penetration. In their estimation they assumed a semi-circular pool shape, which does not apply to the majority of weld joints. Also in the Gas Metal Arc Welding process, spatter and fume occurs which can impede the application of cameras for measuring the pool width during welding. Matteson et al. (65) used the sound pressure produced by the Gas Metal Arc Welding process during welding, and an Artificial Neural Network to classify acceptable or unacceptable welds. In the production environment other sources of noise can interfere with the arc acoustic signals which may reduce the application of the system. Boo and Cho (142) developed a system to control the quality of welds in Gas Metal Arc Welding by monitoring the temperature on the top surface of the workpiece but only for bead on plate welds. Bead on plate experimentation cannot accurately represent the heat flow occurring in GMAW of typical Vee groove joints.

To control the welding process in real time, special Artificial Intelligence (AI) modelling techniques may be used to identify the condition of a weld from sensed features, and provide a corrective procedure. One possible approach to controlling welding is to construct an intelligent process control model that learns the relationship between top surface temperature, the welding variables, and weld quality, predicts the temperature for given welding variables and adjusts the appropriate welding variables to achieve welds with acceptable quality. This is the subject of the research reported in this thesis.

1.3 Objective of the research

Automatic control of Gas Metal Arc Welding is difficult because there are many welding variables affecting the quality of welds. It is difficult to model their

relationships and effect on weld quality accurately by mathematical modelling, due to the complexity of the process.

The objective of this research has been to develop a practical control methodology, and associated models, to alleviate the difficulties and limitation associated with alternative methods. The following solution is proposed in this research to overcome these difficulties:

- Perform on-line temperature measurement at a point in the top surface of the workpiece during welding;
- Model the relationship between welding variables and the measured temperature;
- Model the relationship between the weld penetration and the measured temperature;
- Develop a model to perform on-line correction of controllable welding variables depending on surface temperature measurement, in order to achieve welds with acceptable penetration.

An approach integrating Neural Network and Fuzzy Logic artificial intelligence techniques will be utilised to achieve these goals. The reason for using this integrated approach is to take advantage of the strengths of each technique in order to increase the reliability and accuracy of the proposed process control model. The research experimentation is based on Gas Metal Arc Welding of a Vee groove joint to properly represent industrial application.

1.4 Structure of thesis

There are eight remaining chapter in this thesis as follows:

CHAPTER 2 discusses the principle of Gas Metal Arc Welding, including the fixed, and controllable welding variables, and equipment. It also discusses spatter

and fumes in GMAW, in particular the effect on satisfactory sensing. **CHAPTER 3** presents a review of relevant research work in adaptive control of the Gas Metal Arc Welding process. Approaches to sensing, mathematical modelling, statistical modelling, and AI techniques such as expert system, neural network, and fuzzy logic are discussed. The strengths and weaknesses of these approaches are also summarised. **CHAPTER 4** deals with the theory of heat distribution in a weldment. This is extended to theoretical modelling of heat distribution in the workpiece. **CHAPTER 5** describes the experimental procedure adopted for collecting data for the purposes of modelling. This includes the selection of inputs and outputs, experimental design, and experimental apparatus. **CHAPTER 6** considers Neural Network modelling. Different types of neural network modelling techniques including back propagation, radial basis function, and reinforcement networks are discussed, constructed and evaluated. This is followed by discussion of the selection of the most appropriate neural network technique, and architecture for the prediction of the temperature at a point on the top surface of the weldment, for a set of welding variables, and corresponding to achievement of acceptable penetration. **CHAPTER 7** discusses a Fuzzy Logic control model, and includes the procedure for constructing the fuzzy model. Development of the appropriate fuzzy logic rules for controlling the welding variables, in order to achieve a weld with acceptable quality is discussed. This is extended to the development of a Neuro-Fuzzy Control Model (NFCM). This is in turn extended to develop a software to integrate the Neural Network model, Fuzzy Logic model, and the output of analog to digital converter of the infrared sensor employed. **CHAPTER 8** discusses the results of the evaluation of the proposed method for controlling penetration in welding. The application scope, advantages and limitations of the Neuro-Fuzzy Control Model are discussed. The specific and general conclusions that can be drawn from this research are presented. Finally **CHAPTER 9** presents suggestions for the further work needed to be done for the continuation and extension of this research.

Chapter two Gas Metal Arc Welding process

2.1 Introduction

Today's emphasis on reliability, speed and economy in assembly has led to the development of a wide variety of joining processes and techniques. One of the most important of these techniques is welding.

Although there are many welding processes currently applied in industry, arc welding and resistance spot welding are the most common techniques and are also the most commonly automated. Resistance welding is widely used in sheet metal fabrication, such as in automobile body construction. For thicker materials, and for welding with metal deposition, arc welding is the most widely used process in industry and construction.

In arc welding the heat is generated by an electric arc that is maintained between the electrode and the workpiece. This heat will melt the base metal and in most cases a consumable electrode. There are several different welding processes categorised as arc welding including: Shielded Metal Arc welding, Submerged Arc welding, Gas Tungsten Arc welding, Gas Metal Arc welding, Flux Cored Arc welding and Plasma Arc welding. Each process has particular application scope and advantages, based on technical or economic considerations.

The demands of industry for reduced welding cost, consistent weld quality and to remove personnel from what is an unpleasant and sometimes hazardous environment, has led to development in welding automation. This includes automated manipulation of the workpiece, or the welding arc, and automated control of various welding parameters. Flexible automation is achieved through application of reprogrammable robots. Gas metal arc welding is capable of producing high-quality welds at high welding speed, and is widely used in automatic robotic arc welding. In this research adaptive control of **R**obotic **G**as **M**etal **A**rc **W**elding (GMAW) will be investigated.

2.2 Gas Metal Arc Welding

Gas metal arc welding (GMAW) is probably the most common method for arc welding of steels. The process can be used for welding of most common metals and alloys. However, some require special procedures, e.g., copper alloy that contains a high percentage of zinc, cast iron, titanium and titanium alloy, and refractory metals. Metals that cannot be welded by GMAW includes, lead, tin, and zinc which have a low boiling temperature, for example the boiling temperature of zinc is 946°C which is far below the arc temperature (7).

2.2.1 Principle of operation of GMAW

In the GMAW process electric energy is converted to a useful electric arc between a consumable electrode and the workpiece. The electrode is a bare wire which is fed into the weld area and arc, melts and is deposited into the weld pool. The electrode, arc, weld pool, and the whole welding area of the workpiece are protected from the atmosphere by a shielding gas, which flows through the welding gun. The small diameter electrode wire melts rapidly and transfers across the arc and into the weld pool. Up to about 90% of energy is transferred into the workpiece and weld pool, giving highly efficient and productive welding.

The arc is struck by starting the wire feed, which causes the electrode wire to short circuit to the workpiece and initiate the arc. This self-striking mechanism is a useful feature for automated welding. The arc is then traversed along the weld joint in order to fuse the adjoining edges and form a weld pool. The weld pool solidifies behind the arc and completes the welding process (22). The quality of weld produced depends to large extent on heat and mass transfer from arc and electrode into the weld pool, and the mass of parent material in the joint, which has to be fused. For automation of welding, various parameters affecting these factors must be monitored and controlled.

2.2.1.1 Metal Transfer in GMAW

In gas metal arc welding there are various modes of metal transfer from electrode tip to weld pool, spray transfer, pulse transfer, short circuiting and globular transfer are consider the most practical modes of transfer. These transfer modes show different arc stability, weld pool penetration, spatter production, and level of potential gas entrapment. Lesnwich (7) showed that the modes of metal transfer depends on many operational variables such as welding current and voltage, electrode extension, electrode diameter, and shielding gas type. With so many factors influencing metal transfer, much research has been done to analyse and model this phenomenon, e.g., Kim and Eager (8) analysed the droplet size and droplet transfer frequency both theoretically and experimentally.

In the following sections each method of metal transfer and the significance to automated robotic welding is discussed.

2.2.1.1.1 Spray transfer

In this mode metal is transferred from the end of the electrode wire to the pool in an axial stream of fine droplets. Spray transfer occurs at relatively high voltage and high current density. The high current used produces strong electromagnetic fields and aerodynamic drag force due to high arc plasma flow. These cause rapid detachment of small droplets. The shielding gas used influences the surface tension of the molten electrode material and the magnitude of drag forces, therefore it has a significant affect on the value of current at which spray transfer occurs. This mode of metal transfer is a high deposition rate technique, it is usually recommended for thicker sections requiring heavy single or multi-pass welds or for any filler pass application where speed is advantageous. It is usually applied in the flat position or for horizontal /vertical fillets (9), in which case it is particularly appropriate for robotic welding when used in conjunction with a programmable work manipulator. In this mode metal transfer is very stable, directional, and essentially spatter free. The absence of spatter makes this mode of transfer useful for this research, as spatter could interfere with the operation of the sensor employed and impair the accuracy of temperature measurements recorded.

2.2.1.1.2 Pulsed current transfer

This mode is a type of spray transfer. The welding current is pulsed in a square wave form at a fixed frequency, typically between 50 and 100 HZ, from a high value during which spray transfer occurs, and a low value.

A steady arc is produced with spray transfer at effective mean welding current below that required for conventional spray transfer. Due to the lower heat input this mode can be used for welding thinner plate than practical with the conventional high current spray transfer. This method has the benefit of offering all position welding with almost no spatter, and the regulation of droplet transfer gives a smooth stable arc and weld pool. A solid state and an inverter power supply, with or without a synergic controller, is normally used for this method of welding.

2.2.1.1.3 Globular transfer

This mode occurs at lower current densities compared with spray transfer mode. It is characterised by the formation of a relatively large drop of molten metal at the end of the electrode wire. The drop remains attached to the end of the wire until the forces of gravity and shielding gas flow overcome the surface tension of the molten drop, which then detaches and falls into the weld pool. Globular transfer occurs with all types of shielding gas, but it cannot be used for out-of-position welding due to it being predominantly dependent on gravity. Globular transfer typically produces a large amount of spatter, which comes from splashing of the molten pool and violent droplet detachment. This mode of transfer is not well suited to robotic manipulation or sensor based process control.

2.2.1.1.4 Short circuiting transfer

This mode of transfer, which is also called dip-transfer, occurs with relatively low current, a low voltage which produces a short arc, and small diameter electrode wire. In this mode the wire feed rate must just exceed the burn-off rate so that intermittent short circuits will occur. When the wire touches the pool and short circuits the arc there is a momentary rise of current which must be sufficient to

melt the wire tip. A neck is then formed, due to magnetic pinch effect, causing detachment of the droplet, which is sucked into the molten pool, aided by surface tension (10). The wire short circuits to the workpiece an average of 100 times per second. In this mode of metal transfer careful control of parameters, particularly the rate of rise of current during short circuits, is essential to minimise spattering (11). Because of relatively fast weld pool solidification compared with spray transfer, this mode of transfer can be used in all positions. It is also suitable for automatic welding. Low power short circuiting transfer is essential for welding thin sheet. In figure 2.1 different modes of metal transfer and typical current/voltage combinations at which they occur in GMAW are shown.

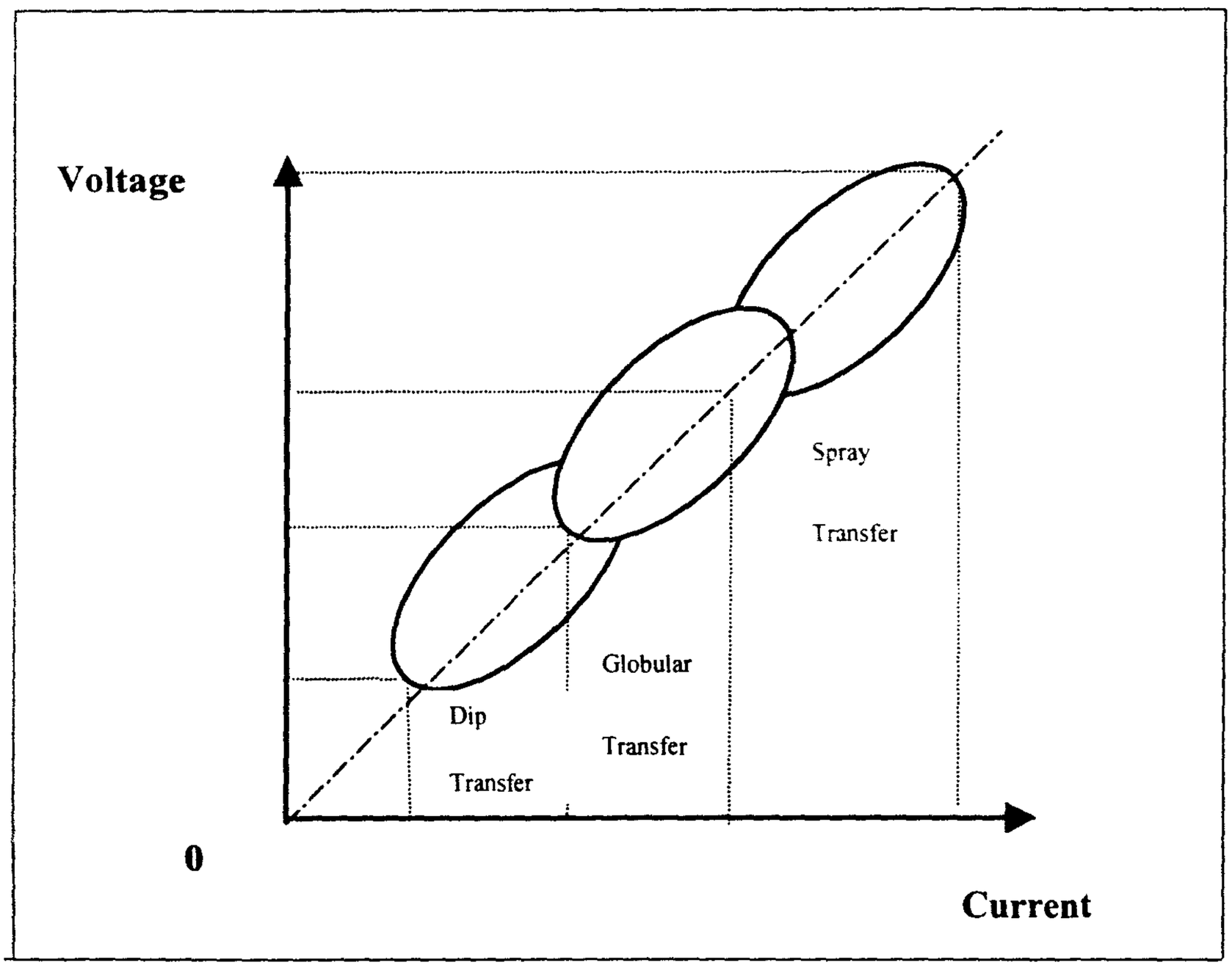

Fig. 2.1 Metal transfer mode in GMA

2.2.2 Gas metal arc welding equipment

Equipment used in GMAW generally consists of power source, wire feed unit, gas supply unit, and welding gun. Additional equipment such as sensors for seam

finding, seam tracking, process control, arc on and gas flow detection, etc. can be added for automatic robotics application.

2.2.2.1 Power sources

In gas metal arc welding alternating current is seldom used (12), direct current electrode positive is used for all practical applications giving maximum electrode melt-off rate and thermal efficiency of the process. Two types of power supply commonly used in GMAW are:

- Constant voltage transformer or transformer / rectifier;
- Inverter.

The essential requirement of the power supply is constant, or virtually constant voltage with changes in current. This characteristic provides the process with self regulating arc length, which simplified the requirement for manipulation and control of the arc length in automated welding, as well as reducing skill requirement for manual welding.

In this work an inverter type power source is employed. Mains A.C. is converted to H.F. (high frequency) A.C. and transformed, still at H.F., to a voltage suitable for welding. It then passes through a reactor, which smoothes the current, and a final rectifier gives D.C. for the arc. A final electronic switching arrangement enables the welder to select D.C. or A.C. at high frequency and the resulting arc is easy to strike, smooth, and stable (13). The wave shape generated in an inverter is rectangular and, since the output is no longer synchronised with mains frequency, the frequency can be varied between, typically, 50 HZ to 300 HZ. The output volt-ampere relationship can be accurately predicted and controlled. Irving(14) described that on changing from conventional to an inverter with rectangular output wave form, there was an average reduction of fume measurement of 67% in GMAW. This is significant to the good performance of optical sensors such as the infrared thermography sensor used in this research.

2.2.2.2 Wire feed unit

A wire feed unit consists of a wire feeder and a controller. There are two types of wire feeder used in GMAW, pull type and push type feeders. Pull type feeders with the drive system integral with the welding torch are used for soft electrode wires such as aluminium wires, or for steel wires of very small diameter, where buckling of a pushed wire would cause feeding problems. It is also used when the wire is to be fed a greater distance. Push type feeders, in which the drive system is typically up to five meters from the welding torch, are used for stiff steel wires, and that allows for torches of a very small size to be constructed. The wire feeder controller maintains a pre-set wire feed rate, and also provides control of shielding gas flow, and the cooling water in a water cooled welding gun. The wire feed rate is maintained constant in manual welding but can be used as a control variable in automated welding.

2.2.2.3 Welding gun

The Gas Metal Arc Welding gun, or torch, must withstand the heat generated by the welding process, and can be connected to the following supplies:

- Flexible conduit through which the electrode wire is fed;
- Shielding gas, and possibly cooling water input and return;
- Cable carrying the welding current, often water cooled.

The welding current from the power supply is transferred to the welding electrode via the torch contact tip. Any spatter present in GMAW may accumulate around the contact tip causing the wire feed to become erratic. Therefore the tip must be cleaned or replaced periodically, which is particularly disadvantageous for automated welding. Shielding gas passages and nozzle surrounds the wire emerging from the contact tip and direct the shielding gas around the arc and molten pool. It has been reported by Kirk (15) that the delivery of gas at a reasonable flow rate through a tubular shroud is effective in reducing defects, but

is extremely susceptible to side draughts. This is aggravated by the relative movement of the gas shroud and contact tip over the workpiece creating a trailing gas shield. Kirk proposed a new design of gas shroud with two gas flow paths to overcome these problems.

Cooling is required in the welding gun to remove the heat generated within the gun as well as the heat radiated from arc and molten pool. In the water-cooled type torch the cooling water flows around the cable carrying the welding current, therefore this cable can be smaller in cross sectional area. Water-cooled torches tend to be larger and heavier and that has implications for access and manipulation. However air cooled torches which are constantly rated for currents up to 500 Amps are now available. This covers the majority of application in GMAW including automated welding with high percentage 'arc-on' time or duty cycle.

2.2.3 Welding parameters

The operation of gas metal arc welding, like most production processes, can be defined by a series of qualitative or quantitative parameters. Welding parameters affect the characteristics of welding such as penetration and fusion of the weld, metal deposition geometry (height, width), and deposition rate. The most important parameters that govern weld characteristics, and that have affect on the thermal cycle during welding are:

- Welding current and voltage;
- Welding gun travel speed;
- Welding electrode feed rate, size, and extension;
- Welding shielding gas;
- Torch angle;
- Weaving frequency, amplitude and pattern.

2.2.3.1 Welding current

The amount of welding current has a great effect on wire melt-off and deposition rate, penetration of the weld, and the size and shape of the weld pool and weld bead deposit. In turn, penetration in particular will influence the design of the weld joint. In the constant voltage case as the wire-feed speed is increased the current increases. As the current increases the deposition rate is increased. When other welding parameters are held constant, increasing the current will increase the depth and width of weld penetration and the size of weld bead. However, excessive current will result in excessive spatter, instability, or an unfavourable mode of metal transfer. The welding process may also become unstable or ineffective at lower currents, due to inadequate heat input or to an unsuitable mode of metal transfer. In automated welding, current is used as a controllable variable because it is relatively easy to monitor and adjust. In this work current is used as one of the welding variables because it has a strong influence on the temperature distribution in the welded region.

2.2.3.2 Welding voltage

The distance between the tip of the electrode and the weld pool surface, the arc length, together with the anode and cathode voltage drops in the arc determines the welding voltage or arc voltage. The voltage required for an application depends on the electrode material and size, type of shielding gas, position of welding, type of joint, etc. If other welding variables are held constant and voltage is increased, arc length increases and the weld bead becomes flatter and wider. The penetration will increase up to an optimum level, beyond which energy loss from the arc column is greater than the increase in arc energy (V x I). Further increase in the voltage and arc length results in the arc discharge being non-sustained and intermittent arcing occurs. Lower arc voltage produces a narrower weld bead and greater convexity, too low an arc voltage at a low current can result in electrode stubbing. Arc voltage is one of the variables used in the empirical work of this research.

2.2.3.3 Welding gun travel speed

The travel speed of the gun has an effect on the distribution of the filler metal transferred from the electrode wire, and the penetration in to the base metal. As the travel speed is increased the heat transferred per unit volume of base metal is decreased, limiting the penetration. At the same time the bead width is reduced. Increasing the travel speed can result in undercutting along the edge of the weld bead, if there is not enough filler metal to fill the groove fused by the arc. If travel speed is reduced, greater penetration will be achieved but excess filling may result. Travel speed has been used as a controllable variable in this work.

2.2.3.4 Electrode feed rate, size, and extension

The electrode feed rate in gas metal arc welding has a similar effect to the welding gun speed. It effects the deposition of the filler metal and penetration in the workpiece. These are also a function of current density, which is related to electrode diameter. The choice of electrode wire size and its metal composition is dependent on the metal to be welded and its thickness, the metal transfer mode, the amount of penetration, the deposition rate, and the bead profile required.

There are two types of electrode wire used in GMAW, solid wires which are used for welding of many high strength low-alloy steels as well as carbon steel, and flux-cored wires of which there are two types, gas- shielded and self-shielded. These are used for welding low carbon steel, high strength low-alloy steel, and stainless steel. Flux-cored wires provide improved arc stability and additional alloying elements. They are used for high current, high deposition rate welding. Wire size, type and composition cannot of course, be changed in-process, in real time.

The electrode extension should also be controlled in GMAW. Too long an extension results in high I^2R heating of the wire extension and excess weld metal being deposited with low arc heat. This will cause poor weld bead shape and reduced penetration in addition to a less stable arc.

2.2.3.5 Shielding gas

The primary purpose of the shielding gas is to protect the molten weld metal from oxidation, and to alleviate gas porosity.

Originally inert gases such as Argon and Helium were used as shielding gases. Now carbon dioxide or a mixture of oxygen or CO_2 with an inert gas, is extensively used. Mixed gases improve the operation of GMAW, addition of CO_2 gives a broader penetration bead and higher arc energy, oxygen gives good wetting and spatter reduction. The shielding gas and flow rate affects arc characteristics, mode of metal transfer, penetration, speed of welding, under-cutting tendency, bead shape, weld metal mechanical properties, spattering, and fume (27). Although monitoring and adjustment of shielding gas parameters is possible, it is not usual to use these in automatic control of welding. They are kept constant in the work reported here with sufficient flow to give good shielding.

2.2.3.6 Torch angle

Torch angle is measured as the angle between the wire and the workpiece surface in the direction of welding , and is usually about 10 to 20° each side of vertical. It has been found (16) that spatter is minimised and penetration increased with an angle greater than 90° (backhand welding). On the other hand, the bead is flatter with a torch angle less than 90°(forehand welding). The selection of torch angle depends on joint type, material thickness, and edge preparation. Through interfacing with the robot controller, this variable can readily be used to control weld penetration in automated robotic welding. In this research torch angle has been chosen as a welding variable.

2.2.3.7 Weaving

Weaving is a side to side motion of the welding torch, as it moves along the joint. It gives better side wall fusion, and helps assure complete filling of the joint. Weaving pattern and frequency are important factors in weld bead geometry, heat affected zone, and heat distribution in fusion welding. However, to the author's

knowledge, few attempts have been made to investigate the effects of weaving. Grong and Christensen (17) developed a mathematical model, based on Rosenthal's three-dimensional heat distribution equation, for GTA welding to quantify the specific effects of weaving on the temperature distribution. They concluded that when the peak temperature was fixed there was a difference in the width/depth ratio of the weld when weaving was applied. In addition weaving is also used in through the arc sensing for seam tracking as discussed in the next chapter. Weaving was not required for the joint considered in this research. It would add considerable complexity to the modelling and is not included as a modelling parameter.

2.2.4 Spattering and fume

The subject of this research is to control welding parameters in real time, by means of measuring the temperature in the metal adjacent to the weld pool with a non-contact temperature sensor. Spatter and fume can interfere with the accurate function of the sensor, therefore minimising spatter and fume is a vital requirement of this work. Smith (19) described the mechanisms of spattering and the means of suppressing it through proper parameter selection. He also described developments in power source design to provide control of spattering. To overcome the effect of spatter on a sensor lens, Dufour (20) developed a rotating window with a protective particle-intercepting blade placed in front of the sensor lens. This technique was effective for dip transfer welding. Lockwood Corporation reduced spatter by 50% when they switched from CO_2 shielding gas to argon rich shielding gas(21).

Welding fume can arise from several sources. It can be caused by over heating of the welding wire and fluxes, from the effect of the arc on the shielding gases, or from coatings on the workpiece. Deere & Co. (14) consider that the temperature of the forming molten droplet in solid wire, GMAW at 5400°C (which is well above the vaporisation temperature of steel), was the main source of welding fume. They suggested that using an inverter power supply will reduce fume generation by 50% to 90%.

This research uses argon rich gas, inverter power supply and low spatter welding parameters, which minimise the effects of fume and spatter. The sensor optics are also purged with air, as described in chapter 5, to further alleviate any possible adverse effects.

2.2.5 Joint geometry

In GMAW in order to achieve the required degree of penetration when welding thicker plates, it is usually necessary to locally thin the edges or leave a gap between them. Various types of such joint edge preparation are employed to suit the requirements of particular applications. In principle it is possible, by using a sufficient input power, to fuse through the complete section even in very thick plate (23). However, the large weld pool, which is produced, may be difficult to control, and will probably require use of a backing to support the weld pool. Also the large amount of weld metal and wide heat affected zone (HAZ) may reduce the mechanical properties of such a weld. Carefully designed joint preparation is particularly required in multi-pass welds, so as to give access to the root and all parts of the joint, thereby ensuring that each pass is properly fused to parent metal and to the previous passes (24). If the plate is thin (typically less than 2mm). it is possible to make a full penetration butt weld with closed joint edges. For metal thicker than 2mm a gap has to be left between the edges to be welded to allow the heat source to penetrate between and fuse the sheet edges. An open square butt joint can be used on plate up to 6mm thickness, depending on the arc welding process used, but there is a risk that the restriction on electrode manipulation will produce lack of side wall fusion. Therefore common practice for material thickness greater than 3 or 4 mm is to bevel the edges of the plate. The bevelled joint preparation may also include a root gap between the plate edges. This allows reduction in the arc force necessary to penetrate the joint but will increase the amount of weld metal needed to fill the joint. To avoid excessive melting of the bevelled edge, it is usual to leave a one or two millimetre root face. With increasing thickness of the plate the amount of weld metal required to fill the joint becomes very large, and it may be economical to bevel both sides or machine a more complex J shape. Figure 2.2 shows some common preparation types.

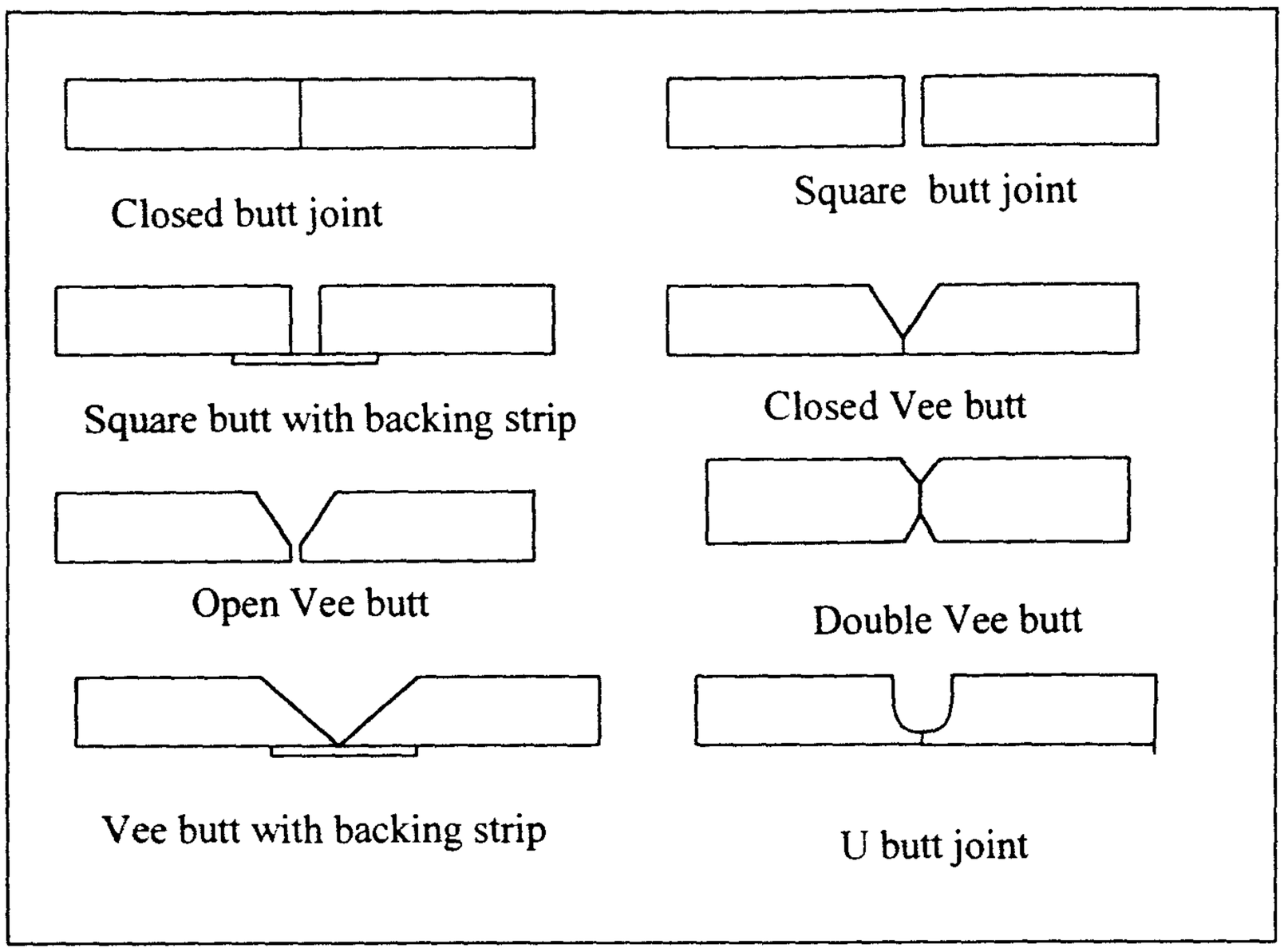

Fig. 2.2 Common joint edge preparation.

The choice of joint preparation has the following effect in welding.

- ***Heat distribution and penetration control.*** The main purpose of a joint preparation is to make the best use of the heat input to produce the desired weld penetration. Much research has been done to recommend the welding input required for different joint types and geometry (25,26, 46).

- ***Access.*** The joint preparation for welding must be wide enough to allow manipulation of the welding torch, such that the arc can be directed at the joint faces to ensure proper fusion.

- ***Multi-pass welding.*** For thick plate where multi-pass welding is required, joint preparation is essential. The single sided or double-sided vee or 'J' preparation is usually used for multi-pass welding.

- ***Distortion.*** Joint preparation has a significant effect on distortion. Distortion tends to increase as volume of metal deposited is increased. Therefore

preparation of the joint which minimises the volume will offer reduced distortion and cost. Welding from both sides can also reduce distortion.

A thorough discussion of the factors affecting joint edge preparation design will be found in (18).

Joint design and manufacture introduces potential dimensional and geometric variability to the problem of automatic process control and the achievement of acceptable quality welds. This research uses 6mm thick plate, with a single sided 60° bevel angle joint, no root gap and 2mm root face. However, experiments have been included for root gaps, ranging from zero to 1.5 mm, to simulate the affects of poor assembly fit-up and in process distortion. These are discussed in chapter 5.

2.3 Conclusion

In this chapter the main aspects of Gas Metal Arc Welding that influence this research have been reviewed.

The important welding variables are the voltage and current of the arc, position and orientation of welding torch, the filler wire feed rate and the traverse speed of the welding torch. The type and size of the filler wire and the shielding gas composition might also be varied. The quality criteria that must be satisfied are the weld penetration, the subsequent mechanical and metallurgical properties of the joint and the shape of the weld bead. In addition a number of defects must be avoided such as cracking or tearing in the weld or heat-affected zone, porosity in the weld, or lack of fusion. This process is characterised by its fairly high deposition rate with a continuously fed consumable electrode, making it attractive for automated robotic application.

In the next chapter the adaptive control of robotic GMAW is discussed, and extended to include the use of Artificial Intelligent (AI) incorporating sensors, to control the quality of the weld in real time.

Chapter three Adaptive control in GMAW

3.1 Introduction

In this chapter robotic arc welding and adaptive control of welding are described. Different modelling techniques including theoretical, statistical and empirical models are described and extended to application of Artificial Intelligence (AI) in welding. Three basic approaches to intelligent control including expert systems, fuzzy logic and Artificial Neural Networks and their application to welding is given in section 3.9. In section 3.11 the application of sensors in adaptive control of welding is investigated, with special attention being given to thermal sensors.

3.2 Robotic arc welding

An industrial robot is the most flexible of the automated systems used in manufacturing operations by virtue of the reprogrammable capability. A robot is an electro-mechanical device that can perform a variety of tasks under automatic control. A variety of motion configurations are available, two common systems being articulated (jointed) and rectilinear. The choice of robot configuration depends upon the nature of the work. Rectilinear robots tend to be useful for the fabrication industry due to weld joints being predominantly in straight lines which requires less manipulation of robot axis. For convoluted shape workpieces articulated robots are commonly used.

For welding applications the welding gun can be mounted on a multi-axis "wrist" at the end of the robot arm, this provides the degree of dexterity needed for the welding process.

Welding robots may be regarded as blind and deaf without sense of touch and not capable of creativity. However, developments in technology enables robots to be used more effectively in manufacturing operations. They may have computer intelligence for decision making capability, sophisticated programming languages

for readily accepting complex instruction, and electronic sensors to detect events and conditions in the working environment. In this work Artificial Intelligence, and the application of sensors, are investigated for the adaptive control of GMAW. These subjects are discussed further in the following sections

3.3 Adaptive control of GMAW

Today many metal fabricators are adapting welding technology towards automation, because automation will be a matter of survival not only for large shops creating a high volume of pieces but for the small fabricator, to raise productivity, flexibility, and quality while reducing costs. As is shown in figure 1.1 (27) 77% of total manual welding cost is labour, and this labour is generally poorly utilised. The flexibility, speed and accuracy of robots give them inherent advantages for improving welding operations from both technical and economical points of view.

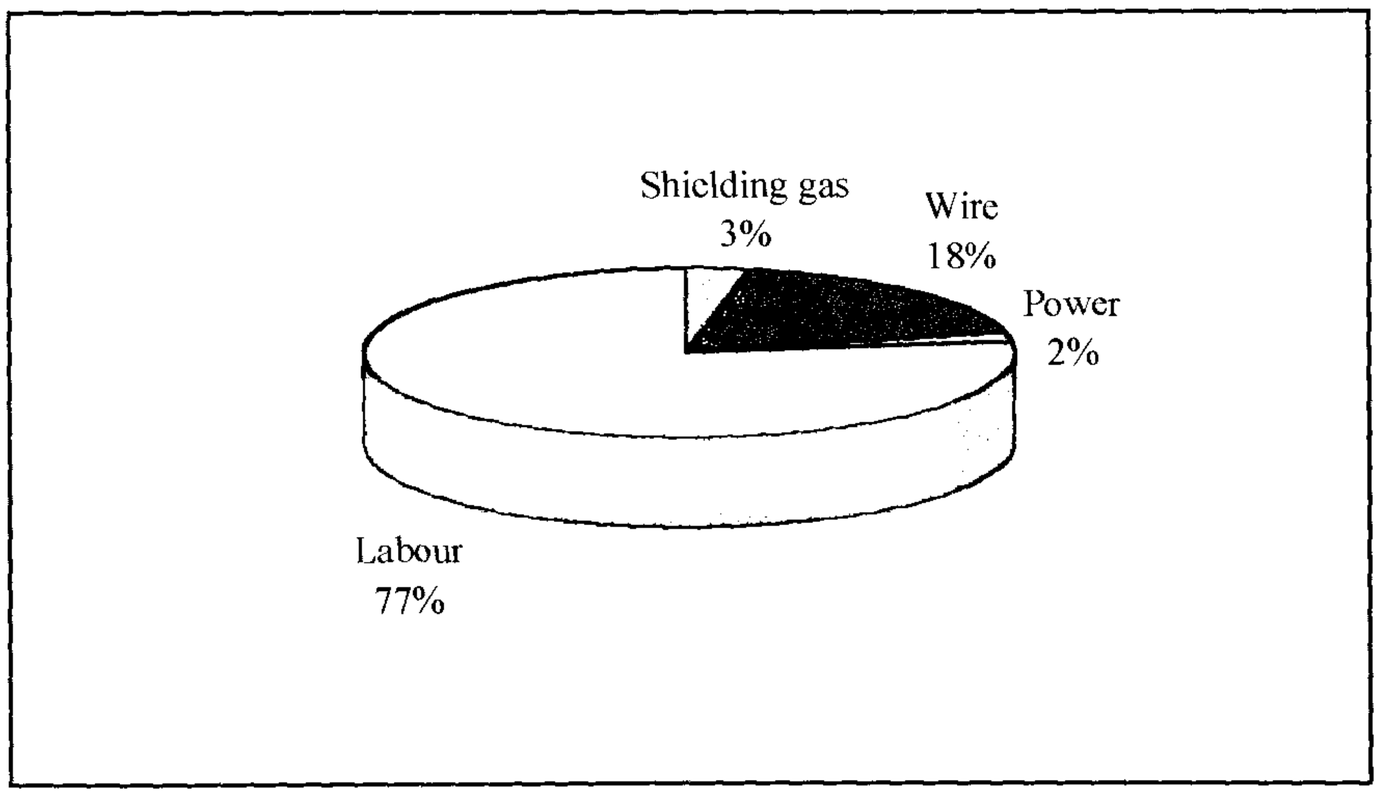

Fig. 3.1 Total welding cost.

The procedures, system and process control used for manual arc welding can not easily be adapted to automatic welding, because most manual welding relies heavily upon the skill and actions of the welder. However adaptive control of welding parameters such as arc length and voltage, electrode feed rate, welding speed, and other variables are possible with the introduction of micro-processors

in arc welding, and the development of a wide variety of sensors that can to some extent emulate those of the human welder.

Development in Artificial Intelligence (AI) methods also enables human knowledge and inferencing to be incorporated into control systems or to deal with situations of lack of knowledge or uncertainty.

3.4 Theoretical modelling

Theoretical models of the welding process attempt to present independent (input) and dependent (output) welding variables in the form of mathematical relationships, the relationship being derived purely by theoretical considerations such as mass and energy balances, the heat transfer laws, the stress - strain relationship etc. These derivations usually include assumptions and simplification. An early contribution to the theoretical formulation related to welding was made by Rosenthal (28). He determined the temperature distribution around the moving heat source and predicted the shape of the weld bead in two and three dimensions. This work will be discussed further in chapter 4.

Jonnson et. al. (29) described a theoretical investigation into arc parameters and metal transfer in GMAW, using argon and helium gases. Masao et. al. (30) developed a theoretical model for the shape of the weld bead and the temperature distribution around a moving heat source in TIG welding. They concluded that the experimental data for pool width was close to the theoretical predictions. On the other hand, ripple lag length and pool length obtained by experiment were longer than those obtained by theory. This was considered to be attributed to convective heat transfer in the molten pool, due to fluid dynamical motion of the molten weld metal. Doumanidis (31) developed dynamic models, which combine theoretical, statistical, and experimental techniques to describe all essential thermal, mechanical, electrical, and other phenomenon taking place in a welding process. The model integrates separate mathematical descriptions for the solid region, the weld pool and the torch efficiency. He concluded that the accuracy of the simulated responses of the bead geometry requires either off-line calibration of the torch efficiency and distribution parameters at the nominal welding condition, or

their in-process identification based on non-contact temperature measurement. He also stated that the model may be used as a reference model for design of weld geometry control systems.

Theoretical models are useful in providing an insight into the nature of the phenomena involved in welding, and in explaining the various interrelations between the welding variables on the basis of theoretical principles. However, their value in predicting the welding outputs is limited. Shinoda (32) has reviewed the literature and concluded that although theoretical modelling requires less empirical experimentation, for validation, it is difficult to ensure all relevant factors are considered and that the model adequately describes every welding situation. McGlone (33) has also reviewed these approaches, and reported that the theoretical approach is not successful in deriving equations capable of reliably relating the arc welding variables to the resulting weld bead geometry. The difficulties in theoretical models are due to complexities of interaction and reaction between the variables, coupled with often vastly over-simplified assumptions. In the next chapter the theoretical modelling of heat distribution in GMAW will be discussed in more detail.

3.5 Numerical modelling

Numerical models employ the same fundamental principles as theoretical models but, instead of formulating welding inputs and outputs, they attempt a computational simulation of the entire process. They typically apply the finite difference or the finite element method and consider discrete time steps. This method provides additional flexibility, since most local and transient phenomena of the process can be considered more easily. Giedt et.al. (35) studied the weld pool surface temperature variation during cooling of stationary GTA welds, using an infrared sensor, as well as the fusion zone joint penetration. The measured results were compared with prediction for the transient temperature responses of the 2D finite difference numerical model. An equivalent conduction factor in the pool was identified to match the experimental results. Fitzpatrick and Bak (36) used the Finite Element technique to model the thermal gradients and weld

geometry, using estimated values of the arc efficiency and energy distribution. They verified the model responses experimentally using thermocouple measurement and infrared thermography images for GTA welding bead on plate experiments. The intention was to extend the use of the model to process development and to use simpler models for real-time control, since the numerical model was too slow for this purpose. Lambrakos (37) also developed a numerical model for calculating the temperature and fluid velocity field in a three-dimensional workpiece in deep-penetration laser welding.

In conclusion, the flexibility of the numerical model has helped to overcome many of the limitations of theoretical models by reducing the assumptions, and therefore extending their application range in practice. However, numerical models usually demand computation, which, in terms of memory and time requirements, makes them unsuitable for real time modelling of complex processes. Developments in computing technology will naturally reduce this limitation.

3.6 Empirical modelling

Empirical or statistical models are similar to theoretical models, they express the relationship between a limited number of inputs and outputs of the welding process by analytical formulas. However, these relationships are not derived from theoretical principles, but from analysis of actual experimental data. It is usual to attempt to recognise those independent inputs that exert essential influences on specific dependent outputs, and then to determine this dependence by applying the techniques of statistical analysis to experimental data. The main effort is to express the welding output in terms of a small number of essential welding inputs, by a relationship having the broadest possible scope of application and the smallest possible scatter of data. Shepherd (38) developed empirical models of bead geometry and welding variables for a self-shielding flux cored electrode welding process. He established a comprehensive data base containing information on 1000 actual test weld beads, each test characterised by 76 pieces of data, in order to generate eight predictive equations. Thorn et.al. (39) considered the theoretical prediction of the weld bead geometry in GMAW, and realised that

modifications are required to obtain better agreement with experimental data. They adapted significant welding inputs in the theoretical relationships and used regression analysis to determine corrective factors.

In this work empirical modelling has been used to determine the correction factor for an infrared temperature measurement sensor, and the theoretical temperature on the surface of the workpiece along the weld line during welding.

Empirical models of welding tend to be restricted in application, they usually apply for one welding technique and a very limited range of conditions. To generate an adequate model, a large amount of experimental data is required which is costly and time consuming. However, since they are derived experimentally, the correlation between experimental validation data with respect to the model predictions, is usually good for the particular case.

3.7 Artificial intelligence

Artificial intelligence (AI) is a part of computer science concerned with designing intelligent computer systems. Typical applications are mechanical devices coupled to sensor technology, to enable the performance of tasks with intelligent behaviour emulating that of human beings.

Examples of AI application include problem solving, natural language processing, pattern recognition, expert systems, robotics, neural network, fuzzy logic, and computer vision. Among these subjects, expert systems, neural networks, and fuzzy logic will be discussed in this chapter. Application of artificial neural network and fuzzy logic modelling to the control of robot and welding parameters is the subject of this research work.

3.7.1 Artificial intelligence in arc welding

Arc welding is a complex manufacturing process, a welder must be trained very intensively to decide how to control the quality of the weld in process. He must learn not only how to position and move the electrode correctly in relation to the

seam and know the parameters for a given task, but his most important task is to react appropriately when unexpected variations occur. For example, if the joint preparation geometry changes due to manufacturing tolerances, an unstable arc or discontinuities may occur in the welding process. The welder must react immediately to correct these problems. This ability to maintain permanent feedback control, based on his experience, puts the human welder beyond any welding machine. Today, by means of Artificial Intelligence(AI), one can reduce the gap between a human welder and a machine. Further application of AI to robotic arc welding has enabled the robot to be more intelligent, make decisions and provide reasoning for their action. Despite the mental capacity of the human welder and his ability to adaptively control the process, he has a number of limitations. The manual welder is affected by fatigue and loss of concentration and possibly limited memory. Given adequate power, computers have none of these limitations. On the other hand capturing large volumes of expert knowledge or experience data accurately within a computer is a difficult task, but once done such a system will perform consistently.

The approach for intelligent control of arc welding may involve integration of off-line inspection of the joint before and after welding, in-process control via the use of sensors for both process and product state, and appropriate control strategies. These can drive the product state to the desired quality. The tools necessary for adaptive control include control strategy, process modelling, sensing and artificial intelligence. In the following section expert systems, artificial neural network modelling, fuzzy logic, sensors and their application in robotic arc welding are discussed further.

3.8 Expert systems

An expert system is a computer program that uses knowledge and reasoning techniques to solve problems that normally require the service of a human expert. The British computer society (40) defines an expert system as " the embodiment within a computer of a knowledge-based component from an experts skill, in such form that the system can offer intelligent advice or take an intelligent decision

about a process function". There are two types of knowledge in expert systems: public knowledge and heuristic knowledge. Public knowledge includes documented definition, facts and theories. Heuristic knowledge is undocumented and based on individual experience or expertise.

An expert system contains three main components (40):

- A data base of knowledge including public and heuristic.
- A set of rules typically of the form "IF" condition, and "THEN" action.
- A monitor (which is sometimes called an inference engine) that executes or fires a set of rules , resolves the conflict if more than one rule can fire, and then executes the chosen rule.

3.8.1 Expert systems in arc welding

Expert systems have been used by many researchers in welding applications, as reviewed by Bahashwan (41). They have been applied in welding either before, after or during execution of the welding process.

Thompson (42) developed a hierarchically structured knowledge-based system (KBS) for welding automation and control. The KBS was designed to co-ordinate a robot and work table movement independently, by examining the initial programmed path and determining the feasible table orientation and robot trajectories that could improve the weld quality. The system was also capable of determining appropriate weld parameters for certain types of seams on the basis of the job description. Budgifvars (43) developed an expert system for diagnostic application. The system was capable of diagnosing malfunctions occurring in the ESAB A21 orbital TIG welding automate when used with the programmable PRO-TIG 250 power source. The input information to the system is performed by interrogation of the user. Each answer is used to test the different components inside the machine and the faults will be ranked in such a way that if a particular set of symptoms implies more than a single fault, the most regularly occurring fault is investigated first. Kerth(44) investigated the concept of a knowledge based

expert system for controlling welding process parameters in real time. The input was the seam profile obtained from a laser vision system. It could detect the variability in root-gap and root-face and, by using a rule based system, update the welding process parameters. Vivek (45) developed an expert system in order to help plan and train welders for the shielded metal arc welding (SMAW) operation. It accumulated available information on a SMAW process, including edge preparation, electrode selection, economic evaluation, analysis of weld defects and trouble-shooting. The expert system also included an explanation sub-system, which shows the reasoning process to reach a conclusion. Ghasemshahi (46) developed a knowledge-based expert system for pre-weld inspection of joint geometry and fit-up in order to control welding procedures in an automated welding cell. Misra (47) developed an expert system for GMAW of aluminium and its alloys, which enabled recommendation of a complete welding procedure such as type of power source, welding current and voltage, torch angle, welding speed, stand off distance, shielding gas type and flow rate, etc. Reeves et.al. (48) used an expert system as a means of providing intelligence for in-process control with particular emphasis on small-batch arc welding operations. Two elements were used in his investigation: expert system, and sensor fusion. In sensor fusion, a combination of sensors is used to gather the information during the welding process. By combining the input of two or more sources, sensor fusion derives an intelligent picture of events transpiring in the target environment. For example, sensor fusion plays a role in making intelligent fill-rate decisions. For materials sensitive to heat input, the fill-rate decision requires combined support from both vision and temperature sensors. A vision sensor is used to capture the joint geometry and torch-to-workpiece location. The information collected is then transferred to an expert system module to provide the mechanism for making decisions based on the above interpretation. It uses sensor fusion output in conjunction with a rule base to pre-set the weld procedure, analyse the condition and modify the welding procedure accordingly, i.e. reconcile computing goals, such as cost, quality and productivity. Pierr and Levine (49) developed an expert system which can be used for automation of the welding process. They concluded that a sophisticated expert system should be able to guide the user in the preparation and planning phase of the welding process. The system also must be

able to plan the welding task in accordance with user specification. Vandeveldt (50) developed a welding expert manufacturing cell called WELEXCELL, it consisted of two components: weld job planner and weld job controller. The system is able to plan the joint design and welding schedule, including details such as suitable voltage, electrode choice and heat treatment for the weld. It then downloads the planned welding job to the robot controller for robotic welding. The system also controls welding by using a voltage sensor. Taylor et.al. (51) investigated the application of expert systems in arc welding and they concluded that expert systems techniques are not only a suitable approach to the solution of combining knowledge from related domains, but they are also a catalyst for the rigorous and logical scrutiny of the domain knowledge, its gaps and its inconsistencies. Therefore there is as much to be gained from the process of building an expert system as there is from the final product.

3.8.2 Advantages of expert systems

Expert systems in contrast with algorithmic languages such as Pascal or Fortran, have the following advantages:

- Within their chosen fields, they can demonstrate expert abilities;
- They can handle uncertainty through bayesian rules and fuzzy logic;
- They can provide the user with an explanation for the advice they offer;
- They have reasoning capabilities;
- They are more reliable and consistent;
- They are programmed in a declarative style, usually by means of rules.

3.8.3 Limitations of expert systems

A number of problems and limitations exist within expert systems (52) as follows:

- Lack of resources: the expertise, knowledge or resources are not always available to build an expert system;
- A useful expert system can take a long time to build;
- Maintenance of expert system: the system will lose its power once the knowledge it holds is outdated which will result in loss of credibility. Therefore, the expert system knowledge base should be updated.

3.9 Artificial neural networks

Neural networks are an attempt to understand the operation of the human brain and nervous system, and to simulate or emulate this as a program in a computer system. Neural networks represent an alternative computational paradigm compared to the conventional approach, which is based on an explicit set of programmed instructions. In neural networks the solution to a problem is learned from a set of examples.

A feed forward neural network can be regarded as a non-linear mathematical function, which transforms a set of input variables into a set of output variables. The precise form of the transformation is governed by a set of parameters, called weights, the value of which can be determined on the basis of a set of examples of the required mapping. This process is called training or learning. When the weights have been fixed, new data can be processed by the network. Neural network architecture and design will be discussed in chapter 6.

3.9.1 Artificial neural networks in arc welding

Artificial neural networks provide a range of powerful techniques for solving problems in pattern recognition, data analysis, and control. Neural networks are ideal for complex pattern recognition problems for, which solution requires knowledge which is difficult to specify but which is available in the form of examples. Neural networks represent a complex trainable non-linear transfer function between inputs and outputs. This allows an effective solution to be found

to complex non-linear problems, such as heat distribution in arc welding without requiring any knowledge as to the nature of the solution. Artificial neural networks, unlike expert systems and statistical modelling (43, 46), have the ability to extract and discriminate information from a limited number of data. Artificial neural networks have been employed by many researchers in order to control arc welding. Cook (55) used ANN to control gas tungsten arc welding. He constructed a closed-loop process control model which was able to control the welding variables (current, travel speed, and arc length) by monitoring the weld bead geometry (bead width, and height) in real-time. Middle (56-57) investigated applications of neural networks in intelligent post -weld inspection of a flexible robotic welding cell. He compared predictions with validation data and concluded that the use of ANN is viable for modelling the robotic arc welding process. They require only a small amount of experimental data for satisfactory training of the network. Stroud et.al. (58) applied an ANN to the diagnosis and control of submerged arc welding using an ultrasonic sensor. They concluded that neural networks are a powerful enabling technology for use in diagnostic and control systems. They can be implemented as part of a more complex system where their abilities are best suited. Ohshima (59) investigated the application of neural networks for seam tracking. He used a neural network model in order to recognise the form of the welding line, and the result is used to adjust a fuzzy variable. White et.al. (60) developed an artificial neural network to model heat flow in the tungsten arc welding process. The input parameters to the network were welding process variables including voltage, current and travel speed. The output from the network was the predicted thermal profile including the isothermal lines around the weld. A finite element model (FEM) of the GTA welding process was prepared and used to train the network. The FEM produced a steady state thermal map of material surrounding the weld. The model was verified experimentally with a series of welds made on 1.9 mm, 2.5 mm, and 2.8mm thick stainless steel plates. These welds were examined using metallographic technique to determine the fusion zone size, and the data was used to verify and adjust the finite element code. The trained neural network runs in a fraction of the time required by the FEM. To produce a single steady state thermal map of the GTAW weld the finite element code requires approximately 1.5 hours, while the neural network required

only a fraction of a second to produce the same result on the same workstation. They concluded that neural network have the capability to dynamically model the relationships between input and output parameters in welding, which is a complex and highly non-linear process. Andesen (61) applied an ANN model in open-loop control of gas tungsten arc welding. He used current, voltage, travel speed and plate thickness as input, and bead width, and bead penetration as a output for training the neural network. A reverse model was developed for closed-loop control in which the input was the bead width and bead penetration, and output was the current, voltage, travel speed and plate thickness. He stated that uncertainty in bead measurements are a significant cause of errors in the models. Einerson et.al. (62) developed an artificial neural network for cooling rate and fill control in gas metal arc welding. An ANN was trained using the back propagation method to learn the functional relationship between the heat input, reinforcement and the electrode and welding speeds. They obtained experimental data by setting the welding speeds prior to welding and measuring temperature during welding. Then they constructed an inverse model in which the temperature measurement was the input and welding variables were the output. Smart(63) states that the difficult part of their work was the fact that reinforcement and heat transfer rates are both functions of welding speed, and in gas metal arc welding, current is a function of voltage and electrode feed rate. This problem was handled by deriving models of these relationships, and teaching them to an artificial neural network, using a look-up table. Jones (64) developed an artificial neural network for modelling the welding parameters in the flux cored arc welding process. Input to the model was voltage, current and travel speed, and output was arc stability, bead geometry, amount of spatter, bead undercut and ease of slag removal. He concluded that artificial neural networks have application in producing highly complex non-linear multi-variable models of the welding process, that offer accurate prediction of weld properties from control parameter values. Matteson et.al.(65) developed an ANN for classifying the acoustic signals of acceptable and unacceptable welds from the gas metal arc welding process. Dilthey et.al. (66) developed a system for quality monitoring and quality grading in GMAW using neural network. The criteria for the quality judgement were seam and root reinforcement and undercutting. They concluded that with this model it was

possible to predict whether the quality of the weld was adequate or not in more than 90% of the welds.

In this research artificial neural network modelling has been used for the prediction of workpiece surface temperature during welding. This is discussed further in chapter 6.

3.9.2 Advantages and limitations of neural networks

Neural networks offer high processing speed and have the capability of learning a general solution to a problem from a set of specific examples.

Their main disadvantage stems from the need to provide a suitable set of example data for network training and for model validation, and the potential problems which can arise if a network is required to extrapolate to new regions of the input space which are significantly different from those corresponding to the training data.

The advantage and limitation of neural networks are often complementary to those of conventional data processing techniques. Bishop (67) states that neural networks should be considered as possible candidates to solve problems which have some, or all of the following characteristics:

- There is enough data available for network training;
- It is difficult to provide a simple first-principle or model-based solution, which is adequate;
- New data must be processed at high speed, either because a large volume of data must be analysed or because of real time constraints;
- The data processing method needs to be adequate to show the level of noise on the input data.

3.10 Fuzzy logic modelling

The idea of fuzzy logic is that it allows imprecise and qualitative information to be expressed in an exact way. Zadeh (68) the founder of fuzzy logic introduced the calculus of fuzzy logic, which may be viewed as a parallel representation to probability theory rather than as an alternative. In other words the fuzzy set contains as a special case two valued logic (true and false) and probability theory. In fuzzy logic predicates can be both crisp (non fuzzy) ,and fuzzy. In the crisp set, the parameter value either belongs to the set which it has a membership of u=1, or it does not, in which case it has a membership of u=0. As is shown in figure 3.2 a, the crisp set is represented by a rectangular step function. Fuzzy set theory extends the crisp set concept by defining the partial memberships which can take any value between 1 and 0. As is shown in figure 3.2 b, the fuzzy set is represented by a step function which ramps up from 0 to 1, and then ramps back down to 0. The crisp set is precise in its meaning, having a definite transition from membership to non membership. On the other hand, the fuzzy set, allows the qualitativeness of the measure to be reflected in a gradual membership transition.

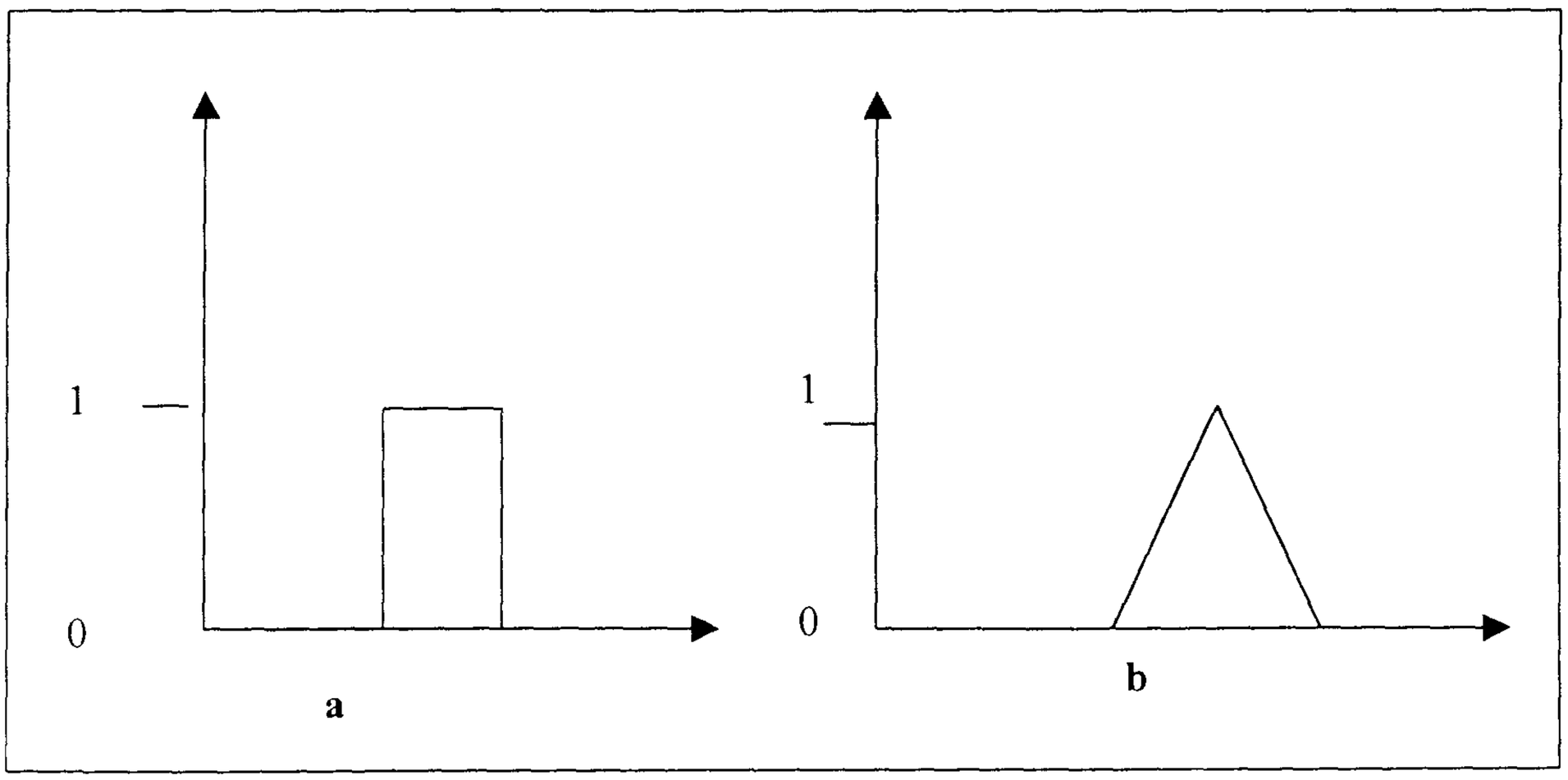

Fig 3.2. a) Crisp set, b) Fuzzy set

3.10.1 The basic architecture of fuzzy logic controller

In the design of a fuzzy logic controller, the main control parameter should be identified and a term set determined which is at the right level of granularity in order to describe the value of the linguistic variable. For example a term set including linguistic values such as *Small, Medium,* and *Large* may not be enough for some domains, and may instead require to use a five term set such as *Very Small, Small, Medium, Large,* and *Very Large.*

Different types of fuzzy membership function have been used in fuzzy logic control. The four common types are monotonic, triangular, trepezoidal and bell shape. The selection of the type of fuzzy variable directly affects the type of reasoning to be performed by the rules using these variables.

In figure 3.3 a simple architecture for a fuzzy logic controller is shown. This architecture consist of four processes, whose functions are described in the following section.

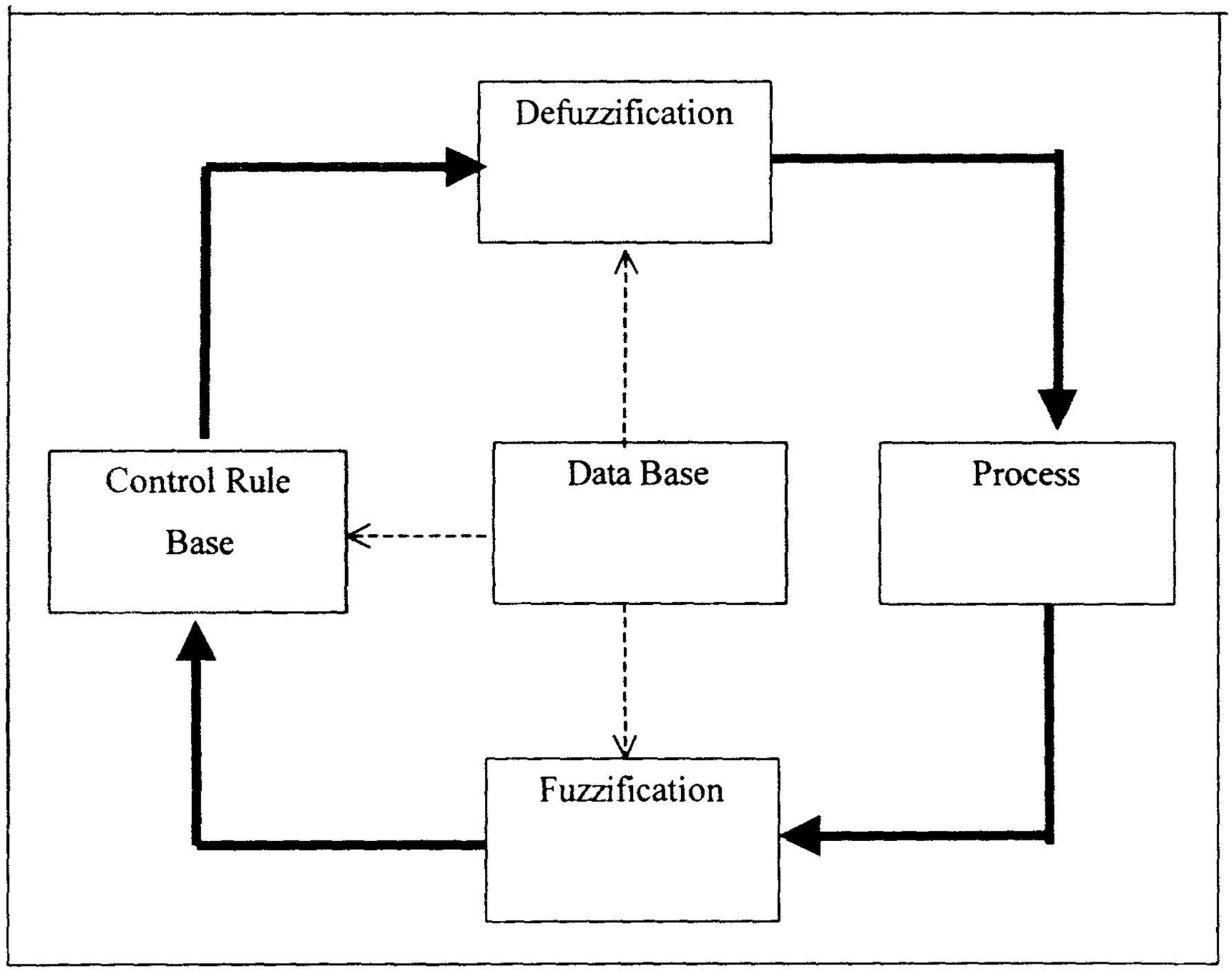

Fig.3.3 A simple architecture of a fuzzy logic controller

3.10.1.1 Fuzzification (Coding the inputs)

The fuzzification process initially maps the measured output variables of the system under control in to a suitable range that corresponds to the universes of discourse used in the control base. If the output of the system contains noise, it may be modelled by using the triangular membership function where the vertex of the triangle refers to the mean value of the data set of system output, and the base refers to a function of the standard deviation. In this case, fuzzification refers to finding out the intersection of the label's membership function and the distribution for the measured data.

3.10.1.2 Control data base

In order to design a control data base first a set of linguistic variables must be selected which describe the values of the main control parameter of the process. Then a control knowledge base must be developed which uses the linguistic variables. In order to develop a control knowledge base, Sugeno (69) suggested four methods:

1- Expert's Experience and knowledge

2- Modelling the operator's control action

3- Modelling the process

4- Self organisation

3.10.1.3 Decision making (control rule base)

This operation provides the formulated fuzzy logic controller (FLC), characterised by a set of linguistic statements generated by experts. The FLC contains the choice of process state variables and control variables, types of FLC rules, FLC order, and number of rules to be fired.

3.10.1.4 Defuzzification (decoding the outputs):

This operation provides a non-fuzzy control action that represents the membership function of an inferred fuzzy control action. There are four methods of defuzzification most often used: (70)

- Tskamoto's defuzzification method;.
- The centre of area method;
- The mean of maximum method;.
- Defuzzification when the output of the rules are function of their inputs.

3.10.2 Application of fuzzy logic in welding

Although the application of fuzzy logic control is a relatively new subject, some researchers have applied this method in order to control the welding process. Messlr, et al. (71) developed a fuzzy logic controller incorporated within a neural network for controlling resistance spot welding. He concluded that the fuzzy logic controller was capable of applying action to every weld whose actual electrode displacement curve deviated from the desired or ideal electrode displacement curve that produced a good weld. Cho (73) developed a fuzzy rule-based on-line searching method to maintain stable arc conditions. In his proposed control system the proportional and derivative (PD) control algorithm was incorporated in parallel with a fuzzy linguistic controller. The advantage of this combination was that the PD stabilised the system when the fuzzy controller could not act properly. Won and Cho (74) developed a fuzzy logic controller for the regulation of weld pool size. In the fuzzy algorithm which they designed, the error between the desired pool size and the predictive size, as determined from the value of an index constructed from multiple surface temperature measurements, was adopted as antecedent variables, and a power increment was adopted as a consequent variable. Ohshima et.al. (75) applied fuzzy inference in order to obtain optimum welding parameters in CO_2 short-arc welding. They used a CCD camera to observe the width of the weld pool at the time at which the amount of spatter was

minimum. They also constructed sets of fuzzy variables and rules expressed in IF-THEN form. The fuzzy controller used the width of the weld and cooling time, and compared it with a reference value. According to the difference and the fuzzy variables the system regulated the power input achieving an acceptable weld. In another research Ohshima et.al. (76) used fuzzy logic and a neural network with a CCD camera for seam tracking in robotic arc welding. In the fuzzy controller the deviation between the welding line and a position ahead of the torch in the direction of movement, and the variation of this deviation were adopted as the input variables. They also used a neural network to improve the tracking performance by recognising the angle of the welding line. Hiroshi et.al. (77) developed a fuzzy logic controller for seam tracking by using the arc sensor. Due to noise in the data output of the arc sensor they developed the composite method of fuzzy filtering by which the arc sensor noise was reduced. They concluded that a fuzzy logic controller with the fuzzy filtering performed better. Einerson et.al (62) investigated the application of fuzzy logic and neural networks for cooling rate and fill control in GMAW. The control strategy they adopted involved monitoring weld joint transverse cross-sectional area ahead of the welding torch, and the weld bead centreline cooling rate behind the weld pool, both by use of a CCD camera. Estimation of the required input process variables necessary to obtain the appropriate heat and mass transfer rate are done by applying a neural network model, and controlling the heat transfer rate by means of a fuzzy logic controller. The value of heat required for reinforcement and weld bead cooling rate, are sent via a fuzzy logic controller to an artificial neural network that maps the electrode speed and welding speed for a given input power. The fuzzy logic controller adjusts the heat input per unit length as required to obtain the desired weld bead cooling rate.

They concluded that the control strategy based on feedback control of cooling rate in combination with feed forward control of reinforcement has potential for application to welding fabrication. Zhang, et al (79) developed a fuzzy model to control the weld fusion zone geometry in a GTA welding process. They used a high shutter speed camera to monitor the top-side pool width. The measured bead width together with estimated under side width are selected as a fuzzy logic

control model inputs to adjust the welding current, and welding speed to achieve a fully penetrated weld.

In this research fuzzy logic control combined with a neural network model will be developed for the control of GMAW. A fuzzy rule base is to be employed to control welding parameters, based on the difference between temperature measured in the surface of the workpiece and the predicted temperature obtained via a neural network model.

3.11 Sensors in arc welding:

When manual arc welding is considered, the welder is capable of recognising and inspecting components prior to welding, recording any defects in assembly and faults requiring special attention during welding. He can orient at the workpiece in the best position for welding and can position himself to gain best access to the seam. During the welding process, the welder gathers information about the process with his visual and auditory senses, and after welding the quality of the weld produced will add to the experience and learning of the welder to take necessary action for future work. He continually observes the weld pool in order to control the penetration, and he also observes the geometry of the joint preparation to keep the electrode in the correct position. While watching the arc and listening to the sound the arc emits, he is able to control the metal transfer. He gathers information during welding and with his knowledge, he draws conclusions and performs the necessary actions.

Development of sensor technology has enabled robots systems to emulate many of the human controls, and to be used more effectively in the welding operation to control both seam tracking of the weld line and adaptive control of welding variables.

Nomura(80) has classified sensors in two groups, Contact and Non-contact as shown in Table 1.

Sensor type		Unit in the sensor configuration
Contact	**Contact probe**	Micro switches, potentiometers and differential transformers (DTF)
	Electrode contact	Voltage and current for contact detection that is applied to the welding wire
	Temperature	Thermocouples and thermistors
Non-contact	**Arc phenomena**	Welding current arc voltage, wire feed speed.
	Optics	Point sensor (photo transistors and photo diodes), line sensor (CCD,MOS and PSD) and area (image) sensors (CCD,MOS,PSD) .
	Temperature	Photo thermometers and infrared thermometers.
	Sound	Ultrasonic and sound pressure detect probes.

Table 1. Classification of sensors

3.11.1 Contact Sensors

The importance of contact or tactile sensing (mechanical or electromechanical) in the field of arc welding systems has been recognised for many years. Applying these sensors is appropriate where relatively linear joints are to be followed. An early review of these systems (81) in tungsten inert gas, gas metal arc welding, and submerge arc welding seam tracking technology showed that these systems are typically mounted to rail mounted tractors (tractor units, gantry, or beam) to permit the seam to be accurately followed. Such systems were mainly used because of their simplicity and low cost. Further research and development into using electromechanical types of tactile sensing enabled robots to be more flexible

in their welding operation. Nicolo (82) investigated the feasibility of applying a tactile sensing technique to robotic arc welding for seam tracking, by mounting the probe on two orthogonal slides driven by stepping motors and sensing the side wall of the joint ahead of the weld. More recent tactile sensors use ultrasound for seam tracking, contact being made via a coupling fluid. Stroud (83) investigated the feasibility of the use of ultrasound for seam tracking and real-time weld penetration control, for robotic welding systems. The robot was capable of tracking the seam, measuring the weld bead penetration depth and position, controlling them simultaneously, and subsequently modifying welding parameters. Many robotic systems use the extended welding wire as a tactile probe for weld start position and seam finding, in a search routine included at the beginning of the taught program. A practical limitation of this sensory method is the difficulty of maintaining satisfactory coupling.

The major drawbacks encountered with tactile sensing when it is applied to robotic welding are:

- Not adaptable to suit a variety of joint geometry;
- Tendency for probe to lose contact with the joint, particularly at high speed;
- Probes cannot easily follow complex contours;
- Contact sensor may limit the welding speed;
- Probes are subject to wear and environmental effects such as spatter.

These types of sensors are not generally viable for most robotic welding applications that require adaptive control sensing.

3.11.2 Through-The-Arc Sensing

Through-the-arc sensing is the most common form of joint tracking used with industrial robots and arc welding. The technique uses electrical signals from the welding arc and requires oscillation of the welding torch, and monitoring of the variation in welding current or voltage. The weaving motion causes changes in the

current sensed at the joint sidewalls. These current changes are directly proportional to fluctuation in distance between the surface of the weldment and the tip of the welding electrode. Eichhorn (84) used through-the-arc seam tracking for TIG welding, and controlled the lateral position of the torch during the welding process. Two seam tracking systems have been developed, seam tracking with constant oscillation amplitude, and seam tracking with self-tuning amplitude. In the former, the sensor is used to measure average arc voltage at the joint sidewall during scanning. The signal difference is then used to correct for an out-off-centre position of the welding torch. In the seam tracking with self-tuning amplitude, the sensor is used to improve response time and be able to compensate for lateral misalignment by self-adjusting the electrode oscillation amplitude using the reverse pulse (from the arc voltage).

Through-the-arc sensing has the following advantages: (85)

- Relatively low cost;
- Not affected by smoke, spatter, or the arc itself;
- Compensation correction for heat distortion during welding;
- Ability to track and weld simultaneously.

The limitations of this arc sensing include:

- Incorrect electrode extension will result in erroneous sensing of the joint start;
- Joint sidewall must be well defined;
- All welds must have weaving of about ± 3 mm;
- Limited ability for non-ferrous material;
- They do not provide detailed geometric information and cannot be adapted for process control purposes, other than arc length control through arc voltage monitoring.

3.11.3 Inductive Sensing

Inductive proximity or eddy current sensors consist of an exciter coil, carrying an alternating current with two coaxial pick-up coils connected in opposition. There are basically two types of inductive sensors, those detecting the seam itself, which use a high frequency oscillation to generate an alternating magnetic field in the surface of the component and those predicting the seam position by locating the component surface (proximity sensor).

Goldberg and Karlen (86) developed a seam tracking sensor base on high frequency induction. The sensor was mounted ahead of the welding gun and it was able to measure the area and height. This type of sensor can be used for all types of welding processes, because the tracking system is independent of the welding process. Nicolo (82) investigated the application of inductive sensing together with a tactile sensor for robotic arc welding systems in order to move the torch toward the nominal position. The sensor uses four transducers, which are not effected by the arc temperature or joint type, mounted orthogonally to the direction of movement of the torch.

The advantages of these sensors are that they are completely independent from the welding process. They are compact and robust and can even operate under water. Eddy current sensors have limited application for robotic arc welding due to the following restriction (38):

- They are sensitive to the temperature of workpiece;
- The sensors are most accurate at a stand off distance less than 10 mm;
- Their physical size may lead to problems where joint access is limited;
- Different sensor configurations are required for fillet and butt welds;
- They are suitable only for seam tracking.

3.11.4 Visual Sensing

Vision sensors can be used to capture detailed information from the joint seam, weld pool or weld bead profile and spatial position by using image processing technique. Joint types can be recognised and dimensionally measured. The welding gun can be positioned correctly in the seam centreline, and information, on the variation in joint geometry and fit-up, can be used in adaptively modifying welding procedures in advance of welding. These sensing systems are mainly based on the use of "structured light" in the form of a strip or plane of light (88), "range finding" in the form of a projected spot of light, or solid-state camera principles where direct visual sensing takes place. Visual seam tracking often requires sensing of the seam to take place in a hostile welding environment. Such an environment can be avoided by using "two-pass" seam tracking (89), where vision sensing is first used to determine the true joint position and measure its parameters (e.g. root gap, root face thickness, etc.). Welding is then conducted in the second pass. This technique increases process cycle time and does not compensate for errors introduced during welding, such as distortion. In "one pass" seam tracking, sensing and welding are done simultaneously. Thermal distortion during welding process is therefore accounted for by modifying welding procedures and torch position. To protect the sensor from the welding environment they are usually secured in a housing with inter-changeable filter glass.

Several researchers have applied vision sensors in robotic arc welding. Richardson (90) developed a vision based sensing and control system in order to view the weld pool through the welding torch. The system was able to achieve real-time joint tracking and weld pool control in GTAW. Nipoled and Bruemmer (91) have used a conventional solid-state camera system together with a special exposure technique to view the weld pool in the GMA welding process. The camera and image processing technique is used to provide seam tracking and measure the three-dimensional profile of the seam. It was also capable of controlling welding parameters by analysing the weld pool shape and position of the electrode relative to the seam. To overcome the problem of measuring the joint near the welding torch in the optically noisy condition caused by strong arc light,

particularly in high-current arc welding, Makato (92) developed a new method. A laser beam, modulated at high frequency, is projected on to the work and detected by a highly responsive photodiode to convert it to an electrical signal, which is passed through filters and detective circuits. He found that in this way the sensor signal within the arc light is detected with an excellent S/N ratio.

3.11.5 Thermal Sensing

Since final mechanical properties of welds such as hardness and toughness are greatly affected by the thermal history (peak temperature and cooling rate), sensing temperature in the weld zone has long been of interest to researchers. The temperature of the base metal near the weld pool is expected to have a relationship to the heat balance and hence weld bead geometry. Infrared and thermocouple devices represent the two primary means for obtaining surface temperature. They can measure the temperature of the front face or back face of the workpiece.

McCampbell, et.al.(93) used a sliding thermocouple in order to measure the surface workpiece temperature in GTAW. They applied a single thermocouple wire in sliding contact with the dissimilar workpiece material to form the thermocouple junction. The wire was placed within 2.5 cm of the weld pool to estimate the surface temperature. This technique is not precise, and cannot be adapted for automated welding process control.

3.11.6 Infrared Sensors

Energy is emitted by all objects having a temperature above absolute zero. This radiant energy increases as the temperature of the object is increased. By measuring the radiation energy from the object in the infrared portion of the spectrum, applying Planck's law (94) which shows the relationship between wavelength and radiation energy, and applying Wien's displacement law which shows the temperature of an object as a function of wavelength, the temperature of an object is measured.

3.11.6.1 Emissivity

Infrared radiation is emitted from all objects. The quantity of this radiation is a function of the surface emissivity, the temperature, and the geometry of the object.

Emissivity is defined as the ratio of the energy radiated by an object at a given temperature to the energy emitted by a perfect radiator, or blackbody, at the same temperature. The ideal surface for IR temperature measurement would be a black body with an emissivity of 1.0. In practice most objects are either *graybodies* which have an emissivities less than 1.0 but the same emissivity at all wave lengths, and *non-graybodies* which have emissivities that vary with wave length and/or temperature. This last type of object can result in serious measurement accuracy problems especially when measuring absolute temperature is required. Metals, in almost all cases, tend to be more reflective at long wavelengths, hence their emissivity improves inversely with wavelength (92).

In any research involving measurement of IR radiation, it is necessary to know or determine the emissivity of the radiating surface. In this research experiments comparing IR measurements with thermocouple measurements were carried out as discussed in chapter 5. These experiments served to evaluate and calibrate the accuracy of the IR sensor, and in turn allow accurate estimation of the emissivity of the weld joint surface. This value of emissivity can be assumed constant at a given temperature providing the condition of the radiating surface remains unchanged. However, in this research relative temperature measurements have been used, and virtually identical conditions will have applied to temperature measurement for the collection of data for training the models, as for the evaluation of the models.

3.11.6.2 Application of infrared sensing in Arc Welding

Infrared sensing is the most common form of temperature measurement in arc welding. Researchers have used this method for seam tracking and process control by front face and back face temperature measurement, and thermography in arc welding (96).

Groom et.al. (97) investigated using infrared thermography for joint tracking in gas tungsten arc welding. An infrared camera was used to record the temperature gradients surrounding the welding torch and workpiece and transmit the images to a central computer. Using an experimentally derived image processing technique, the relationship between distance of the torch from the joint and the resulting thermal profile was determined. Given the monitor thermal profile corrective action for the torch path was possible. They conclude that reliable and repeatable thermal patterns are obtained by infrared measurement of surface temperature distribution during the welding process.

Doumanidis and Hardt (98) developed a model for independently regulating the time-temperature relationship of the HAZ and the centreline cooling rate in the GMAW process. The on-line thermal measurement included scanning the time-dependent temperature field on the top surface of the workpiece, using an infrared radiation sensor. As shown in Figure 3.3 they measured:

- The weld nugget cross-section area, defined by the solidus isotherm, this was adopted as a collective measure of the effect of solidification faults, such as porosity, inclusions, incomplete fusion, etc;

- The heat-affected zone width (HAZ);

- The centreline cooling rate , defined at the location with critical temperature.

They concluded that the effects of in-process emissivity variation are inevitable, as long as radiation measurement are performed at a single wavelength range.

Chin et.al. (99) investigated the application of infrared thermography for detecting perturbations that result in faults during the arc welding process. They stated that the infrared camera is capable of monitoring arc position relative to the seam and can be used to identify joint geometry faults, such as joint gap and offset. Change in the patterns of surface isotherms in front of a moving arc are directly related to depth of penetration, and impurities.

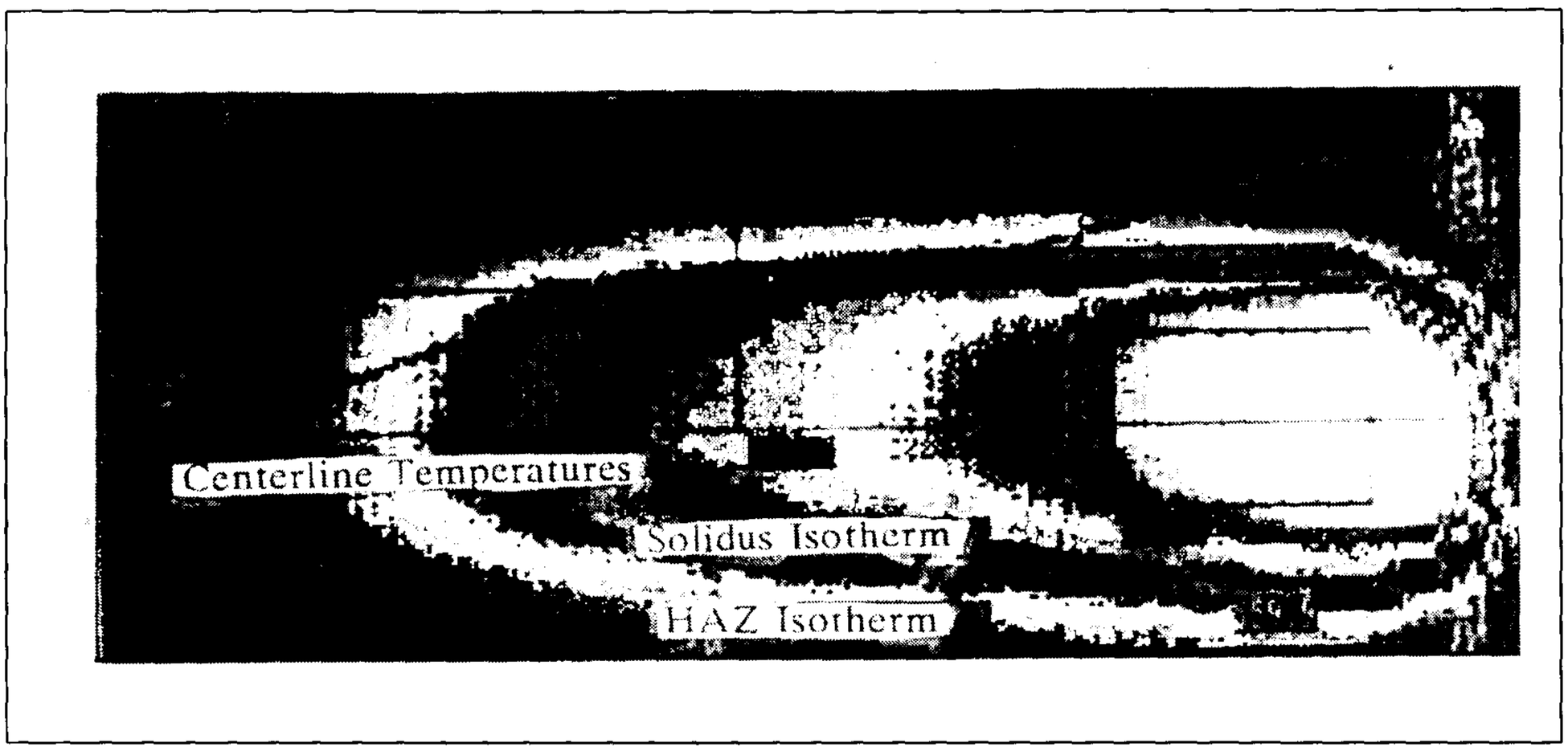

Fig.3.3 Top surface temperature field.

Chen and Chin (100) used infrared sensing techniques in order to monitor the joint penetration. They conducted a series of experiments to relate the depth of joint penetration and bead width to measured surface temperature distribution. Bead width and depth of penetration, measured after welding using metallographic techniques, were compared with magnitude, gradient, area under thermal profile and symmetry of the infrared sensed temperature distribution. As shown in Figure 3.4 there are identifiable changes in surface temperature distribution for each percentage of joint penetration. They concluded that a linear relationship exists between the width of the temperature profile and the bead width, and an exponential relationship exists between the depth of the joint penetration and integrated area under the peak temperature profile, obtained during the welding process.

Betly and Marburger (4) also used an infrared sensor in order to develop a feed back control system for penetration control, by measuring the amount of visible and near-infrared light emitted from the backside of the weld. They state that the visible underbead radiation is concentrated in the weld pool and thus for controlling full penetration weld underbead width, visible radiation is a better feedback parameter than infrared, yet for partial penetration welds, infrared is

more significant. Moreover, it remains that back side monitoring is inconvenient for most welding applications, in particular robotic application.

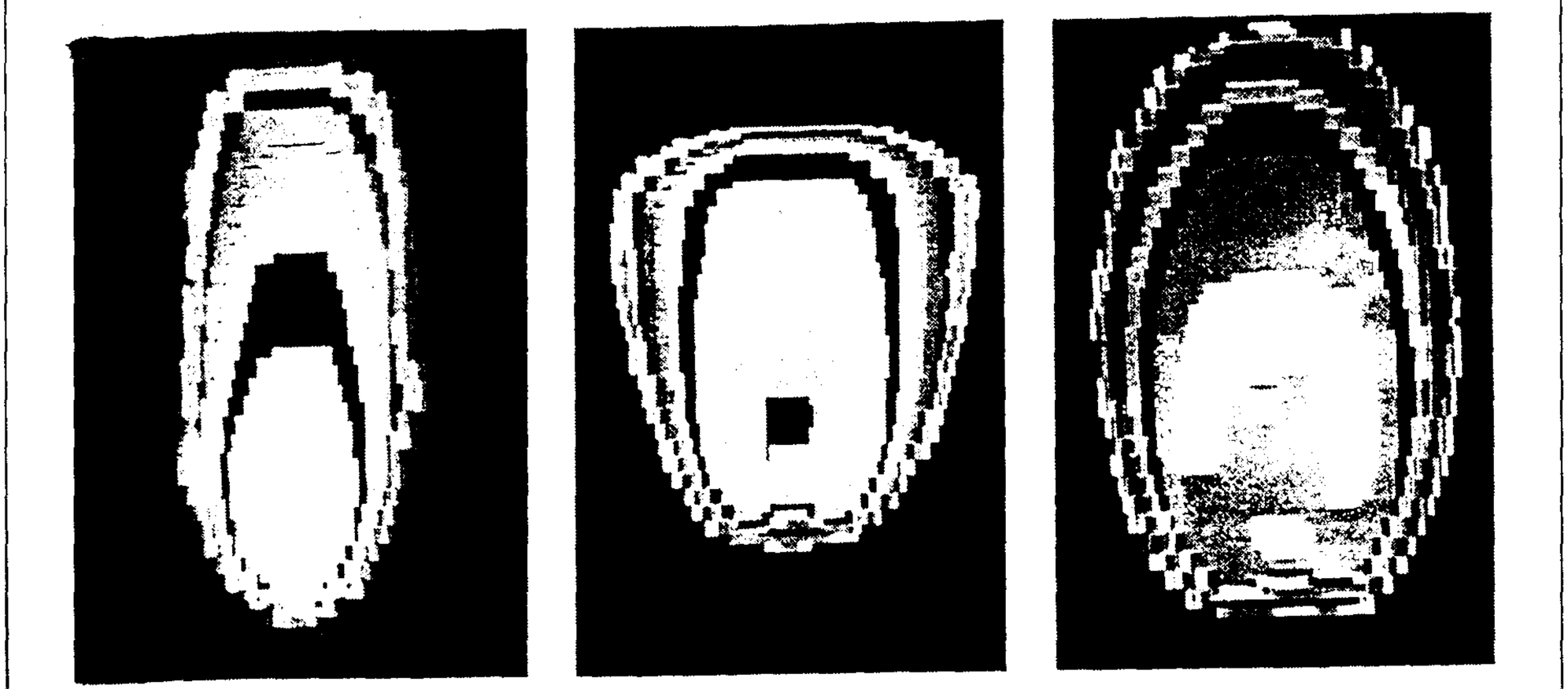

Fig.3.4 Isothermal plots showing surface temperature distribution for 10%, 30%, and 70% penetration.

One problem with an infrared sensor is that the sensor can pick up reflected and transmitted infrared energy from numerous sources, in addition to the emitted energy of the primary target (78). One way to prevent these extraneous sources of radiation is to focus on a small spot on the surface being measured. The infrared sensor, used in this research is able to measure a spot with diameter of 2.3mm.

3.11.7 Sound sensing

Sound sensors can be of two types audible sound, which is detected by microphone, and ultrasonic noise, which is transmitted and received by a transducer. Hardware and software have been developed which can be applied in arc welding to detect and analyse the sounds received in real time (95). Weld penetration monitoring and control by ultrasonic sensing, along with seam

tracking during welding has been implemented by Siores and fenn (72, 32). He states that weld penetration monitoring and control by ultrasonic sensing has been shown to be both realistic and accurate. Shepherd (38) examined the effect of sound pressure during welding, by analysing the pressure level detected by a microphone. A sharp increase in pressure accompanied the onset of penetration. He concluded that "monitoring of the sound pressure level can give information as to whether or not the process is achieving full penetration, but no other information can be derived".

3.12 Conclusion

In this chapter the main concepts of robotic welding and adaptive control for automation of welding, related to this research, have been reviewed.

In order to produce an acceptable weld, monitoring the weld, and possibly the joint via sensors and controlling the welding parameters via modelling is necessary. Developing mathematical, empirical and statistical models needs considerable amounts of experimentation, time and cost, and such models may only be applicable to a single combination of plate thickness, joint type, etc. Among non-mathematical models, neural network and fuzzy logic can be used to control the gas metal arc welding process with a degree of confidence. A neural network mimics the computational architecture of the human brain to achieve intelligent capabilities such as pattern recognition, while fuzzy logic contributes such human traits as the ability to make decisions from a rule-based reasoning.

Different types of sensors for monitoring and controlling arc welding have been developed, which each have their advantages and limitations. Among these sensors the infrared temperature sensor is an appropriate device for measurement of the temperature distribution on the surface of the workpiece. Infrared sensors have distinct advantages over other temperature detecting devices in that it requires no physical contact with the workpiece, thus affording a minimum amount of interface with the welding process.

In this research the use of an infrared sensor has been explored as a means of real-time monitoring of heat distribution on the top surface of workpiece. Then by applying artificial neural network methods the relationship between temperature distribution and input variables is estimated. A fuzzy logic controller will give opportunity to modify welding variables to fulfil the requirement for acceptable weld penetration.

The theoretical relationship between heat distribution on the top surface of the work and welding variables will be discussed in the next chapter. The architecture and design of the proposed neural network will be discussed in chapter 6.

Chapter four Heat flow in arc welding

4.1 Introduction

In Gas Metal Arc Welding a fusion weld is produced by moving a localised intense heat source, an electric arc, along the joint thus melting the metal in the joint to form a weld pool. At the same time molten filler metal from the consumable electrode wire is deposited into the weld pool. As the heat source is traversed along the joint the weld pool flows around and behind the arc, due to capillary action and the force of the arc displacing the molten metal. Since in GMAW, the electrode wire is melted off and transferred to the weld pool at a very high rate, the majority of arc heat, which flows into the electrode, is also transferred to the weld pool. The process is thus highly thermally efficient. There are many potential problems in and around a weld joint such as generation of distortion or residual stress, inadequate joint strength and unacceptable weld bead geometry (101). The primary causes of low joint strength are insufficient penetration and lack of fusion with the side walls of the joint. These faults are mainly a function of the mass of the joint members, energy input from the welding heat source, and heat flow into and through the weld pool and heat affected zone.

Accurate predictions of weld penetration and bead geometry require understanding and analysis of the weld thermal cycle and associated heat flow. The purpose of this research work is to predict the depth of penetration by measuring the temperature at a point in the top surface of the workpiece. Therefore in this chapter, the principles of heat flow in GMAW will discussed. This discussion will be extended to the theoretical relationships between the surface temperature, welding variables, weld penetration and weld bead geometry.

4.2 Heat flow in Gas Metal Arc Welding

The thermal cycle in welding is due to a moving heat source acting along the weld joint. The thermal cycle at a point in the joint material is characterised by the heating stage in which the temperature of the material rises to a maximum, and a cooling stage in which the temperature of the material decreases. The temperature pattern and kinetics at a point in the joint is dependent on the energy parameters of the welding process, including welding speed, and the thermo-physical properties of the joint material. The rate of rise in temperature, maximum temperature and the cooling rate at any point are also a function of the position and distance of the point from the centre of the arc heat source where the energy input is maximum. The maximum temperature is above the melting temperature in the fusion zone, with lower temperature occurring in the heat affected zone (HAZ). Figure 4.1. shows the characteristic shape of the thermal cycle at different distance y perpendicular to joint line during G.M.A.W. (102).

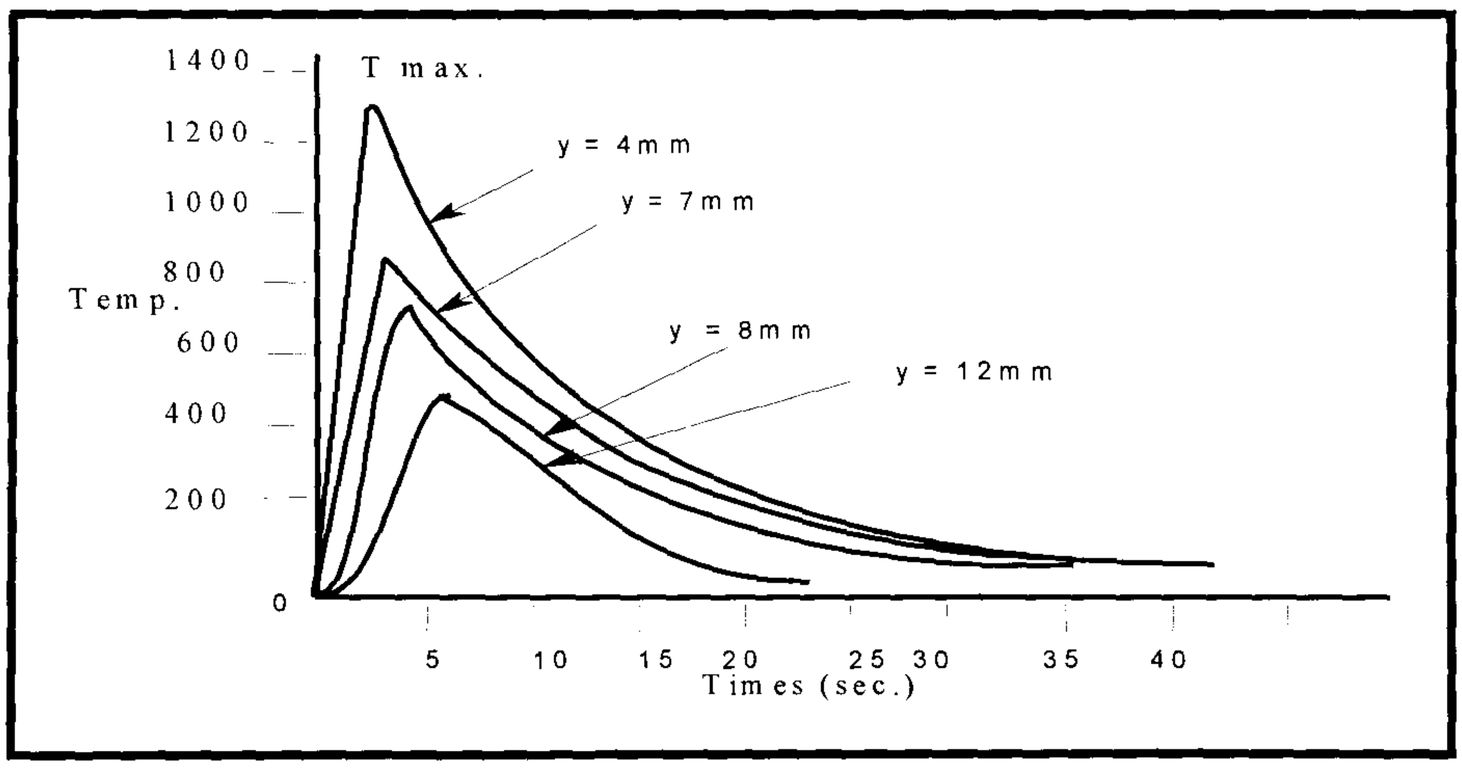

Figure 4.1. Thermal cycle in arc welding

In the first stage of the thermal cycle the maximum temperature at a point in the fusion zone may be taken as a measure of grain growth. Therefore the longer this

heating up time and the time at the maximum temperature, the coarser is the grain. The cooling stage is also important to the structural transformation, and in diffusion. The higher the rate of cooling in the zone above the transformation temperature, the higher the probability of obtaining a transient structure, such as martensite. On the other hand the lower the rate of cooling from temperature below 300°C, the more time there is for diffusion, particularly of dissolved hydrogen, and the greater the probability of hydrogen entrapment in grain boundaries and of hydrogen induced cracking in the joint.

To achieve complete fusion of the sidewalls of the joint, the maximum temperature in the thermal cycle at any point on the joint surface must exceed the melting temperature of the metal. Similarly, to achieve full penetration, the maximum temperature at points on the back surface of the joint close to the root face must exceed the melting temperature.

4.3 Theoretical modelling of heat distribution in arc welding

An understanding of the thermal cycle in welding, and ability to model the heat distribution occurring, has long been considered important to estimating material weldability and the quality of welds in welding processes. Therefore much research has been concerned with the theory of heat flow in arc welding. In 1941 Rosenthal (28) determined the temperature distribution and predicted the shape of the weld pool in two dimensions, figure 4.2.a, and three dimensions, figure 4.2 b, equation 1 and 2.

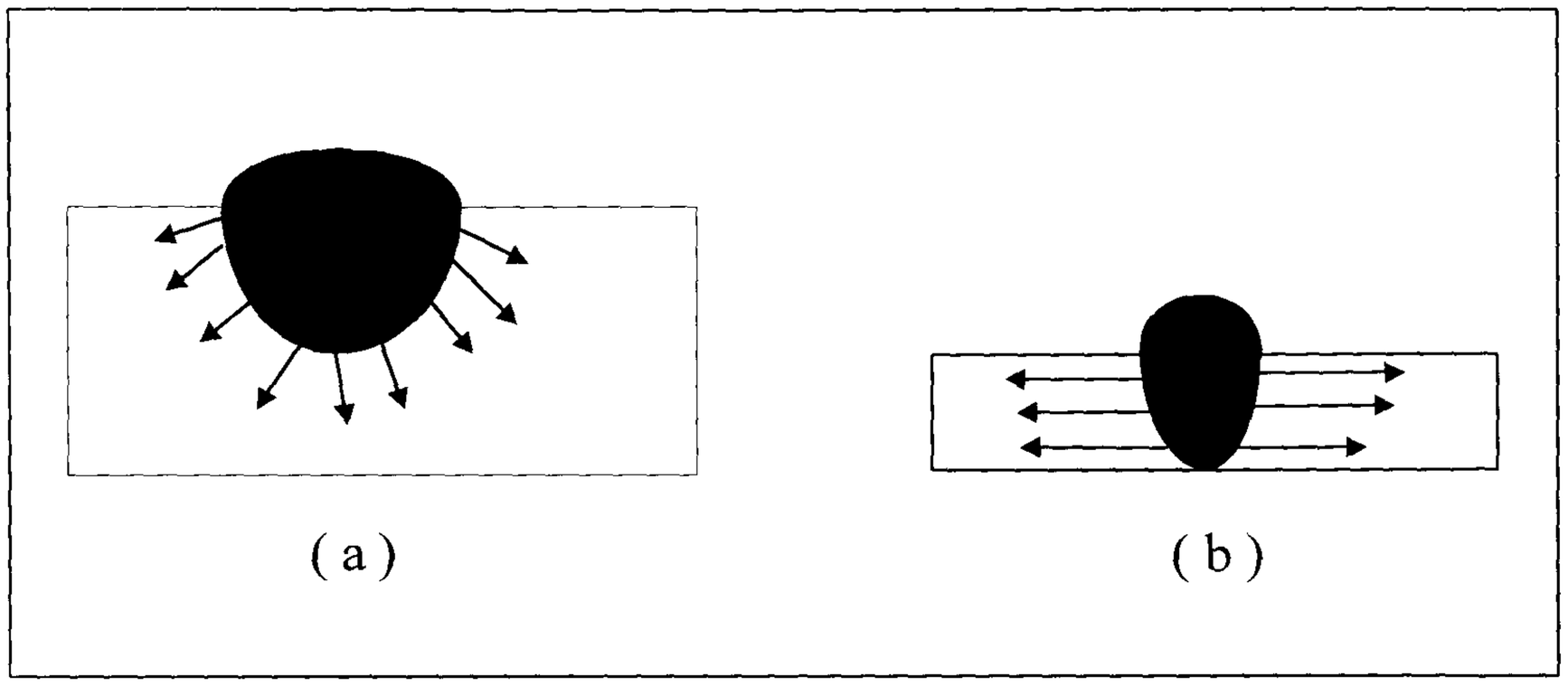

Figure 4.2- a) Three dimensional heat flow, b) two dimensional heat flow.

$$\text{For 2D, Line Source} \quad T - T_0 = \frac{Q}{2\pi\kappa} e^{-\alpha v \xi} \frac{k_0(\alpha v r)}{h} \qquad [1]$$

$$\text{For 3D, point Source} \quad T - T_0 = \frac{Q}{2\pi\kappa} e^{-\alpha v \xi} \frac{e^{-\alpha v R}}{R} \qquad [2]$$

Where:

- T is the temperature at a point on the (XYZ) co-ordinate system moving with the torch (K);
- T_0 is the initial temperature of the plate (K);
- Q is the heat input to the plate (J/S);
- k_0 is the Bessel function of second kind and zero order, the value of this function can be found for each value of $\alpha v r$ in reference(104);
- k is thermal conductivity of the base metal (W m^{-1} K^{-1});

- α is thermal diffusivity $(m^2 s^{-1}) = \frac{k}{\rho C_P}$;

- ρC_p is volume thermal capacity ($Jm^{-3} K^{-1}$);

- h is the plate thickness (m);

- v is the torch velocity ($m\ s^{-1}$);

- ξ is used when the x axis lies in the direction of welding (m) $= x - vt$

- x is the distance from the torch along the weld centreline (m)(positive backwards);

- t is the time (sec.);

- R is the radial distance from the torch centreline (m);

- y is the distance from the heat source perpendicular to centreline (m);

- r is the radius of a circle drawn around the heat source.

$$R^2 = x^2+y^2 \quad \text{and}$$

$$r = \sqrt{\xi^2 + y^2}$$

His assumptions were:

- A concentrated line (2D) or point (3D) heat source. The solution of quasi-stationary state of heat flow has yielded two equations characterising temperature gradients for a two-dimensional flow (thin plates) and a three-dimensional heat flow(thick plates).

- Heat flow is by conduction only. Heat created in electric welding by Joule effect can be overlooked in relation to the heat generated by the arc.

- Heat losses from the surface were neglected. As heating in large welded plate is considered, heat losses through the surface to surrounding atmosphere can be neglected, in relation to the heat flow in the plate itself.

- Infinite length and width of the workpiece. In the 3D heat distribution equation semi-infinite plate and a single bead deposited on the surface of a very large and thick plate was considered.

- Thermally homogeneous and isotropic material. The physical coefficients of the materials are assumed to be constant and temperature independent.

- Temperature-invariant material properties and neglecting the phase transformation (including fusion and solidification) led to steady-state temperature field expressions.

In the above equations, if the physical properties of the plate are assumed constant in the weld pool near the heat source, equation [2] would give $T = \infty$ for $R = 0$, which is not true. This indicates that equation [2] applies only to points outside the fused zone.

Christensen et.al.(105) converted Rosenthal's equation for a point heat source (3D) moving across the surface of semi-infinite body to the dimensionless form

$$\theta = n\frac{e^{-(P+\psi)}}{P} \qquad [3]$$

where the operating parameter n includes the torch speed, the thermal diffusivity and the heat input to the workpiece, and

$$P = \frac{vR}{2\alpha}, \text{ and } \psi = \frac{vx}{2\alpha} \qquad [4]$$

All heat transfer theories result from the basic equation for the conduction of heat in a homogenous isotropic solid which is:

$$k\nabla^2 T - \rho c_p(\vec{V}.\vec{\nabla})T = \frac{\delta T}{\delta t} \qquad [5]$$

In steady state T is constant, therefore $\frac{\delta T}{\delta t} = 0$

velocity $\vec{V}$ in Cartesian coordinate is:

$$\vec{V} = v_1\,\vec{i} + v_2\,\vec{j} + v_3\,\vec{k}$$

where $i, j,$ and k are unit vector in the x, y, and z direction. Thus:

$$(\vec{V}.\vec{\nabla}) = (v_1\,\vec{i} + v_2\,\vec{j} + v_3\,\vec{k}).(\frac{\delta T}{\delta x}\vec{i} + \frac{\delta T}{\delta y}\vec{j} + \frac{\delta T}{\delta z}\vec{k}) \quad \text{and}$$

$$(\vec{V}.\vec{\nabla}) = v_1\frac{\delta T}{\delta x} + v_2\frac{\delta T}{\delta y} + v_3\frac{\delta T}{\delta z}$$

Now, if the direction of $\vec{V}$ is on the x-axis, then :

$$\vec{V} = v_1\,\vec{i} + 0\,\vec{j} + 0\,\vec{k} = v\,\vec{i} \quad \text{or}$$

$$(\vec{V}.\vec{\nabla})\,\mathrm{T} = v\frac{\delta T}{\delta x}$$

Thus equation [5] can be rewritten as:

$$k\nabla^2 T - \rho c_p \quad v\frac{\delta T}{\delta x} = 0$$

or

$$\frac{k}{\rho c_p}\nabla^2 T - v\frac{\delta T}{\delta x} = 0$$

$$\alpha \nabla^2 T - v\frac{\delta T}{\delta \chi} = 0 \qquad [6]$$

when there is no relative movement between the workpiece and the heat source the equation [6] reduces to:

$$\alpha \nabla^2 T = 0$$

which is the Laplace Equation .

The heat may be liberated instantaneously from an instantaneous source, or at a steady rate from a continuous source. The fundamental solution for the temperature distribution in a body of infinite extent after a quantity of heat Q has been liberated instantaneously at a point, assumed to be the origin is given by Lancaster (104) as

$$T = \frac{Q}{8\rho c(\pi\alpha t)^{3/2}} e^{(-\frac{r^2}{4\alpha t})} \qquad [7]$$

where $r^2 = x^2 + y^2 + z^2$

If the heat source is moving with velocity v in direction x and emits heat at a rate q then the integration of equation [7] for a semi-infinite workpiece (2D i.e. one which is bounded by the plane z = 0) is given in [8].

$$T = \frac{q}{4\pi\kappa r} e^{[-\frac{v(r-x)}{2\alpha}]} \qquad [8]$$

If the workpiece is assumed to be infinite (3D thick plate) the integration of [7] is given in [9].

$$T = \frac{q}{2\pi\kappa r} e^{-\frac{v(r-x)}{2\alpha}} \qquad [9]$$

Where xyz are the co-ordinates of the measured spot, T is the temperature (K°), α is the thermal diffusivity ($m^3\ s^{-1}$), x is a distance from the heat source in x direction, v is the torch speed (cm s^{-1}), k is the thermal conductivity, and r is the radius of circle around the heat source.

In the solution of equations [8] and [9] certain conditions are applied.

- Heat source is considered as a point or line for 3D and 2D case respectively;
- Latent heat of the solidifying weld metal, and of the structural transformation are neglected;
- The heat radiation from surface is neglected;
- Material constants are assumed temperature independent;
- Moving of the heat source (torch) is assumed to be constant speed;

These conditions are not strictly realistic and consequently the theoretical outcome does not fully correlate with experimental results. However equations [8] and [9] have been tested with some of the experimental data from this research. The results show that these formula give reasonable approximations for heat distribution during arc welding. Therefore they will be used in this research to analyse and compare the temperature measured with the infrared pyrometer and the calculated temperature. This will be illustrated and discussed in chapter 7 .

For carbon steel the following values of constants are used in calculation (106).

Thermal conductivity (k) 41 W m^{-1} K^{-1}

Thermal diffusivity (α) 9.1×10^{-6} m^2 s^{-1}

Volume thermal capacity (ρc_p) 4.5 x 10^6 J m^{-3} K^{-1}

Melting point (MT) 1800 K

4.4 Prediction and control of weld bead geometry

Weld quality features such as metallurgy and joint strength are not measurable directly on-line. Therefore, for control, some indirect method of assessing weld quality is essential. Approaches to in-process control of welding include monitoring geometric features of the bead, thermal characteristics such as temperature in the heat affected zone and cooling rate. The geometry of a weld bead can be represented by bead width, bead height, and depth of penetration. However although much research has been conducted into measuring the weld pool using computer vision techniques(107,108), monitoring these geometrical parameters in real time during welding is difficult. Many attempts have been made to predict and understand the effect of arc welding variables on the resultant weld bead geometry and include theoretical studies based on heat flow theory, as well as empirical methods.

By applying Rosenthal's heat distribution theory, Roberts and Wells (109) have developed equation [10] to estimated the weld width in the case of thin plates.

$$W = \frac{1}{2}\frac{Q}{Sa}\frac{1}{\rho c_p}\frac{1}{T} - \frac{4}{5}\frac{\lambda}{S} \qquad [10]$$

In the case of thick plate they assume that the plate is infinitely thick, so that heat flow is three dimensional and the weld width is given by equation [11].

$$W^2 + \frac{8\lambda W}{5S} - \frac{16Q}{5\pi\rho c_p ST} = 0 \qquad [11]$$

Where:

W = estimated weld width ;

Q = rate of heat input to the plate (J/sec);

a = plate thickness;

S = welding speed;

T = (melting temperature - ambient temperature);

λ = thermal diffusivity;

ρc_p =volume thermal capacity.

The depth of penetration is predicted to be half the weld width, i.e. a semicircular weld cross section. Apps and Milner (110) compared experimental results with Roberts and Wells theory. They concluded that, the actual width was larger than the predicted width, whereas actual penetration was generally less than predicted.

In an attempt to produce more realistic weld pool profiles, Eagar and Tsai (111) modelled the arc as a Gaussian distributed heat source. The temperature at a point (x, y) at the time t was derived as equation [12]

$$q(x,y) = \frac{\eta Q}{2\pi\sigma^2}\exp\left(-\frac{x^2+y^2}{2\sigma^2}\right) \qquad [12]$$

where q is temperature at a point, Q is heat input, η is thermal efficiency, and σ is the distribution parameter that has dimensions of length and can be considered as half the width of the arc. As is shown in Figure 4.3, with the combination of two adjustable parameters, efficiency η and distribution σ, this model could predict more realistic weld pool shape and size.

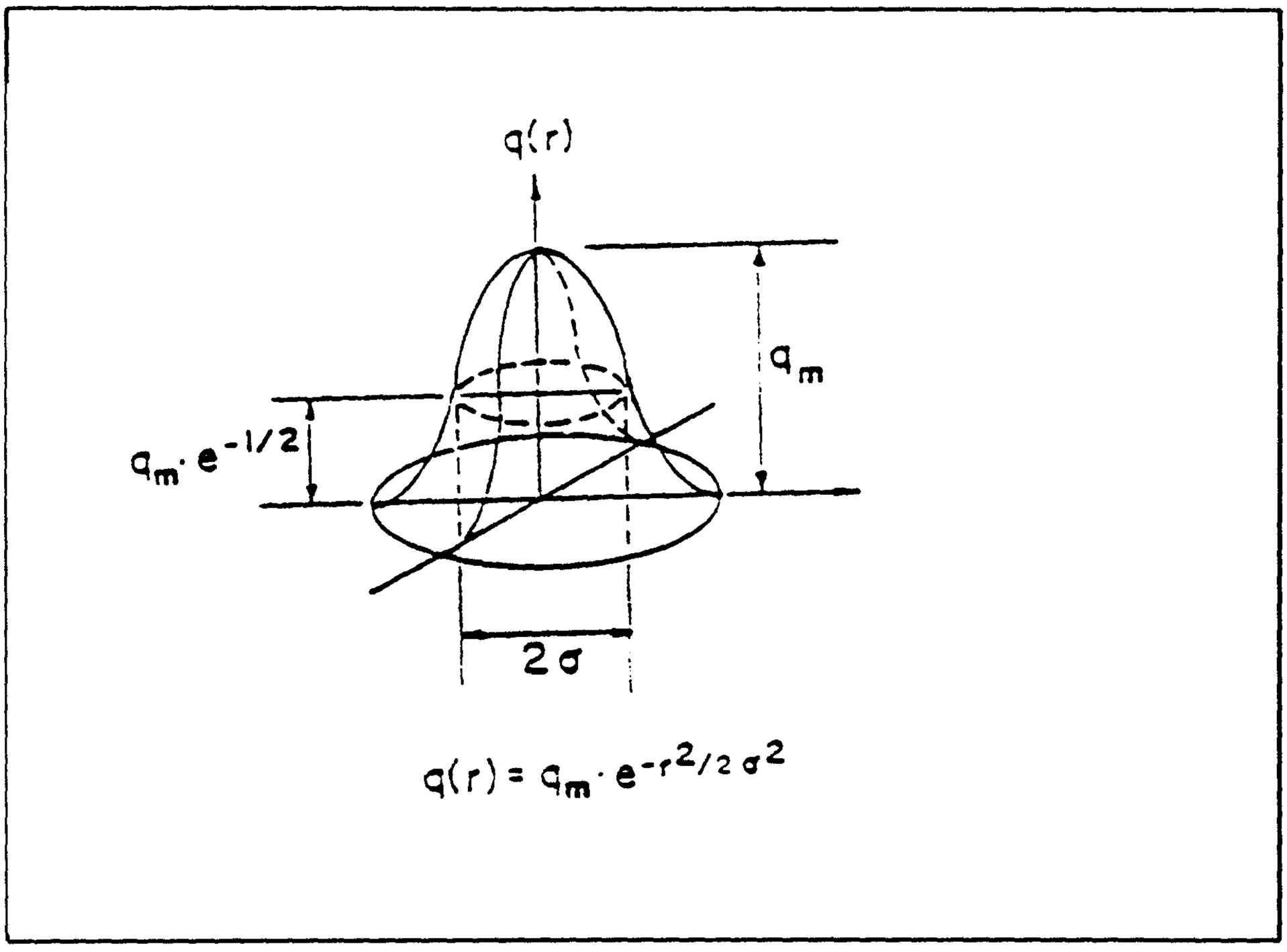

Figure 4..3 A Gaussian distributed heat source moving on the surface of a semi-infinite plate

They tested the accuracy of their model and concluded that the predicted and actual widths were in good agreement, but the depth prediction had considerable error. The error in depth of penetration was considered due to the assumption of a semi-infinitely thick plate, whereas the true plate thickness was 12.7mm. Song and Hardt (5) continued the Eagar and Tsai work and developed a new model where a dual gaussian heat source, top and lateral, was considered instead of single gaussian heat source. As is shown in Figure 4.4 the weld pool shape can be considered in two parts :a horizontal portion caused primarily by the top Gaussian heat source, and a vertical portion caused by the lateral gaussian heat source [13].

$$T(x,y,z,t)-T_0=\int_0^1 \frac{\eta Q}{\pi\rho C_P}\frac{(16\pi\alpha t)^{-1/2}}{2\alpha t+\sigma^2}\exp\left(-\frac{(x+vt)^2+z^2}{4\alpha t+2\sigma^2}-\frac{y^2}{4\alpha t}\right)dt \quad [13]$$

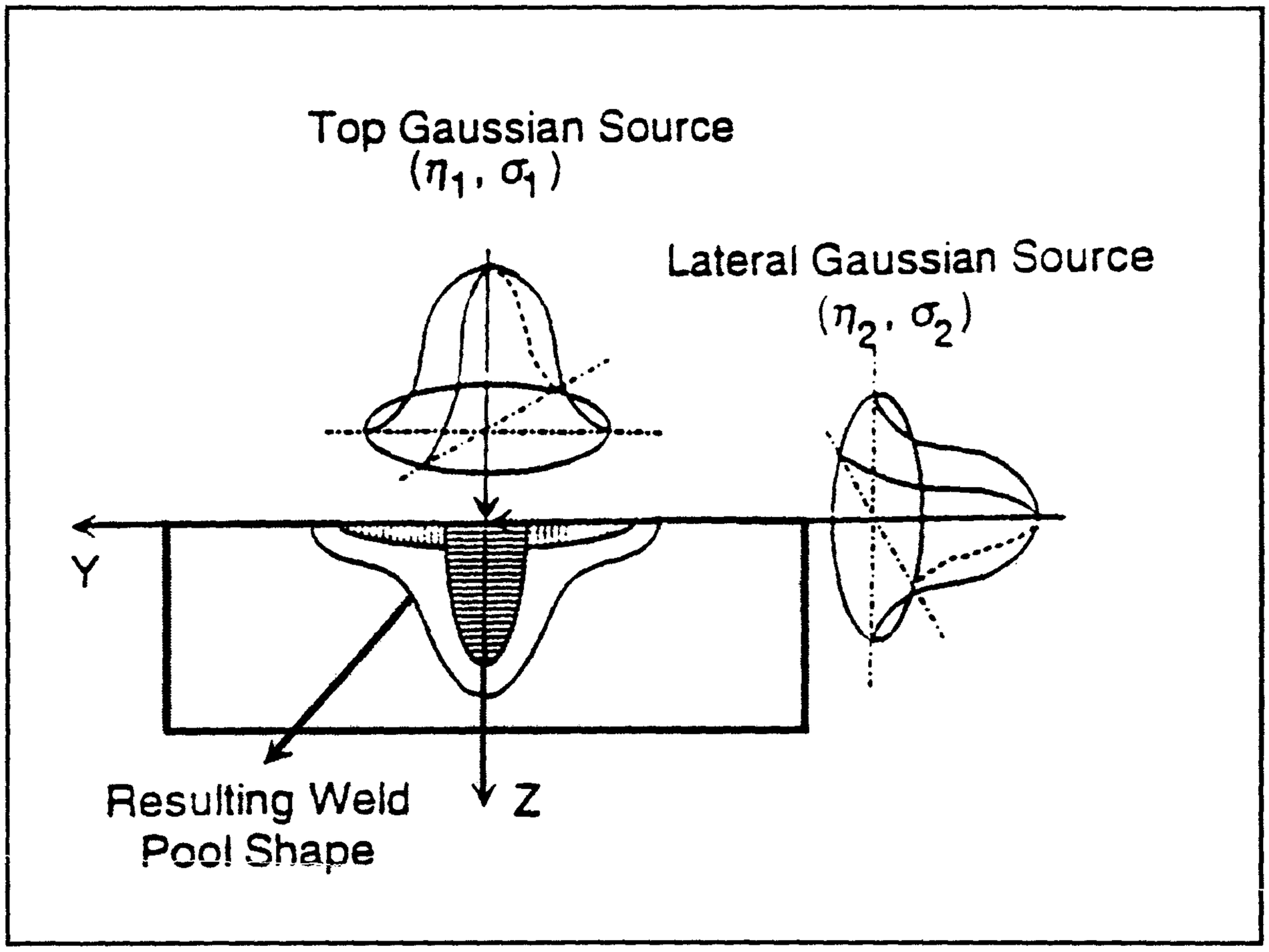

Figure 4.4 Weld pool shape and isotherms in a dual Gaussian heat source model.

Model predictions were compared with experimental results for GMAW. In these experiments they used an infrared sensor to measure the temperature of the back side of the plate. They concluded that the depth can be estimated due to varying welding parameters. The experimental results showed that the wire feed rate and torch travel speed have a significant effect on the depth of penetration when used as a process input.

Thorn, et.al.(39) developed an empirical model of the influence of various parameters on the pool shape in GMA welds, and compared the result with

theoretical models. They also developed a multiple regression model to predict the relationship of welding variables and weld pool shape as follows:

Penetration (mm) = 0.075 + 0.089 WFR + 0.0130E

Width (mm) = 1.89 + 0.750 E

Height (mm) = 2.12 + 5.37 VFA

Where WFR is electrode wire feed rate measured in m/min, E is the heat input [E = η (V x I)] measured in kJ/cm, η is thermal efficiency, VFA(Volume of Filler Added) is measured in cm^3/cm.

Kim and Basu (114) also developed a mathematical model for relationship of weld pool geometry and welding variables as follow:

$$W = (D^{0.4294} I^{0.3518} V^{0.7083} S^{-0.4590}) 10^{0.0905}$$

$$H = (D^{-0.1255} I^{0.6387} V^{-0.7183} S^{-0.2395}) 10^{0.3339}$$

$$P = (D^{-0.5668} I^{1.4005} V^{0.0130} S^{-0.3641}) 10^{-2.3098}$$

where D is plate thickness (mm), S is welding speed cm/min, I is welding current, and V is welding voltage. To assess the accuracy of the model, they conducted a number of experiments and calculated the percentage error. They concluded that as shown in fig 4.5 , 79 % of results of weld bead dimensions were accurate within 0-5% error. The remaining results were lay predominantly in the 5-10 % and 10-20 % error ranges. Therefore the model could be used to control the process input parameters in order to achieve desired weld bead geometry outcomes and weld quality.

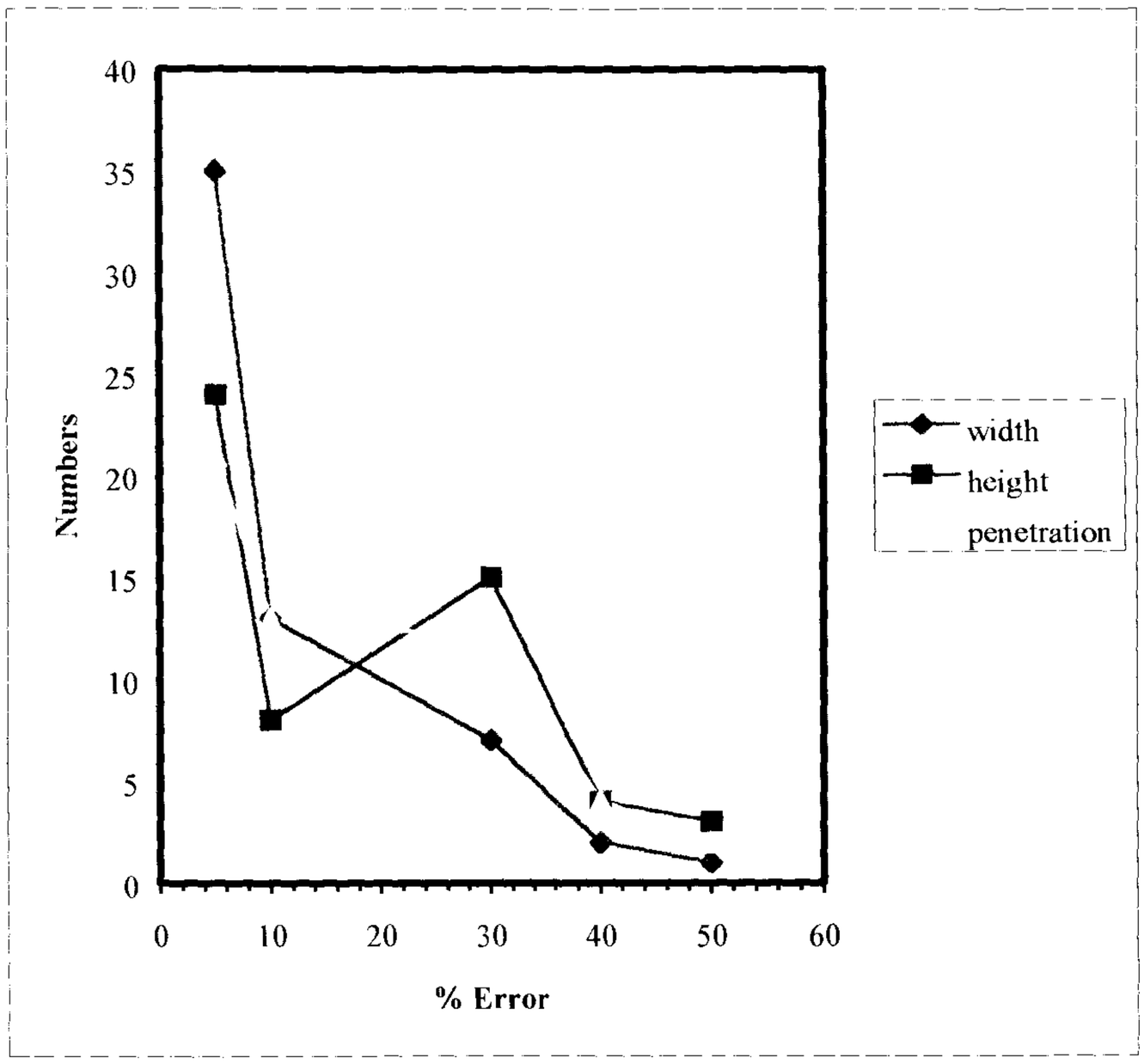

Figure 4.5 Accuracy analysis of mathematical model (114).

Song and Hardt (113) developed a mathematical model to predict the weld geometry. They selected wire feed rate and welding speed as inputs, and bead width and depth of penetration as a outputs for a control model. A CCD camera was used to measure the bead width and an infrared sensor to measure the back side temperature and estimate the depth of penetration. This work has limited application due to reliance on back side temperature measurement during welding, which is often impractical.

Banerjee, et.al (103) developed a gradient technique to monitor weld geometry in cases involving variation in plate thickness, minor element content and shielding gas composition in GTAW and GMAW. The technique was based on the temperature gradient at the solid-liquid metal interface. The cause of the sharp change in temperature at the interface is the difference in emissivity of the solid and liquid metals. Figure 4.6 shows the isothermal map of the temperature distribution in a weld.

which consist of several bands with the temperature increasing from the outer edges to the centre of the weld pool (98).

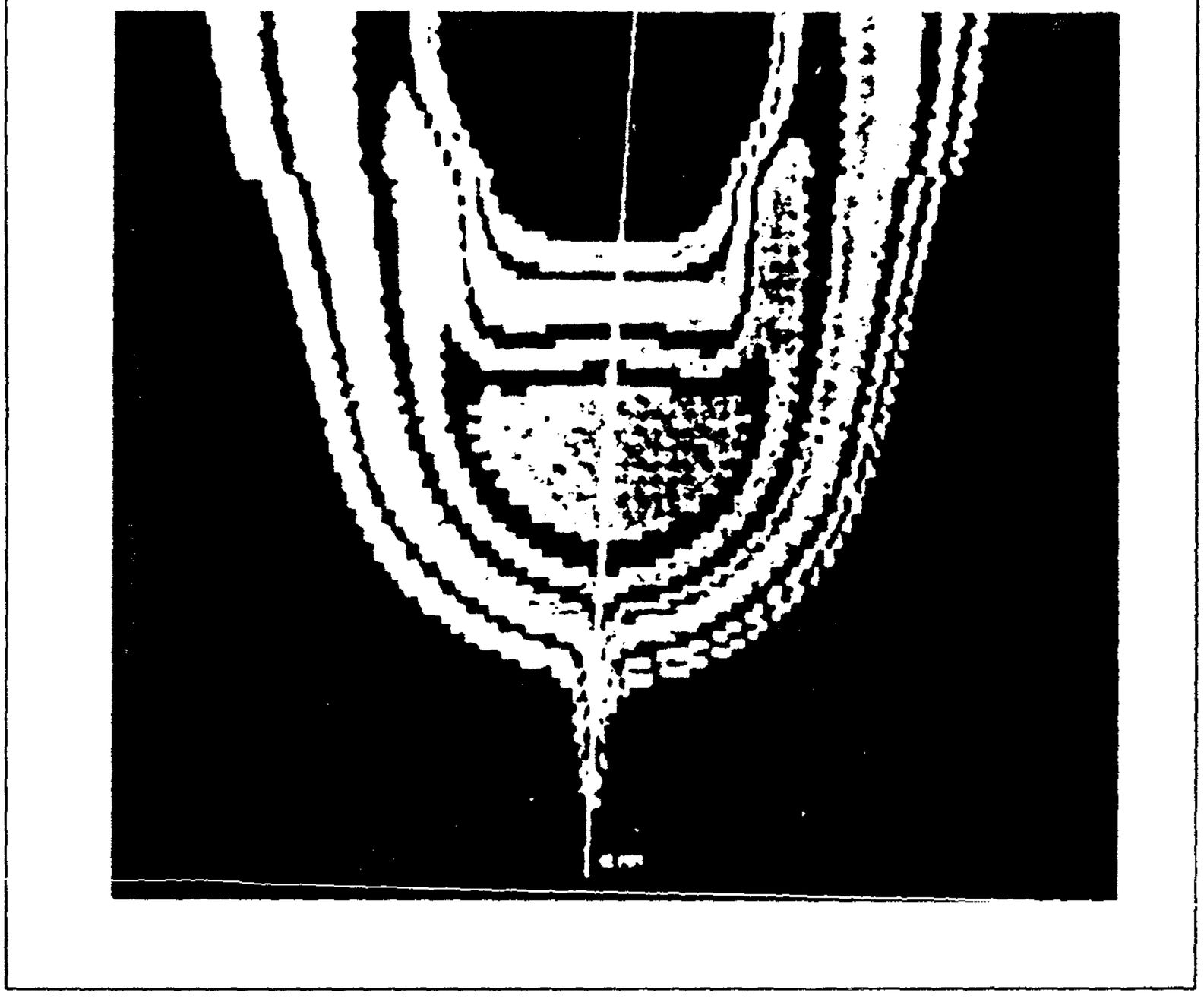

Figure 4.6 Isothermal map of heat distribution in weld.

They concluded that the bead width and the temperature gradient computed along a line transverse to the direction of torch motion showed promise for on-line control of bead width and depth of penetration respectively.

In chapter 7 the effect of temperature distribution on bead geometry is illustrated and further discussed. Also experimental results from this research will be compared with some of the theoretical and empirical models discussed here.

4.5 Discussion

Arc welding involves melting and resolidification of the workpiece to form the joint. The geometry of the weld bead which is represented by the bead width, bead height, and depth of penetration is a good indicator of weld quality. There are restrictions on the direct monitoring of these weld features. An alternative method is to measure the heat flow pattern in the workpiece and derive a mathematical relationship between the measured temperature and the weld bead geometry. Since the welding process causes very complex physical and metallurgical changes in the workpiece, it is practically impossible to establish an exact mathematical model. In particular, the temperature-dependent characteristics of the physical parameters of the metal make the problem very intractable. Various other physical phenomena in the welding process, such as phase change and heat convection due to forced flow of the molten pool, further increase the difficulty of the mathematical analysis. Researchers have coped with these difficulties by simplifying assumptions and the resulting models are not sufficiently precise to be suitable for real-time control of welding (112, 113). Consequently many researchers have proposed welding control based on empirical models. This approach, however, also has a limitation for generality of application because of the extreme non-linearity of the process.

This research examines the use of Neural Network and Fuzzy Logic models to overcome the limitation of previous control methodologies, and is discussed in chapters six and seven.

Chapter five Experimental design

5.1 Introduction

The objective of the experiments was to obtain training and validation data for artificial neural network modelling of the GMA welding process. The data was used in a neural network simulation software (115) to establish models of the relationship between the input welding variables to the welding process and the temperature distribution in the weldment during welding. To achieve the above objective two sets of experiments were conducted, one with zero root gap to model the temperature distribution in the workpiece assuming the work is accurately fitted up and there is no distortion during welding. The second set of experiments, with root gap varying between zero and 1.5 mm, was used to model the temperature distribution in cases where error in assembly, poor fixturing, tacking up or distortion could cause deviation from nominal root gap.

In this chapter the inputs and outputs of the welding process which have been selected for this work are defined. In section 6 the full factorial experimental design is given and discussed. This is followed by description of the experimental apparatus which is also illustrated in section 7.

5.2 Selection of welding outputs

The welding outputs to be derived from the temperature distribution must be chosen so that they adequately characterise the quality of the welded joint. Moreover, since the motivation for this research is real time process control, the measured control output from the thermal sensor must be capable of being processed in a short time. Control of welding typically requires a response time of less than 500 ms.

In the following section the welding outputs which were selected for this research are discussed.

5.2.1 Surface temperature

The neural network models are based on the assumption that an accurate temperature measurement at a specific point on the weldment surface is available in approximately real time. In order to meet this requirement, temperature measurement is obtained by a total radiation pyrometry technique, in which surface temperature is measured by collecting the emitted thermal radiation from the workpiece at all wavelengths in the infrared (IR) spectrum. Figure 5.1 illustrates the workpiece and the temperature measurement point.

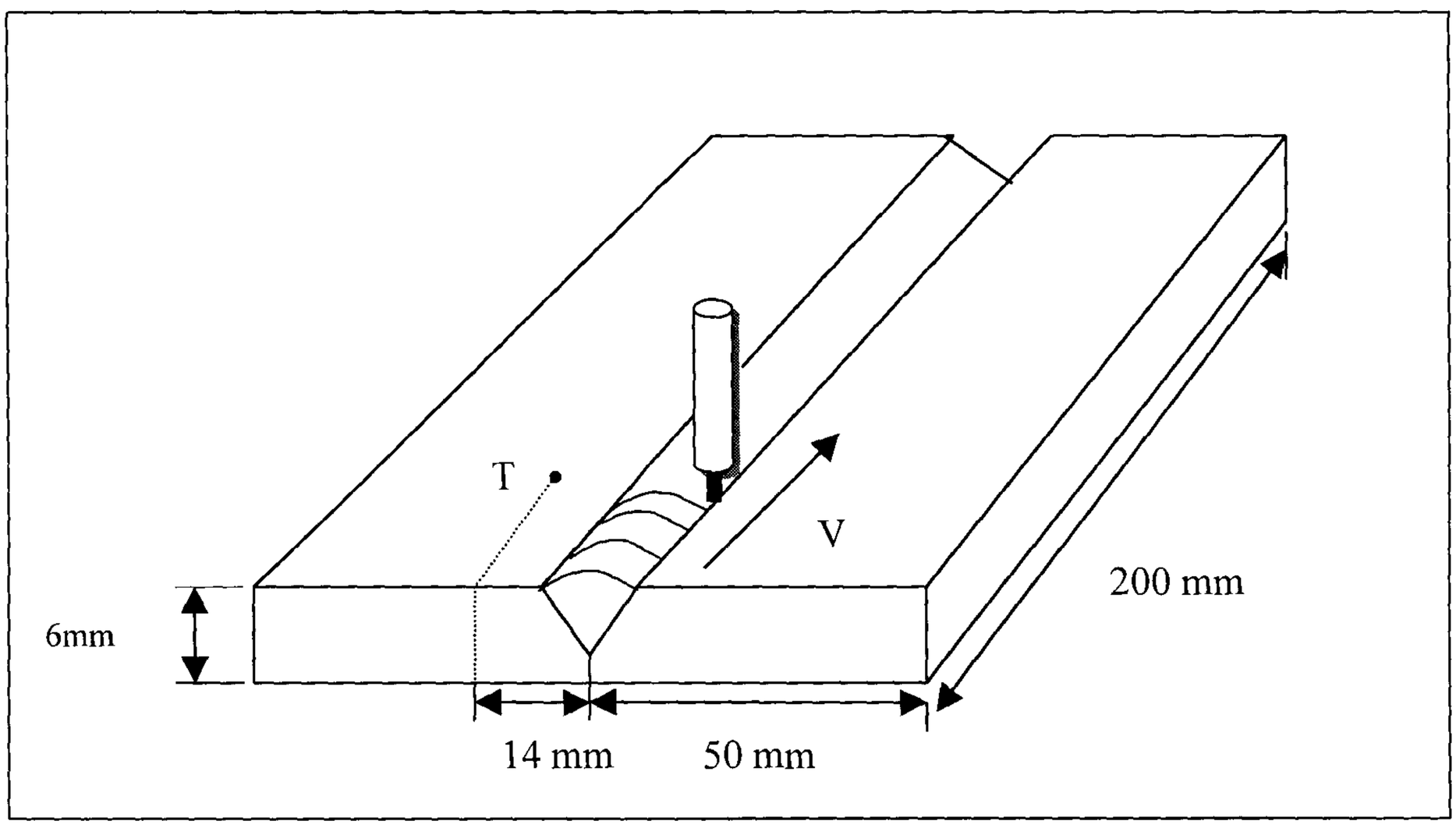

Fig.5.1- Workpiece and temperature measuring spot

The infrared sensor was attached to the welding torch 60 mm above the workpiece.

At this distance the diameter of the measured area was minimum (2.3 mm (94)). A number of experiments were conducted in order to establish the best distance of the measured spot from the centre line of the joint. The temperature was measured for maximum and minimum level of welding variables at different distances across the seam. The results of these experiments are plotted in fig.2. A distance 14 mm perpendicular to the welding line was selected, being the position

at which the change in temperature with change in welding variables was greatest. In subsequent experiments to obtain model training and validation data, and in order to have time to process data in the models, and to feed back control data to the welding system when operating as a process controller the temperature was to be recorded at 10mm increments as welding proceeded.

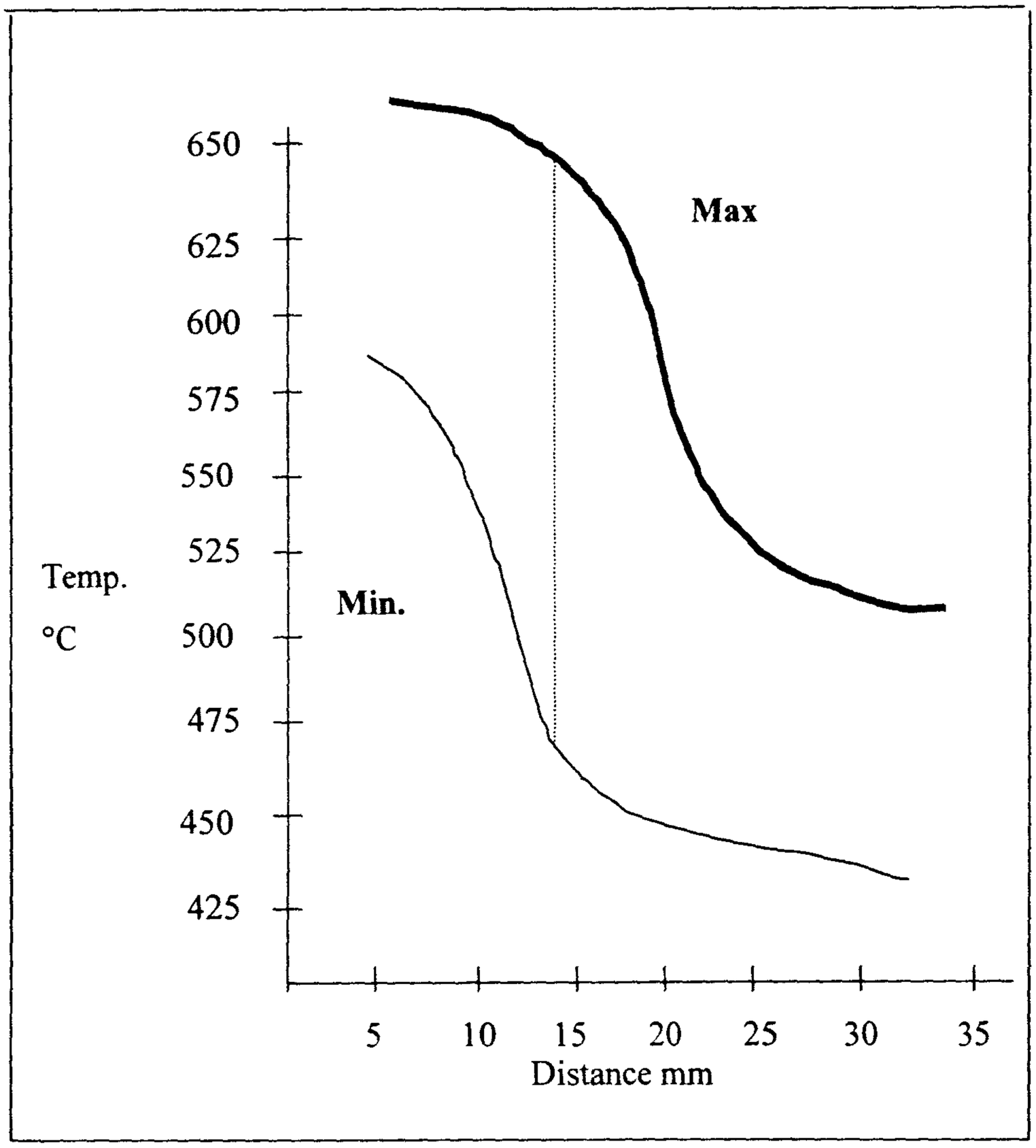

Fig. 2 . Optimum distance for temperature measurement

5.2.2 Weld bead geometry

Gas Metal Arc Welding, involves melting and re-solidification of the joint metal and the filler material from consumable electrode which is deposited into the joint.

The resulting geometry of the weld bead is a good indicator of weld quality. Although it is not the aim of this work to build a weld bead geometry model, on the other hand the data for neural network modelling and for fuzzy logic control should correspond to welds of acceptable quality. In the first set of experiments to obtain training data, with no root gap in the joint, welded test pieces were sectioned at 10 places along their length, the location corresponding to the point at which temperature was recorded. This was to allow modelling to take account of the variability in weld bead geometry and penetration, which occurs due to heat build up in the plate as welding proceeds. The sectioned faces were ground and polished then etched with a 5% solution of nitric acid in alcohol to reveal weld penetration. The bead width, height, and the depth of penetration were measured from the image obtained using a CCD camera with X20 lens and monitor. The bead geometry as shown in figure 5.3 and 5.4 was measured from the screen to an accuracy of 0.5 mm, representing a maximum error of 0.025 mm in the dimension recorded.

In the second experiment, in which root gap was varied between 0-1.5mm the resulting weld was inspected visually. Those points along the weld line with penetration between 100% -110% of the material thickness, being the criterion for acceptable weld quality, were selected, with the corresponding point surface temperature, for NN modelling. The results of experiments are included in appendix A1.

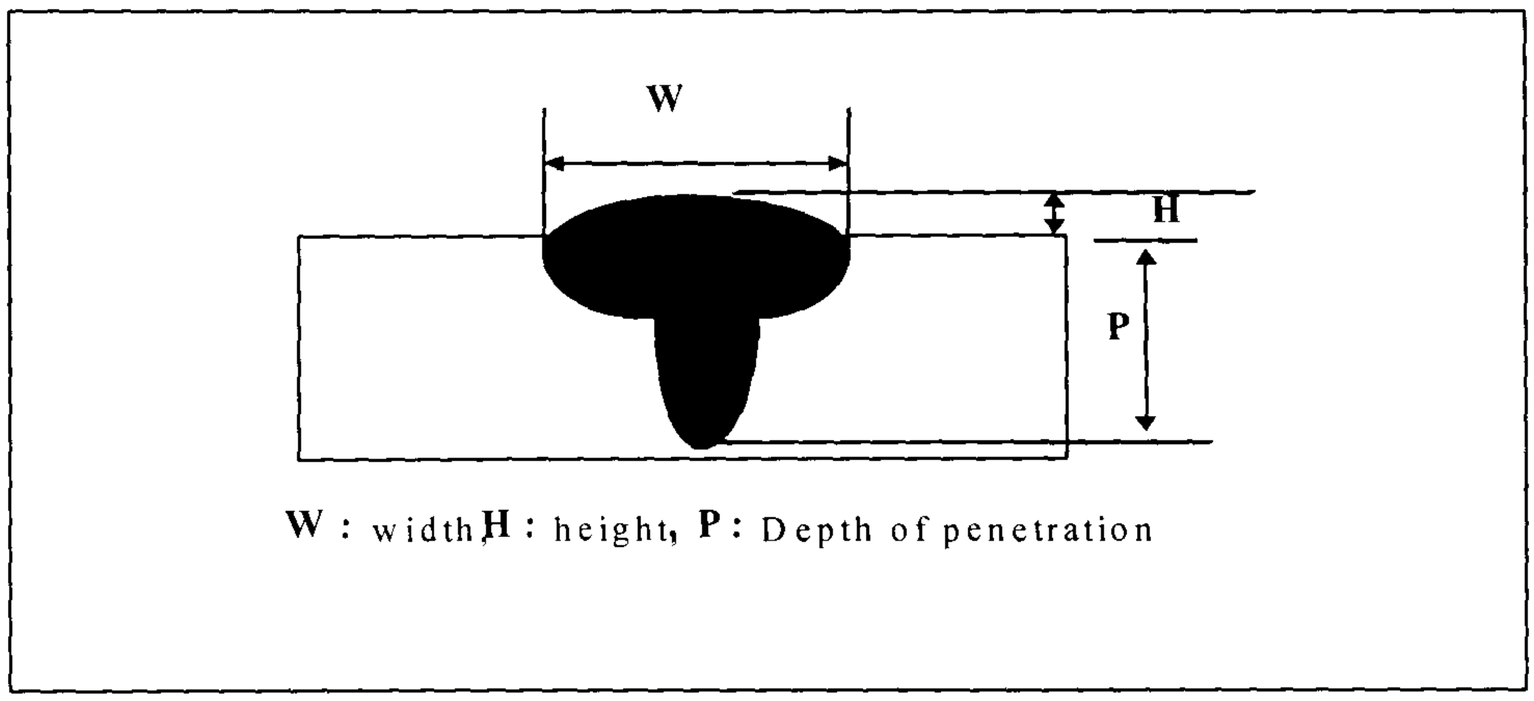

Fig 5.3 Weld bead geometry

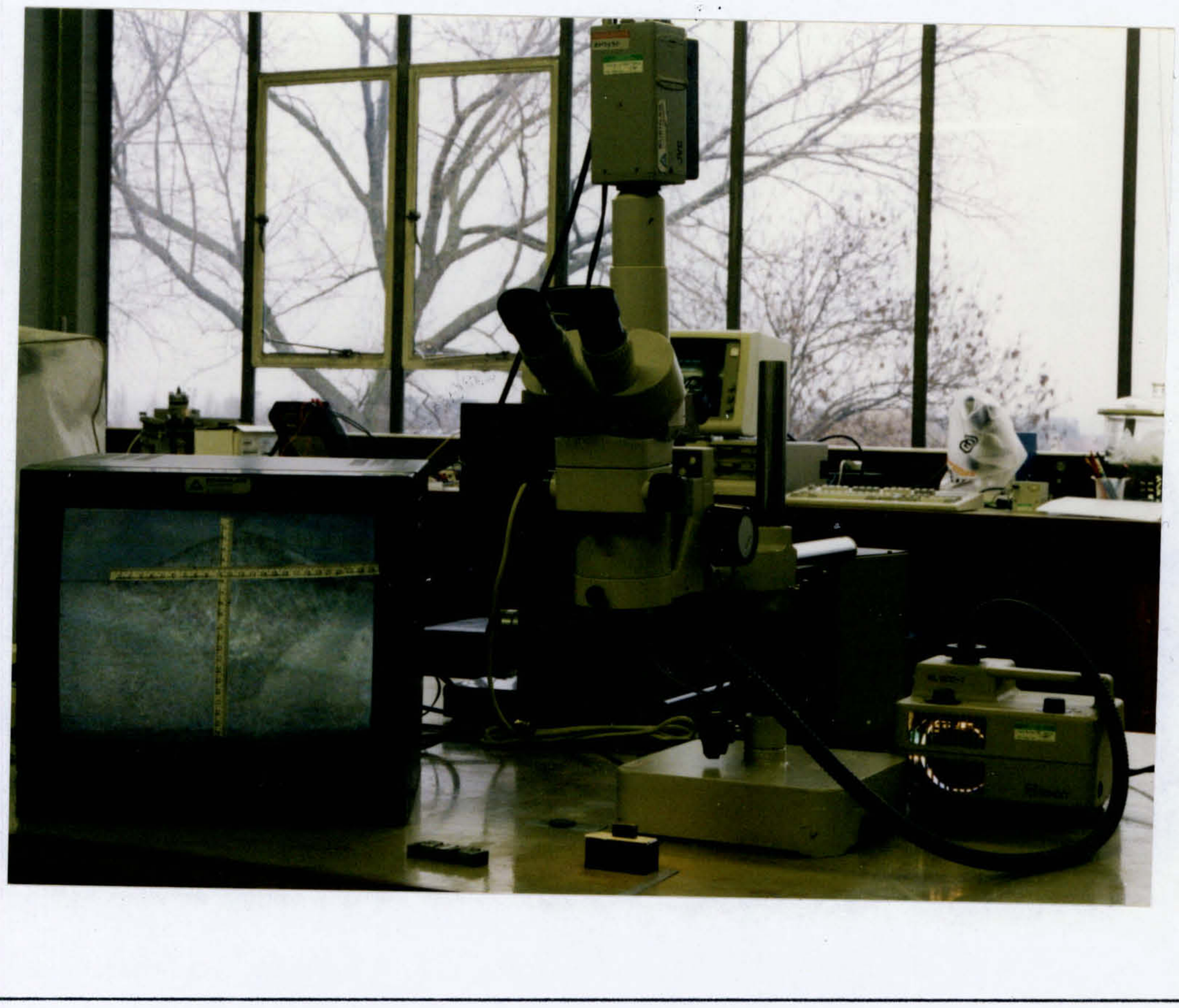

Fig.5.4 Apparatus for measuring the weld geometry

5.3 Selection of welding inputs

Gas Metal Arc Welding variables can be categorised in two distinct groups. First those which can be modified during adaptive welding, the important ones being welding voltage, welding current, travel speed, torch angles, weave pattern, shielding gas flow rate, and electrode extension. The second group of variables can be monitored but cannot be modified during welding. These include joint geometry, plate thickness, wire diameter, shielding gas, etc. Although the joint geometry is normally considered as a fixed variable, in the second set of experiment, reported here the root gap was varied between 0-1.5 mm. This was to

allow modelling of the situation when the root gap might vary during welding due to poor assembly, fixturing or distortion.

Four controllable welding variables, which significantly affect the heat distribution in the workpiece surface, and the weld penetration, were selected for experiments in this research. These variables are discussed in the following sections.

5.3.1 Welding voltage

Arc voltage is the sum of the voltage drops at cathode and anode surfaces, which are approximately constant, and the voltage drop across the column of the arc. Therefore distance between the tip of the electrode and the weld pool surface, the arc length, and the ionisation potential of the arc plasma determines the welding arc voltage. The arc voltage required for an application is dependent on the electrode size, type of shielding gas, welding position, joint type and workpiece thickness. In order to evaluate the accuracy of the infrared sensor via a mathematical model the actual welding voltage was required. The voltage across the arc was measured during welding using a Voltmeter placed between contact tip (cathode) and workpiece(anode). These measurements were used for analytical calculations where the absolute values of voltage were needed. A regression equation was developed in order to determine the relationship between voltage set for the power supply and actual arc voltage as follows.

$$V_1 = 15.3 \div 0.367\ V_2$$

Where V_1 is the actual value and V_2 is the set value.

For all welding experiments the minimum voltage level was chosen such as to prevent electrode stubbing and arc discontinuity during welding. The maximum level was chosen such as to achieve high penetration and prevent non-sustained and intermittent arcing. The value chosen, with corresponding current, produced a

weld with acceptable penetration and avoiding a high amount of spatter and fume during welding. Levels chosen are shown in table 5.1.

5.3.2 Welding current

The actual welding current during welding was measured through a low resistance shunt (0.0001Ω) placed in series with the welding power supply cable. Measuring the voltage drop across the shunt and applying Ohm's law gives the current flowing through the shunt. A number of experiments were conducted to establish the correlation factor between the actual arc current and the current set at the welding controller. The results are shown in appendix A2. The regression equation is

$$C_1 = 7 + 0.85\ C_2$$

Where C_1 is the actual value and C_2 is the set value.

For all welding experiments three levels of current have been used as shown in table 5.1. The minimum level was set to prevent an unstable welding process, low penetration, due to inadequate heat input or an unsuitable mode of metal transfer. The maximum value was set in order to prevent excess penetration or burn-through, excessive spatter and instability. The third level was chosen as the midpoint of maximum and minimum values.

5.3.3 Travel speed

As the travel speed is increased, the heat transferred to the joint per unit metal volume is reduced. This reduces the melting of the parent metal and, hence, the depth of penetration. Sidewall and inter-run fusion will also be affected. In all experiments three levels of travel speed were chosen as shown in table 5.1. The minimum level was chosen such as to prevent an uncontrollable large weld pool, and excessive penetration or burn through. The maximum level was chosen in order to prevent low penetration, small bead width and undercutting along the edge of the weld bead due to insufficient filler metal deposition, to fill the groove

melted by the arc. The midpoint of maximum and minimum values was used as the third level.

In order that temperature measurements were taken at the same positions along the joint for all welded samples, regardless of travel speed, the interval of sensor sampling was correspondingly changed.

5.3.4 Torch angle (in direction of travel)

Changing the torch angle in the direction of travel has an affect on heat distribution and depth of penetration. When the torch angle is changed from 90° to a push angle (forehand welding), the depth of penetration is decreased and the weld bead becomes wider and flatter. When the torch angle changed from 90° to a drag angle (backhand welding), the depth of penetration will increase (117).

In all experiments three levels of torch angle have been selected as shown in table 5.1 and figure 5.5 The mean level was chosen as 90°. The minimum level was set as forehand technique with an angle of 70°. The maximum torch angle was set as a backhand welding technique with an angle of 110° from horizontal. This angle produces a high level of penetration and lower spatter. At these angles the sensor was still capable of accurately measuring average target temperature.

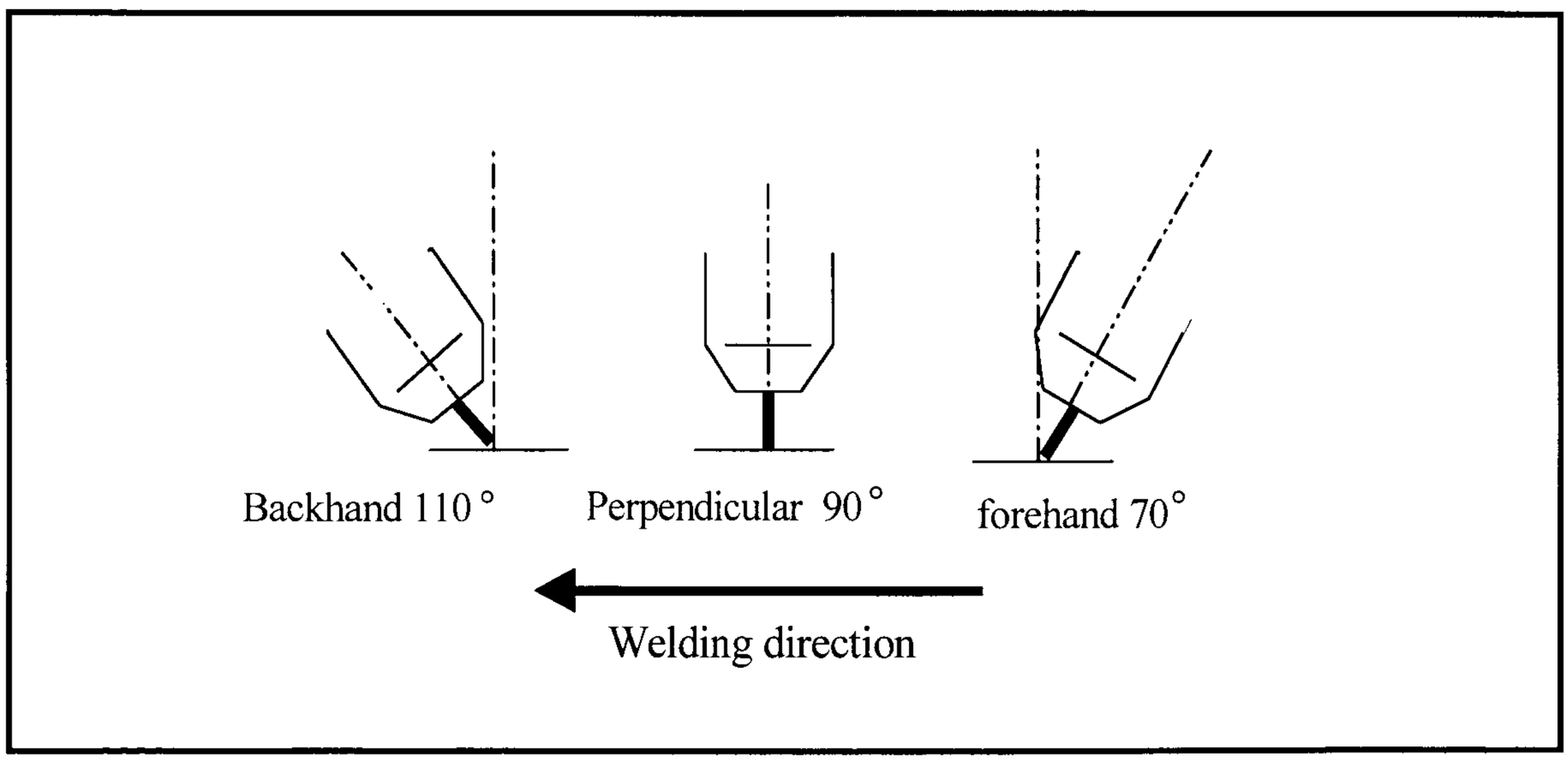

Fig.5.5 Selection of The Torch angle

5.3.5 Joint Root Gap

Two sets of experiment were conducted one with a zero root gap and 60° "Vee" prepared joint, and the other with root gap varying between 0.0 and 1.5 mm in both cases root face thickness was 2.0 mm. This was to enable modelling of circumstances in which root gap may vary due to distortion, poor assembly or fixturing. The values of root gap at positions along the joint where temperature was measured are shown in table 5.1.

Variables	**Set levels of variables**			**Actual level of variables**		
	low	**mean**	**High**	**low**	**mean**	**high**
Current (Amps)	300	320	340	275.6	287.8	300
Voltage (Volts)	37	42	47	27.5	30.2	33
Travel speed (mm/min)	800	850	900	800	850	900
Torch angle (degree)	70	90	110	70	90	110
Root gap (mm)	0.39,0.45,0.56,0.64,0.75,0.86,0.97,1.08,1.12,1.24					

Table 5.1 Selected welding variables.

5.4 The Fixed variables

The variables that were fixed in the welding experiments are listed below. They can be categorised into those which can not readily be changed in process, those which the initial tests have shown to have little influence on weld penetration, and those which could reasonably be fixed for the application scope of this research.

- Electrode type: Bostrand LW1 (BOC Murex)
- Electrode diameter: 1.2 mm
- Plate type: Carbon Steel, 0.15 % C (EN 1A)
- Plate thickness: 6mm
- Shielding gas type: ArgoShield 5 (93% Ar +5% CO_2 + 2% O_2)
- Shielding gas flow rate: 18 litres / min
- Electrode stickout: 16mm
- Welding position: Flat. Welding position has a profound influence on the other welding inputs and the weld penetration achieved. However experimentation and resultant modelling were constrained to the flat position, as is particularly appropriate for robotic welding utilising an integrated work manipulator.
- Weaving: No electrode weaving motion was used. Weaving, and the weave pattern and frequency will effect the specific heat input to the joint and consequently weld penetration. It is used primarily to assure sidewall fusion and complete filling of the joint. However, for the plate thickness and joint design in the experiments no weaving was necessary.
- Transverse torch angle: For flat position butt welding of equal thickness material the torch is normally held perpendicular to the surface.

5.4.1 Joint geometry

Nominal joint geometry for the experimental welds is shown in figure 5.6 and was determined as suitable for full penetration welding according to initial experimentation and literature (118).

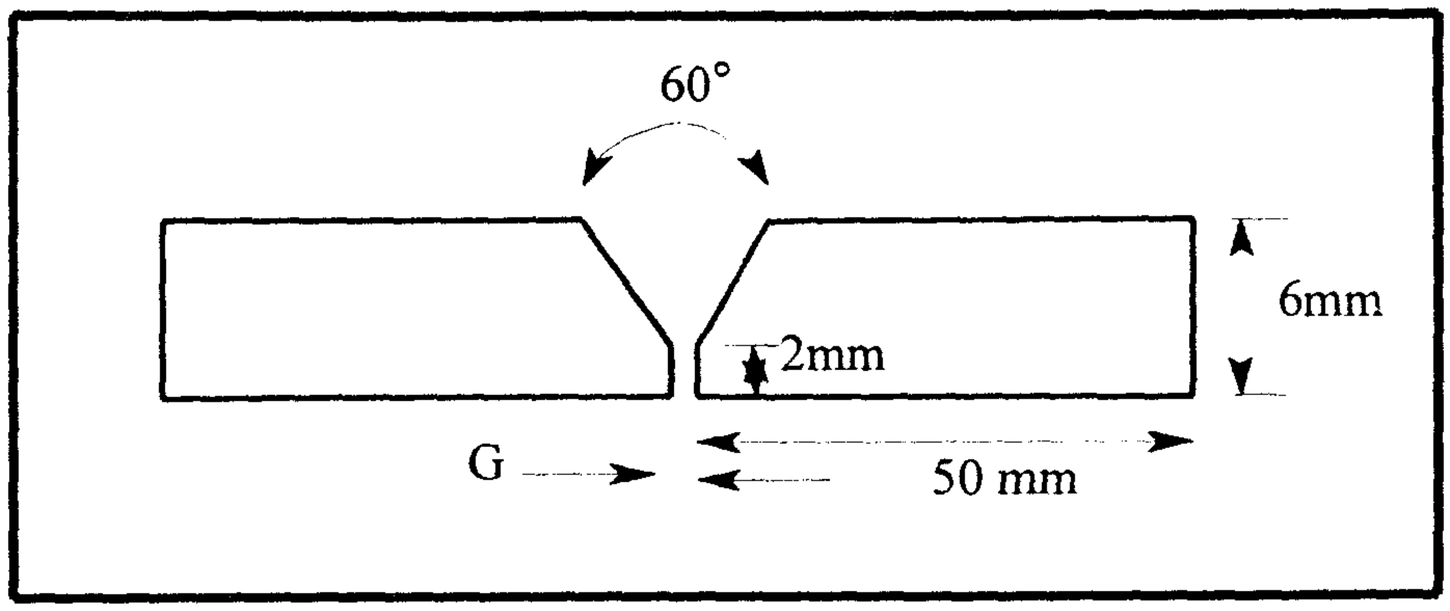

Fig. 5.6. Joint geometry of workpieces G = 0 and G = 0-1.5mm

5.5 Experimental design

The objective of the experiments was to obtain training and validation data for neural network modelling. The models are intended to define the relationships between input welding variables, temperature distribution in the weldment, and the output weld geometry as defined by penetration and bead geometry

For the experiments reported in this research the four most important adjustable variables current, voltage, travel speed, and torch angle were used. In the second set of experiments root gap was also varied but was not treated as an input variable for modelling. Other variables were maintained constant. Tests were first carried out to establish the combination of the variables giving acceptable penetration. This was set as the mean level in a four variable, three level, full factorial experiment, as shown in table 5.1, settings for high and low levels was discussed in the previous section .

For all welding experiments, mild steel plate, 200mm long, 50mm width with thickness of 6mm has been used. After degreasing and machining they were tack welded together to produced the workpiece as shown in fig 5.6. The dimensions of workpieces have been chosen that satisfied the following criteria.

- Heat lost from the edges of plate before measuring the temperature is minimised.

- Enough data can be obtained.

The first and last parts of the weld are ignored to eliminate the effect of initial instability in welding, and the local chill effect of the specimen holding fixture. Data was collected at 10mm intervals along the weld giving a total of 810 sets of data.

5.6 Experimental apparatus

The experimental facilities are schematically shown in figure 5.7. These include an infrared thermography sensor, industrial 6-axis robot, robot controller, welding machine, analog to digital convertor and computer for ANN modelling. In the next sections these elements will be discussed briefly.

5.6.1 Welding robot

In this work the Fanuc robot model S-100 has been used. The robot is an articulated robot, with six controlled axes. The maximum load capacity at the wrist is 10 kg. The robot is controlled by the R-MODEL C controller, which consists of the control unit, setting / display panel, and the teach pendant (119). The robot is equipped with the KEMPPI model FU20 solid state programmable welding machine, which provides welding current up to 500 Amps, voltage up to 50 Volts, and is allied to a wire feed unit providing a wide range of wire feed speed. A water cooled torch continuously rated at 500 Amps was employed.

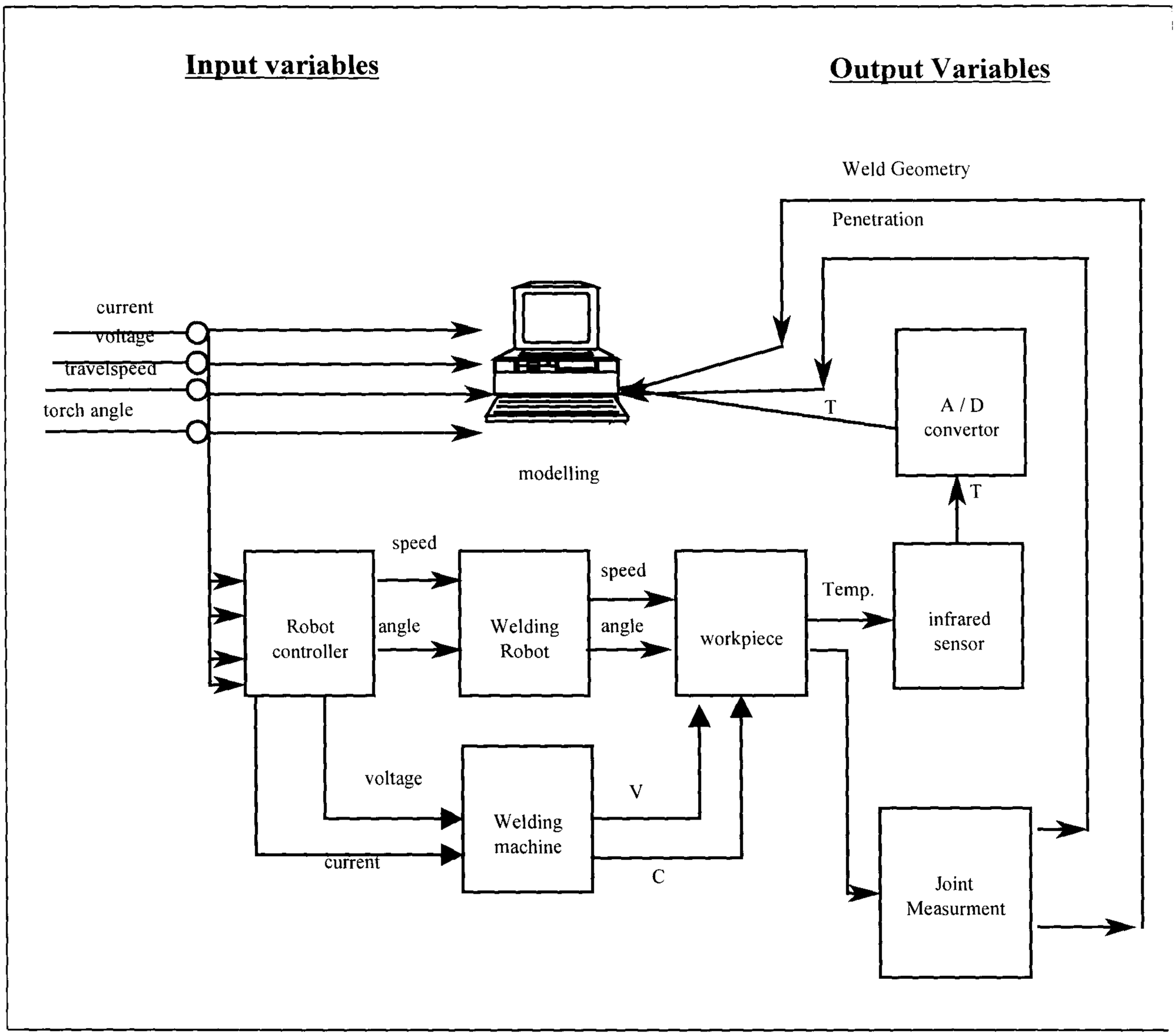

Fig. 5.7 Schematic diagram of welding controller modelling

5.6.2 Infrared sensor

The Calex model TR 7420 (94) has been used in this work. This pyrometer uses a fibreoptic bundle to transmit the infrared radiation emitted by the workpiece to a remote sensor. The pyrometer can be used to measure the temperature of a target spot with minimum 2.3mm in diameter when the distance between the lens and target is 60mm.

The measuring system as shown in figure 5.8 consists of:

- An optical head to focus the radiation;

- A fibreroptic cable with metal sheath;
- The detector and amplifier;
- Signal processing and display unit.

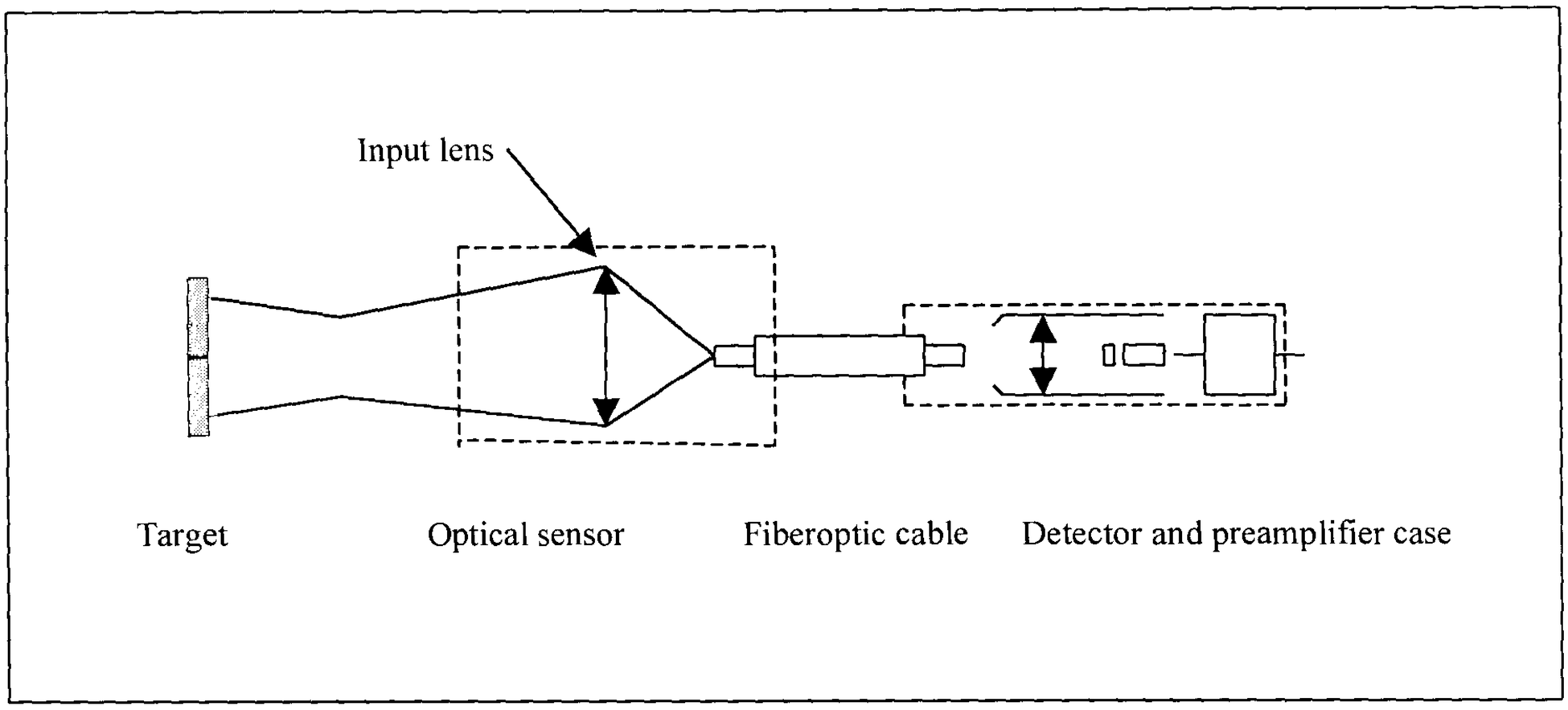

Fig 5.8 Schematic diagram of the sensor.

Important characteristics of the sensor are (120):

- Temperature measurement range: 350-1700°C;
- Measurement distance range: 20 mm to 1m;
- Target diameter: from 2.3 mm;
- Accuracy ± 0.5% of the measurement;
- Response time: ≤ 20 ms.

The selection of emissivity is very important in infrared temperature measurement. In order to establish the emissivity for workpieces used in

experiments, the workpiece was heated to a known temperature, as determined by a thermocouple, and the temperature of the plate measured with the IR sensor. The emissivity compensator was adjusted until the indicator displayed the correct temperature. The resultant value of emissivity was 7%, which is used for all of the experiments.

The optical head was attached to the welding torch at 60 mm distance from the workpiece surface giving the minimum spot diameter of 2.3 mm. To prevent the effect of spatter and smoke interfering with sensing, the optical head was installed in a housing purged with compressed air, and protected by a replaceable window.

5.6.3 Computing hardware and software

This research has utilised various software for modelling and data acquisition purpose. These are:

- Neural Works Professional II/plus version 5.2. This software has been used for construction, simulation and evaluation of neural network models;
- Pico data logger. This software has been used with the Pico analog to digital convertor for the selection of data samples, the sampling interval, and capture of data. Data is achieved in < 120 msec. ;
- Matlab Fuzzy Logic tool box. has been used for building and testing of the fuzzy logic model;
- Control model software. Was developed to combine the C^{++} neural network model and pico data logger software for the evaluation of Neuro-fuzzy control model.

All of the software was operated on an IBM compatible PC having a Pentium 75 MHz processor, 32 Mb RAM, and 1Gb HD. These provide processing of data and operation of the models in less than 200 msec. With improved A-D convertor hardware and more powerful computing facility processing time could readily be reduced to less than 100 msec.

5.7 Experiments Results

Experiments were conducted in order to obtain the training and evaluation data for the neural network modelling. For the purpose of the modelling reported in this research, data was needed to establish the relationship between controllable welding variables and temperature at a point in the surface of a workpiece during welding. Temperature was measured at appropriate intervals depending on the welding speed, to give measurements at 10 mm increments and recorded along with the value of welding variables used to produce the weld. After welding the joint geometry was measured at the positions where temperature measurement was taken. Data was classified by depth of penetration in five classes:

100 - 110% depth of penetration;

90 - 99% depth of penetration;

80 - 89% depth of penetration;

70 - 79% depth of penetration;

less than 70%.

The data then was randomly divided into training and evaluation sets for each class of penetration as shown in table 8.3, to be used in the construction of neural network models as described in the next chapter.

The complete set of experimental results are shown in appendix 1. In appendix 2 the neural network training and evaluation data for each model are given.

Chapter six Neural network modelling

6.1 Introduction

An Artificial Neural Network (ANN) is an information processing paradigm that is inspired by the way biological nervous systems, such as the brain, process information.

ANNs have been applied to an increasing number of real-world problems of considerable complexity. Their most important advantage is in solving problems that are too complex for conventional technologies, problems that do not have an algorithmic solution or for which an algorithmic solution is too complex to be found. In general, because of their abstraction from the biological brain, ANNs are well suited to problems that people are good at solving, but for which computers, or rather conventional computer programs, are not. These problems include pattern recognition and forecasting (which require the recognition of trends in data).

In this chapter, a general overview of the Artificial Neural Network approach and methods is given. These methods are applied in this research in the context of approximating the temperature attained at a point in the weldment surface, for a set of welding variables. Neural Network architectures are discussed and different modelling techniques are demonstrated in the following sections. In section 6.8 modelling of Gas Metal Arc Welding process by various types of neural network technique are demonstrated and discussed as a guide to the selection and development of suitable models to fulfil the objectives of this research.

6.2 Historical overview

The field of neural networks was initiated by the introduction of the model of a simple neuron by McCulloch and Pitts in 1943 (121). In their work, they showed that even simple types of neural networks could, in principle, compute any arithmetic or

logical function. This idea was quite attractive and was quickly taken up by Rosenblatt (122). He invented the perceptron in which, as shown in figure 6.1, a weighted sum (net) of input x_i's is produced and compared to a threshold (T_0). The output is 1, if the net value is larger than the threshold, otherwise it is zero. Rosenblatt also proved that, given linearly separable classes, a perceptron will, in a finite number of training trials with no dependence on the initial states, develop a weight vector separating the classes.

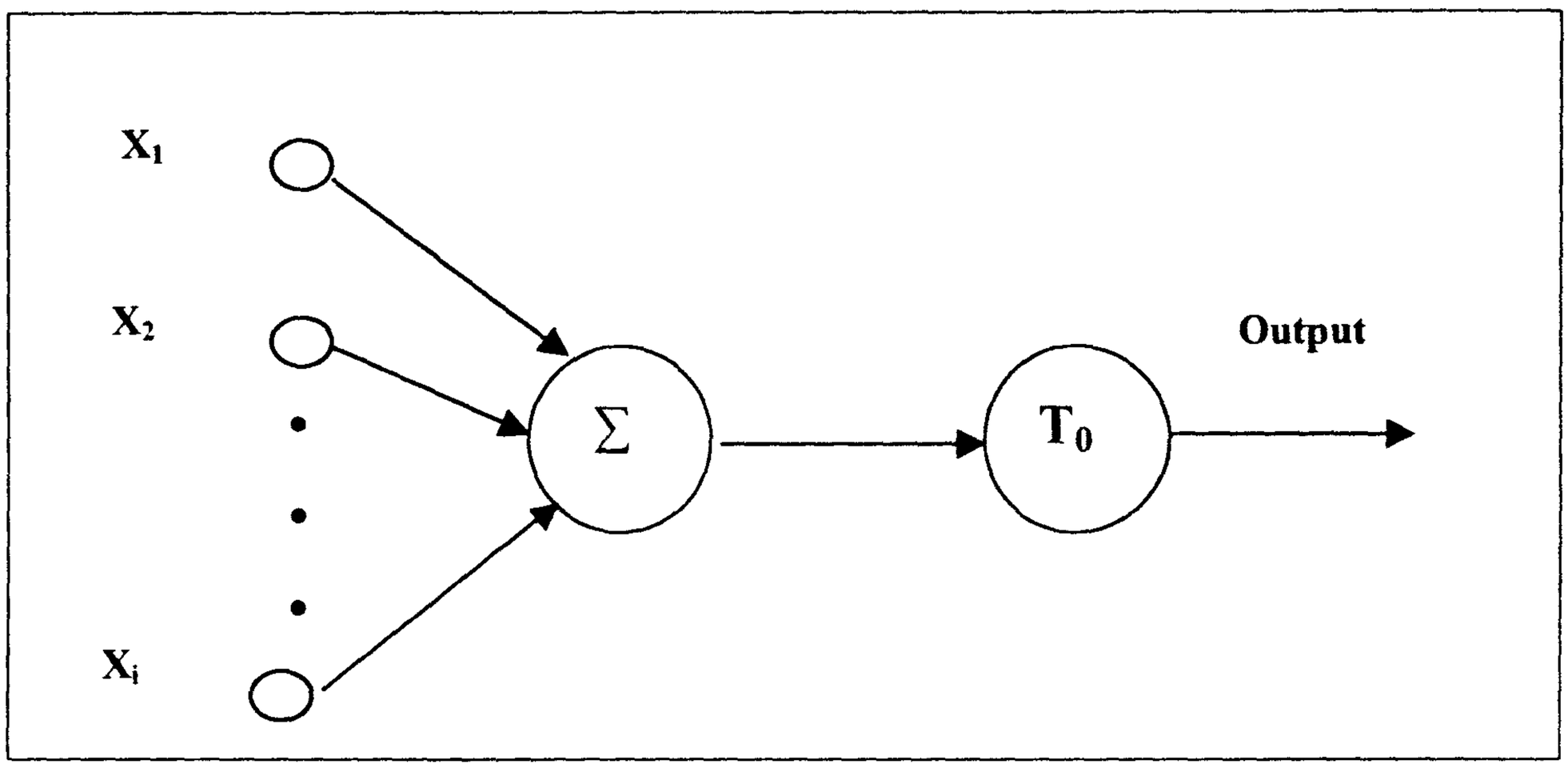

Fig.6.1 Rosenblatt's model of the perceptron.

This was the start of development of the first successful neurocomputer, the Mark I Perceptron which was demonstrated in 1957 (122). However, no learning methods existed at the time for multilayer perceptrons and the field of neural networks became dormant.

The revival came in the early 1980's with the works of John Hopfield (123), and later with the works of Rumelhart and McClelland (124), in introducing learning rules for multilayer perceptrons (the backpropagation learning rule). A resurgence in the development of neural networks occurred and many new paradigms and architectures with successful applications are reported, often in areas where conventional programming and other AI techniques found considerable difficulties.

6.3 Biological neuron model

Artificial neural networks draw their strength in mimicking biological neuronal systems in their basic functional behaviour. Hence, a prerequisite to understanding the working of the ANN and adapting it to engineering application is to understand the basic workings of the biological neurons.

The biological information processing system can be broken down into:

1. Receipt of sensory information (input);
2. Localised pre-processing (filtering and differentiating);
3. Transmission and post-processing by the central nervous system (interpretation and perception).

At first the information is received via a complex sensory system (visual, auditory, etc.). This is followed by a local level pre-processing, for example, noise reduction, gain control, motion detection or edge enhancement. At this stage, the information is broken down into localised parameters, that are passed to the brain where they are put back together and a coherent perception of the object is formed (analogous to inverse solution). The first two steps have been utilised in designing sensors and various signal processing tools. The third aspect is the driving force behind artificial neural networks research. Literally the objective is to mimic and explain, "how does the brain do what it does".

According to the limited knowledge at the present time, the anatomy of the neuron as shown in figure 6.2 is comprised of a series of *dendrites* which act as the input terminals to the *soma* (cell body). The cell body processes the information received by the dendrites and transmits its response via the *axons* to the next layer of neurons. The connection of this axon and the dendrites of the next layer is via s*ynapses*. The synapse secretes a neurotransmitter which stimulates the dendrites of the connecting neuron. All incoming stimuli are summed at the cell body and if a threshold value is passed an action potential is generated passing the signal to the next layer for further processing.

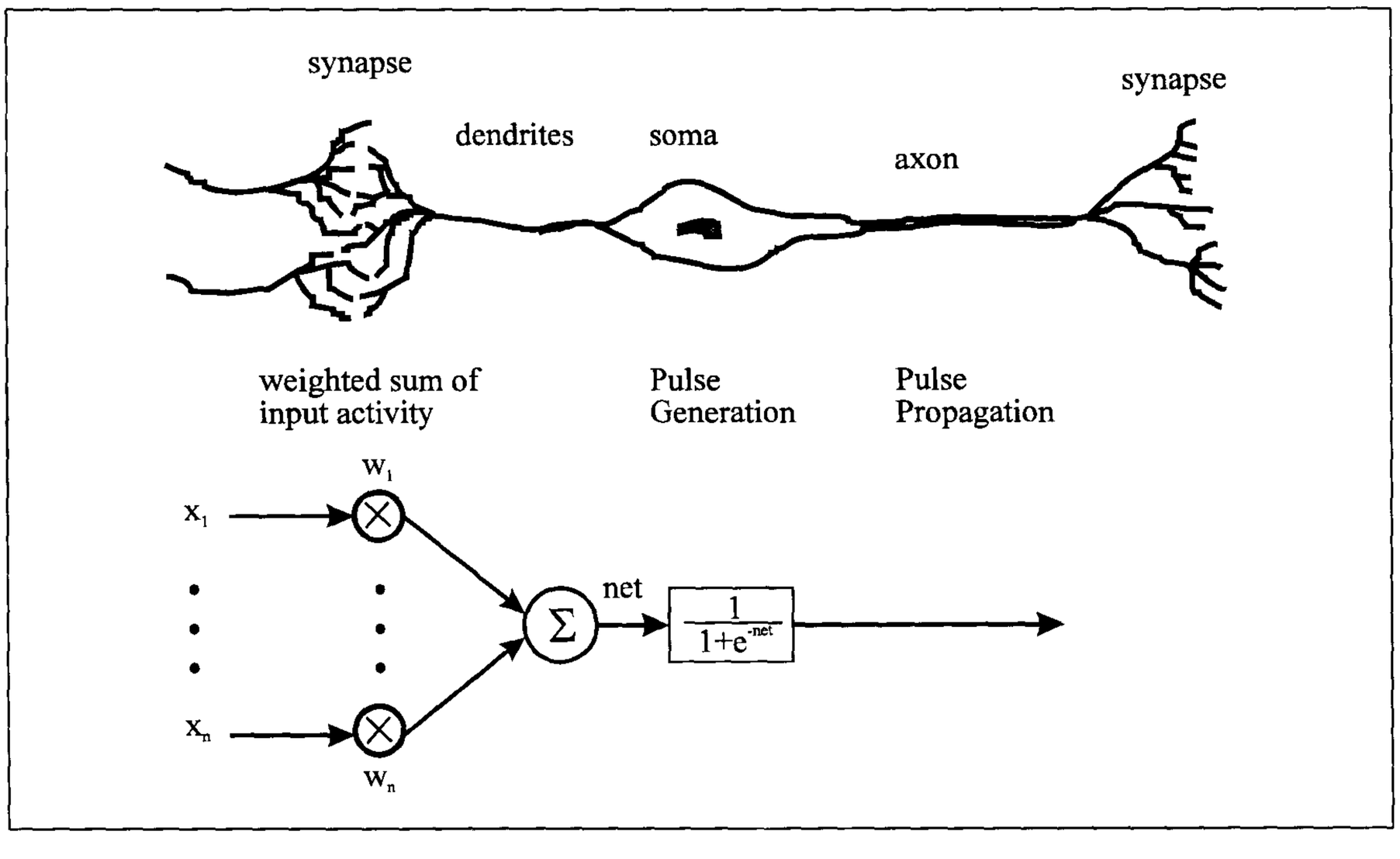

Fig. 6.2: Comparison of the biological neurones and a perceptrons (125)

The transmission of the signal is only in the forward direction. In summary, the basic operation of the biological neuron includes weighted summation and thresholding. The analogous artificial neuron-like structure invented by Rosenblatt, the perceptron also shown in figure 6.2, has the same functionality as the biological neuron and has a number of inputs and a number of outputs. The perceptron receives signals from inputs and performs a weighted sum of the inputs. The artificial neuron (Processing Element, P.E.) performs a mathematical transformation to achieve output, which may in turn be the input to a next layer of neurons (125)

6.4 Neural network modelling

In general, Artificial Neural Networks (ANN), perform an input-output mapping. This mapping may be either discrete or in the continuous domain. In mathematical modelling, usually there is a need to know about the domain theory in guiding the

design of the model. In contrast, ANNs do not make any assumption about the governing physical theory, and instead they fit a generic model to the data. Therefore ANNs can be thought of as universal data-driven modelling techniques capable of learning the underlying mathematical functions governing system operation.

Given a physical system, an ANN can model on the basis of a set of examples encoding the input-output behaviour of the system. The modelling performed by the ANN can be ascribed to its ability to learn. This learning, which is known as training, is a process by which the network internal parameters (weights) are adapted and as a consequence the model is formed. If the network is designed and trained properly, it can perform generalisation and be relatively immune to system variations and noise.

For a given problem, the best model is possible. However, even the best model may not guarantee full accuracy because every model has its limitations. Instrumental to the success of every model is an understanding of the problem. Therefore, the more is known about the system, the more accurate models can be constructed. Two points need to be stressed in any successful application of ANNs. First, a good understanding of the ANN architecture is essential especially the requirements and limitations. Fortunately, available powerful and high speed computers make empirical testing of a wide range of architectures a viable research option. Secondly, although they are capable of dealing with arbitrary problems, the learning task is often simplified by orders of magnitude if more is known about the problem. This could be in the form of data normalisation or input parameter expansion (125). Different types of ANN architecture, which have been employed in this research, will be discussed in subsequent sections.

6.4.1 Neural network training

A Neural Network has to be configured in order to produce the desired outputs from a set of inputs. Various methods to set the weights of input connections exist. One way is to set the weights explicitly, using a priori knowledge, but such knowledge is rarely available. Another method is to train the neural network by

patterns and allowing it to change its weights according to some learning rule. The training can be categorised as two different types, supervised learning and unsupervised learning.

6.4.1.1 Supervised learning

In supervised or associative learning the network is trained by providing it with input and matching output patterns. These input-output pairs can be provided by an external teacher, or by the system which contains the network (self-supervised). In this research, because of the availability of empirically determined input-output data, for various levels of penetration depth all the models have been trained employing supervised learning.

One problem with all supervised learning is that the network can recognise patterns that are similar to those learnt, but finds difficulty in recognising new ones. In order to recognise new patterns, the network needs to be retrained with these patterns added to produce a larger training set. If only new patterns are provided for retraining, then old patterns may be forgotten. In this way, learning is not incremental over time. This is a major limitation for supervised learning networks. This problem is dealt with by careful problem consideration in choosing the training data to be a true representative of the domain, which is being modelled.

6.4.1.2 Unsupervised learning

In unsupervised or self-organisation learning, the output PE is trained to respond to clusters of patterns within the inputs. In this paradigm the system is supposed to discover statistically salient features of the input population. Unlike supervised learning, there is no a priori set of categories into which the patterns are to be classified, rather the system must develop its own representation of the input PE.

Unsupervised learning often has less computational complexity and less accuracy. In general the task of unsupervised learning is more abstract and less defined (125). The learner must focus its attention, observe the regularity in the environment and draw

hypotheses which are not suitable for highly-non-linear, multi-variable process modelling such as the Gas Metal Arc Welding process.

6.4.2 Neural Network Evaluation

Validation is to determine whether the system can perform at an acceptable level in terms of accuracy and efficiency. Artificial neural network validation includes both validation of system performance and validation of the learning system. For example the capability of network for generalisation is evaluated in the learning system.

6.4.2.1 Learning system evaluation

The learning system usually learns its knowledge from training data. If only the training data is evaluated the performance level will reflect how well the knowledge fits the data, but is not necessarily a reliable estimation for unseen data. For this reason an independent validation or test data set is required. Frequently, the experimental data is randomly partitioned into two subsets, one used for training and the remainder for testing.

Several techniques are available for evaluation of learning system performance. These techniques include cross-validation, consistency analysis and sensitivity analysis. Among these techniques cross-validation is more appropriate for supervised learning (126).

The performance measure for a network is directly dependent on the performance of the learning system. The performance of the learning system in a classification task is measured by the rate of correct classifications over the entire set of test patterns. In pattern recognition and function approximation, the performance is measured by the percent error or mean squared error (MSE) over the test set. In this work, the reported results have been tested by cross validation and performance measures are reported accordingly.

6.4.2.2 Validation of system performance

A system performance evaluation must be done to determine if the system can meet the predefined objective. The system performance evaluation for the neural network and fuzzy logic model is discussed in the next chapter.

6.4.3 Optimisation of neural network

There are several techniques for network optimisation divided into two general heuristic methods, building up and pruning methods. In the building up techniques, such as cascade-correlation (127) and dynamic node creation (128), the starting network is small and units are added and trained to minimise the error. Other methods start from a large network and remove weights and nodes. Alternatively, a combined method can be used to add and remove hidden units dynamically. Examples of such methods are given in (129, 130). All of these approaches have been used to reach generalised networks.

Generally, in a fully connected network, there is a large amount of redundant information encoded in the weights. Thus, it is possible to remove some weights without effecting the network performance. This process is known as pruning. Reduction in the number of weights leads to better generalisation and makes learning faster (131). For models reported in this work the pruning method has been used to reduce the number of hidden layers.

6.4.4 Multi-layer perceptron (MLP) network

A multi-layer perceptron (MLP) or multi-layer feed-forward network is constructed from the successive connection of individual perceptron layers as shown in figure 6.3.

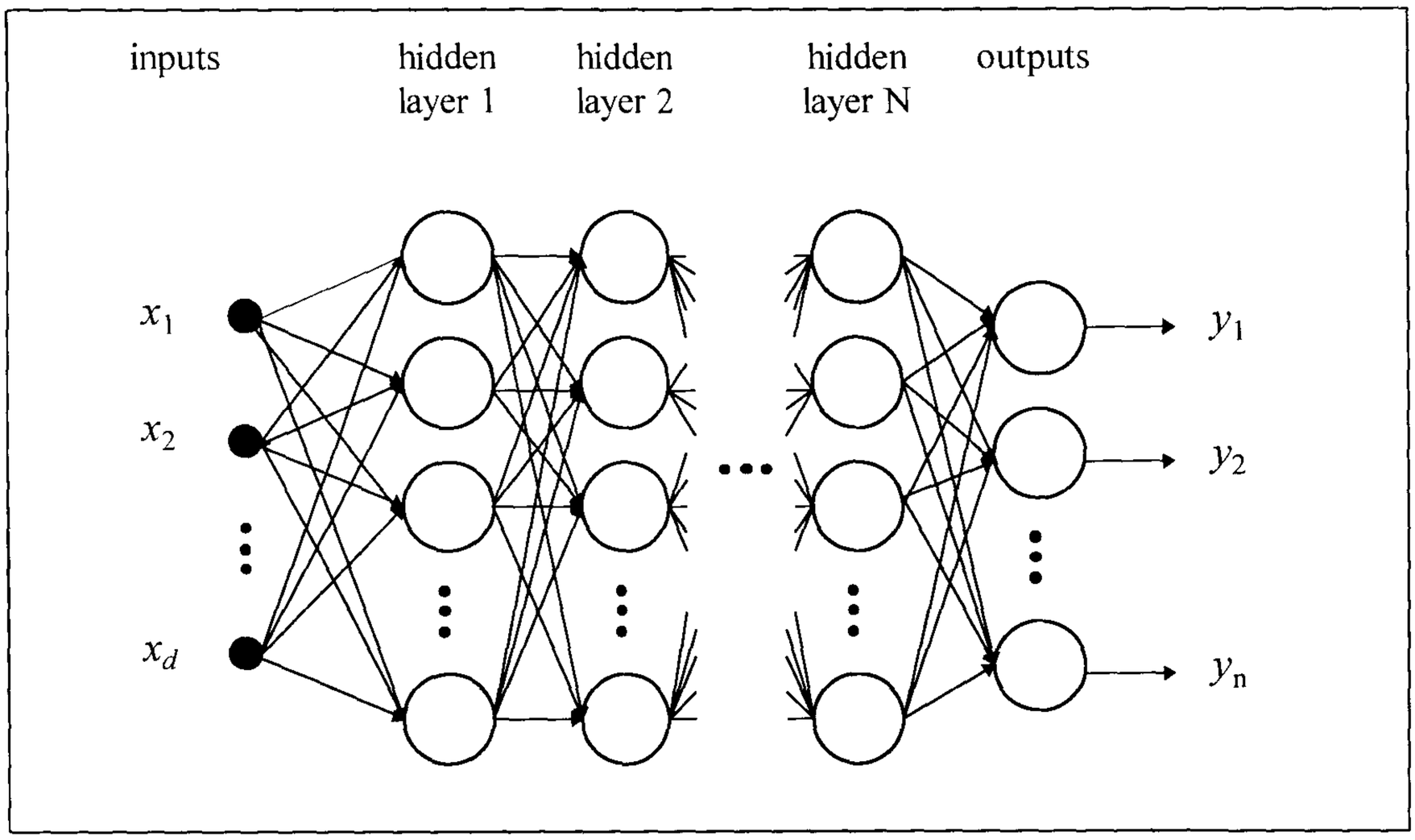

Figure 6.3 The structure of multi-layer perceptrons.

The inputs are indicated by (x_i's) and the outputs as (y_j's). Commonly there is full connectivity between consecutive layers, i.e. each perceptron is connected to all of those in the next layer as indicated by lines. Each connection has a weight associated with it. Furthermore, each processing element (PE) has a common non-linear differentiable transformation function, which is a requirement of the gradient descent learning algorithm. The main characteristics of MLP include the following:

- The ability to learn from example. Whilst the theoretical understanding and modelling of a welding process is difficult, sensor technology enables the rapid collection of data which can be exploited by the neural approach;

- The ability to cope with complex non-linear problems such as the relationship between welding variables and temperature distribution which displays a high degree of non-linearity;

- The ability to abstract essential information from noisy data. On-line sensor measurement has to deal with a variety of noise inherent in the measurement (i.e. background , electronic, etc.). Neural networks have the ability not only to extract the signals from the noise but also to build up an understanding of the sensor characteristic in such situations (filter application);

- The ability to generalise from examples. Neural networks can interpolate and extrapolate from the experience generated from a limited set of examples;

- The ability to construct effective solutions quickly. Being trained rather than programmed, neural networks are less reliant on expert domain experience;

- The ability to work in real time, a trained network is computationally efficient and its massively parallel architecture is ideally suited to modern processing technology, such as automated robotic welding.

Therefore, when there is ample data available from a process that is difficult to characterise analytically, ANNs can be used to extract and learn the underlying relationships. An implication of this ability has a direct consequence on theoretical development in the sense that if the ANN is able to model a process within reasonable accuracy, then there is a mathematical model which can define the process.

Due to their flexible nature, MLPs are used for a variety of tasks such as function approximation, and classification. In classification tasks, often the network is assigned an output node for each class with the appropriate number of features as inputs. In function approximation the network has usually a single output node with a non-linear or linear activation function and a number of appropriate input variables.

Generally it is accepted that the performance of a well designed MLP neural network is comparable with, but not better than, that achieved by good classical statistical technique. On the other hand the MLP uses less time than statistical techniques (132).

6.4.5 Back-propagation network

As described earlier the MLP learns in a supervisory mode by, fine tuning the parameters and minimising the network "mistakes". Amongst these procedures, back-propagation (BP) is the most popular and well known learning algorithm for training of the MLP networks (129).

Back-propagation is a general purpose network paradigm that can be used for system modelling, prediction, classification, function approximation and many other general types of problem. Back-propagation learns by calculating an error between desired and actual output and propagating this error information back to each node in the network. Back-propagated error is used to drive the learning at each node. In BP learning, the weights are initially set at small random values and the learning is achieved in two stages:

- Feed forward phase, in which each training pattern (x_p) is presented to the MLP and the network response (o_j) is evaluated by a forward pass and compared with the target output (t_j), as equation 6.1;

$$E_p = \frac{1}{2}\sum_j (t_j - o_j)^2 \qquad [6.1]$$

- Error back propagation phase, in which the weights are adapted by applying the chain rule to the successive layers of PE in estimating the direction of the gradient of error surface.

$$\Delta w = -\eta \frac{\partial E_p}{\partial w} \qquad [6.2]$$

In the above equation, η is the learning rate or learning coefficient, which controls the convergence speed and the learning precision. This process is repeated for all training patterns. A formulation of the BP algorithm and relevant equations are found in general neural network textbooks (129).

A standard back-propagation network can learn either in cumulative (batch) mode or in standard delta-rule mode. With the cumulative mode, weight changes are accumulated over an "epoch" before they are applied to the network, where the epoch size is a number less than or equal to the number of training data. Standard Delta-Rule mode corresponds to an epoch of 1, in this case weight changes are applied as soon as they are calculated.

6.4.6 Radial basis function (RBF) network

Radial basis function is a statistical transformation based on a gaussian distribution function. In principle, they could be employed in different types of models (linear or non-linear) and different types of network (single-layer or multi-layer). Radial basis function networks can be used for applications such as function approximation, pattern discrimination and classification, pattern recognition, prediction and forecasting, and process modelling. RBF networks have traditionally been associated with radial functions in a single-hidden layer network (133), which is shown in the figure 6.4.

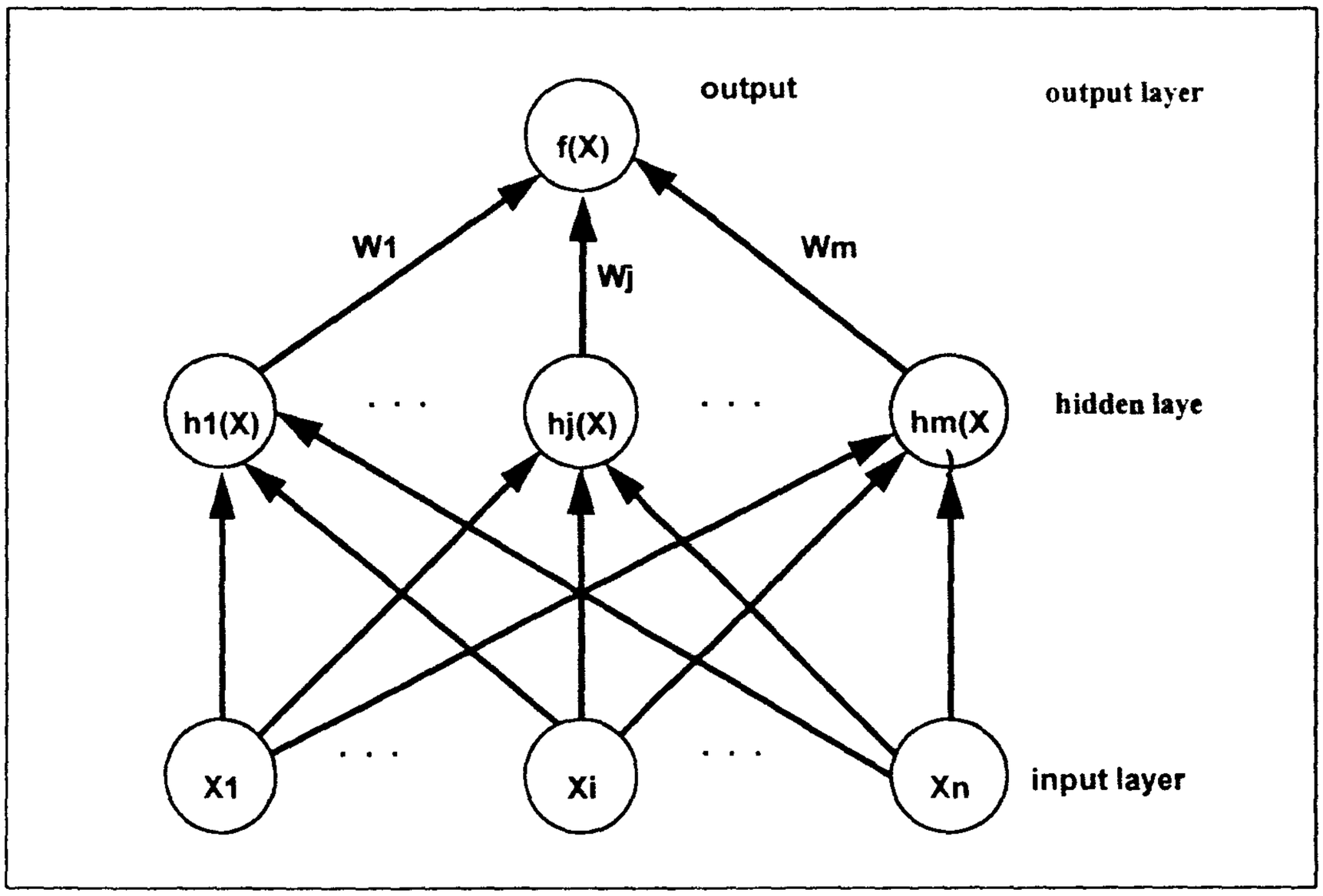

Fig. 6.4: The radial basis function network.

Each of ***n*** components of the input vector feeds forward to ***m*** basis functions, whose outputs are linearly combined with weights into the network output.

In the hidden layer of an RBF network, each PE takes as its input all the outputs of the input layer. The hidden PE contains a basis function, which has the parameters of centre and distance. Centre is a vector in the input space, which is typically stored in the weight vector from the input layer to hidden PEs. A radial distance, ***d***, is used to determine how far an input vector is from the centre of the basis function. Typically this is standard Euclidean distance. The basis function is a curve (normally Gaussian function) which has a peak at zero distance and which falls to smaller values as the distance from the centre increases. Therefore the PE gives an output of 1 when the input is centred but which reduces as the input becomes further from the centre.

6.4.6.1 Comparison with Back-propagation

The radial basis function network is typically used in situations in which using a back-propagation network may also be considered. Comparisons of RBF networks with BP networks are summarised as follows:

- RBF trains faster than a BP network;
- RBF leads to better decision boundaries than BP, especially when used for classification and decision problems;
- The internal representation of hidden layers in RBF has more natural interpretation than the hidden layer of a BP network (134);
- The initial learning phase of an RBF network (135) is an unsupervised clustering phase. Therefore important discriminatory information can be lost in this phase;
- A BP network can give a more compact distributed representation compared with a RBF network.

6.4.7 Reinforcement network

Reinforcement learning refers to learning schemes, which proceed by iterating the following steps until performance no longer improves.

- A set of weights is selected in some methodical or semi-random way, depending on previously selected and saved weights;

- The performance of the network is assessed by running the training data through the network and evaluating an objective function by a control layer (figure 6.5);

- If the weights show an improved performance, they are saved, replacing the previously saved weights;

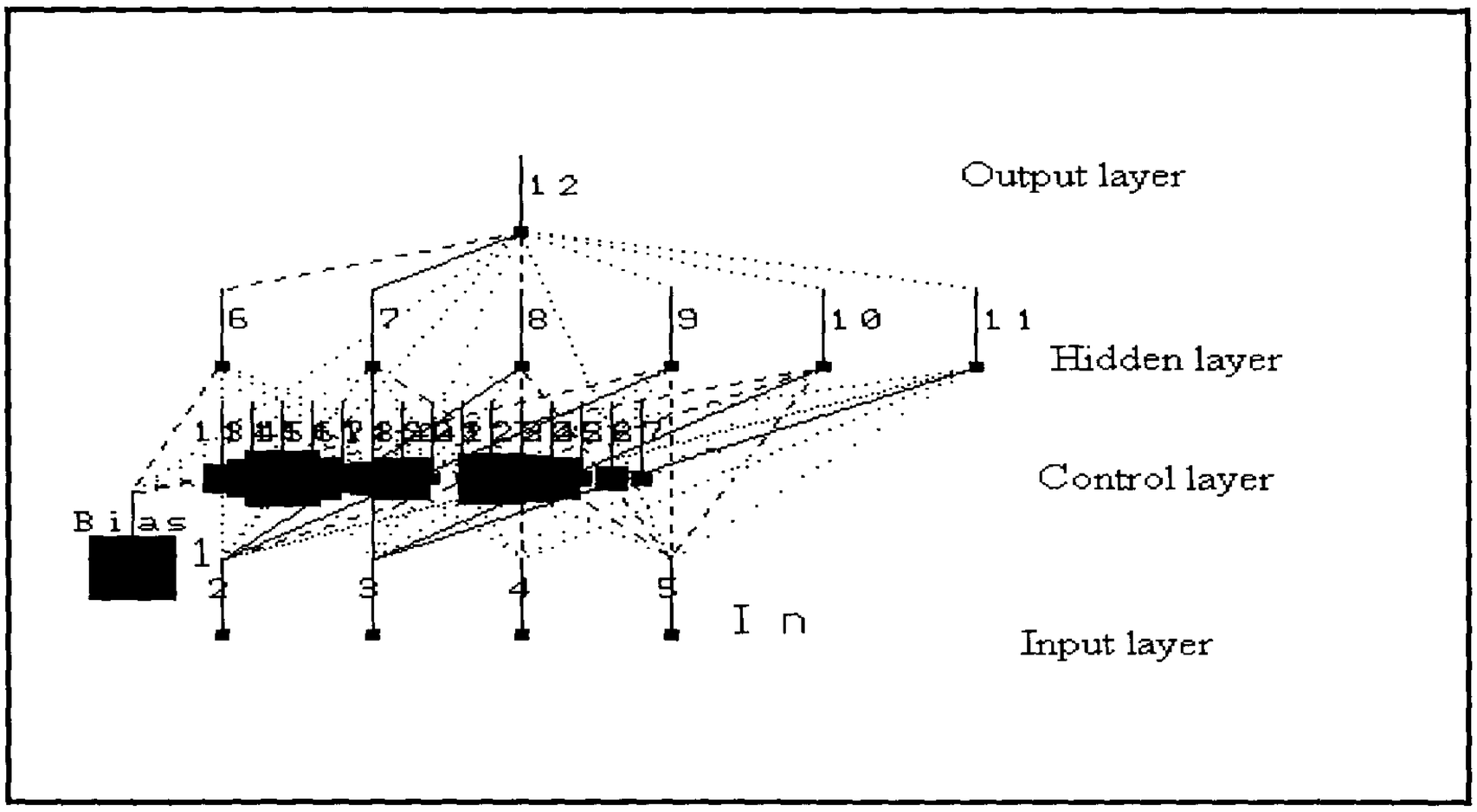

Fig.6.5 The schematic diagram of reinforcement network

Reinforcement Networks have the following advantages over paradigms such as back-propagation:

- They can be used when gradient information is not available to drive the learning. This means that, unlike BP, reinforcement learning does not have to compute derivatives. This feature makes it suitable in a complex system where derivatives are difficult to obtain. For example, the performance of a classification network is more appropriately evaluated by classification rate rather than by RMS error;

- They can be used with non-orthodox architectures. For example, cascaded connections can be used;

- They are able to learn their way out of local minima since they can take large steps in weight space;

The main disadvantages are:

- They are very time consuming;

- If the initial population is not diverse enough, large regions of the weight space may not be searched.

6.5 Neural network welding modelling

The main objective of this research is to model the relationship between temperature distribution in the weldment and the welding variables. The models should fulfil the control requirement of assuring acceptable quality welds (penetration, fusion, bead shape). The temperature at a point in the weldment surface can be correlated to the joint geometry, welding process variables, and resultant weld quality. In practice temperature measurement of a point on the weldment surface during welding is to be measured using an infrared sensor. When there is a variation in this point temperature compared to that predicted by the model for full penetration, the model must be able

fulfil this requirement three approaches to ANN modelling have been taken. These are one-to-many modelling, inverse mapping and many-to one modelling which are discussed in the following sections.

6.5.1 One-To-Many (Temperature-To-Welding variables) modelling

To find the relationship between the temperature measurement and the welding variables directly, back-propagation feed-forward neural network models have been constructed. After training the models with experimental data, they should be able to predict the welding variables for a given workpiece surface temperature as measured during welding. The neural network model is to map the input (temperature) and output(current, voltage, torch angle, and welding speed), therefore the network should have one PE in the input layer, some PEs in a hidden layer, and four PEs in the output layer fig 6.6.

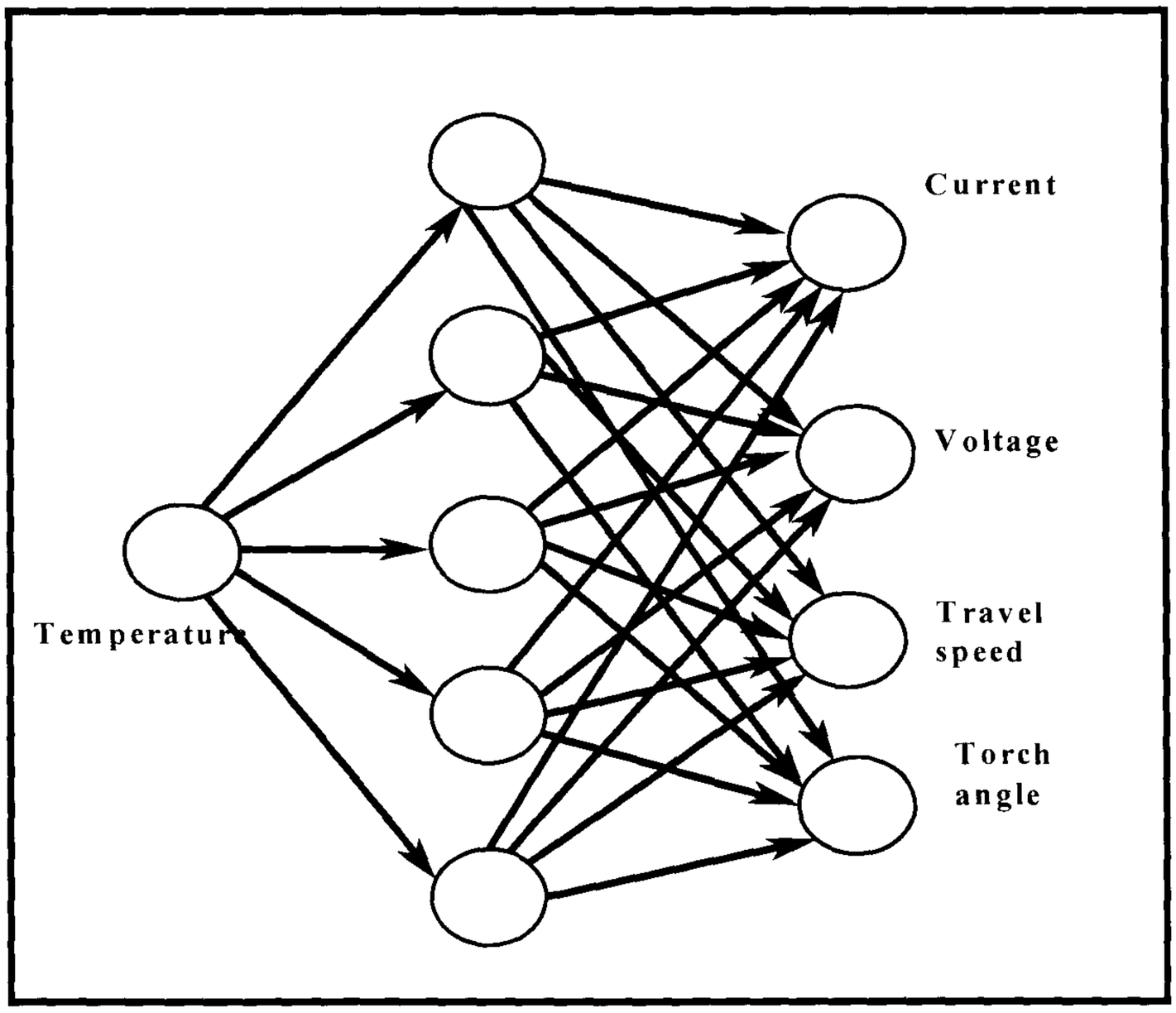

Fig.6.6 One to four feed forward model.

A number of different neural network architectures have been constructed and trained. Each of these architectures have then been evaluated with unseen testing data. Training and evaluation data sets were as shown in table 8.3 and appendix 2. Table 6.1 summarises the minimum error instances or 'best' results from the trained networks.

data type (Penetration)	No. of Hidden PE	Angle Error %	Current Error %	Voltage Error %	Speed Error %	Average Error %
70%-79%	6	12.15	1.65	6.7	3.67	6.04
80%-89%	8	11.82	1.8	8.15	3.76	6.38
90%-99%	5	15.55	2.11	6.95	4.1	7.17
100%-110%	6	9.49	1.33	5.31	3.27	4.85

Table 6.1. Result of one-to-four back- propagation models.

In table 6.2 the range of error when models were tested with validation data are shown.

Data type (Penetration)	Angle Error degree	Current Error Amps.	Voltage Error Volt.	Speed Error mm/min
70%-79%	±6.5	±6.5	±3.4	±31
80%-89%	±7.3	±7.3	±3.1	±32
90%-99%	±8.2	±8.2	±3.2	±35
100%-110%	±5.4	±5.4	±2.1	±28

Table 6.2. Welding variables error via one-to-four back-propagation models

It is clear from the magnitude of the errors that the networks failed to learn the functionality required. This is expected because the mapping is ill-defined and

there exists an infinite set of possible solutions. It is seen in table 6.3 that improved learning is possible, when reinforcement learning incorporating Genetic Algorithms (GA) is used. However, this is only a small improvement and does not render a reliable functional mapping. One way to achieve a better functional mapping may be to increase the number of input parameters to the network providing, additional degrees of freedom. The inputs would be provided from additional sensors monitoring the process during welding, such as sound pressure, weld pool (image), etc. Other input could be joint geometry (root gap, plate thickness, root face, etc.) which can be monitored prior to welding. Although it is conceivable that a network would be able to learn this function with the additional input parameters, in reality the incorporation of the additional sensors would increase the system complexity, and will reduce the flexibility of the robot welding system.

Another way is to indirectly predict the welding variables corresponding to point temperature, such as inverse mapping, or incorporating other intelligent systems such as an expert system or fuzzy logic.

No.	Type of data (penetration)	% of angle Error	% of current Error	% of voltage Error	% of speed Error	% of average Error
1	70 %-79%	11.8	1.79	7.56	3.33	6.12
2	80% - 89%	11.4	1.88	6.6	3.1	5.74
3	90% - 99%	12.12	2.13	5.3	3.5	5.76
4	100% - 110%	8.0	1.4	4.6	3.2	4.3

Table 6.3. GRL one - to- four modelling with corresponding depth of penetration.

In the following sections neural networks with additional input (joint root gap) and reverse modelling are illustrated. In the next chapter the addition of a fuzzy logic system for control modelling is discussed.

6.5.2 Two (temperature and root gap) to four (welding variables) modelling

For this modelling purpose data for training and evaluation of the neural network models was extracted from the welding experiments in which joint root gap varied between 0 - 1.5 mm. During welding the surface temperature on the plate was measured and data was sorted according to root gap and depth of penetration. Welds with 100-110 % penetration and the corresponding root gap were selected for training and evaluation of the networks, which are shown, in appendix 2.

Several models with different modelling techniques and architectures have been constructed, trained, and evaluated. The summary of evaluation results of the models is shown in table 6.4.

Network Type	Angle Error %	Current Error %	Voltage Error %	Speed Error %	Average Error %
BP	10.8	1.6	5.1	3.1	5.15
RBF	6.5	1.4	3.8	3.2	3.75
GRL	7.4	1.5	5.17	3.4	4.3

Table 6.4. Result of two-to-four mapping models for 100-110% penetration with 0-1.5 mm root gap.

The results show that using a two-to-four network incorporating RBF gives a small improvement but not sufficient to make it a viable model. With GRL the network performance virtually unchanged, and the BP network had inferior performance.

6.5.3 Reverse neural network modelling

Reverse modelling is a process that a network undergoes to simplify and facilitate pattern recognition by allowing the output level to be stimulated first, and progress backward through the network. The system will then show what should be expected as an input solution by stimulating the pattern backward (136).

As discussed in the section 6.5.1, mapping one to many with a neural network model is difficult. The association of an input with selection of an output, in a one-to-many mapping relationship may required an indirect method based on the inverse mapping of a many-to-one trained neural network model. On the other hand, the objective of inverse mapping is to generate an input vector corresponding to the desired output vector. First the network is trained to learn non-linear many (current, voltage, speed, and torch angle)-to-one(point temperature) mapping relationships. This network has an input layer with four PEs, some PEs in the hidden layer and one PE in output layer. After training the network, the model is modified to be able to map an inverse path. This means that the input of the model will be the temperature and the outputs are the welding variables for the control of the process. In the following section the procedure for the construction of reverse mapping will be discussed further.

6.5.3.1 Reverse mapping of welding variables and temperature modelling.

In order to construct the inverse mapping of the many-to-one network the following steps were taken. More detail of the method can be found in references (137-138)

- A back-propagation feed-forward model with the following configuration was constructed Fig 6.7 :

Four PE in input layer, which receives the welding variables (current, voltage, torch angle, and travel speed) as an input;

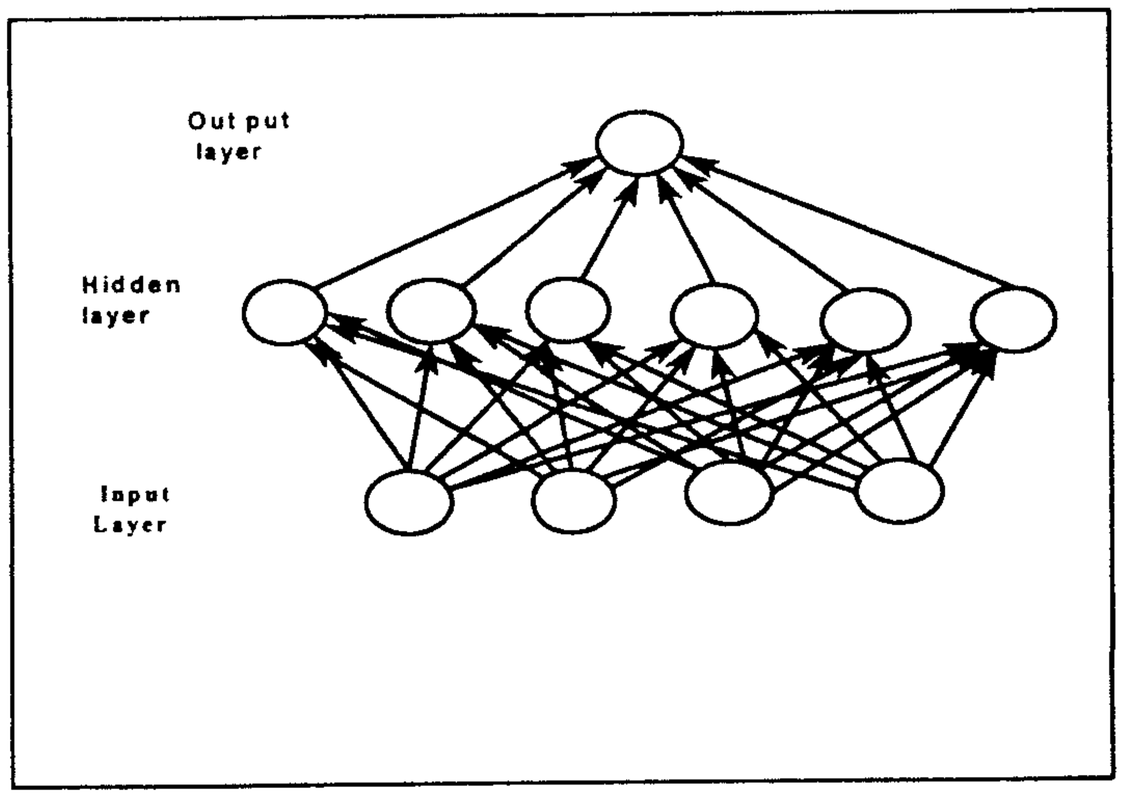

Fig 6.7 Four-to-one feed-forward welding variables-temperature model

- One hidden layer with six PE;.

This number was extracted from following equation (115), and by trial and error method.

$$h = \frac{T_c}{5x(m+n)} \quad \text{where}$$

h = number of PE in hidden layer

T_c = number of training case

m = number of input

n = number of output

- One PE in output layer, which outputs the temperature of the plate during welding;

- The Delta-rule for learning rule was selected.

  This rule is based on reducing the error between the actual output of PE and its desired output by modifying incoming connection weights.

- Sigmoid transfer function was selected.

  This is the transfer (activation) function for PE where the output value changes continuously from 0 to 1 over a range of values. PEs with Sigmoid transfer function generated graded response. Thus, selection of this function creates more "states" for the neural network.

- The network was trained for 20,000 training iterations, in which the RMS error became constant, and the network did not converge any more.

- After training the network, all of the weights were fixed.

- A new input layer with one PE was added to the network below the old input layer

Fig.6.8

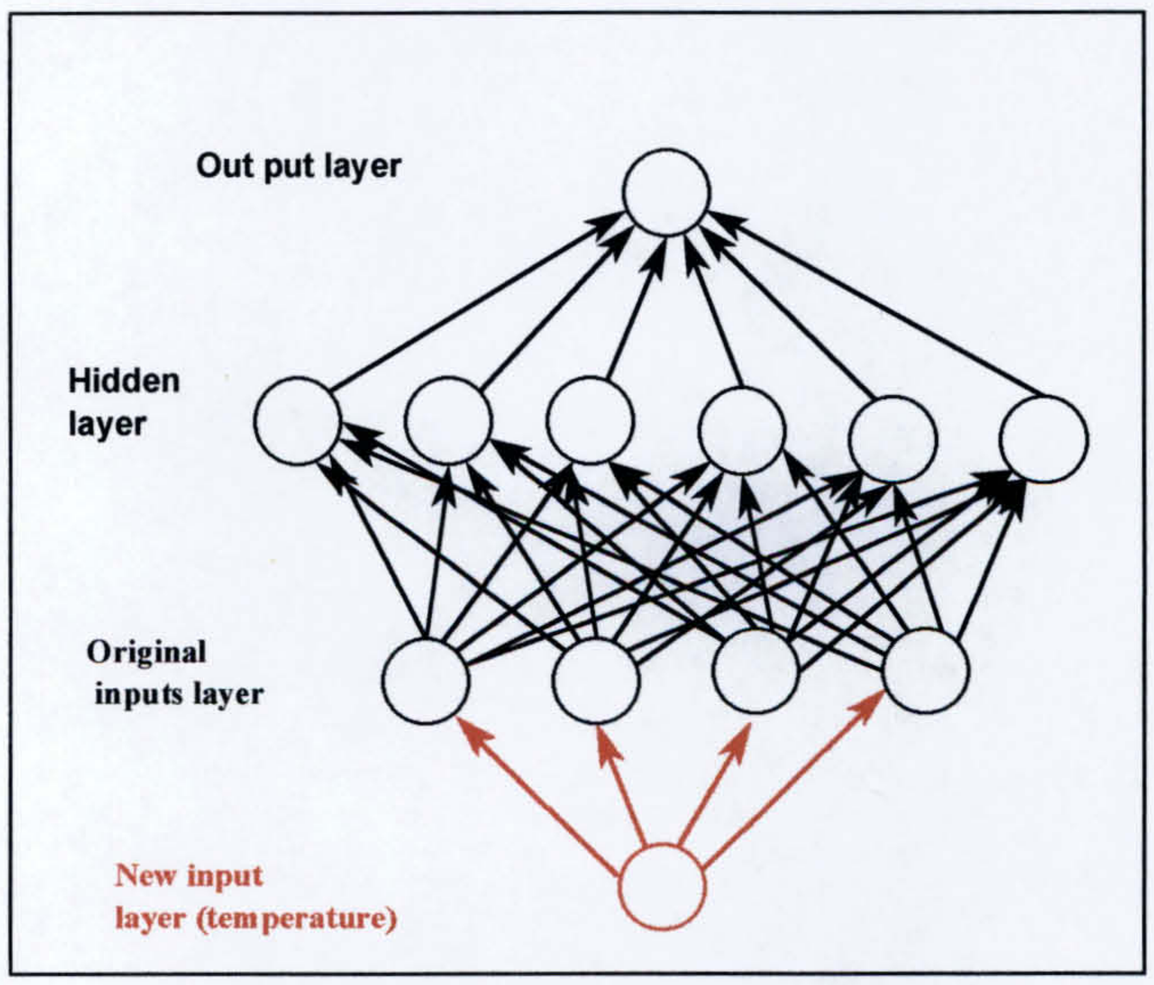

Fig 6.8 Inverse model diagram.

- the delta learning rule was applied to the old input layer therefore this layer became a hidden layer for the modified model.

- A new training file was made. This file which was a single piece of data, in the form of 1,X where X is the measured temperature that we want to find the corresponding input variable for.

- The new network was trained with the single piece of data until the minimum output error was obtained

- When the network converged the weights from the new PE to the old input PEs were recorded. These were the values for the new model which give the predetermined output for the original model.

The result of this modelling is shown in table 6.5.

Evaluation of this model has shown that this method provides improved mapping of temperature to welding variables compared with the 1-4 BP, and 2-4 RBF networks. The disadvantage of this technique is that it cannot be used for real time control of dynamic systems, because for each new temperature the network must retrain to calculate the relevant welding variables.

No.	type of data (penetration depth)	No. of original input PE	No. of original Hidden PE	No. of original output PE	No. of original training iteration	No. of inverse model iteration	% of average Error
1	70 %-79%	4	6	1	20,000	500	4.9
2	80% - 89%	4	6	1	20,000	500	5.17
3	90% - 99%	4	6	1	20,000	500	3.9
4	100% - 110%	4	6	1	20,000	500	3.2

Table 6.5. Result of reverse modelling.

6.5.4 Four-to-one (Welding variables-Temperature)neural network modelling

Since 1-4 (temperature to variables) modelling has not been found to be sufficiently accurate, and since reverse neural network control models discussed in the previous section are not suitable for real time control in GMAW, an alternative indirect approach has been taken. In this approach a four-to-one(welding variables-temperature) model is used as a reference model to predict the surface temperature for a set of welding variables. A fuzzy logic model is then to be used to compensate the welding variables corresponding to the actual temperature measured during welding. For this purpose various types of neural network model with different configurations have been constructed and evaluated. The modelling techniques used were: Backpropagation (BP) network, Reinforcement network with Genetic Algorithm (GA), Radial Base Function (RBF). These modelling techniques, which are appropriate for modelling complex and non-linear systems such as welding, have been investigated in the following sections.

6.5.5 Back propagation welding variables-temperature modelling

Back propagation models have been constructed trained and evaluated for different sets of data. As described in chapter five, data in one set of experiments was categorised by percentage of penetration depth, with corresponding welding variables and measured temperature for each depth of penetration. The classifications were less than 70%, 70%-79%, 80% - 89%, 90% - 99% and 100% - 110%. For each class of penetration depth a different model with different configuration has been constructed and evaluated. The most appropriate modelling architectures are shown in table 6.6. The other back-propagation model properties were kept constant for all of the models and are as follows;

- Learning rule : delta Rule
- Transfer function: Sigmoid
- Number of epoch: 16
- Data pre-processing: normalising
- Learning Iteration : 20,000
- Test Iteration: One pass all of the test data.

Results for the BP network are shown in table 6.6.

No.	type of data (penetration)	No. of input PE	No. of hidden 1 PE	No. of hidden 2 PE	No. of output PE	Temperature Error	% of Average Error
1	70 %-79%	4	6	3	1	± 29-34°C	4.40
2	80% - 89%	4	6	-	1	± 31-43°C	4.46
3	90% - 99%	4	6	3	1	± 36-48°C	5.63
4	100% - 110%	4	6	-	1	± 25-34°C	3.77

Table 6.6. Result of Back-propagation modelling

6.5.6 Genetic reinforcement Learning modelling

To create a Reinforcement Network the following steps were taken:

- Select the number of PE for the input layer as 4 (current, voltage, torch angle, and welding speed);
- Select the number of PE for output layer as 1 (temperature);
- Select the number of PE for the hidden layer, according to equation in section 6.5.3.1, and by trial and error method;
- Select a Learning Rule: Genetic Reinforcement Learning (GRL) has been used for all the reinforcement modelling. Unlike back propagation learning, GRL does not have to compute derivatives. This feature makes it suitable in a complex system such as arc welding modelling;

- Select the Number of Individuals: This should be large enough (50 to 100) to provide good starting points to explore most of the weight space (140), Various numbers of individuals were tested and the model was found to perform best with a value of 60;

- Select the Transfer function: The choices for selecting the transfer function are: Linear, Hyperbolic Tangent, Sigmoid, Exponential Function. Due to non-linear relationship, between welding parameters and temperature distribution, the Sigmoid transfer function has been selected;

- Select a training set and a test set from experimental data for training and evaluation of the network.

Results of the GRL models are shown in table6.8.

Type of data (penetration)	No. of Input PE	NO. of Hidden PE	No. of Output PE	No. of Individual PE	Temperature Error	Average % Error
70 %-79%	4	6	1	60	±32-47 °C	4.89
80% - 89%	4	6	1	60	±30-40 °C	4.23
90% - 99%	4	6	1	60	±26-35 °C	4.1
100% - 110%	4	6	1	60	± 25-36°C	4.09

Table 6.8. Result of GRL modelling with corresponding depth of penetration.

The results show that the welding variables-temperature models developed by Genetic Reinforcement Learning technique are able to predict the output (surface temperature) for specified welding variables inputs(welding current, welding voltage, torch angle, welding speed) with a reasonable degree of accuracy. A problem with this modelling technique is that they are very slow in training.

6.5.7 Radial Base Function (RBF) modelling

The Radial Basis Function network is usually used for modelling of highly non-linear problems (139), such as modelling of welding variables and surface temperature of a work piece. The Radial Base Function used in this research is based on the technique proposed by Moodey and Darken proposed technique (136). It consists of three layers, an input layer, a prototype (hidden) layer and an output layer

For construction of the feed forward RBF network the following steps have been taken:

- Selection of the number of input PEs as 4 (torch angle, current, voltage, and welding speed);

- Selection of the number of output PE as one (temperature);

- Selection of the number of prototype PEs, this number cannot be determined in advance. The suitable number is found by trial and error method. The network was first constructed, trained and evaluated with a small number for prototype PEs, then with other network variables kept constant, the number of PEs are increased by 10 each time. This was continued until the minimum error was obtained, as is shown in figure 6.8, where the number of prototype PEs is 70 and the error is minimised as 1.88 % for the case of 100 – 110 % penetration;

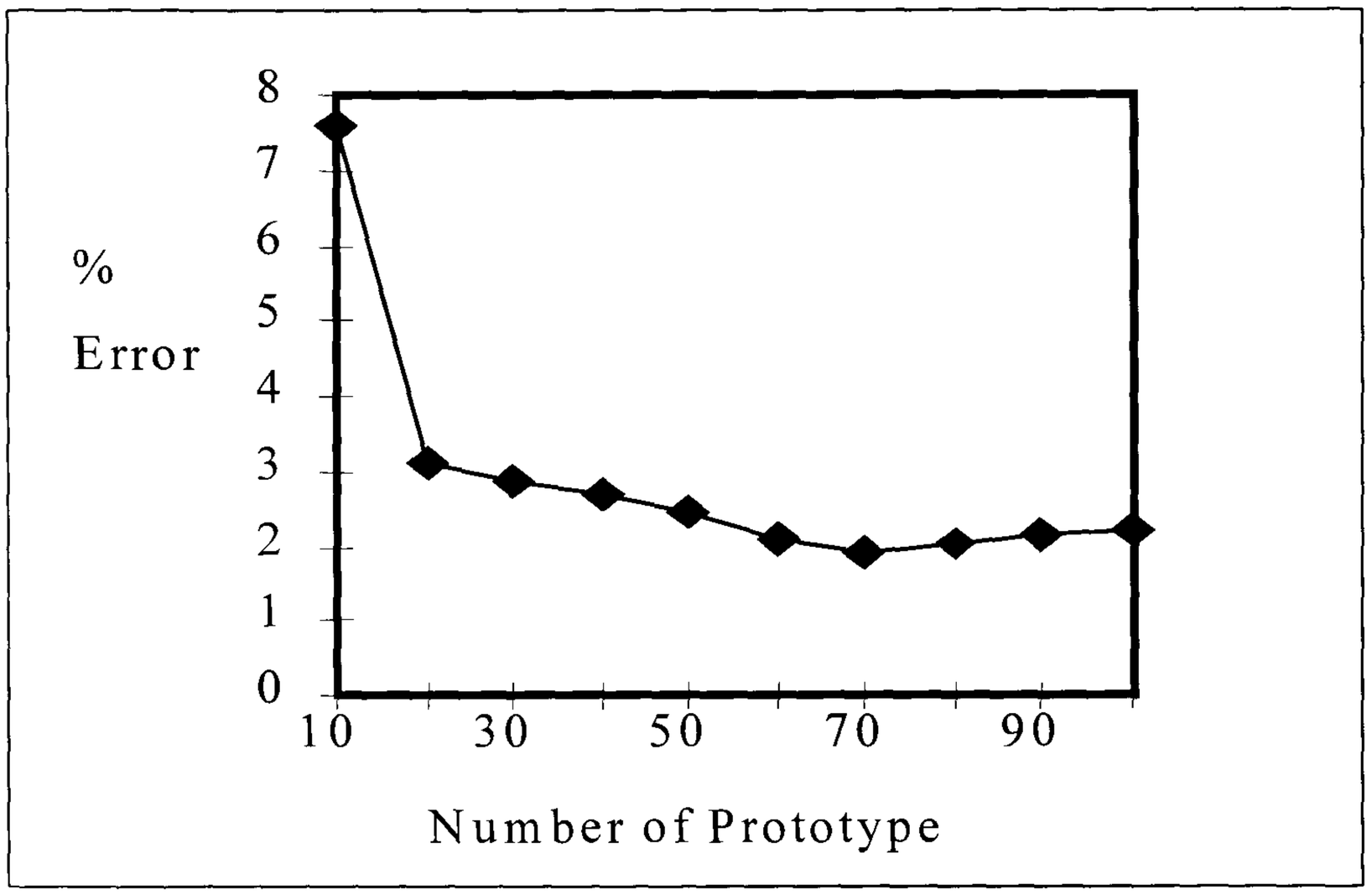

Fig 6.8 Result of trail and error prototype selection for 100%-110% depth of penetration mode.

- Selection of learning coefficient (0.500). Learning coefficient or learning rate can be selected between 0 - 1. With a large learning rate, a network may experience large oscillation during training. In fact, if the rate is too large the network may never converge. Smaller rates tend to be more stable, but with rates too small, the training of the network takes a very long time;

- Selection of the Learning rule as Delta-rule, and transfer function as Sigmoid which are appropriate for non-linear mapping;

- Selection of the training and test data for each model.

After construction and training the models were evaluated by calculating the percentage of error between the network output predicted temperature and the actual temperature of the evaluation data set.

Several models with different configurations for each data set, classified by depth of penetration have been constructed, trained for 30,000 iterations(which the RMS

error was constant) and evaluated. The result of the most appropriate models are shown in table 6.7.

No.	type of data (penetration)	No. of input PE	No. of prototype PE	No. of output PE	Temperature Error	Average % Error
1	70 %-79%	4	70	1	± 19-27°C	2.82
2	80% - 89%	4	70	1	± 24-33°C	3.5
3	90% - 99%	4	70	1	± 17-23°C	2.69
4	100% - 110%	4	70	1	± 11-16°C	1.88

Table 6.7. Result of RBF modelling with corresponding depth of penetration.

Results of evaluation of the models shows that the RBF network can predict the surface temperature for a set of welding variables with a good degree of accuracy and better than the GRL networks. Also the training time was shorter in comparison with other network techniques. Among the above results, the performance of the RBF models for 100% - 110% of penetration was considered adequate, and this was selected as the final ANN model for the welding control model. This is discussed further in the next chapter.

6.6 Discussion

In this chapter the effectiveness of using neural networks for process modelling of welding variables and temperature distribution was demonstrated.

In the preliminary modelling experiment reported by the author, and not included in this theses (136), the data used was mixed in terms of depth of penetration. Although the result of evaluation of the network was acceptable(the average error for surface temperature measurement was ± 28°C), on re-evaluation of the experimental results it was found that some of the output temperatures were identical to those from entirely different sets of inputs as shown in table 6.9. After sectioning of those joints and measuring the depth of penetration it was discovered that when the depth of penetration increased due to increasing current or voltage or decreasing the welding speed, the temperature on surface decreases probably due to heat loss from the backside of the plate. These identical outputs for different inputs make the network confused in attempting to find the accurate relationship between input and output. Therefore for this research the data was classified according to the depth of penetration. This classification makes the models more accurate, and effective, in terms of application, because weld depth of penetration may be varied for different joint applications.

Different networks with various mapping techniques have been constructed and evaluated. Direct one(temperature) to four (welding variables) models, were not satisfactory, probably due to the high non-linearity of welding phenomenon. The inverse mapping model has the limitation that the network must re-train every time for each new set of inputs. These networks are also not consistent. This is because an inverse model will use the trained weights to find a proper set of outputs for the input. Therefore it is possible that it will generate different output (welding variables) for the same input (temperature).

Torch Angle °	Current	Voltage	speed	temperature °C	Depth of Penetration %
70	380	37	80	733	93
70	390	47	90	733	77
90	380	37	85	733	102
110	400	37	80	733	110
70	380	37	85	687	65
70	390	37	80	687	103
70	400	42	80	687	107
70	400	47	90	687	78
110	390	37	85	781	102
110	400	37	90	781	85

Table 6. 9. Some identical temperature measurements with different welding input (from136)

The non-direct approach for predicting the appropriate sets of welding variables for specific surface temperature measured during welding was found to be more suitable for achieving the objective of this research. This approach is to use a four to one neural network model to predict the temperature for corresponding welding variables, in conjunction with a fuzzy logic system, to compensate the welding variable due to variation of the temperature during welding. In order to select the most suitable network technique and architecture, different types of network with various configurations have been constructed and evaluated.

The result of evaluation of the networks shows that the Radial Basis Function (RBF) network achieves the minimum error. The average error of temperature prediction via the network is ±13°C (1.88%) which is considered acceptable for controlling the welding variables via fuzzy logic rule base system discussed in the next chapter.

Chapter Seven Neuro-Fuzzy Control Model

7.1 Introduction

This chapter describes the application of a control model using neural network and fuzzy logic modelling to control a Gas Metal Arc Welding process. These control models may be used to improve weld quality, by adjusting the controllable welding variables in response to changes in workpiece surface temperature measured at a point adjacent to the weld line during welding. Neural network modelling, described in the previous chapter, was employed to develop a reference model of temperature in relation to welding variables. The fuzzy logic model is used for compensating welding variables when the temperature in the surface is varies from that predicted by the reference model.

Design of the Fuzzy Logic model is described in section 7.3. Development of the Neuro-Fuzzy control model is then discussed in section 7.4. In section 7.5 the control model is evaluated and the performance of the models discussed. Fuzzy modelling has been confined to achievement of 100-110 % penetration.

7.2 Welding control model

The most important quality feature in butt welding is the depth of penetration. Unlike bead width, height, and toe angle which can be measured in process from the top face of the joint, the penetration can only be measured directly from the back face, this is often difficult or impossible. Therefore non-direct methods as discussed in chapters three and four have been researched and developed.

The quality characteristics of a fusion welded joint are strongly dependent on the amount of heat transferred to the base metal. The temperature distribution in the top surface of the joint is a function of the heat input. ANN models of the relationships

between the temperature at a point in the surface of the workpiece, satisfactory depth of penetration, and the welding variables that achieve them have been developed. The application potential for control using these models is significant since, unlike many other top surface monitoring methods, it does not require sensing of the highly transient weld pool shape or surface. As is discussed in the previous chapter it has proved difficult for neural network models to directly map the surface temperature and the four controllable welding variables. For this reason the control model developed in this research consist of two parts;

- A Neural Network model which is used as a reference model and predicts the point temperature on the surface of the workpiece corresponding to a set of welding variables.

- A Fuzzy Logic control model which regulates the welding variables, depending on the difference between the neural network's temperature estimation and the actual point temperature measured by an infrared sensor.

The integrated Neuro-Fuzzy control model compensates the welding variables to achieve the desired weld quality as indicated by the depth of penetration. The design of the Fuzzy Logic rule base control model is discussed in the next section.

7.3 Fuzzy logic control model

Using the top surface temperature measured, via an infrared sensor, to control the welding variables with a dynamic mathematical model or a neural network model, as discussed in chapters four and six does, not guarantee sufficiently accurate control performance. This is mainly due to the highly non-linear nature and complexity of GMA welding. One approach to this problem is to apply fuzzy modelling which is appropriate for controlling a complex and non-linear process such as GMA welding (141). Fuzzy rule-based control can realise heuristic rules obtained from human experiences which cannot be expressed in mathematical form, and does not require a large amount of computation time as would traditional adaptive algorithms (142).

The fuzzy logic model will compensate the welding variables to provide acceptable control performance at different welding conditions. The block diagram of the fuzzy logic control model is shown in figure 7.1 The system consists of fuzzification, inference engine, control rules and defuzzification. The inputs to the model are the temperature difference (ΔT) between measured temperature and that predicted by the neural network reference model described in chapter 6, and the initial welding variables which are discussed in the following sections.

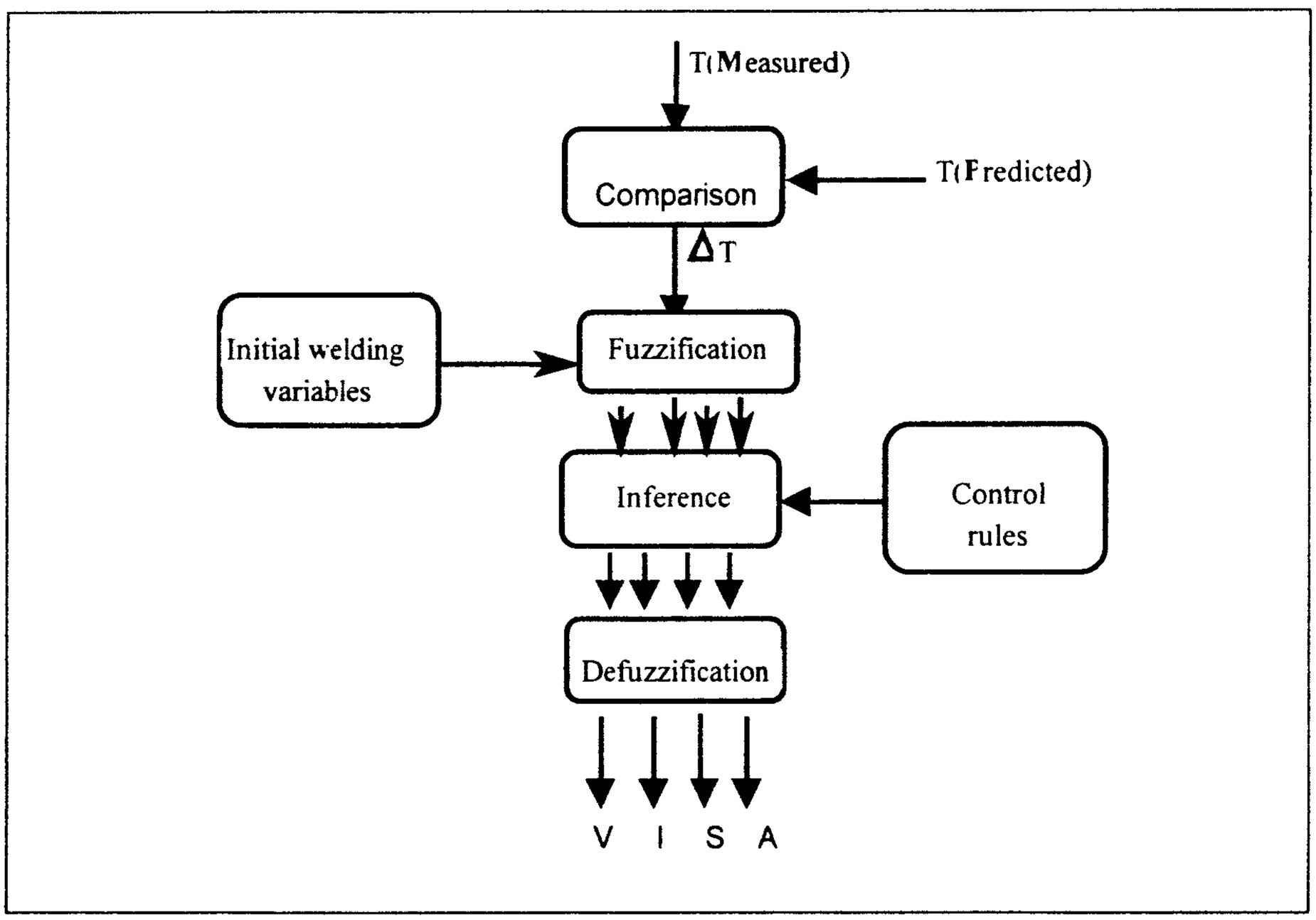

Fig 7.1 Block diagram of fuzzy controller

7.3.1 Comparison of temperature

The variation between the surface point temperature T_p predicted for the set of welding variables by the neural network model, and temperature measured T_m via the infrared sensor is calculated. If this is outside the predefined allowable range an error message is passed to the fuzzy model. At the same time an error message may inform

the operator of the condition to prompt him to check for possible causes of error such as sensor position, wrong welding position, or inaccurate setting of initial welding variables.

7.3.2 Fuzzy model input variables

In the proposed model five input variables (antecedent): difference in temperature ($\Delta T = T_m - T_p$), initial welding current (I_I), initial welding voltage (V_I),, initial torch angle (A_I),, and initial welding speed (S_I), have been selected. Four output variables (consequent) have been chosen which are: welding voltage (V), welding current (I), travel speed (S) and torch angle (A), which are predicted corresponding to the difference in temperature ΔT and the initial welding input variables.

7.3.3 Fuzzification

The process of fuzzification converts an input value into linguistic terms and determines the corresponding grade of membership for that value. For example, an input welding speed can be fuzzified into a fuzzy set with members **LOW** for 800 mm/Min, **MEDIUM** for 850mm/min, and **HIGH** for 900 mm/min. Fuzzifying requires specifying membership functions, one for each fuzzy set member. Fuzzification of difference in temperature sets are defined as follow:

BN : big negative

N : negative

NC : no change

P : positive

BP: big positive

For other input variables to the model, current, voltage, welding speed and torch angle only 3 fuzzy subsets are defined as follows:

L : low

M : medium

H : high

The numerical values of these levels are the same as for the actual welding variables used for the welding experiments reported in this research.

To achieve a good control performance via a fuzzy model, close partitioning of fuzzy sets are advantageous. On the other hand when partitioning is increased, especially in multi-input variables, the number of rules increases.

As described in chapter 3, different types of membership function have been used in fuzzy logic control models. The Triangular membership function, spaced equally, (fig.7. 2), which is popular with fuzzy logic practitioners (143), has been used for this research due to its simplicity.

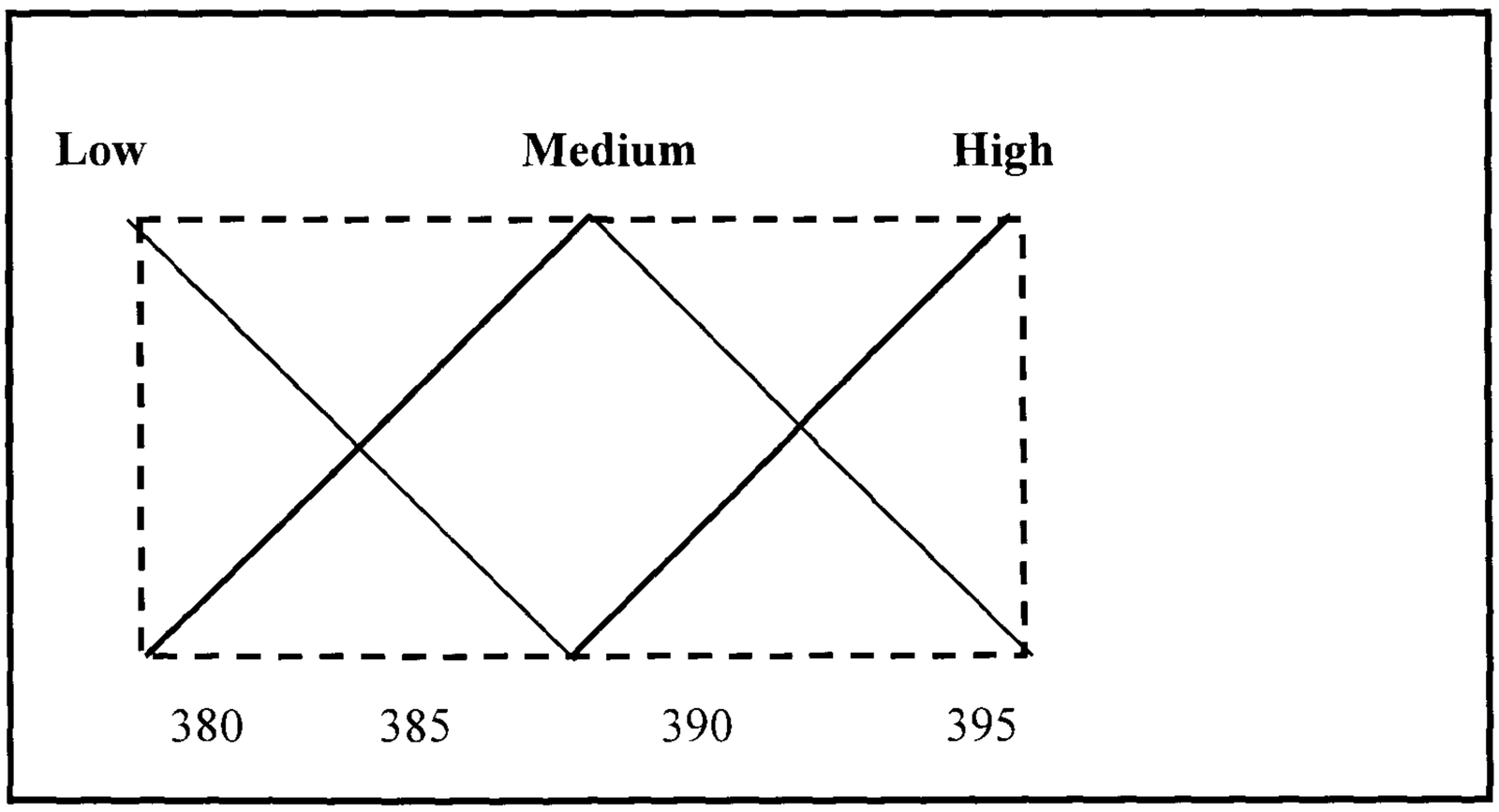

Fig 7.2 Current as Input (antecedent) variable.

For output (consequent) variables (current, voltage, welding speed, and torch angle) five levels with triangular membership function (fig.7.3) have been defined as follows:

VL : very low

L : low

NC : no change

H : high

VH : very high

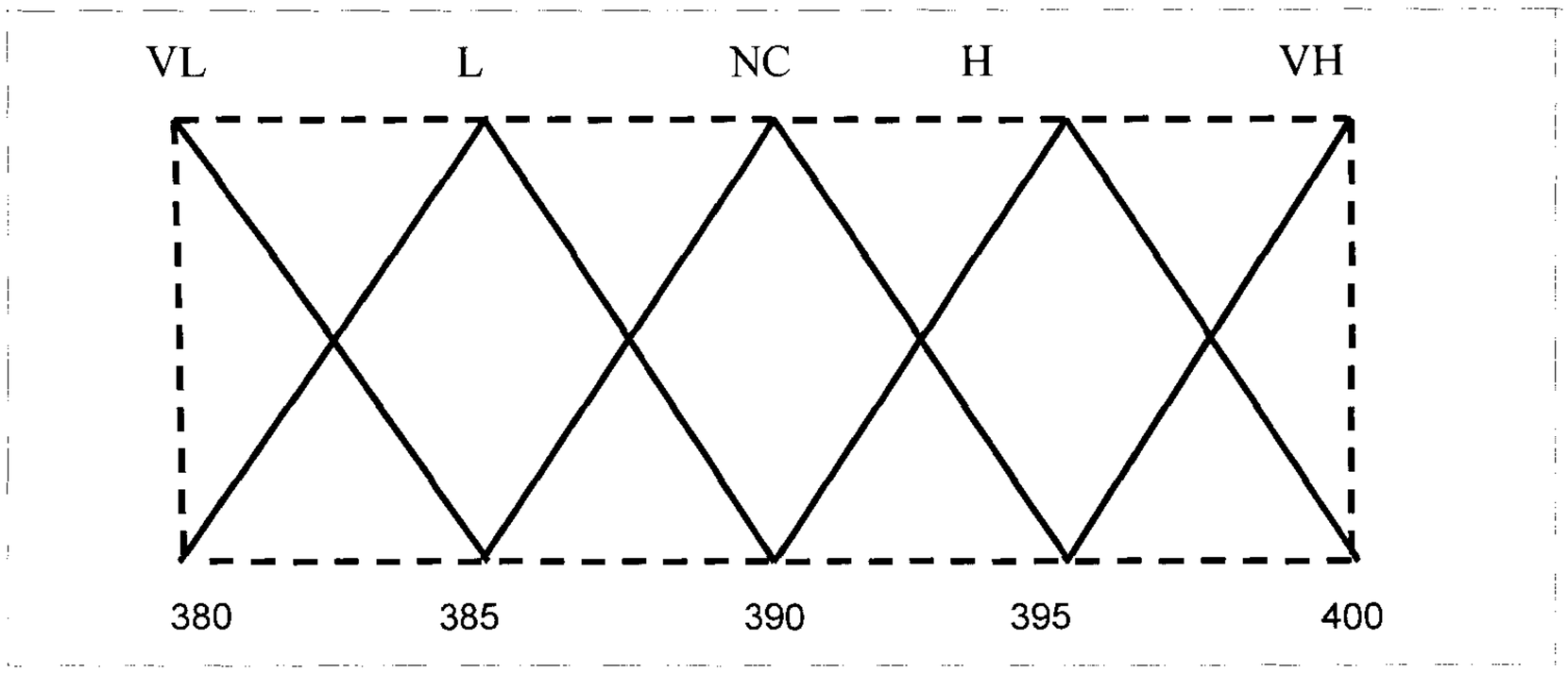

Fig.7.3 Current as an output(consequent variables).

7.3.4 Fuzzy operator

In fuzzy logic where computation of imprecise knowledge is concerned, the linguistic operations, such as ***AND, OR*** and ***NOT,*** use different mathematical operators. The basic operations in fuzzy sets include:

- **Intersection of Sets** : a new set is generated from the intersection of two given sets A and B, if the new set contains exactly those elements that are contained in A ***AND*** in B.

- **Unification of Sets** : a new set is generated from unification of two given sets A and B, or B and A, if the new set contains all elements that are contained in A ***OR*** in B or in both.

- **Negation of Sets**: a new set containing all elements which are in the universe of discourse but ***NOT*** in the set A, the negation of A.

Zadeh (144) suggested the minimum operator for the intersection and the maximum operator for the union of two fuzzy sets. It is easy to notice that these operators coincide with the crisp unification and intersection if membership degrees consider only 0 and 1.

7.35 Rule base

The rule base consist of a set of rules which is used to formulate and represent expert knowledge in the form of :

IF (condition or antecedents)

THEN (conclusion or consequence).

Each rule has two essential parts, the condition or antecedents and the action or consequences. The rule can be a single or multi condition. The number of rules depends on the number of input variables, and corresponding number of membership functions. In the fuzzy logic welding control model the rules are in the form of: **IF** a set of input variables, (ΔT, I_i , V_i, S_i , A_i) **THEN** output one modified variable, (I_p or, V_p or, S_p or, A_p). Rules have been extracted from the experimental welding data using the author's experience. In each rule fired, the set of 5 inputs causes one of the

variables to be output. A total of 327 rules have been developed and are included as appendix 3

7.3.6 Inference system

A fuzzy inference system is the actual process of mapping from a given input to an output. The process applies membership functions, fuzzy logic operators and if-then rules. As shown in fig 7.4 the system stores separate fuzzy rules and fires in parallel the set of 4 rules that give the 4 output variables, that apply for the given set of inputs.

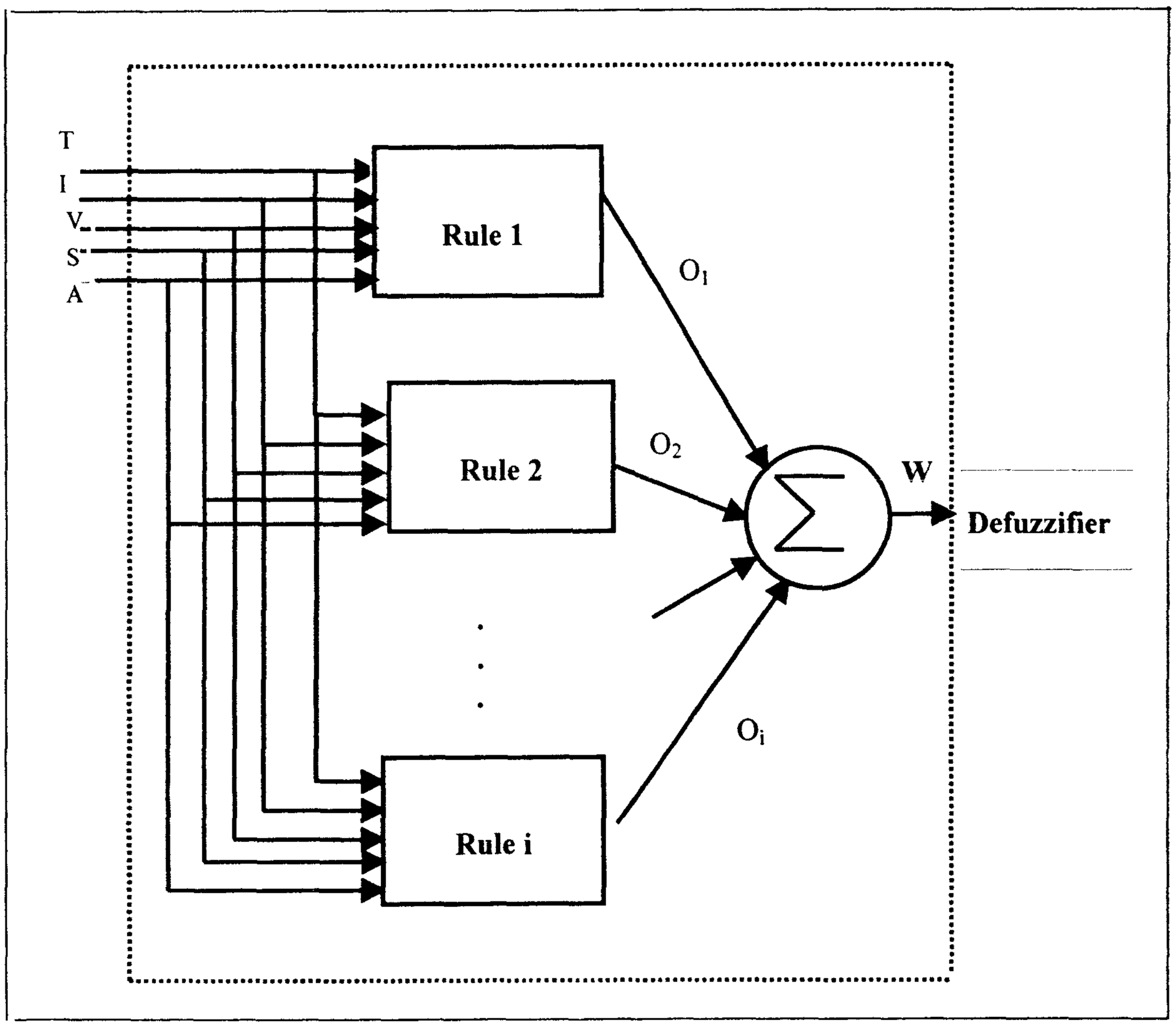

Fig. 7.4 Fuzzy system architecture.

In the figure 7.4 T, I, V, S, and A are the fuzzy system inputs. Each rule which is fired transforms only one variable and outputs its new linguistic value O_i. W is a set of predicted welding variables (current, voltage, travel speed and torch angle) in linguistic form. This process is known as Mamdani's fuzzy inference method and is the most commonly applied fuzzy methodology for control systems. In this method the fuzzy sets from the consequent of each rule are combined through the aggregation operator, and the resulting fuzzy set is defuzzified to yield the output of the system (145).

7.3.7 Defuzzification of fuzzy set

Defuzzification is the calculation of a crisp numerical value as the output based on the linguistic result. The input for the defuzzification process, as shown in fig 7.4, is the fuzzy output which resulted from aggregation of the rules output. Output of the process is a crisp number. The process of defuzzification in fuzzy logic control systems is not standardised (146). There are several methods in use such as:

- average of maximum (maxav);
- centre of the area;
- largest of maximum;
- smallest of maximum.

Alternatively, rules may be written to implement almost any desired defuzzification scheme.

Perhaps the most popular defuzzification method is the centre of area method (145), which calculates the centre of gravity of the distribution for the control action. In the modelling discussed in this research the centre of area method is employed for defuzzification.

7.3.8 Evaluation of fuzzy model operation

Evaluation of the operation of fuzzy model for controlling the welding variables has been conducted based on an examination of the model performance for sets of constant input welding variables (initial welding current, initial welding voltage, initial welding speed, initial torch angle), and difference in temperature. The model prediction of welding variables should be the same values as the initial input welding variables to the fuzzy model when the temperature difference is within ± 13 °C, the allowed sensor / ANN error. The inputs of the model are listed as follows:

Temperature difference: - 100°C - +100°C

current: 385 Amp.

voltage: 40 Volt.

welding speed: 850 mm/min

torch angle: 90°

For evaluation purposes the torch angle was kept constant. This is due to the limitation of the available MATLAB fuzzy logic software, which has a restricted range for number of outputs and number of rules. Therefore the less important welding variables were selected to be constant for evaluation purposes. This problem can be overcome by rewriting the fuzzy logic software or purchasing professional fuzzy logic software. Results of evaluations are shown in table 7.1.

As shown in table 7.1, the predicted welding variables are close to the initial welding variables when the temperature difference is in the range of ±13°C. The model should propose modified welding variables except when the temperature difference is within ±13°C. Also it can be seen that when ΔT is greater than ±13°C the output variables from the model are in the correct order. That is, when penetration is low as indicated by negative ΔT ($T_m < T_p$) the set of output variables causes an increase in heat energy

per unit volume of weld metal. The converse applies for positive ΔT. Therefore, the operation of the fuzzy logic model was considered to be satisfactory. Section 7.6 describes evaluation of the accuracy of output variables.

Temp. Difference °C	Initial Current Amp.	Initial Voltage Volt	Initial Speed mm/min	Initial Angle degree	Predicted Current Amp.	Predicted Voltage Volt	Predicted Speed mm/min	Predicted torch angle °
-100	385	40	850	90	399	47	800	90
-80	385	40	850	90	397	46	810	90
-60	385	40	850	90	396	46	805	90
-40	385	40	850	90	395	42	800	90
-20	385	40	850	90	393	41	820	90
-10	385	40	850	90	388	41	830	90
0	385	40	850	90	385	40	850	90
10	385	40	850	90	385	40	860	90
20	385	40	850	90	385	40	860	90
40	385	40	850	90	384	39	870	90
60	385	40	850	90	383	39	900	90
100	385	40	850	90	380	37	900	90

Table 7.1 Evaluation of fuzzy logic model.

7.4 Neuro-fuzzy control model

The Neuro-fuzzy welding control model consists of the following programmes:

- Neural Network Model to predict the surface temperature expected for a set of initially set welding variables:

- Analog to Digital conversion to convert the analog infrared sensor output to digital input to the control mode;

- Fuzzy logic model to compensate the welding variables according to the difference in temperature between that predicted by the neural network model and the surface temperature measured via the infrared sensor.

The flowchart of Neuro-fuzzy Control Model is shown in figure 7.5. In order to integrate the above programmes into the welding process, software has been written in C++. This is described in the next section.

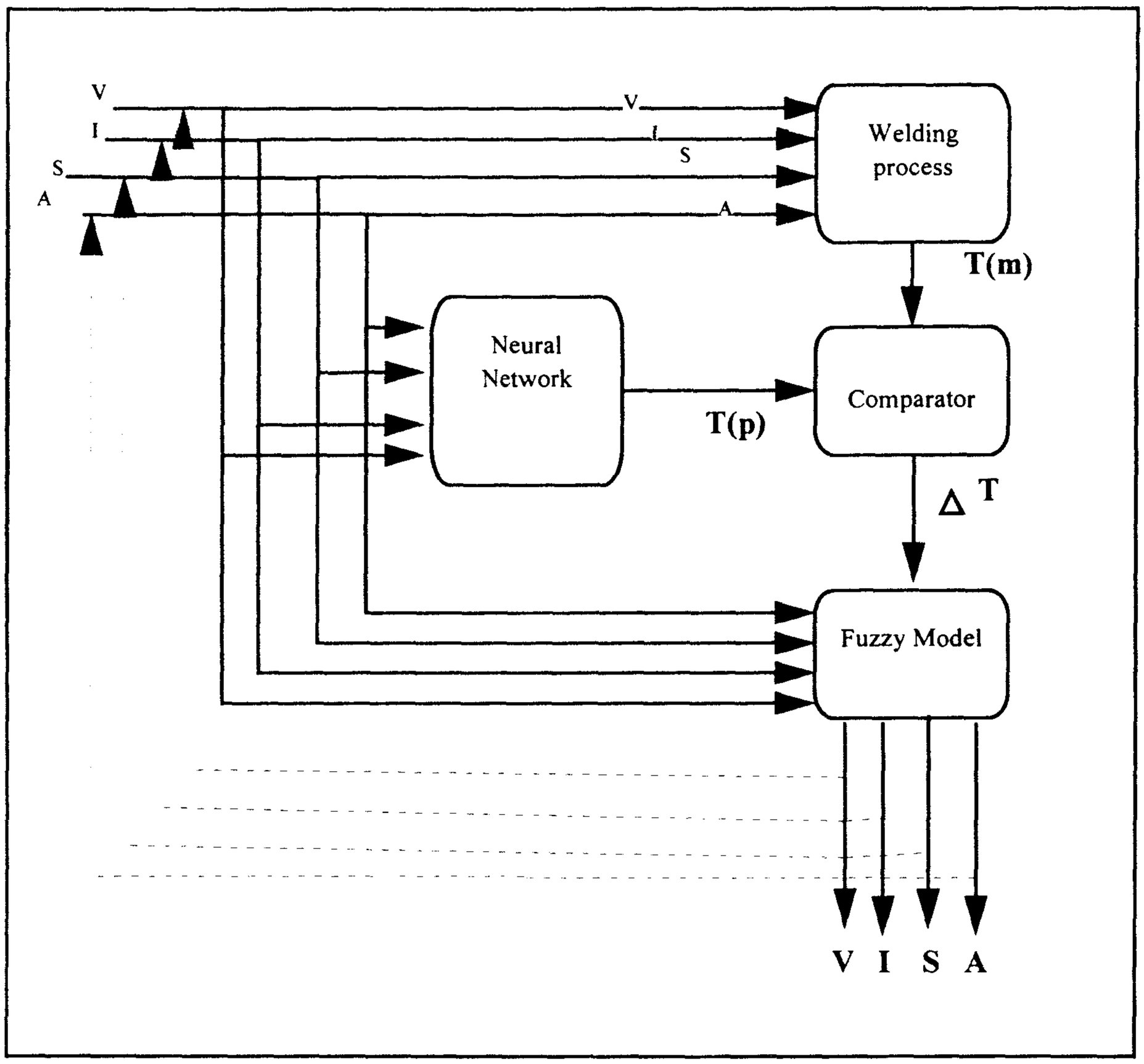

Fig.7.5 Neuro-Fuzzy control model flowchart.

7.4.1 Control model software

The software was written for the evaluation of the Neuro-Fuzzy Control Model. For evaluation of the model, the software operates as follows:

1. The user enters the required depth of penetration into the software. Although most welded parts require 100 percent depth of penetration, some low or non-load bearing structures may not require 100 percent penetration. A family of 4

neural network models covering the range of weld penetration 70-110% is available in the control model.

2. The nominal values of the initial welding variables (current, voltage, welding speed, and torch angle) are entered. These values should be within the range of the experimental welding variables as described in chapter 5.

3. The software then executes the neural network model, and prints out the predicted surface temperature. The temperature is also communicated to the comparator.

4. Welding is then initiated, the infrared sensor measures and displays the point surface temperature on screen and communicates this to the comparator. The sensor records temperature measurement along the welding line at 10 mm intervals. For the purposes of the research the software was programmed to ignore the first five and last two records in which instability of welding may be present, and average the remaining measurements.

5. The comparator subtracts the average temperature measurement from the neural network predicted temperature and displays the result on a screen as a "temperature difference".

6. In this stage if the temperature difference is less than ± 13°C (the neural network error, chapter 6) welding will continue without adjustment in welding variables. In this case, the depth of penetration should be the same as initially selected. If the temperature difference is more than ±13°C, then the Fuzzy Logic model is applied to adjust the welding variables.

To control the weld penetration in real time in a production situation the sampling of surface temperature would be modified as following:

- The model will activate when the arc is struck and after a short delay, say 5 seconds, to allow arc and thermal condition to stabilise, surface temperature would then be measured every 10 mm.

- The Neuro-Fuzzy control model would perform on the data received at these intervals.

7.5 Fuzzy logic control model

As described in the previous section the Fuzzy Logic model is applied if the temperature measurement was 13°C more or less than the temperature predicted via neural network. The Matlab Fuzzy Logic Toolbox has been used to construct the fuzzy system model as described earlier in this chapter. At this time, due to limitations in the Matlab compiler software, the fuzzy model can not be integrated into the control model software, therefore the operator has to enter the inputs to the fuzzy model through the keyboard in the following steps.

1. From the Matlab command window the model will be loaded from disk using the "readfis" command. This command reads a fuzzy inference system from a *.fis file on the disk and brings the resulting file into the workspace. The syntax for this command is:

   a = readfis('filename')

2. The command "evalfis" will be used for evaluation of fuzzy inference. This function computes the output vector of the fuzzy inference system. The syntax for this command is:

   Output = evalfis([temperature difference; current; voltage; speed; torch angle], a)

Where "a " is the fuzzy model, which has been loaded, and the welding variables are as described in previous sections.

After the operator enters the input to the 'evalfis' function the model calculates the output which is the set of new welding variables to achieve welds with 100 % depth of penetration.

7.6 Evaluation of neuro-fuzzy control model

A number of experiments have been conducted for the evaluation of the model for 100–110% penetration. These experiments include the evaluation of models for workpieces with zero root gap, 1mm root gap, and variable 1.5mm – 0 root gap,. The remaining joint geometry of workpieces was kept constant as described in chapter 5.

The general procedure for evaluation of models was the sequence of steps as follows;

1. Select welding variables randomly from the experimental welding data that did not produce welds with 100-110% depth of penetration.

2. Follow steps 1 to 6 as described in section 7.4.1 inputting 100% at step 1.

3. The weld was examined for depth of penetration. If depth of penetration was between 100% - 110% and temperature difference was within ±13°C, then evaluation was stopped and the result recorded. Otherwise the evaluation was continued.

4. The average temperature difference, along with the welding variables, were entered into the fuzzy logic model (evalfis function in Matlab command window) to predict the new welding variables to achieve 100 –110% depth of penetration.

5. The procedure of 7.4.1 was followed using the fuzzy logic model predicted welding variables.

6. If the depth of penetration was less than 100% then the original weld and the new weld were sectioned, polished, and etched to enable measurement of the depth of penetration.

The evaluation of models and their result are described in the following sections.

7.6.1 Evaluation of models for joint with zero root gap.

For this evaluation the fixed welding variables, including joint geometry, plate thickness, and type of material, were the same as those used in the welding experiments carried out to provide training data for the neural network modelling as described in chapter 5. The evaluation experiments were conducted in two series following the procedure described in the previous section. In the first series the welding process was carried out with selected initial welding variables. In table 7.2 the initial welding condition, along with the resultant depth of penetration, are shown.

Exp. NO.	Torch angle	Current Amp.	Voltage Volt.	Speed mm/min	N.N. Temp.°C	Measured Temp. °C	ΔT °C	Penetration %
1	90	385	40	900	736	777	41	67 %
2	90	383	37	860	730	682	- 48	83.5 %
3	90	380	37	900	732	733	1	88.5 %
4	90	390	37	850	728	664	- 64	95 %
5	90	390	40	900	745	746	1	98.6 %
6	90	380	42	900	735	828	93	75 %
7	70	385	40	900	716	694	- 22	86.5 %
8	70	390	37	850	712	689	- 23	92 %
9	70	400	42	900	714	738	24	84.5 %
10	110	385	40	900	751	807	56	67 %
11	110	390	37	850	776	740	- 36	73 %

Table 7.2 Initial welding data

For the second series of experiments the temperature difference (ΔT) along with the initial welding variables were entered as an input to the fuzzy logic model. The welding variables which the fuzzy logic model predicted were then used for the second series of the welding experiments. The welding variables predicted by the fuzzy logic model along with resultant depth of penetration are shown in table 7.3.

Exp. NO.	Torch angle	Current Amp.	Voltage Volt.	Speed mm/min	N.N. Temp.°C	Measured Temp. °C	ΔT °C	Penetration %
1	90	387	41	850	769	772	3	102%
2	90	395	39	810	755	743	-12	105%
3	90	*	*	*	*	*	*	88.8%
4	90	395	38	820	733	730	- 3	108%
5	90	*	*	*	*	*	*	98.6%
6	90	383	37	870	730	714	-16	100%
7	70	395	39	820	704	701	- 3	110%
8	70	393	39	820	704	702	-2	109%
9	70	390	38	830	710	704	-11	104%
10	110	389	38	870	768	780	12	98%
11	110	395	37	820	753	747	- 6	100%

* : Workpiece for which the welding variables were not modified due to the value of temperature difference being within ±13°C.

Table 7.3 Modified welding variables with resultant depth of penetration.

In figure 7.6 the cross section of the weld in experiments 1, 6, and 10 with initial and optimised welding variables are shown.

Experiments.1 initial

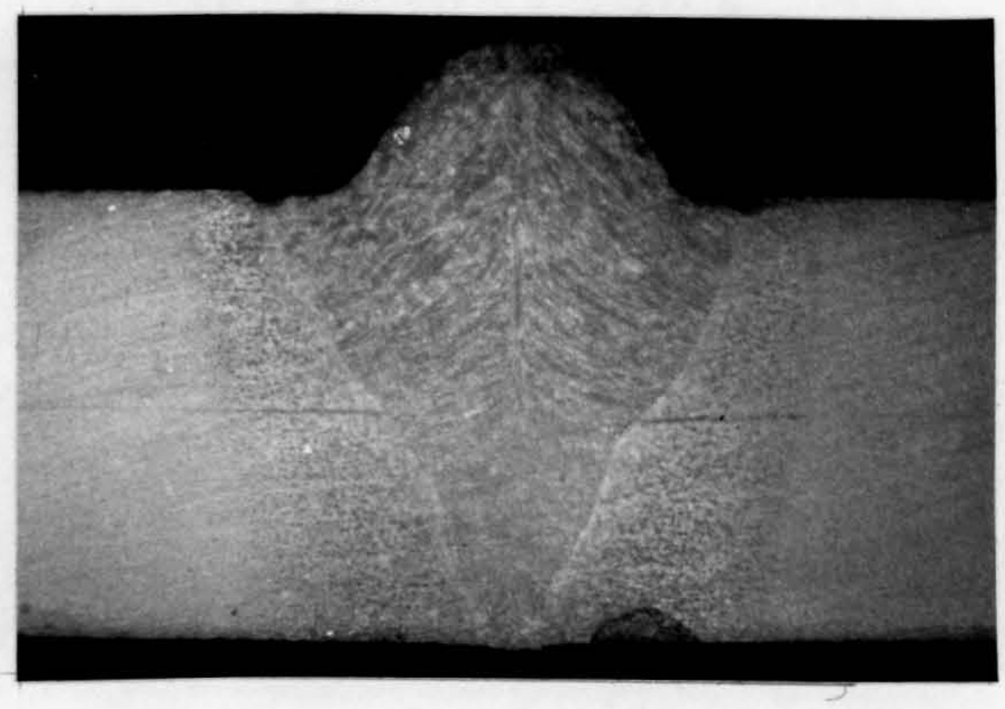

Experiment 1 final

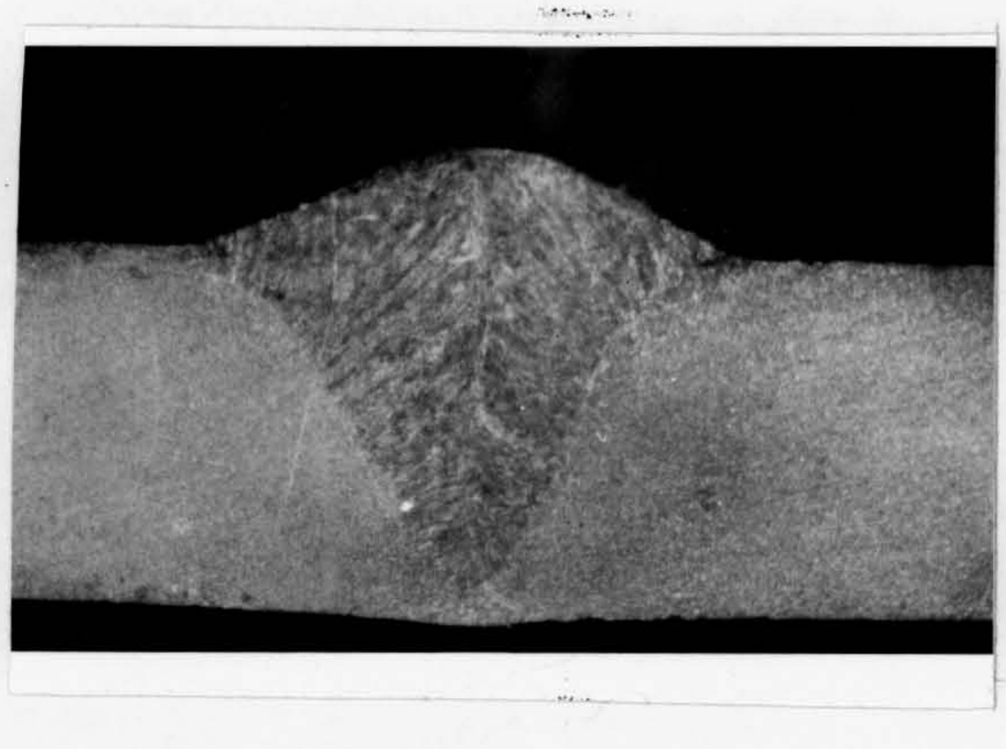

Experiment 6 initial

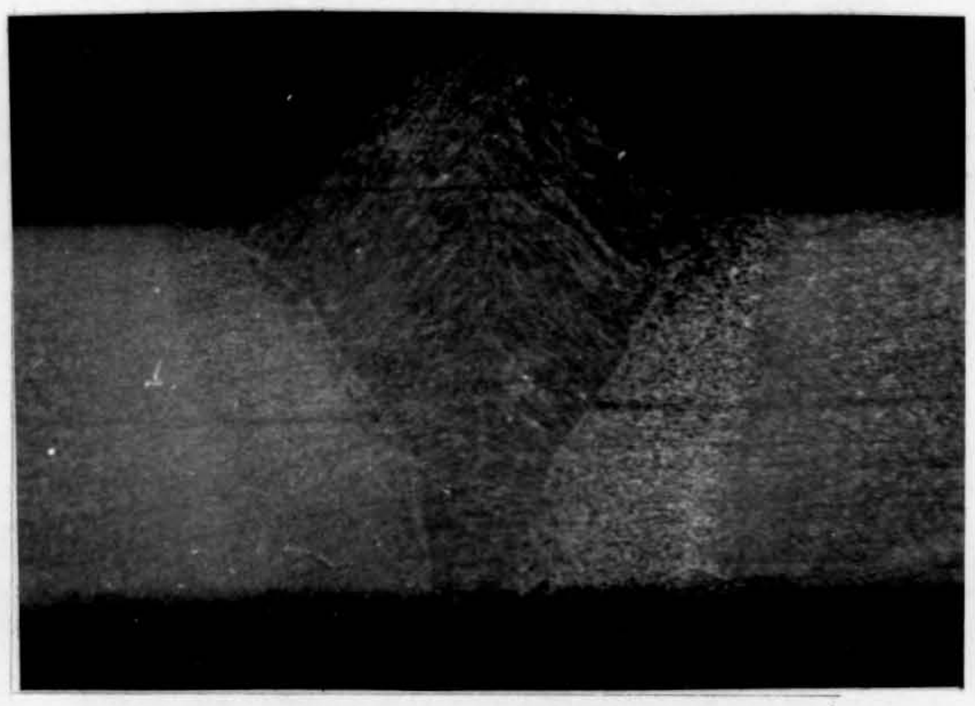

Experiment 6 final

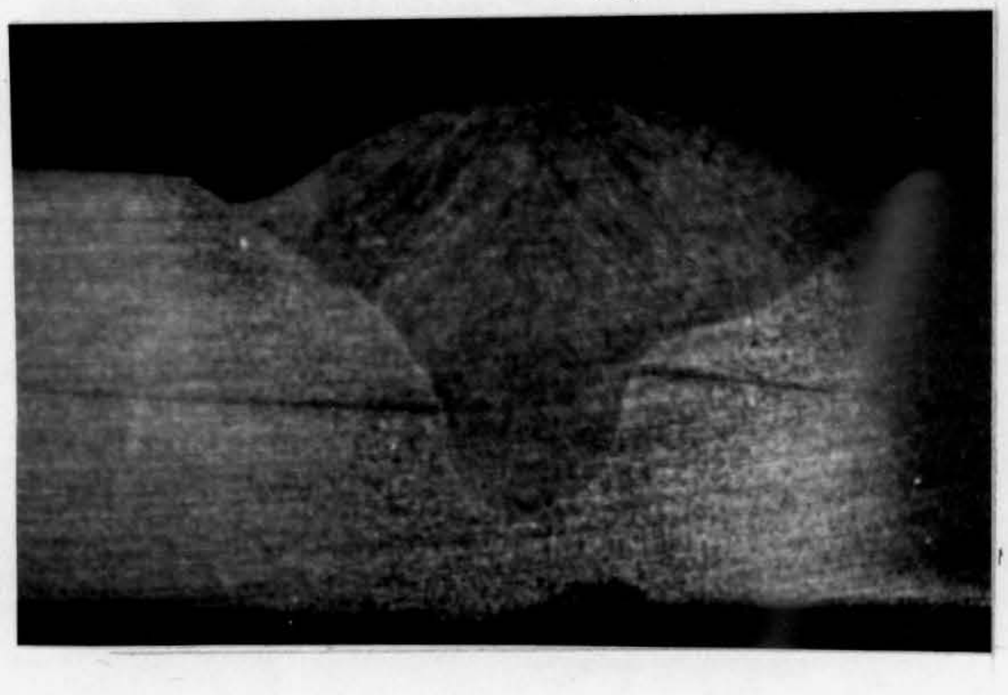

Experiment 10 initial

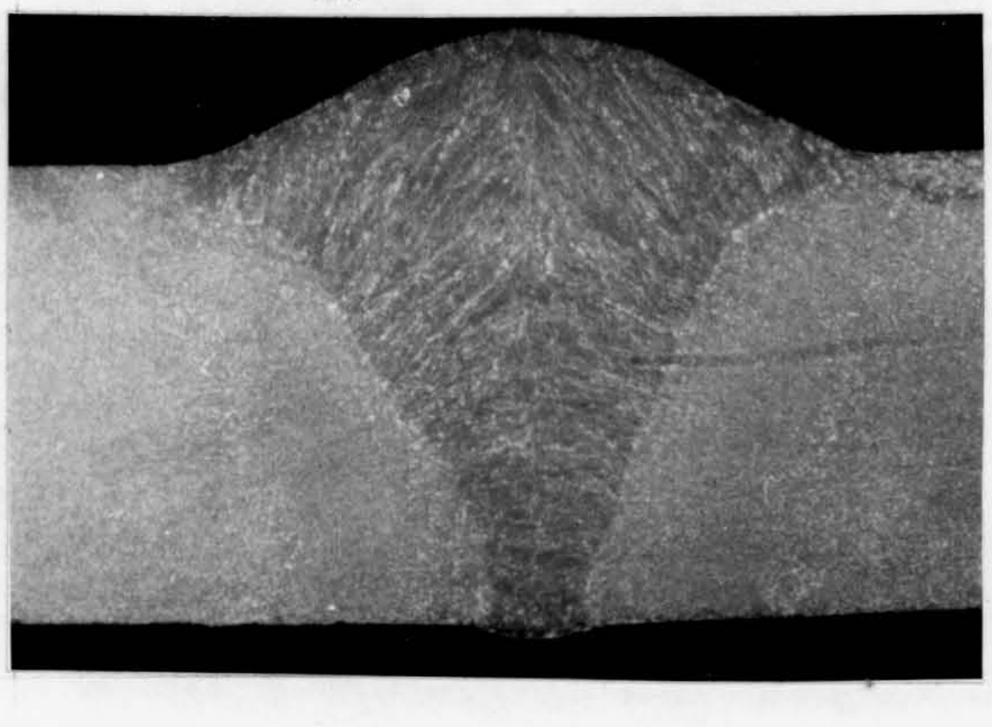

Experiment 10 final

Fig. 7.6 the cross section of the weld in experiments 1, 6, and 10

For experiments 3, 5, and 10, it was necessary to section, polish, and etch the joint to reveal the depth of penetration. In experiments 3, 5, the average temperature difference was within the acceptable range of ±13°C and was repeated with the same welding conditions. Closely similar penetration was achieved. According to the neural network model 100-110% penetration should have been achieved according to value of ΔT but experiments 3 and 5 did not do so. Experiment 5 may be considered to be within the margin of experimental error. However experiment 3 which showed only 88.5% penetration needs explanation. It is first noted that the conditions of experiment 3 were the extreme condition of the test at which the penetration would be expected to be minimum. Also there was no similar set of input variables in the neural network training data set for 100-110% penetration. The remaining experiments produced results in which temperature difference was greater than ±13°C and hence the fuzzy model was invoked. All results showed an improvement in penetration to the desired level except experiment 10 where, however, the penetration achieved is considered to be within the margin of experimental error.

The temperature differences between neural network prediction and sensor measurement, and the measured depth of penetration for initial and final welding experiments are shown in figures 7.7 and 7.8 respectively. These graphs indicate that the Neural Network model prediction and fuzzy logic welding variable modification model can control the quality of welding with reasonable accuracy.

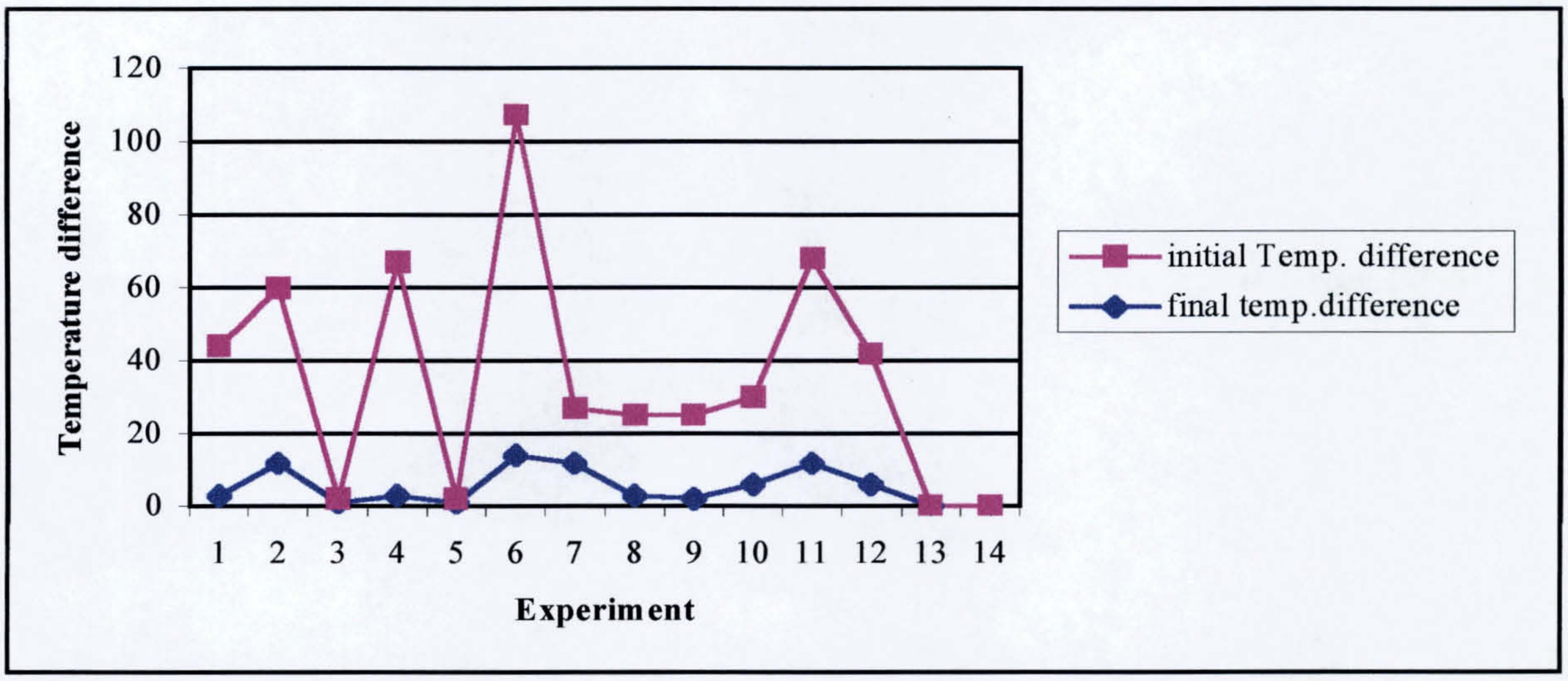

Fig 7.7 Temperature differences in Initial and final welding experiments

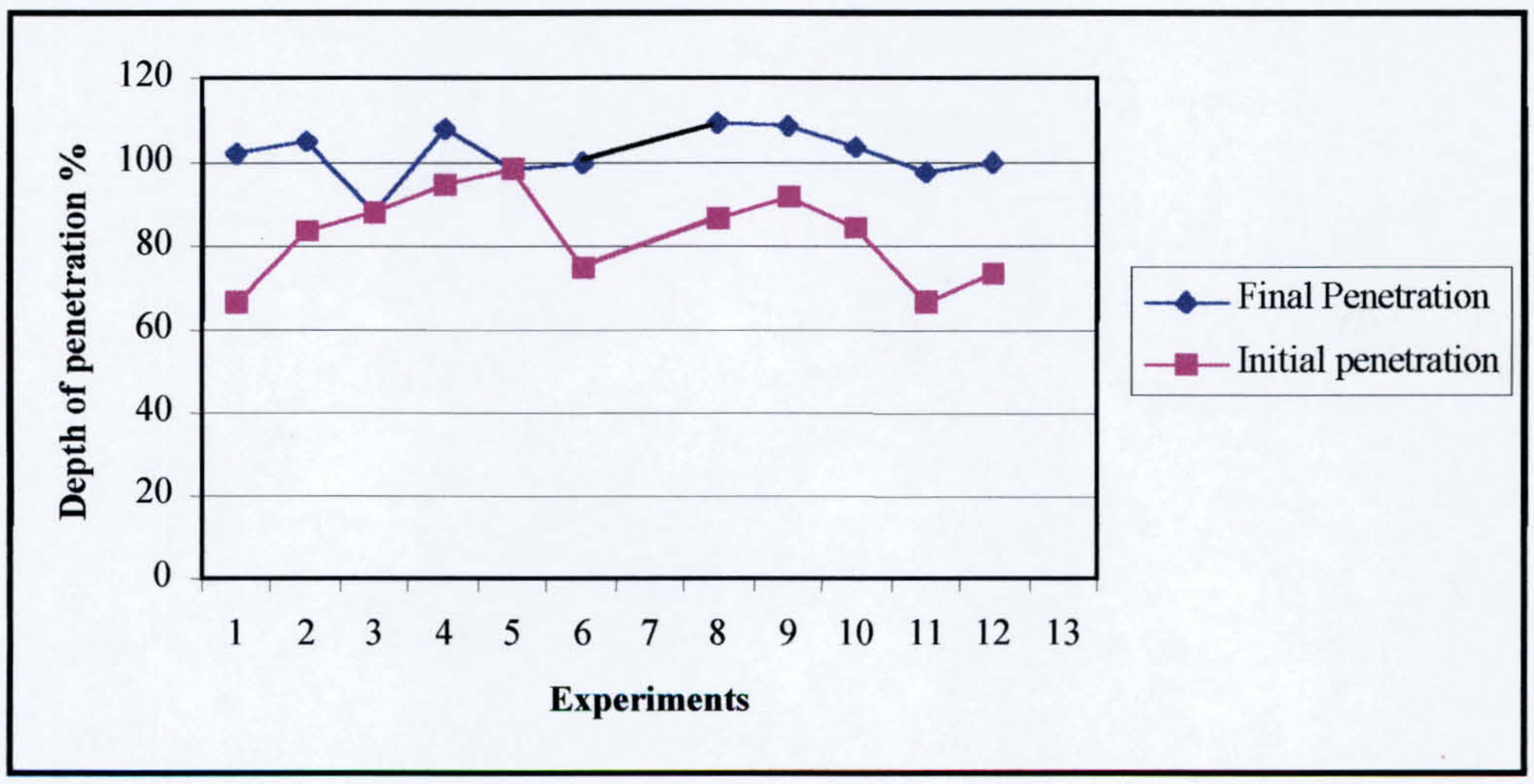

Fig 7.8 Depth of penetration in initial and final welding experiments

7.6.2 Evaluation of models for joint with root gap.

The Neuro-fuzzy Control Model was designed for joints with 60° Vee preparation and zero root gap. However due to misfit of the joints during assembly or distortion during welding a root gap may appear in the joint. To evaluate the models capability

of dealing with such a problem two sets of experiments were conducted. In the first set of experiments a constant 1mm root gap was included in the test pieces, and in the second set of experiments the root gap was varied between 0-1.5mm. These experiments are described in the following sections.

7.6.2.1 Evaluation of models with 1mm root gap

The plates for these experiments were tacked together with 1mm root gap. The other joint geometry remained as described in chapter 5. A number of experiments were conducted with initial welding variables, chosen from those previously used for closed butt joint experiments and which had achieved less than 100 % depth penetration (75-85%). This was to assure that burn through of an open joint was unlikely to occur. As described in the previous section, final welding variables were determined through application of the neural network model, to predict surface temperature, and the fuzzy logic model. For these open root gap experiments the membership functions of the fuzzy logic model required modification in order to provide accurate prediction of welding variables. The modifications included changes to the range and number of linguistic terms in the model outputs, as follows:

Output variables	**Zero root gap**	**1mm root gap**
Voltage range	37 – 47 volt.	30 – 40 volt.
Voltage linguistic terms	3 (L, M, H)	5 (VL,L,M,H,VH)
Current range	380 – 400 Amp.	350 – 400 Amp.
Welding speed range	800 – 900 mm/min	500 – 900 mm/min

In table 7.4 the values of the initial welding variables with resulting depth of penetration are shown, and photographs of joint cross sections are shown in figure 7.9. It is clear that these conditions produce excessive penetration.

Exp. NO.	Initial values of welding variables				Measured Temp. °C	N.N. Temp.°C Prediction	Ave. ΔT .°C	Penetration %
	Torch Angle	Current Amp.	Voltage Volt.	Speed mm/min				
1	90	380	37	900	677	732	-55	135 %
2	90	380	47	900	848	745	103	153 %
3	90	380	40	850	820	736	84	142 %
4	90	395	37	800	640	720	-80	168 %

Table 7.4 Results of experiments on workpieces with 1mm root gap using initial welding variables

For the second set of experiments workpieces with the same joint geometry were used. The modified welding variables predicted by the fuzzy logic model were used for welding. The final welding variables with the resulting depth of penetration for each experiment are shown in table 7.5. Photographs of the initial and final joints from the experiments 1 and 4 are shown in figure 7.9

As can be seen, the weld produced, using the values of variables predicted by the neuro-fuzzy model exhibit, satisfactory penetration. Figure 7.10 shows the

comparison of penetration achieved using uncontrolled and fuzzy controlled variables.

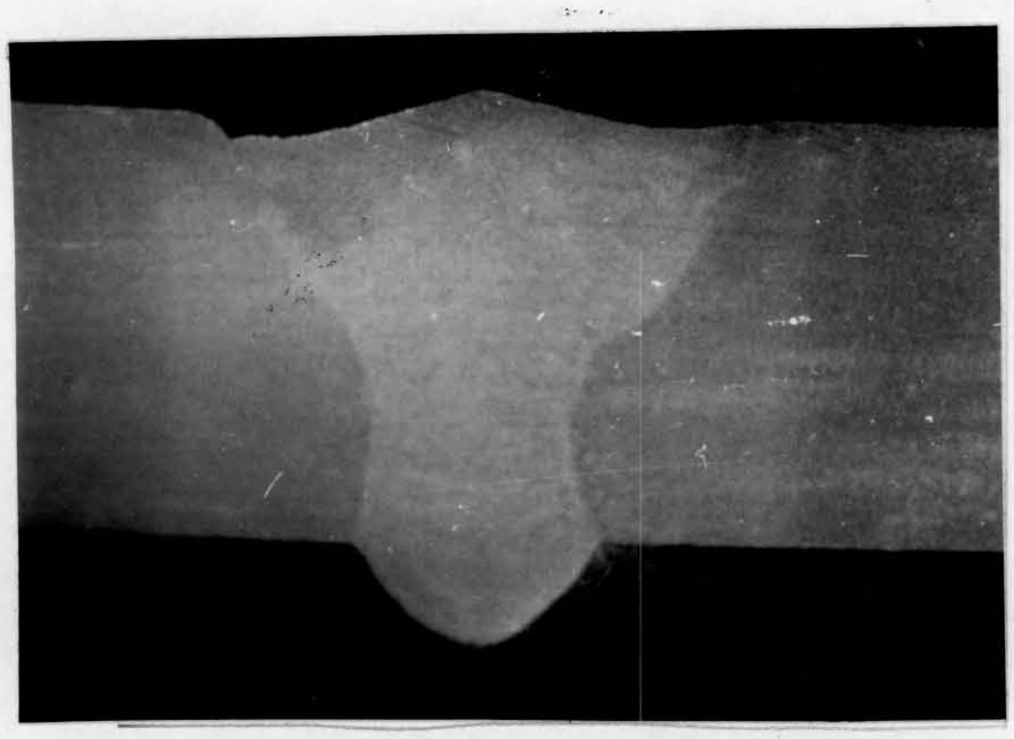

Experiment 1 initial condition

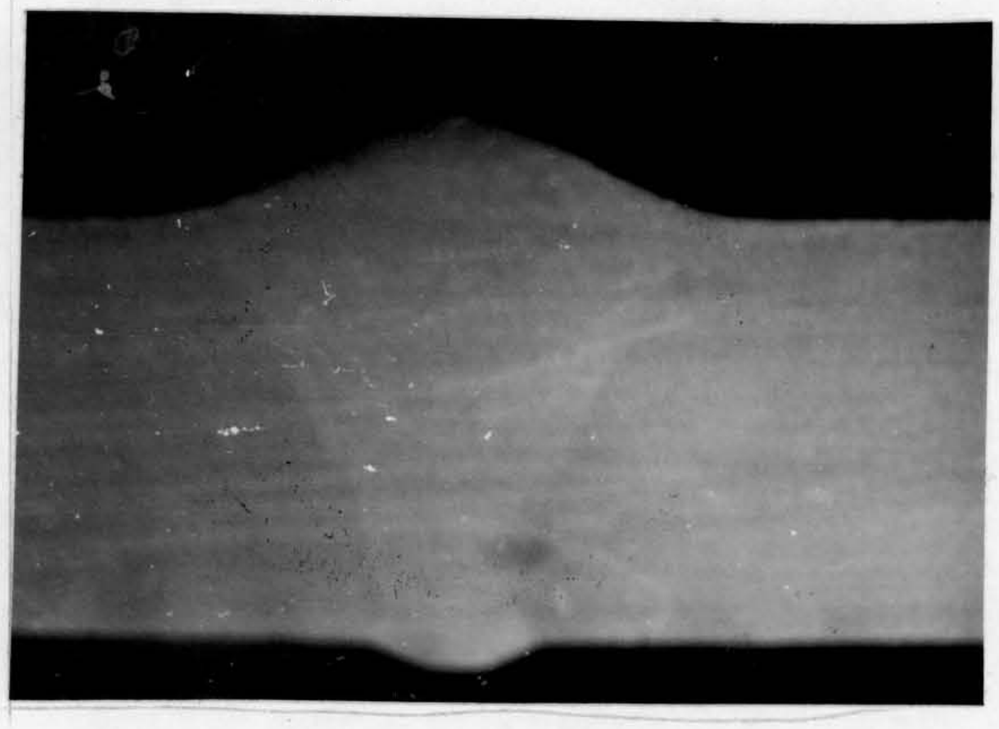

Experiment 1 final condition

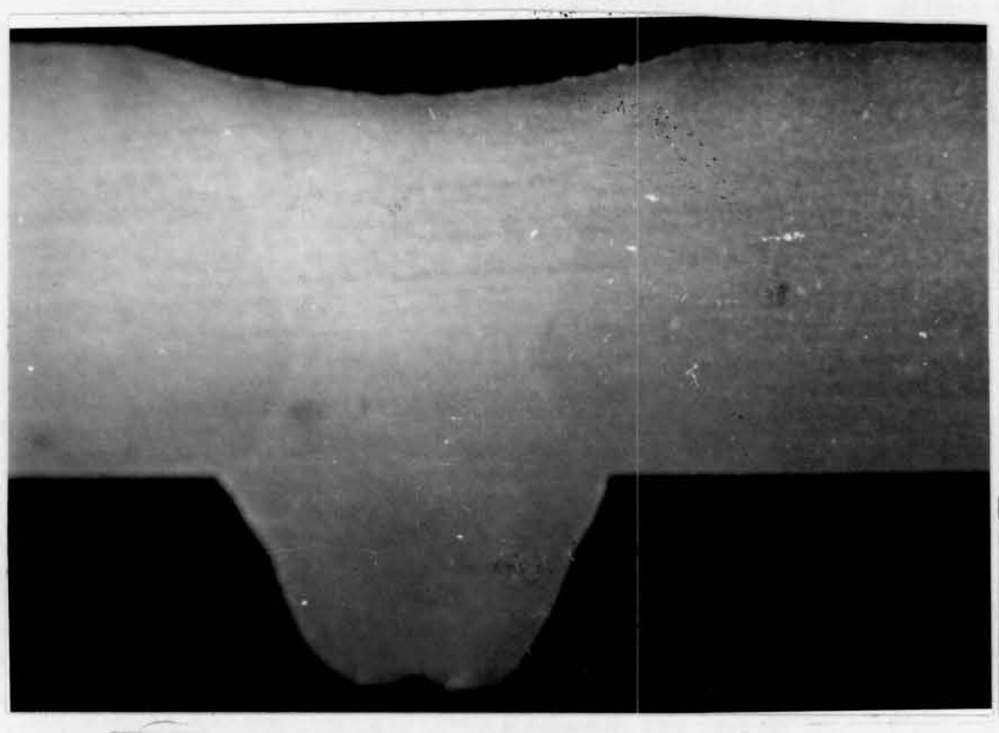

Experiment 4 initial condition

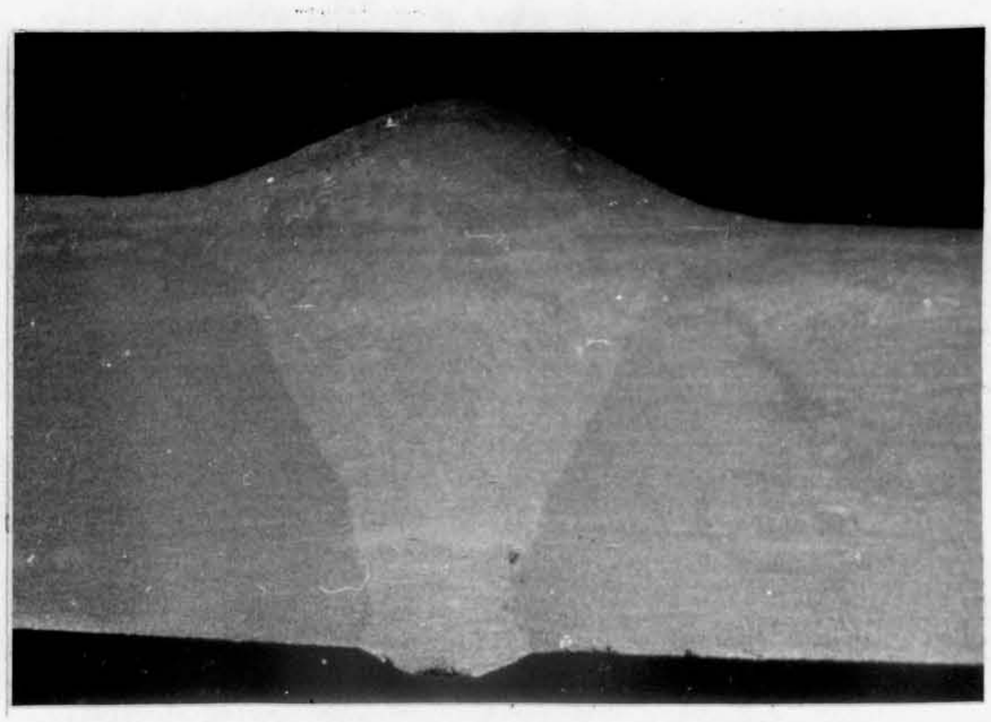

Experiment 4 final condition

Fig. 7.9 cross-sections of joints welded with initial and fuzzy model output welding variables in experiments 1 and 4 .

Exp.	Fuzzy model prediction variables				Penetration
NO.	Torch angle	Current Amp.	Voltage Volt.	Speed mm/min	%
1	90	360	31	570	105 %
2	90	362	30	830	108 %
3	90	362	31	830	102 %
4	90	362	31	590	110 %

Table 7.5 Results of experiments on workpieces with 1mm root gap using output variables from Fuzzy Logic model.

As indicated in table 7.5, the depth of penetration was improved to the required level using new predicted welding variables through fuzzy logic models. In figure 7.10 the resultant depth of penetration in the initial and final experiments are shown.

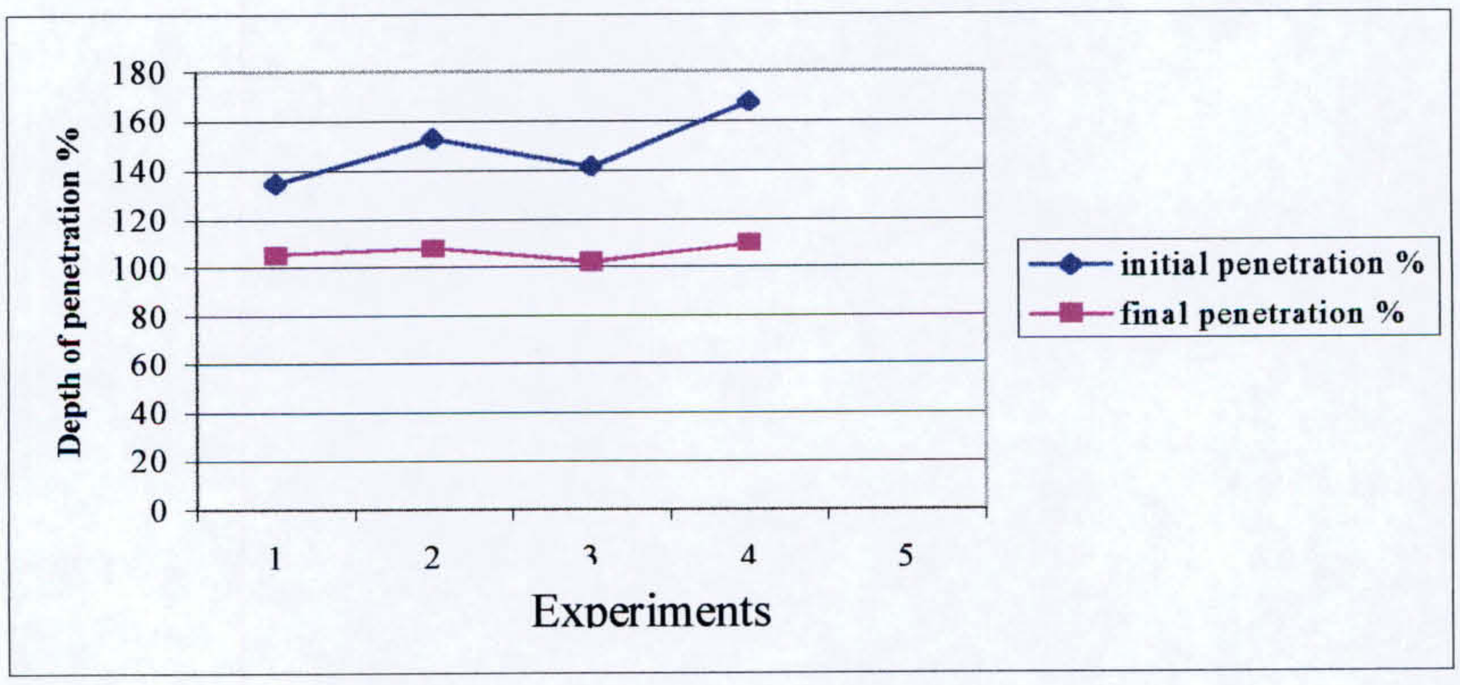

Fig. 7.10 Depth of penetration in initial and final experiments on workpieces with 1mm root gap.

7.6.2.2 Evaluation of model for joint with a 0 – 1.5mm root gap

An experiment was carried out to test the ability of the neural network model when changes occur in the workpiece gap during welding.

For this purpose workpieces were tack welded together to have a varying root gap between zero and 1.5mm. A number of tests were conducted with randomly selected welding variables. The welding variables and the resultant depth of penetration for one set of experiments is shown in table 7.6. The cross section of the weld is shown in figure 7.11. Figure 7.11a is the longitudinal cross section of the weld. Figure 7.11b is drawn from measurements taken from micro examination as described in section 5.2.2.

No.	Gap mm	Torch Angle	Current Amp.	Voltage Volt.	Speed mm/min	N.N. Predicted Temp.°C	Measured Temp. °C	ΔT °C	Penet. %
1	1.35	90	400	42	850	835	730	-105	156
2	1.27	90	400	42	850	835	754	-81	150
3	1.12	90	400	42	850	835	762	-73	138
4	1.05	90	400	42	850	835	785	-50	130
5	0.97	90	400	42	850	835	784	-51	112
6	0.82	90	400	42	850	835	782	-53	112
7	0.75	90	400	42	850	835	819	-16	106
8	0.67	90	400	42	850	835	828	-7	106
9	0.52	90	400	42	850	835	840	5	100
10	0.45	90	400	42	850	835	767	-68	90
11	0.37	90	400	42	850	835	754	-81	80

Table 7.6 Welding variables with results for a workpiece with 0-1.5mm-root gap

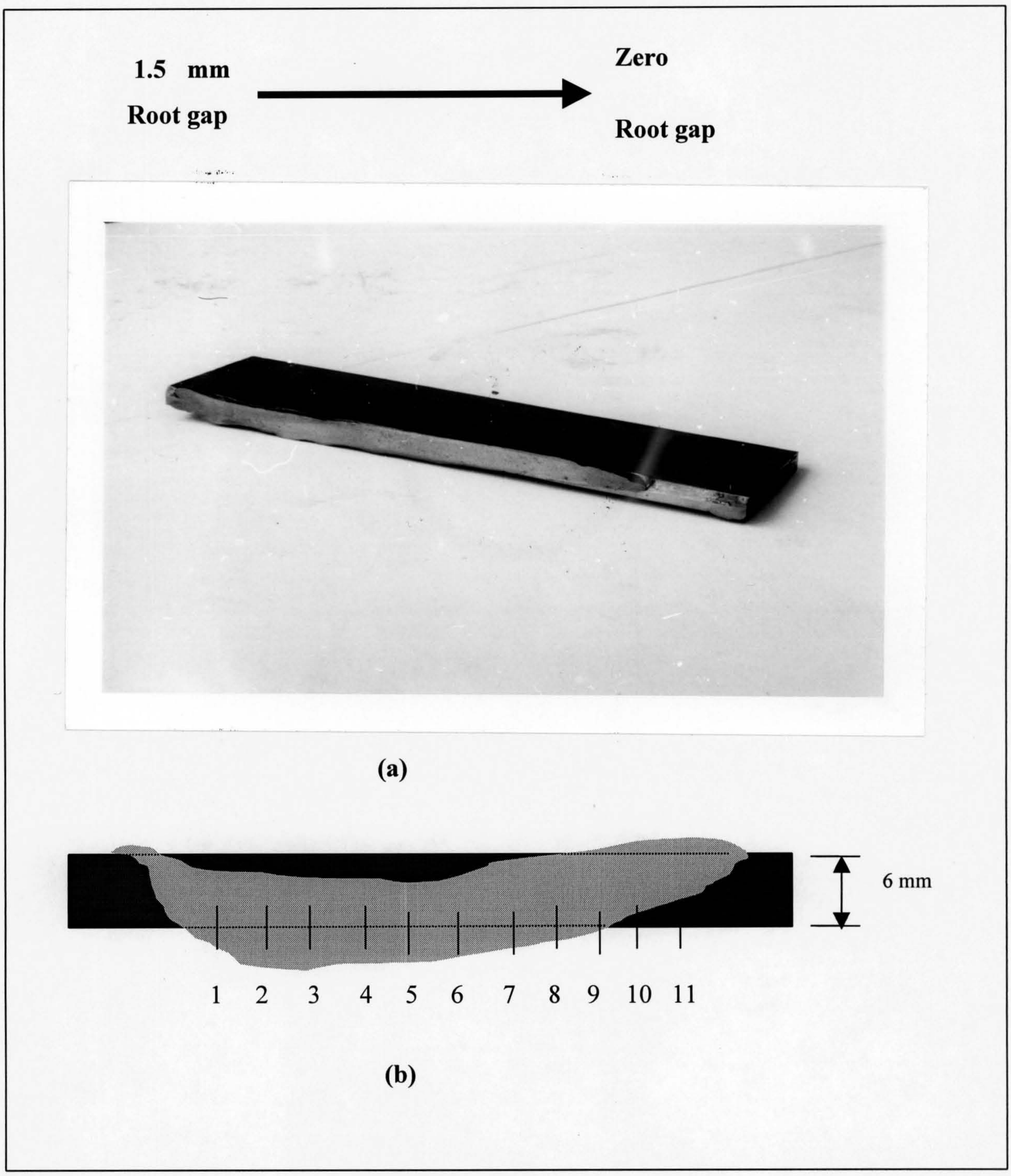

Fig. 7.11 cross section of weld with 0-1.5mm root gap.

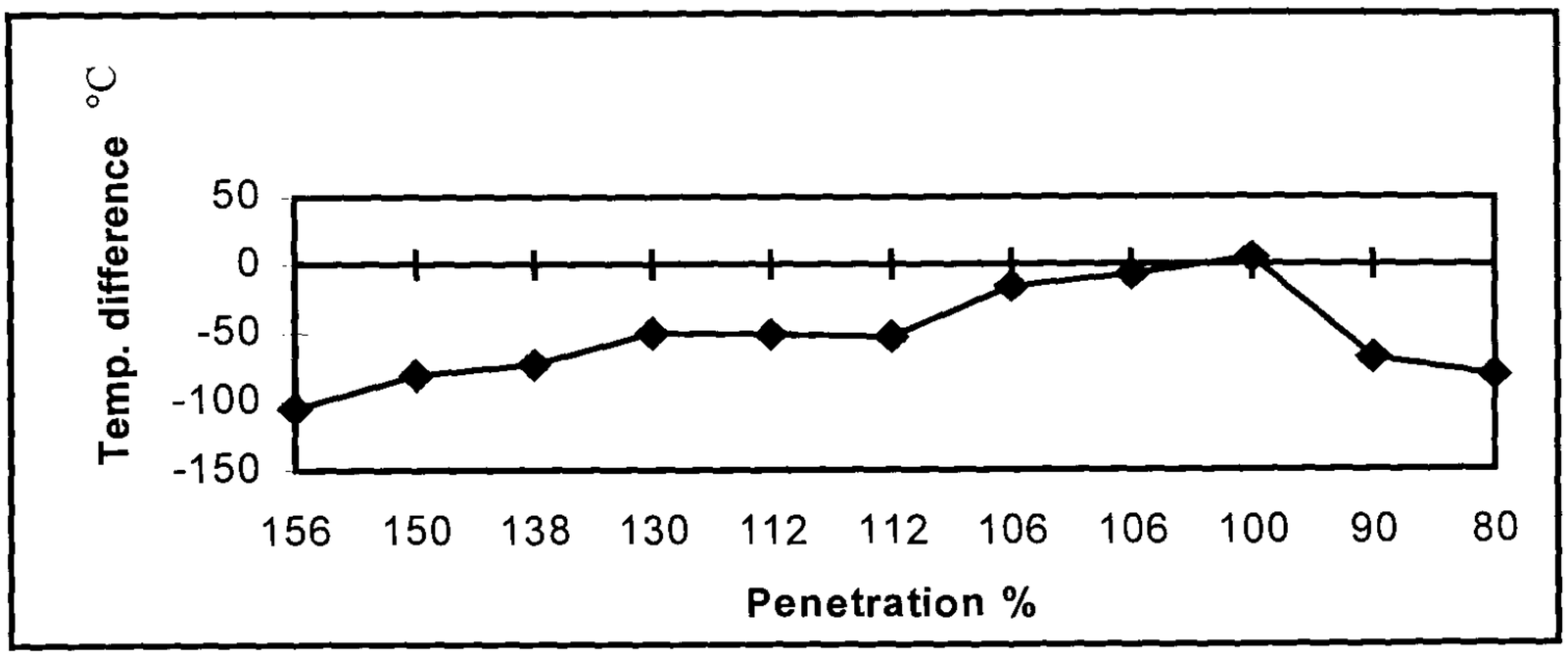

Fig. 7.12 Relationship between temperature difference and depth of penetration when the root gap varies between 0-1.5 mm. Welding variables are as in table 7.6.

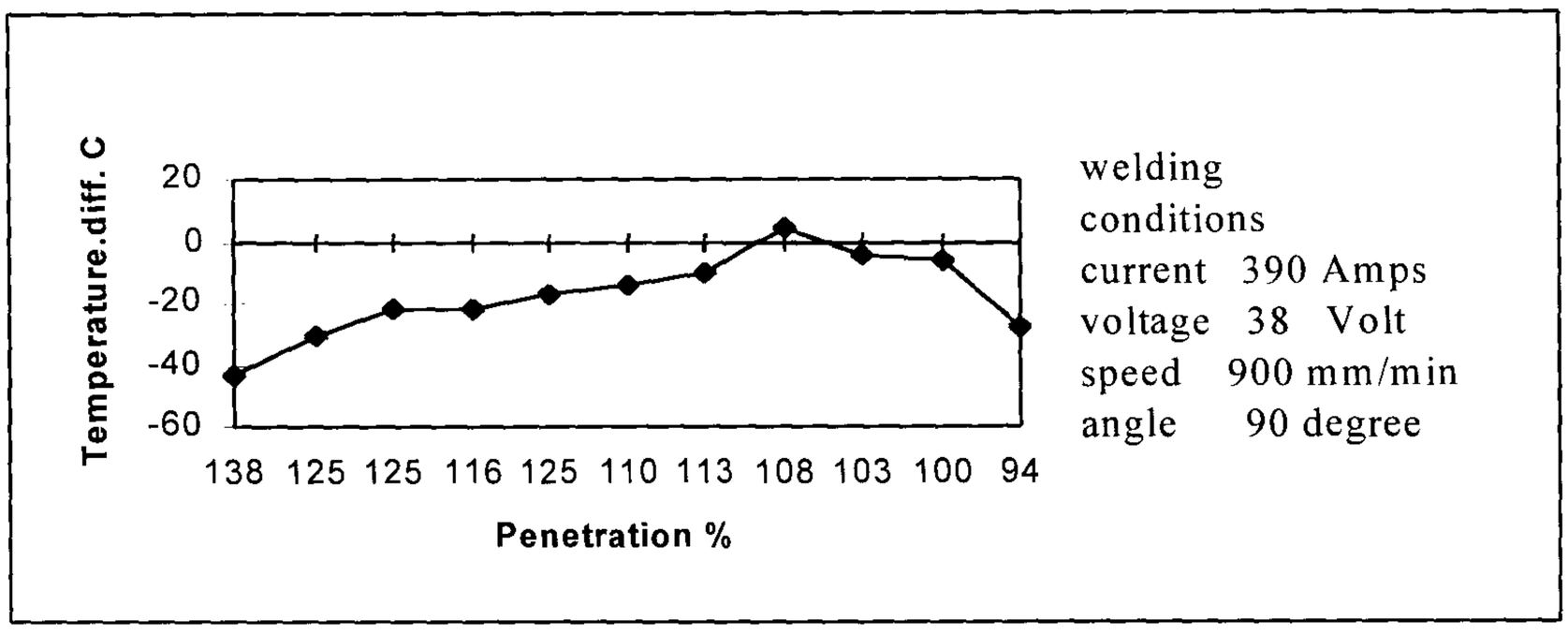

Fig. 7.13 Relationship between temperature difference and depth of penetration when root gap varies between 0-1.5mm.

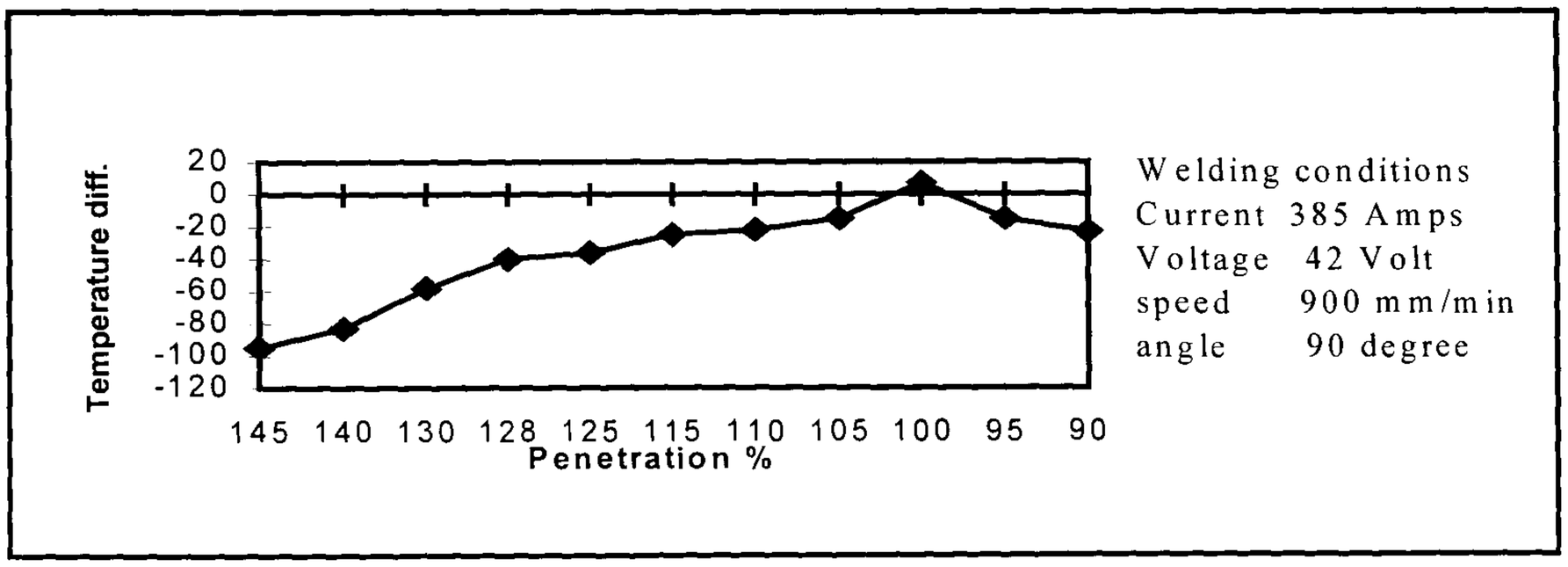

Fig. 7.14 Relationship between temperature difference and depth of penetration when root gap varies between 0-1.5mm.

The results of these experiments show that the difference in neural Network temperature prediction, and measured surface temperature during welding is still a good indication for depth of penetration when the root gap varies substantially. It can be seen from table 7.6 and figure 7.11 to 7.14 that ΔT at first increases as the gap reduces but as the gap approaches zero ΔT then reduces. This is accompanied by progressive change in penetration from large excess penetration to less than complete penetration. At one extreme, with, large excess penetration, heat flow is approximately 2D and, also, energy efficiency is reduced due to increased radiation losses thus reducing the temperature at the joint surface. At the other extreme energy is insufficient to cause penetration and heat flow is approximately 3D which increases conduction of heat into the work material away from the surface.

7.7 Discussion

In this chapter the construction and testing of the fuzzy logic model is described. The fuzzy logic model has five inputs (temperature difference between neural network prediction and measured temperature, and initial welding variables of current, voltage, travel speed and torch angle). The model has four outputs: current, voltage, welding speed and torch angle. These outputs are the models prediction of welding variables to produced a weld with 100-110 % depth of penetration.

Initially only temperature difference was selected as the model input. This model failed in the case when the initial values of the welding variables gave heat input in excess of that needed to produce a weld with 100% penetration. Therefore the arc burned through the plate, decreasing the temperature on the surface of the plate. The measured temperature was then less than the temperature predicted by the neural network model. On the other hand if the values of welding variables were selected lower than needed to produce a weld with 100 % penetration, the measured temperature is also lower than the predicted temperature. In the first case the welding variables (current, voltage) should be reduced, while the latter case the welding variables (current, voltage) should be increased. The model could

not differentiate these cases by the temperature difference alone. Therefore, the initial welding variables together with temperature difference were selected as inputs to the models.

The neuro-fuzzy control model (NFCM) was developed for controlling the weld depth of penetration by measuring a point surface temperature on the weldment during welding. For this purpose a software was written to integrate the sensor measurements and neural network models. However, at this time, the fuzzy logic model could not be integrated with the software due to problems in the Matlab C compiler, which was not able to convert the fuzzy logic command into C^{++} language. Therefore the fuzzy logic model was run in a separate window.

The neuro-fuzzy control models were evaluated by welding experiments. These experiments were conducted to cover different possibilities, which may have occurred during welding.

The depth of penetration in the workpiece was compared with initial welding variables and modified welding variables, as predicted by the fuzzy logic model. Results of the experiments show that the models are able to use surface temperature to monitor penetration being achieved to an acceptable level of accuracy. If acceptable penetration is being achieved the neural network model alone will detect this state. If penetration is outside the acceptable limits, in this research 100-110%, then the fuzzy logic model is invoked to output modified welding variables which will achieve the acceptable penetration.

Experiments were carried out on workpieces with different root gaps. These experiments show that that the neural network model for zero root gap is capable of indicating the state of penetration in the presence of substantially varying gap.

Chapter Eight Discussion and associated results

8.1 Introduction

In this chapter the characteristics of the welding control models will be discussed, and compared with theoretical models. In addition, this chapter will discuss and compare the merits and limitations of infrared temperature measurement and theoretical and neural network modelling prediction of surface temperature, to support the selected methodology in this research. In section 8.3 the empirical relationship between surface temperature and weld bead geometry will be discussed and the results compared with theoretical predictions of weld bead geometry. This chapter will conclude with an overall evaluation of the neuro-fuzzy control model.

8.2 Theoretical surface temperature prediction

As described in chapter four, much research has been undertaken in attempts to develop a mathematical model to predict the heat distribution during GMA welding. In order to understand the capability of a neural network model for prediction of top surface temperature of a workpiece during welding, the following section compares the results of theoretical temperature calculations with actual temperature measurement obtained via an infrared sensor, and with the neural network temperature prediction.

8.2.1 Surface temperature calculation

In order to calculate the temperature T at a spot in the top surface of a joint during welding the following steps were taken.

- The actual arc current and voltage was calculated using the equation determined by calibration of the robot controller and welding power supply as described in section 5.5.

$$V_1 = 15.3 + 0.367\, V_2 \qquad [1]$$

and

$$I_1 = 7 + 0.85\, I_2 \qquad [2]$$

Where V_1 and I_1 are the actual voltage and arc current value and V_2 and I_2 are the voltage, and current value set in the robot controller.

- For full penetration welding the equation for 2D heat distribution is applied (see section 4.3).

$$T = \frac{q}{4\pi\kappa r} e^{\left[-\frac{v(r-x)}{2\alpha}\right]} \qquad [3]$$

- for welds with partial penetration the equation for 3D-heat distribution is applied, (see section 4.3).

$$T = \frac{q}{2\pi\kappa r} e^{-\frac{v(r-x)}{2\alpha}} \qquad [4]$$

Where x y are the co-ordinates of the measured spot from the centre of the heat source (m) as shown in figure 8.1, T is the spot temperature (°K), α is the thermal diffusivity ($m^3\ s^{-1}$), v is the welding speed in the y direction ($m\ s^{-1}$), k is the thermal conductivity, q is the heat input to the welding which is:

$$q = \eta(V \times I) \qquad [5]$$

Where η is the efficiency (section 4.4), V is voltage, and I is arc current, and r is the radius of the circle around the heat source (m) (fig 8.1).

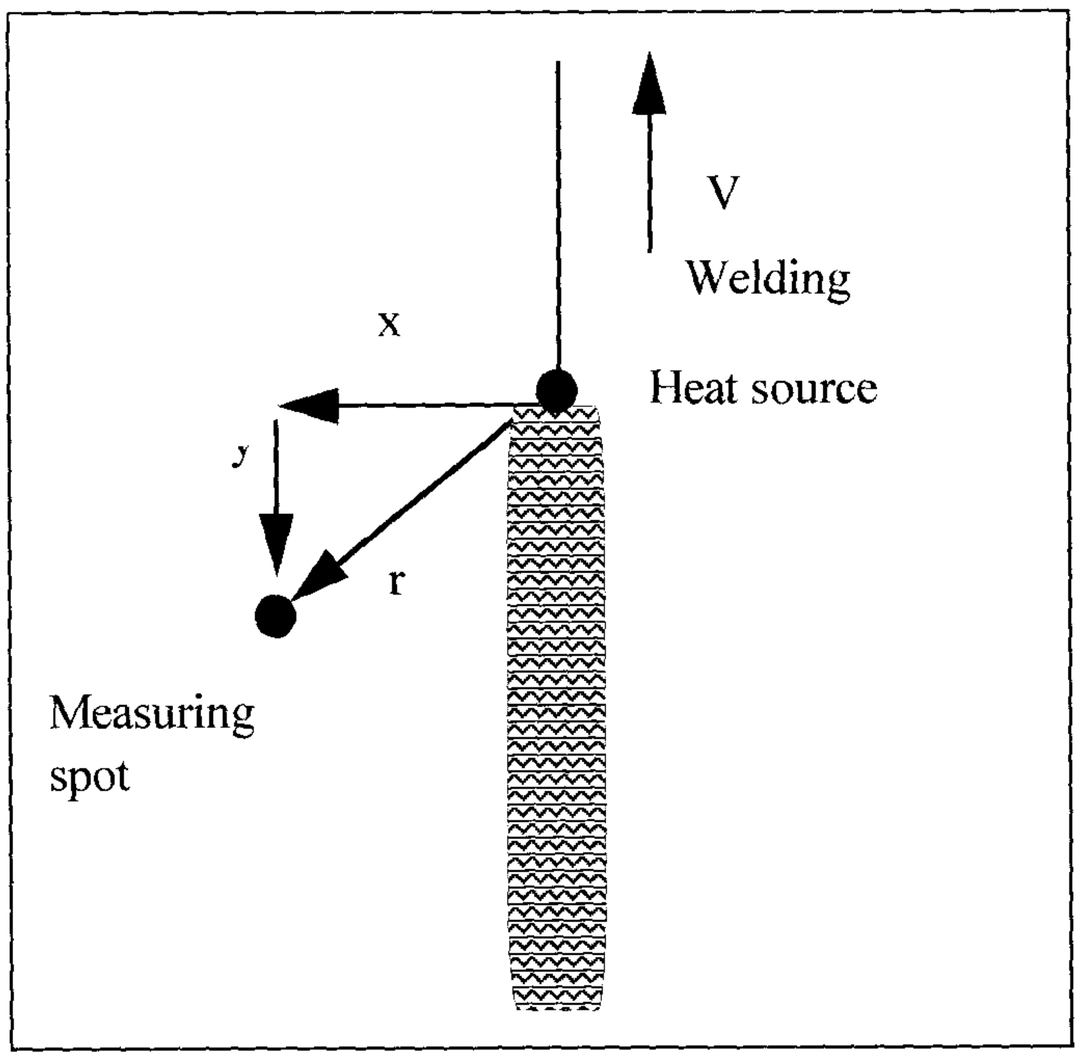

Fig.8.1 Position of temperature measurement.

In figure 8.2 the relationship between heat input and calculated 3D surface temperature is shown and compared with the temperature measured with a calibrated infrared sensor. As shown in table 8.1 welding current and voltage only were varied, other welding variables remained constant. As would be expected spot temperature increases with increasing heat input. As can be seen the measured temperatures do not correlate with calculated values nor do they show a linear relationship with heat input. This is due to simplification in the calculations and the dependence on estimation of arc efficiency (η).

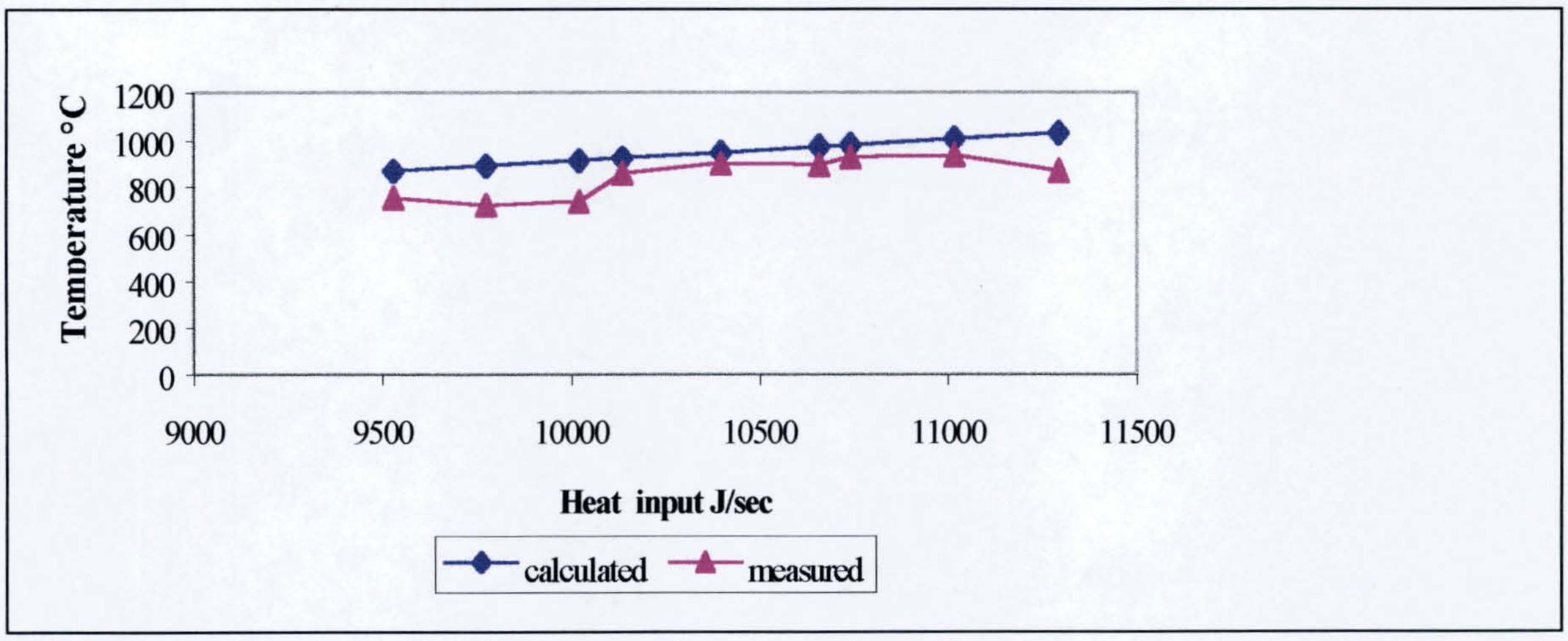

Figure 8. 2 Relationship between heat input and surface temperature for the welding condition shown in table 8.1.

No.	Torch angle °	Current (A)	Voltage (V)	Welding Speed mm/min
1	90	400	37	800
2	90	390	37	800
3	90	380	37	800
4	90	400	42	800
5	90	390	42	800
6	90	380	42	800
7	90	400	47	800
8	90	390	47	800
9	90	380	47	800

Table 8.1 Welding variables for comparison between calculated and measured temperature.

In figure 8.3 the relationship between welding speed and calculated and measured surface temperatures are demonstrated. Other welding parameters (current 380, voltage 37 and angle 90°) were maintained constant.

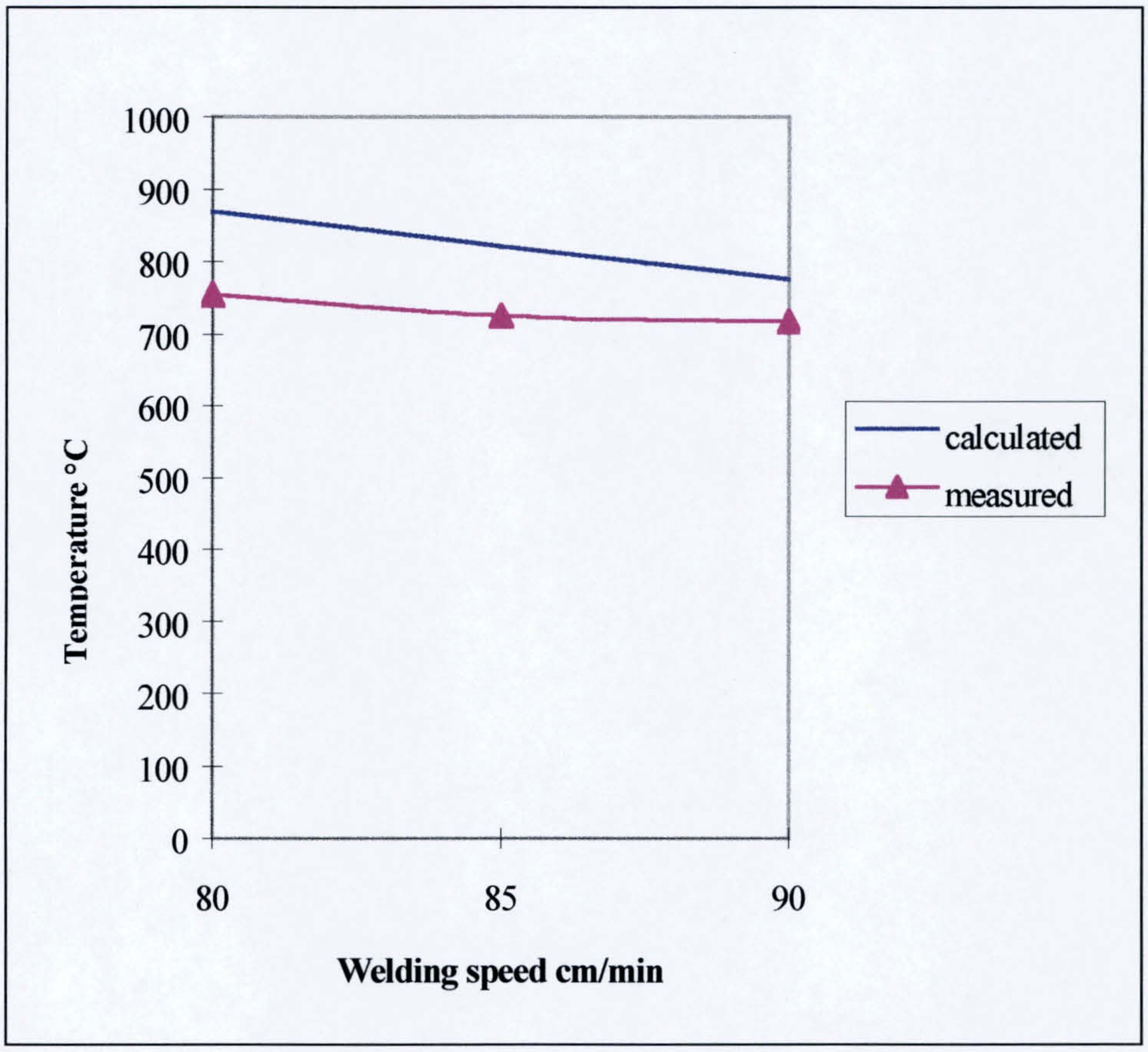

Figure 8. 3 Effect of welding speed on surface temperature.

As would be expected figure 8.3 shows that the surface spot temperature decreases as welding speed is increased. Again the measured temperatures are less than the calculated values, for the reason previously explained.

8.3 Comparison of neural network prediction with measured Temperature

The temperatures predicted by the neural network model for full penetration welding and the measured temperatures for the same welding conditions are shown in fig.8.4. For this comparison the neural network validation data have been used (appendix 2).

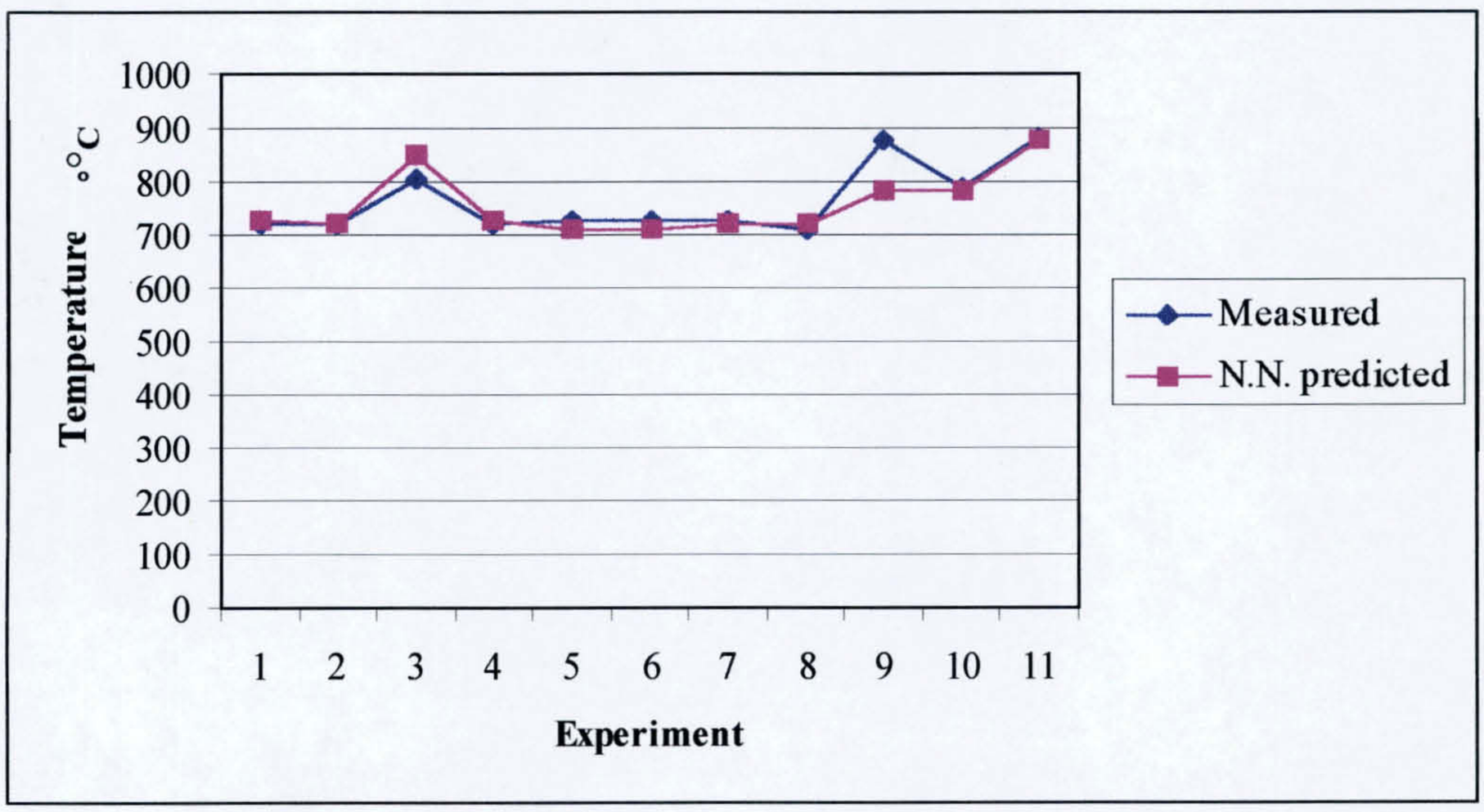

Figure 8.4 Comparison between measured and Neural Network predicted temperature.

It can be seen that the predictions of surface temperatures by the neural network model are close to the measured temperatures. An ideal model should predict the surface temperature without any error. However, for a non-linear complex system such as welding this is virtually impossible. In the neural network modelling the goal has been to minimise the error through experimenting with different modelling techniques, and model architectures.

Experiments have been conducted to compare the predictions of the trained neural network with measured spot temperature when 100-110% depth of penetration was achieved. The result of these experiments, which used combinations of welding variables not included in the training or validation data of the model, are shown in figure 8.5.

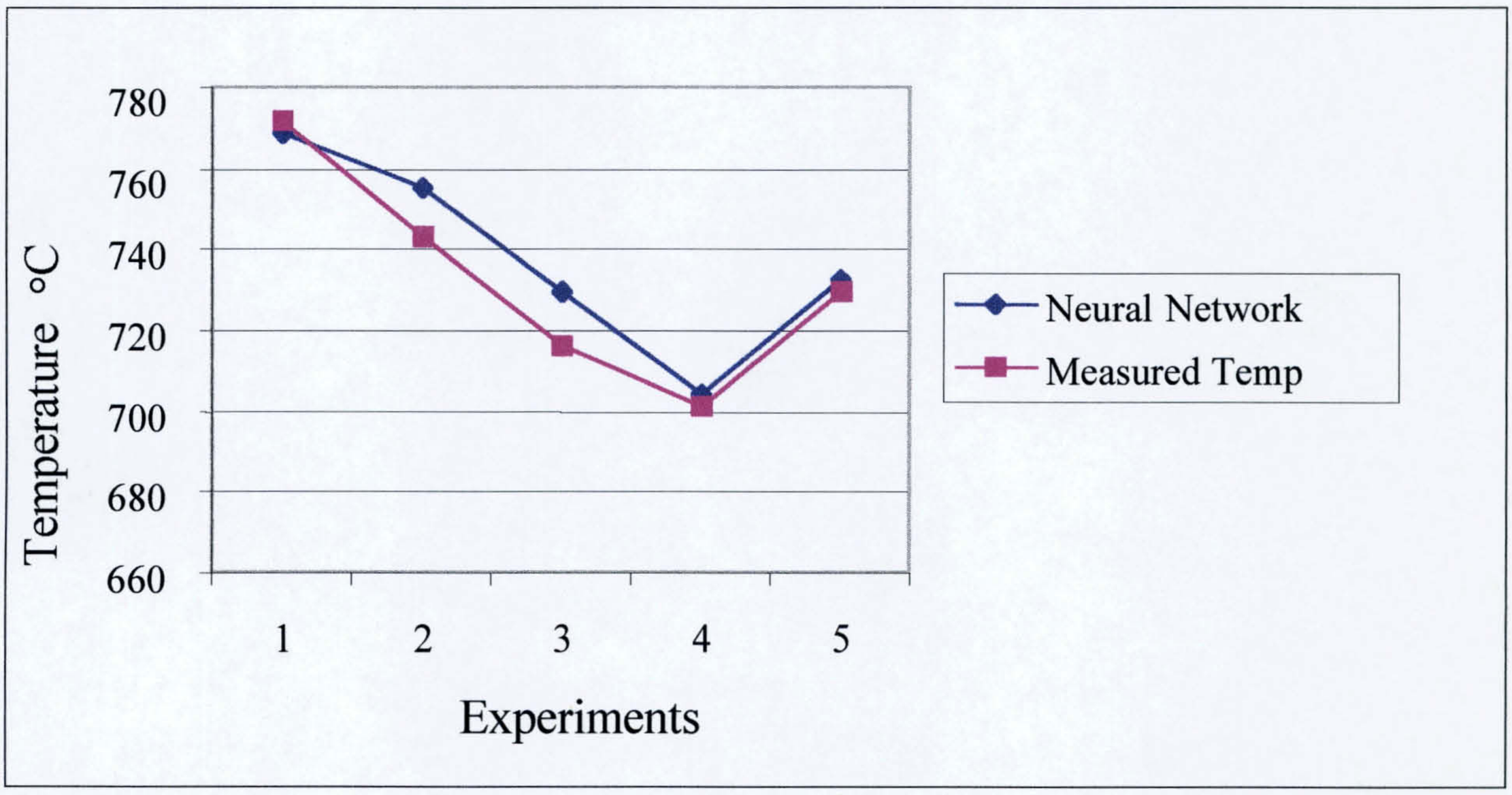

Fig.8.5 Comparison of measured and predicted temperature for 100-110% penetration.

The model has predicted temperature to within 0.4 – 1.9 % of the actual measured values. this demonstrates the ability of the model to be used in a real time control system for controlling penetration by measurement of temperature at the surface of the welded plate.

8.4 Comparison between the one – to – four neural network and the neuro-fuzzy control model.

The One-to-four neural network model was evaluated as a control model. The neural network which was described in chapter 6 has one input (measured temperature), and four welding variables (current, voltage, welding speed, and torch angle) as outputs.

In the evaluation tests, sets of nominal initial welding variables were selected and the weldment spot surface temperature during welding, and the resultant weld penetration were recorded. These are shown in table 8.2.

Exp. NO.	Torch angle	Current Amp.	Voltage Volt.	Speed mm/min	Measured Temp. .°C	Penetration %
1	90	385	40	900	777	67 %
2	90	383	37	860	682	83.5 %
3	90	390	37	850	664	95 %
4	90	390	40	900	746	98.6 %

Table 8.2 Initial welding variables.

The measured temperature from these trials was then used as an input to the neural network model which then predicted modified welding variables, which were expected to achieve full penetration. Welding was carried out using the modified variables on workpieces with zero root gap as described in chapter five. The modified welding variables and resultant depth of penetration are shown in table 8.3.

Exp. No.	Torch angle	Current Amp.	Voltage Volt.	Speed mm/min	Penetration %
1	90	390	42	890	95 %
2	90	400	47	810	87 %
3	70	390	38	870	98 %
4	90	390	44	800	100 %

Table 8.3 Modified welding variables with resultant penetration.

As can be seen output variables from the neural network model have achieved improvement in penetration, but not 100% as required (except experiment No. 4)

The above results from neural network modelling alone were compared with results of welding when variables were modified by the neuro-fuzzy control model. Figure 8.6 compares the weld penetration achieved using the initial parameters, parameters adjusted by neural network model, and those resulting from application of the neuro-fuzzy Control model. It will be observed that the welds produced using parameters modified by the neuro-fuzzy model have more consistence penetration and within the required limits of 100 to110%.

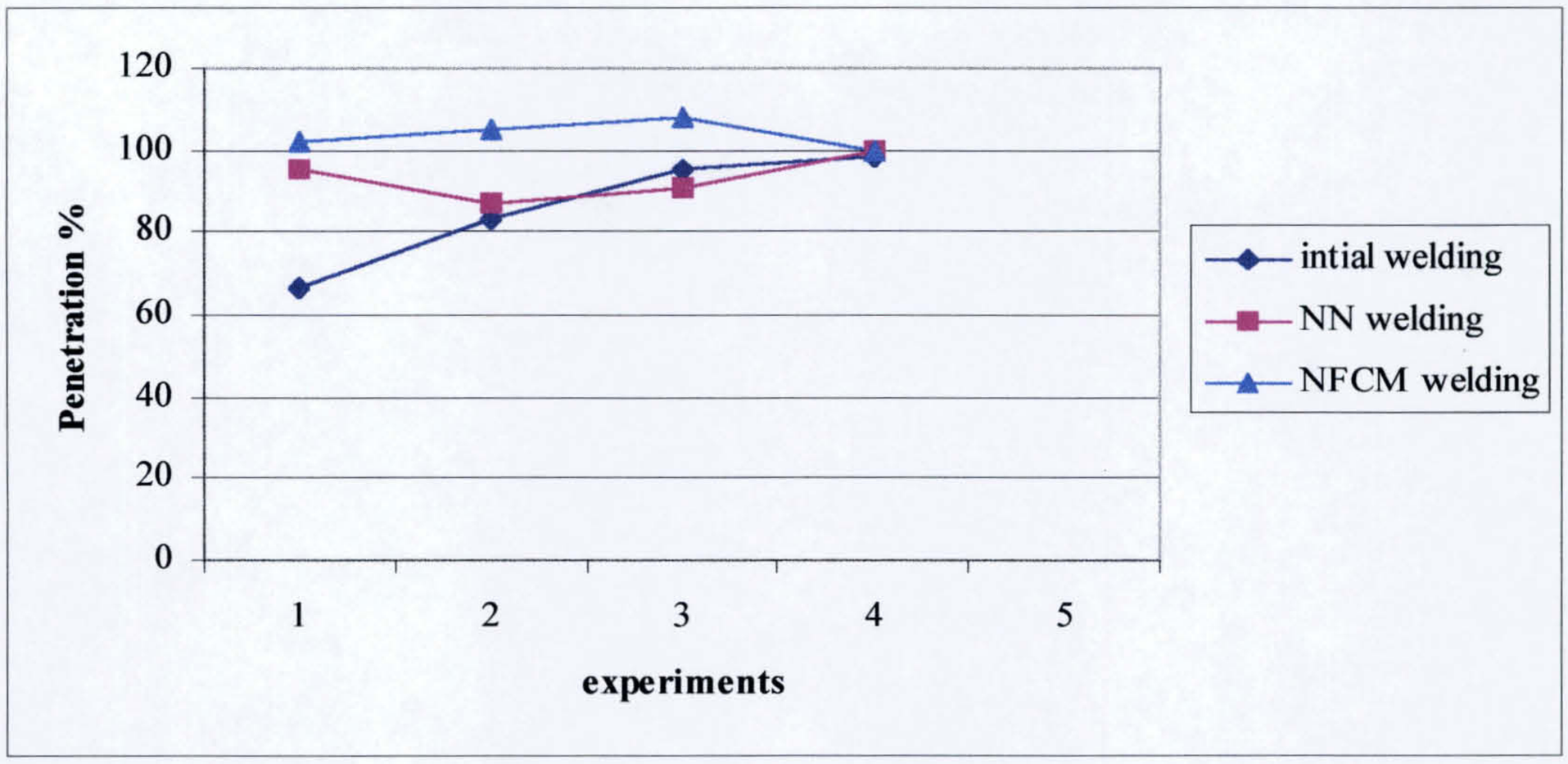

Figure 8.6 Comparison between neural network and neuro-fuzzy control model.

8.5 Comparison of neural network model with statistical regression model

The predictions from the developed neural network model were further compared with result from a statistical regression model of temperature relative to welding variables. The regression model equation [6] was developed using Minitab software.

Temperature = 308 + 2.75 angle – 1.31 current + 11.9 voltage + 2.95 speed [6]

The data, which was used for training the RBF Neural network (Appendix 2), was also used to develop the regression equation. Similarly the data used for evaluation of the neural network was also used for evaluation of the regression equation. The temperature predicted by the neural network, statistical regression, and the actual temperature measured by the infrared sensor, together with the associated welding variables, are shown in table 8.5.

Torch angle	Current	Volt V.	Speed	T_M	A.N.N. Prediction		Statistical regression		Δ % Error
			Mm/min	°C	°C	% error	°C	% error	
70	390	37	800	689	678	1.60	666	3.34	1.74
70	400	37	850	634	657	3.63	668	5.36	1.74
70	400	37	850	663	657	0.90	668	0.75	-0.15
70	400	37	800	726	730	0.55	653	10.06	9.50
70	400	37	900	665	654	1.65	682	2.56	0.90
70	400	42	850	704	706	0.28	727	3.27	2.98
70	400	47	800	709	716	0.99	772	8.89	7.90
90	380	37	850	724	731	0.97	749	3.45	2.49
90	390	37	800	721	724	0.42	721	0.00	-0.42
90	390	47	800	806	853	5.83	840	4.22	-1.61
90	400	37	850	723	726	0.41	723	0.00	-0.41
90	400	37	800	728	714	1.92	708	2.75	0.82
90	400	37	800	726	714	1.65	708	2.48	0.83
90	400	37	900	726	722	0.55	737	1.52	0.96
90	400	37	900	711	722	1.55	737	3.66	2.11
90	400	42	800	878	786	10.48	767	12.64	2.16
90	400	42	800	788	786	0.25	767	2.66	2.41
90	400	47	800	885	877	0.90	827	6.55	5.65
110	380	37	850	815	767	5.89	804	1.35	-4.54

Table 8.4 Comparison of predicted surface temperature with measured values.

Torch angle	Current	Volt V.	Speed Mm/min	T_M °C	A.N.N. Prediction		Statistical regression		Δ % Error
					°C	% error	°C	% error	
110	390	37	800	796	762	4.27	776	2.51	-1.76
110	390	37	800	757	762	0.66	776	2.51	1.85
110	400	37	800	759	730	3.82	763	0.53	-3.29
110	400	37	800	728	730	0.27	763	4.81	4.53
90	390	37	650	693	697	0.58	677	2.31	1.73
90	390	42	800	846	808	4.49	780	7.80	3.31
90	390	42	800	846	808	4.49	780	7.80	3.31
90	390	47	700	754	755	0.13	810	7.43	7.29
90	400	37	800	699	714	2.15	708	1.29	-0.86
90	400	37	750	687	693	0.87	693	0.87	0.00
90	400	37	700	675	672	0.44	678	0.44	0.00
90	400	42	750	790	763	3.42	753	4.68	1.27
90	400	47	700	775	772	0.39	797	2.84	2.45
90	410	37	800	642	642	0.00	695	8.26	8.26
90	380	42	750	733	738	0.68	779	6.28	5.59
70	390	37	700	625	616	1.44	636	1.76	0.32
70	390	47	800	707	711	0.57	785	11.03	10.47
70	400	42	800	697	702	0.72	712	2.15	1.43

Table 8.4 Continued

In table 8.4 T_M is the measured temperature, and Δ% error is (statistical regression error - N.N. prediction error).

Although in a few cases the statistical regression predictions were better than neural network predictions, The average error for statistical regression was 4.08% compared with that of the neural network which was 1.88%. this shows the neural network model is more accurate than the statistical regression equation for prediction of surface temperature. In fig. 8.8 the predictions, and measured temperature are compared.

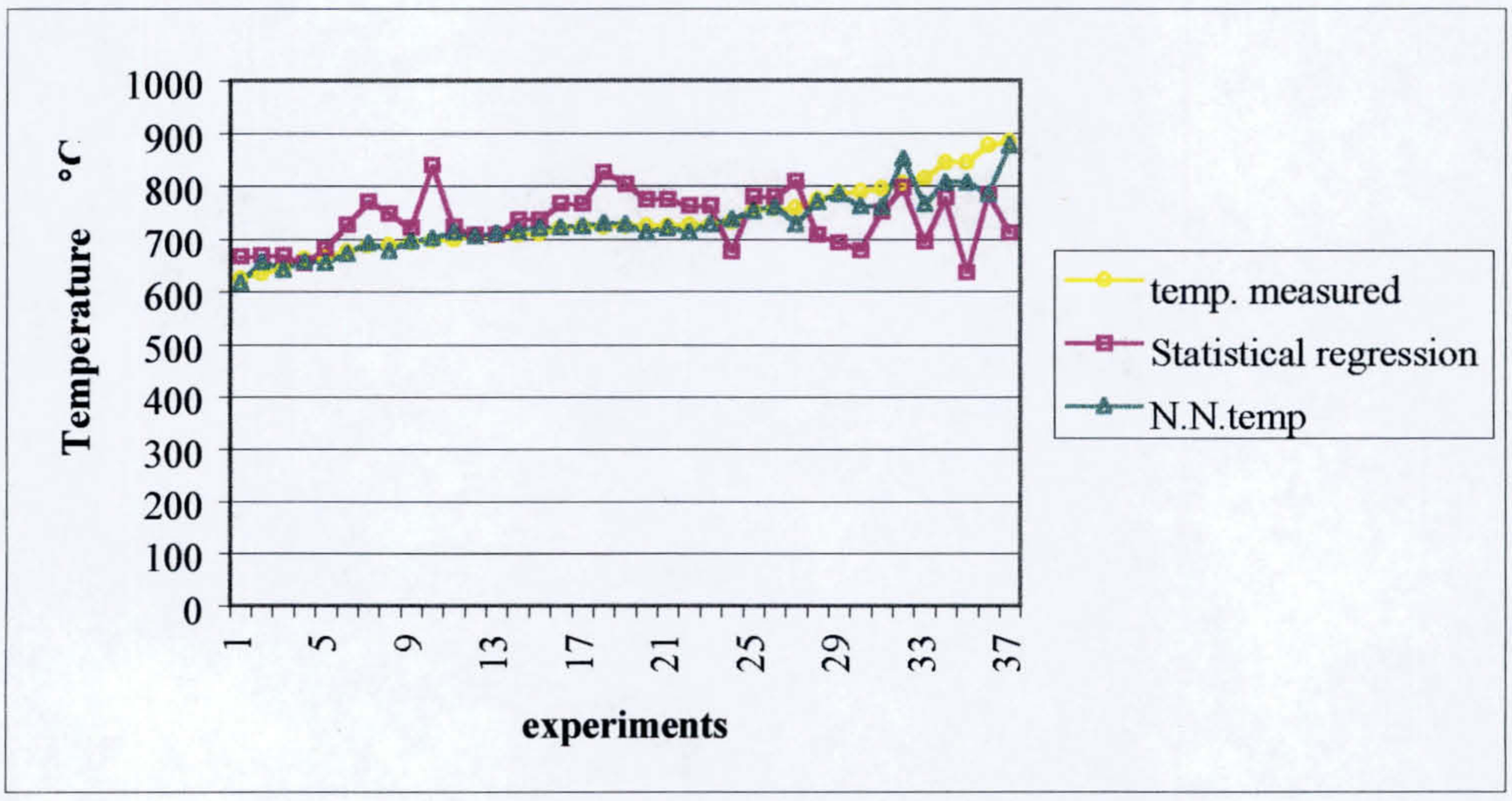

Fig.8.7 Comparison between NN, Statistical, and measured surface temperature.

Neural network modelling has a number of advantages and limitations when compared with other modelling techniques, as described in chapter 3. One of these advantages is the relative accuracy and generality. If training data for the model are sufficiently general, spanning the entire range of welding variables, the resulting model will capture the complexities of the process, including non-linearity and cross-coupling of variables, over the same range. Also the neural network can be refined with the addition of further training data at any time. This capability will allow the user to change the range of welding variables covered by the model to those required by the application.

The results of evaluation of the control model shows (table 7.2 and 7.3) that the neural network model has predicted the surface temperature with a good degree of accuracy.

8.6 Discussion of results

In the following sections the result of experiments and modelling are discussed further.

8.6.1 Discussion of experimental results

All modelling techniques need data. Data can be gathered from theoretical calculations, expertise, or experimental work. For the purpose of the modelling reported in this work, data was needed to establish the relationship between controllable welding variables, depth of penetration, and temperature at a point in the surface of a workpiece during welding. As described in chapter five experiments were conducted in order to obtain the training and evaluation data for the neural network modelling. The controllable welding variables were welding current, welding voltage, welding speeds and torch angle. These variables have the greatest effect on depth of penetration, a major indicator of weld quality. Therefore in this research fixed welding variables such as plate thickness (6mm), joint type (V-groove butt joint), and geometry of the joint (60° included angle, 2mm-root face), which are commonly found in fabrication practice have been used. Most research, in which heat distribution in a workpiece has been studied, has collected data from bead on plate welding experiments (142, 73, 149, 87). While this may be appropriate for autogenous closed butt joints, it does not properly represent the heat distribution in the most commonly encountered welding procedure, i.e., welding in a Vee grove.

The nominal levels of welding variables used were determined experimentally as being appropriate to avoid either burn through or very low depth of penetration, that is, the extremes of poor welding performance.

The experimental results were also used for the creation of the rule base for the fuzzy logic model. These results gave the opportunity to produce an accurate rule base for the compensation of welding variables based on the difference between neural network predicted surface temperature for full penetration and the temperature measured during welding.

8.6.2 Discussion of modelling results

In this work two different approaches of Artificial Intelligence techniques were adopted for constructing the neuro-fuzzy control model for Gas Metal Arc welding. An Artificial Neural Network model is used to predict the temperature expected at a point on the surface of the workpiece corresponding to the welding variables being used for welding. The FL (fuzzy logic) model is used to compensate the controllable welding variables by reference to the temperature difference between predicted and measured temperatures. In the following sections the results of each model are discussed further.

8.6.2.1 Discussion of neural network models

Artificial Neural Networks have been used in a wide variety of applications, ranging from classification and pattern recognition, to optimisation and control of the welding process (107,136, 147, 148).

Initially in this research, neural network modelling alone was to be used to predict directly the welding variables required to achieve the desired weld depth of penetration from an input of temperature measured on the surface of the workpiece. Different network modelling techniques, various network architectures, such as inverse modelling (chapter 6.3.10.4), and the addition of another input (root gap) to the models (chapter 6.3.10.2) were tested. Results of validation experiments showed the difference between predicted penetration and that actually achieved (table 8.2). This was not considered to be satisfactory. An alternative approach was then

considered in which the neural network would be used to predict the surface temperature expected for a set of welding variables, the difference between predicted and actual measured temperature would then be employed as a control signal in a further model for adjustment of welding variables.

As described in chapter 6, different types of network were built and evaluated, the results show that for the arc welding process the Radial Base Function (RBF) network was the most suitable technique. A number of RBF network models with different number of layers, physical elements (PE) and different learning coefficients were constructed and evaluated. The final RBF network model consisted of four PEs in the input layer, these are the controllable welding variables, 70 Gaussian radial basis function as an hidden layer, and one PE in the output layer, which is the spot temperature on the surface of the workpiece. This network predicted the surface temperature for a given set of welding variables when full penetration would be achieved. The training of the models was carried out until the RMS(Root Mean Square) error reached the minimum value, which for 100-110% depth of penetration was 0.03. In table 8.4 the value of RMS error for other models and the number of data used for training and evaluation of the models are summarised. Once the network had been trained with the training data, its performance was evaluated with validation data. The neural network model for 100-110% penetration was able to predict the surface temperature with average error of 1.88%. In other words the temperature was predicted to an accuracy of ±13°C. The results of the neuro-fuzzy modelling (chapter 7.3) shows this accuracy to be acceptable for welds with 100-110% depth of penetration. The evaluation results for other models are given in chapter 6.3.10.7. From the test results it was concluded that the trained neural network models were effective for the prediction of temperature on the surface of the weldment during welding.

Depth of penetration %	Number of training data	Number of validation data	Network RMS error
100 – 110	254	37	0.03
90 – 99	107	11	0.07
80 – 89	207	20	0.03
70 – 79	278	27	0.04

Table 8.5 Number of training and validation data for neural network models.

8.6.2.2 Discussion of fuzzy logic model result

A fuzzy logic model has been used to compensate welding variables relative to the difference between actual and neural network predicted surface temperature.

The fuzzy logic model modifies the welding variables depending on the difference between the surface temperature predicted, by the neural network for a set of welding variables, and the temperature measured at a point on the surface of workpiece during welding. The fuzzy logic rule-based control model was constructed as described in chapter seven. The necessity of having the initial welding variables in addition to the temperature difference as an antecedent to the model was discussed. The model then predicted the welding variables to achieve the desired weld depth of penetration, i.e. full penetration. A number of experiments were conducted to evaluate the accuracy of the model. The results of the experiments show that the fuzzy logic model performance is accurate and consistent. The model can be applied for different fixed welding variables such as plate thickness or joint geometry, and/or different controllable welding variables such as welding current, and welding voltage, by modifying the membership function and/or rule base of the fuzzy logic model.

8.6.2.3 Discussion of control model result

The control model developed from this research was achieved by combining the neural network model, fuzzy logic model and data acquisition software. It may be used to monitor and control the quality of welding by regulating the controllable welding variables in real time. The key input to the control model is the temperature measured at a spot on the surface of the workpiece during welding, and the outputs are welding current, welding voltage, welding speed and torch angle. Due to unavailability of some software and hardware as discussed in section 8.4.3 it was not possible to evaluate the control model in a real time closed loop system. However the result of the evaluation of the control model in a manual closed loop shows that the model is capable of controlling weld penetration. Requirement for practical implementation of the model is discussed in chapter 9.

8.7 Practicability of the neuro-fuzzy control model

This research is intended to demonstrate how infrared sensing of surface temperature in the top face of a welded joint, coupled with a neuro-fuzzy control model, can be used to achieve control of penetration in Gas Metal Arc Welding. In the next sections the practicability of the proposed method, which includes methodology, equipment, and accuracy, will be discussed.

8.7.1 Practicability of methodology

The depth of penetration in fusion welding is the primary indicator of weld quality features such as weld strength or sidewall fusion which are not measurable during welding. However there is no direct method of measuring this quality indicator, other than from the back face of the weld, which is often impractical.

In the Gas Metal Arc Welding process, heat due to the electric arc fuses the workpiece so that the weld pool is generated and the remaining heat is conducted to

In the Gas Metal Arc Welding process, heat due to the electric arc fuses the workpiece so that the weld pool is generated and the remaining heat is conducted to the workpiece and dissipated to the environment by radiation and convection. Heat is applied to the joint until the melting point isotherm spreads by conduction through the thickness of the joint, or its root, to achieve full penetration. Other isotherms have similar shape to that of the melting point isotherm. (see figure 4.2).

Therefore, the heat flow pattern or temperature profile in the weldment may be an indicator of the performance of the welding process and can be used to monitor weld penetration. In this research it has been shown that the measured temperature on the surface of the workpiece during Gas Metal Arc Welding is a reliable source for estimation and control of weld penetration. The reasons for selecting surface temperature for modelling the relationship between depth of penetration and controllable welding variables include:

- The temperature in surface can be related to controllable welding variables such as voltage, current, welding speed and torch angle;
- There is a theoretical relationship between the depth of penetration and the heat distribution on the surface of the workpieces;
- The infrared sensor (fibre optic pyrometer) for measuring temperature is robust and of relatively low cost and, when attached to the welding torch, allows relatively easy access to the top surface of the joint during welding;
- Processing of data from the sensor is done rapidly;
- The neuro-fuzzy model when implemented, for example on a powerful P.C., can provide feedback response, less than 100 msec, quite adequate for welding process control.

8.7.2 Validity and Practicability of modelling technique

Gas Metal Arc Welding is a complex and non-linear process, which is difficult to control because of inadequate knowledge of the inter relationships of the variables in the process (152). This lack of knowledge limits the use of conventional analytical modelling. Artificial Intelligence techniques are widely applied to such problems and have been used to improve the control of the arc welding process. These techniques include Artificial Neural Networks, Fuzzy Logic and Expert Systems. The Artificial Neural Network (ANN) and Fuzzy Logic (FL) models, which have been developed and applied in this research, have been reviewed in previous chapters.

The neural network model was trained to model the relationship between a set of welding variables and the spot temperature measured at a position on the weldment surface, and the depth of penetration achieved. The networks have been trained using experimental data, extracted from more than 1000 weld samples. The model is able to predict the workpiece surface temperature which should occur for specified welding variables when 100-110% penetration is achieved. As with other modelling techniques neural networks have advantages and limitations. They are suitable for non-linear mapping, they learn from example, and require less development skill than mathematical or statistical modelling. However unlike expert systems they are not able to offer explanation of the final result. It has been found through evaluation of models that neural network modelling produces the best results when the application input data to the network is in the same range as that with which the network had been trained. Neural networks do not extrapolate particularly well for extensions beyond the learned input regions. To overcome this problem the network must be trained with a wide range of data, requiring more experimental empirical data.

The fuzzy logic model has been used to predict the required control adjustments to welding variables. The model predicts the modified welding variables as a function of the difference between the temperature measured during welding and the output temperature of the neural network model. Initially only the temperature difference

was used as input to the fuzzy logic model. However due to inaccuracies in the prediction of output modified welding variables, the initial nominal welding variables were also used as an input to the FL model. It was found that the fuzzy logic model has its best performance when the inputs are in the same range as the predefined membership function for each input and output.

For practical application of the control model it would be necessary to integrate the fuzzy logic model, the neural network model, the input from the analog to digital converter of the infrared sensor and the initial welding variables. Unfortunately there was no proper tool available to convert the developed fuzzy logic model by MATLAB to C^{++} language for this integration. Therefore the fuzzy Logic model was operated separately.

8.7.3 Practicability of equipment

In this research the major equipment used included, an infrared temperature sensor, a thyristor controlled GMAW power supply and a 6 axis general purpose robot with standard welding application software.

The Fanuc welding robot used was capable of communication to external computer facilities. However access to the robot control software language was not available, therefore it was not possible to integrate the developed control models with the robot and welding power supply controls on-line.

8.7.3.1 Practicability of temperature measurement sensor

In this research a fibreoptic pyrometer was used for measuring temperature. This sensor uses a fibre optic cable to transmit the infrared radiation from the surface of the weldment to a remote infrared sensor. They are typically used when access to a target is difficult, or where the temperature at the location of the sensing head is high (up to 200 °C), such as in arc welding, thus preventing thermal damage to the sensor. Due to the small size of the head, in this research it could be attached to the welding

torch. Other advantages of infrared temperature sensors were discussed in chapter 3. In the next section the effect of spatter and fume on the accuracy of the sensor is discussed further.

8.7.3.1.1 Effect of spatter and smoke on sensor accuracy.

In order to fulfil the objective of this research, an accurate temperature measurement from a spot on the surface of the workpiece should be available in real time during welding. Also the accuracy of the neuro-fuzzy control models depended on the accuracy of the temperature data used in the modelling process. In Gas Metal Arc Welding spatter and fume will occur. In this research, to avoid damage and hence inaccuracy in the temperature measured, the fibre optic head was assembled in a housing, purged with compressed air, and fitted with a glass window to prevent the spatter damaging the sensor lens. Spatter and fume deposited on the glass window, would affect the temperature measurement. Therefore it was necessary to periodically clean or replace the window.

An experiment was conducted to evaluate the effect of spatter and fume on temperature measurement, based on the amount of welding completed. In this experiment a constant heat source (the radiating filament of a tungsten light bulb) was used, and the sensor used to measure the temperature through glass windows, which had been used for specific amounts of welding. The results are summarised in figure 8.7.

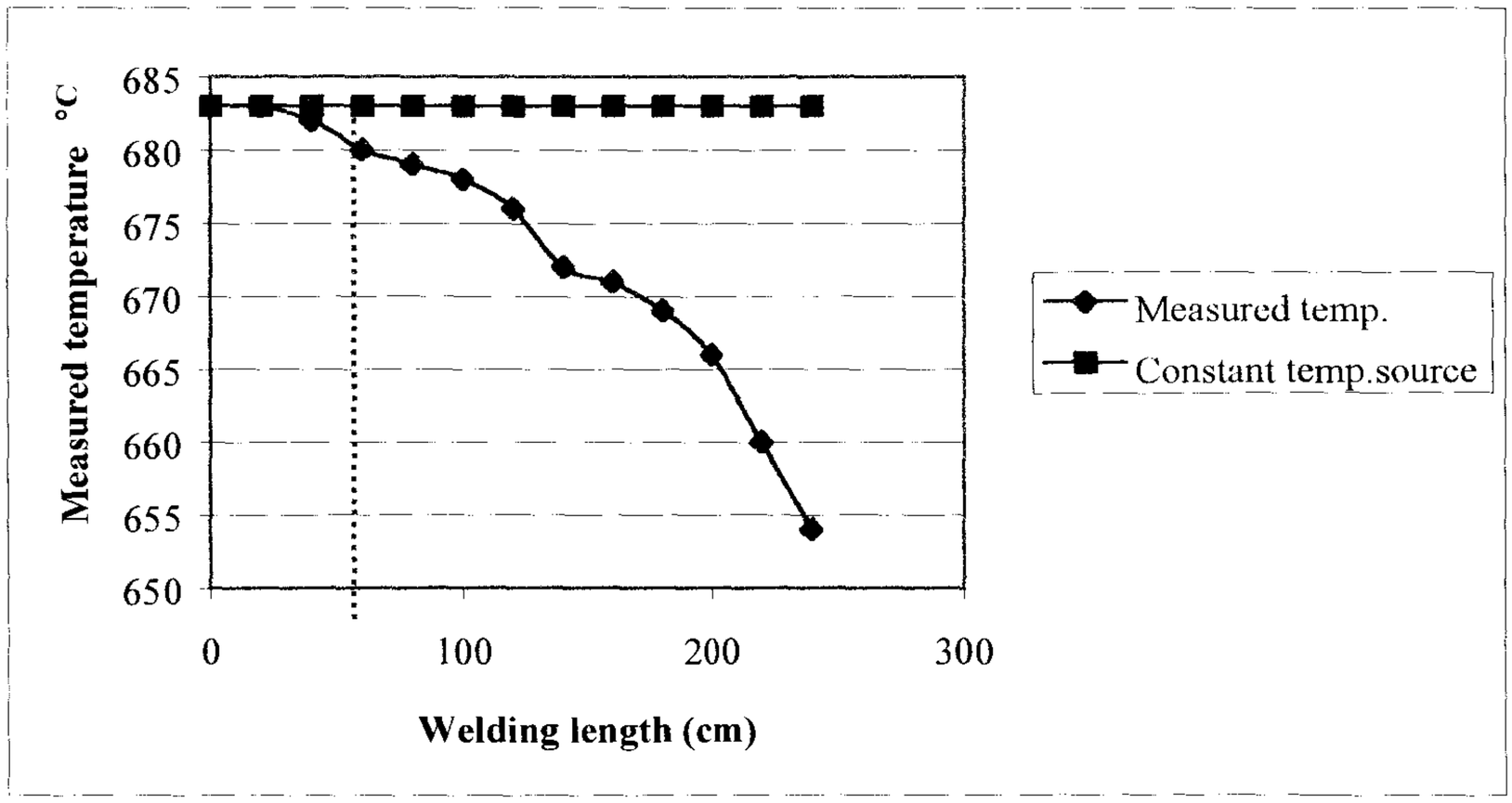

Fig.8.8 The effect of spatter and smoke on temperature measurement

As shown in the 8.7 figure the sensor is still accurate after 600mm of welding, this will permit ±5° error in the measurement. In experiments to obtain modelling data the glass windows was replaced every 200mm of welding.

As described in chapter two, the amount of spatter is different for each metal transfer mode. It has been found that if welding is by spray transfer mode, due to a lower rate of spatter, two times the amount of welding can be completed before the temperature measured was significantly effected. The problem was most serious with dip transfer welding due to the deposition of very fine spatter on the glass window.

In practise this problem will require periodic replacement of the sensor window, a limiting factor, or as has been used by other researchers (153) an indexible window could be used to extend the life of the window between replacements. It is also possible that development of gas or air flow for purging the sensor head could eliminate the problem, but care would be needed to assure the welding gas shield was not disrupted.

8.8 Advantages of the control model

The proposed control model has a number of advantages over other control techniques for assuring the penetration in the automated Gas Metal Arc Welding process. These are listed as follows:

- It has been shown that the heat distribution in the workpiece and the temperature at a point in the top surface of the joint have a direct relationship with the weld penetration, and therefore the quality of the weld.

- Measuring the top surface temperature of workpiece during welding by infrared sensor is a relatively easy and cost effective method compared with other sensing method such as ultrasonic, vision, and sound pressure sensors, which were described in chapter three.

- In the control model the neural network was used to predict the expected top surface temperature from nominal welding variables. This method has been shown to be more efficient compared to mathematical modelling as described in chapter three, in which a number of simplifying assumptions have to be made, or statistical modelling which needs a large amount of empirical data.

- The result of the evaluation of the control model presented in chapter seven shows the neuro-fuzzy control model was capable of predicting the welding variables required in order to achieve welds with the desired depth of penetration.

- The fuzzy control model is easy to design by constructing a proper rule base suitable for the control of welding variables. Fuzzy logic control models have a number of advantages over other control modelling techniques, as discussed in chapters three and seven.

- Most of the research on modelling of welding processes, including modelling of heat distribution in a workpiece (73, 142, 148, 116), is based on bead on

plate welding. This is not representative of many industrial welding applications. The control model developed in this research is based on experimental data collected from welding in a Vee groove joint in 6-mm plate thickness, which is a common real welding application in the fabrication industry.

8.9 Limitations of the control model

The control model has number of limitations, which are listed as follows:

- The scope of the model is limited in that the welding variables must be within the range used for training the neural network model. If different values of welding variables are to be used, the neural network model must be retrained with new data.

- The input of the fuzzy logic model should be within the range of the membership functions for the input variables. If different input values are used the membership function or the rules must be modified.

- The sensor head needed to collect input temperature data is placed in the vicinity of the welding zone and must be protected from the effect of fume and spatter or else error in temperature measurement will occur.

Chapter nine Conclusions and future work

9.1 Introduction

This chapter presents the conclusions drawn from this research and suggestions for further research and development on the neuro-fuzzy control model in order to improve the utility of the proposed system.

9.2 Conclusions

The research work reported has shown the feasibility of developing Artificial Intelligence modelling techniques, including Artificial Neural Network and Fuzzy Logic, for controlling the penetration of welds in a Robotic Gas Metal Arc Welding process. The research investigated a single sided V groove joint welded in the flat position. The following conclusions have been reached:

1. A comprehensive database has been established containing information on actual weld beads, workpiece surface temperature at a defined point, and weld bead geometry including weld penetration. This data was used to generate the models in this research and may be useful to other researchers working in this area (Chapter 5). The data base listing is included as appendix 1.

2. It has been demonstrated that a fibre optic pyrometer is suitable for measurement, with good accuracy, of the workpiece surface temperature at a specific position relative to the welding line during welding.

3. It has been shown that Artificial Neural Network modelling is an appropriate tool for developing the relationship between welding variables; welding current, welding voltage, welding speed, torch angle and spot temperature on surface of workpiece. It has been demonstrated that the neural network model developed can be used as a reference model to predict the temperature on the

surface of the workpiece at a specific point along the weld line during welding.

4. Different types of neural network modelling technique were applied and evaluated. Evaluation of those tested shows that the Radial Base Function (RBF) feed forward network model is the most appropriate technique for prediction of surface temperature.

5. It has been demonstrated that a neural network model alone cannot be used for adjusting the welding variables corresponding to measured temperature on the surface of the workpiece. The evaluation results shows that welding variables prediction was not accurate enough for controlling the process.

6. The neural network model was compared with an analytical model, and with statistical regression. It has been shown that neural network prediction of welding variables was more accurate than these other two methods.

7. It has been demonstrated that a fuzzy logic control model is capable of compensating the welding variables depending on the difference between measured temperature and the temperature predicted by the neural network model. The rule base for the fuzzy model was developed in order to assure production of a weld with 100%-110% depth of penetration.

8. The quality of welds is strongly dependent on the weld bead geometry especially the depth of penetration. Weld bead geometry has a relationship with heat distribution in the workpiece, and furthermore the heat distribution in the workpiece has a relationship with controllable welding variables (current, voltage, and speed, torch angle). Therefore monitoring the temperature on the surface and adjusting the controllable welding variables is a reliable technique for controlling the quality of welding.

9. The results of the evaluation of the neuro-fuzzy control model show that the model is capable of detecting conditions at which the welding process is not

achieving full penetration welds. The model can then suggest appropriate modification to the welding variables.

10. It has been shown that the difference in temperature between the infrared sensor measured value and that predicted by the RBF neural network is a good indicator of achievement of satisfactory penetration, even in the presence of substantially varying root gap.

11. The developed Neuro Fuzzy Control model is capable of implementation in a real time adaptive control for robotic Gas Metal Arc welding, and this is discussed in chapter 9.

9.3 Future work

The study reported here has shown that by using suitable Artificial Intelligence techniques the quality of weld can be controlled in real time. The neuro-fuzzy control model is capable of controlling the weld penetration by monitoring the temperature measured at a point on the surface of the workpiece. This research can be extended in a number of ways:

1. The neuro-fuzzy control model (NFCM) should be implemented as an automatic closed loop system, in which the controllable welding variables can be adjusted in real time. For this purpose it is necessary to have access to robot controller language and to develop appropriate software interfaces between the models and the robot controller.

2. In order to make the model more general in dealing with variable root gap, in particular when gap is of such size as to possibly lead to burn through, a neural network model can be constructed to have the joint geometry as additional input. For this purpose a striped laser sensor (46) could be used to measure the joint geometry such as, root face thickness and root gap prior to the welding.

3. Other controllable welding variables such as weaving, and stand–off distance could be introduced to the control modelling, as these two variables have an strong influence on the penetration and quality of weld and the stability of arc (17, 117).

4. Different neural network and fuzzy logic models could be constructed for different plate thicknesses.

5. The area of the joint can be calculated prior to the welding, then the neural network trained with the area of the joint and welding variables. This could improve the generality of the NFCM by controlling the welds with a wide range of plate thickness, and joint geometry.

6. In order to reduce the effect of spatter and smoke on the infrared sensor temperature measurement, the sensor assembly on the torch, and the design of housing could be reconsidered. Also it may be possible to design a device which automatically changes or cleans the glass windows periodically.

7. The basic principle of the fuzzy logic model applied in this research is that the relationship governing the model inputs and the outputs are assumed to be represented by a fuzzy system in terms of IF – THEN rules, which is extracted from domain experts. This approach relies on the availability of domain experts. Another approach called self – organising controller (SOC) (141, 54), is to construct the rule-base by directly operating the welding process. In this method the fuzzy logic model is able to develop the rule-base, and fine tune membership functions for controlling the welding process in real time.

8. Develop fuzzy logic models to take account of constant or variable root gap.

References

1 Matton, R.A. "Maximising arc welding productivity, minimising its cost", Tooling and Production, Vol. 56, No. 1, 1990, pp. 58-63.

2 Tay K.M., and Butler C. "Modelling and optimising of a Mig welding", Quality and Reliability Engineering International", Vol.13, 1997, pp. 61-70.

3 Nadew F., et.al. "Method and apparatus for controlling root pass weld penetration open butt joint", United State Patent No. 4733051, 1988.

4 Bentley A.E., and Marburger Quantitative feedback theory", Welding Journal, 1992, pp.397-404.

5 Song J.B. and Hardt D.E "Close-loop control of weld pool depth using a thermally based depth estimator", Welding Journal, Oct.1993, pp.471-476.

6 Hardt D.E.and Katz J.M., "Ultrasonic measurement of weld penetration", Welding Journal 63 (9), 1984, pp. 273-28.

7 Lawsuit A. "Control of melting rate and metal transfer in GMAW", Welding Journal 37 (9) pp. 418-425.

8 Kim Y.S., and Egar T.W. "analysis of metal transfer in gas metal arc welding", Welding Journal, Jun. 1993, 72(6), pp.269-277.

9	Uttrachi G.D., and Meyer D.W.	"The basic of semiautomatic welding, Welding Journal Aug., 1993, pp. 47-51.
10	Davies A.C.	"The science and practice of welding",8th edition vol.2, Cambridge university press (1984) p.87.
11	Smith D.	"Welding skills and technology", McGraw-Hill, (1986) pp. 425.
12	American Society of metals	"Metals hand book", vol. 8 welding , ASM, pp. 154- 173.
13	Davies A.C.	"The science and practice of welding",10th edition, Cambridge university press, 1993, p.105.
14	Irving B.	"Inverter power source check fume emission in GMAW", Welding Journal, Feb. 1992, pp.53-56.
15	Kirk C., and Mileham A.	"Gas shielded metal arc welding improving quality by minimisation of defects", Advance in Manufacturing Technology VIII, Taylor & Francis, 1994 , pp.617-621.
16	Smith A.A.	"Co_2 welding", The Welding Institute, Keyworthe & Fry Ltd., 1970, pp. 70-71.
17	Grong O., and Christensen N.	"Effects of weaving on temperature distribution in fusion welding". Material Science and Technology, September 1986, pp. 967-973.

18 Gray, T.G.F., et.al. "Rational welding design", Newnes-Butterworths, 1975, pp.39-70.

19 Smith A.A. "Co_2 welding", The Welding Institute, Keyworthe & Fry Ltd., 1970, PP.145-146.

20 Dufour M.L., and Maldge X. "Prevention of spatter and molten particle adherence to protective windows in welding application", Welding Journal, Jan 1987, pp. 43-46.

21 Anon "Farm equipment fabricator reduces weld spatter", Welding Journal , Jan 1986, p46.

22 American welding Society "Welding hand book",8th edition vol.1, Welding Technology ,AWS,1987, pp. 4-8.

23 Gray T.G.F., and Spence J. "Rational welding design", Second edition, Butterworths & Co., 1982, pp. 41-49.

24 Lancaster J.F. "Metallurgy of welding", Fourth edition, Allen & Unwin, London, 1987, pp.17-20.

25 Anon "Recommended joint preparation for steel", Welding in the World, Vol.37, No.4, Jul-Aug 1996, pp.177-185.

26 Ghasemshahi M. "P.I.K.B.E.S. expert system for welding process quality control" PhD theses. Loughborough university, 1991.

27	Irving B.	"Trying to make some sense out of shielding gases", Welding Journal, May 1994, pp.65-69.
28	Rosenthal D.	"Mathematical theory of heat distribution during welding and cutting", Welding Journal, Vol. 20 No.5, 1941 pp. 220-234.
29	Jonsson P.G., et.al.	"Heat and mass transfer in GMAW using Argon and helium", Metallurgical and Materials Transaction B, Volume 26B, April 1995, pp. 383-395.
30	Ushio M., et.al.	"Theoretical calculation on shape of fusion boundary and temperature distribution around moving heat source (Report I)",Transaction of Japan Welding Resarch Institute (JWRI), vol.6, No. 1, 1977, pp. 1-6.
31	Doumanidis C.C.	"GMA weld bead geometry : A lumped dynamic model", Proceeding of 3rd International Conference on Trends in Welding Research, USA, 1992, pp. 63-67.
32	Fenn R.	"Ultrasonic monitoring and control during arc welding", Welding Journal, vol.64. (1985) pp.18-22.

33 Shinoda, T., and Doherty, J. "The relationship between arc welding parameters and bead geometry- a literature survey", The Welding Institute Research Report No. 74/1978/PE, Oct.1978.

34 McGlone J.C. "Weld bead geometry prediction - a review", Metal Construction, July 1982, pp. 378-384.

35 Giedt W.H., et.al. "Effect of surface convection on stationary GTA weld zone temperature, Welding Journal, Dec. 1984, pp. 376-383.

36 Fitzpatrick P.R., and Bak M. "Thermal analysis and experimental correlation of the GTA welding process, Computer Technology in Welding, vol.38, Welding Inst., UK, 1986.

37 Lambrakos S.G., et.al. "A numerical model of deep penetration laser welding", Proceeding of 3rd International Conference on Trends in Welding Research, USA, 1992, pp. 51-56.

38 Shepherd P.R. "A contribution to adaptively controlled robotic arc welding",Phd thesis, Loughborough University, 1985.

39 Thorn K., et.al. "The interaction of process variables - their influence on weld dimensions in GMA welds on steel plates", Metal Construction and British Welding Journal, vol 14(3). March 1982, pp. 128-133.

40 Sowizral H.A., and Kipps J.R. "A programming environment for expert system", Expert system, Addison-Wesley publishing co., pp.27-69, 1986.

41 Bahashwan A.A., and Garg S.B.L. "A Review of the application of expert system to welding", Int. Jour. of Materials and Product Technology, Vol. 11, No.1-2, 1996, pp.89-97.

42 Thompson D.R., et.al. "A hierarchically structured knowledge-based system for welding automation and control", Journal of Engineering for Industry, vol.110, pp.71-76, 1988.

43 Budgifvars S. "The computer welding expert- the use of Artificial intelligence to facilitate welding",, ESAB. Svetsaren 2.88, part 2, Sweden, pp 4-5, 1988.

44 Kerth W.J. "Knowledge-based expert welding", Robots 9th Conference Proceedings, USA, pp.98-110, 1988.

45 Vivek G., and Lee K.S. "A shielded metal arc welding expert system", Computer in Industry, vol. 21, pp.121-129, 1993.

46	Ghasemshahi M., and Middle J. E.	"An expert system approach to the control of welding procedures", Proceeding of 4th International Conference in Automated Welding System , paper 5, Gateshead, UK.1991.
47	Misra S. and Subramaniam S.	"Expert system for GMA welding of aluminium", International Trends in Welding Science and Technology, Proceeding of the 3rd International Conference on Trends in Welding Research, pp.959-953, Gatlinburg, USA, 1992.
48	Reeves R.E., et.al.	"Expert system technology an avenue to an intelligent weld process control system", Welding Journal, pp.33-41, Jun., 1988.
49	Pierre S., and Levine M.D.	"Mars: An expert robot welding system", Machine Intelligent and Knowledge Engineering for Robotic Application, NATO ASI series, Vol. f33, 1987.
50	Vanderveldt H., and Xu X.	"Weldexcell a pc-based welding engineering station", Welding and Weld Automation in Shipbuilding, 1996, pp. 195-215
51	Taylor W., et.al.	"Knowledge acquisition and synthesis in a multiple source multiple domain process context", Expert Sytems with Application, Apr.1995, pp.. 295-302.

52 Beerel A.C. "Expert system-strategic implications and applications", Ellis Horwood. Ltd, 1987.

53 Street N.J., et.al. "Adaptive robotic welding of controlled penetration root welds",1st. International Conference on Advanced Welding System, Welding Institute, p5-1-p5-8, 1985.

45 Procyk, T.J, and Mamdani, E. H. "A linguistic self-organising process controller", Automatica, vol.15, 1979, pp 15-30.

55 Cook G.E., et.al. "Intelligent gas tungsten arc welding control",Automated Welding System in Manufacturing, 4th International Conference, TWI, 1991.

56 Middle J.E. and Li Y. "Artificial neural networks applied to process modelling for robotic arc welding",International Conference on Modelling of Casting, Welding and Advanced Solidification Process, VI, Florida, USA, 1993, pp.127-134.

57 Middle J.E. and Li Y. "Application of ANN to intelligent post-weld inspection in flexible arc welding cell", Intelligent Robotics, Mac Graw-Hill,co. pp.375-384, 1993.

58 Stroud R.R., et.al "Neural network in automated weld control",Automated Welding System in Manufacturing, TWI, paper 22, 1991.

59 Ohshima K., et.al "Application of a fuzzy neural network to welding line tracking",Sensor and Control System in Arc Welding, Chapman &Hall , 1994, pp.147-153.

60 White D.R., et.al "Integration of process and control models for intelligent control of welding", International Trends in Welding Science and Technology, Proceeding of the 3rd International Conference on Trends in Welding Research, Gatlinburg, USA, pp.883-887.

61 Andeson K., et.al. "Gas tungsten arc welding process control using artificial neural networks",International Trends in Welding Science and Technology, Proceeding of the 3rd International Conference on Trends in Welding Research, Gatlinburg, USA, 1992 pp.877-881.

62 Einerson, C.J., et.al. "Development of an intelligent system for cooling rate and fill control in GMAW", International Trends in Welding Science and Technology, Proceeding of the 3rd International Conference on Trends in Welding Research, pp.853-857, Gatlinburg, USA, 1992.

63 Smart H.B. "Intelligent sensing and control of arc welding", International Trends in Welding Science and Technology, Proceeding of the 3rd International Conference on Trends in Welding Research, pp.843-851, Gatlinburg, USA, 1992.

64 Jones J. "Weld parameter modelling", International Trends in Welding Science and Technology, Proceeding of the 3rd International Conference on Trends in Welding Research. pp.895-898. Gatlinburg, USA, 1992.

65 Matteson A., et al. "Real-time GMAW Quality classification using an artificial neural network with air bone acoustic signal as inputs", Material Engineering, ASME, 1993, pp.273-278.

66 Dilthey L. U. et.al "On-line quality control in gas-shielded metal arc welding using artificial neural network", Schweissen und Schnden (Welding & Cutting), Vol. 49, part 2, 1997, pp E22-24.

67 Bishop C. M., "Neural network and their application",American Institute of Physics 65 (6), Jun., 1994.

68 Zadeh, L.A. "A fuzzy-set-theoretic approach to the composition, disposition and canonical forms",Journal of Semantics, December 1983, pp. 1-23.

69 Sugeno, M. "Current project in fuzzy control", In Workshop on Fuzzy Control System and Space Station Application, Huntington Beach, CA, NOV. 1990, pp. 65-77.

70 Berenji, H. R. "Fuzzy Logic Controller",An Introduction to Fuzzy Logic Application in Intelligent Systems,

Kluwer Acadamic Publishers, 1995, pp. 69-92.

71 Messler, W., Jr., et.al. "An intelligent control system for resistance spot welding using a neural network and fuzzy logic "Conference Record - IAS Annual Meeting (IEEE Industry Applications Society), 1995, Vol.2,pp. 1575-1763.

72 Siores E., Fenn R. "Adaptive control in arc welding utilising ultrasonic sensor", Second International Conference in Development in Automated and Robotic Welding, Welding institute, (1987), pp.8_1-8_10.

73 Cho, Hyung S. "Application of AI to welding process automation", Japan/USA Symposium on Flexible Automation, Volume 1, ASME 1992, pp. 303-308.

74 Won, Y.J., and Cho, H.S. "A fuzzy predictive approach to the control of weld pool size in gas metal arc welding process", Manufacturing Science and Engineering, Volume 64, ASME, 1993,PP. 927-938.

75 Ohshima, K., et.al. "Fuzzy control of CO_2 short-arc welding",Sensor and Control Systems in Arc Welding. Edited by Nomura, H., Chapman & Hall, 1994, pp. 137-146.

76 Ohshima, K., et.al. "Application of a fuzzy neural network to welding line tracking", Sensor and Control Systems in Arc Welding. Edited by Nomura, H., Chapman & Hall, 1994, pp. 147-153.

77 Fujimura, H., and Murakami, S. "Arc sensing using fuzzy control", Sensor and Control Systems in Arc Welding. Edited by Nomura, H., Chapman & Hall, 1994, pp. 238-246.

78 Erfer L. "Measuring temperature with infrared sensors", Machine Design, Aug. 1996, pp. 91-92

79 Zhang Y.M., et.al. "Neurofuzzy model based control of weld fusion zone geometry", Proceeding of the American Control Conference, New Mexico, June 1997, pp. 2483-2487.

80 Nomura H. "Sensor and control system in arc welding", Champion &hall, 1994, pp. 15-16.

81 Holder S.J., et.al. "Mechanical approaches to seam tracking for arc welding", The Welding Institute Report, 167/1981.

82 Nicolo V. "Industrial robots with sensory feedback application to continuous arc welding", 10th International Conference in Industrial Arc Welding Robots, 1980, pp.15-22.

83 Stroud R.R. "Seam tracking with ultrasound", Proceeding of 2nd Conference in Development in Automated and Robotic Welding, 1987.

84 Eichhorn F., and Borowka J. "Adaptive through the arc seam tracking system for narrow gap welding process", Proceeding of 2nd Conference in Development in Automated and Robotic Welding, 1987 pp.10_1-10_8.

85 Hanright J. "Robotic arc welding under control", Welding Journal, pp.19-24, Nov.1986.

86 Golderberg F., and Karlen R. "Inductive seam tracking and height sensing system for arc welding method and thermal cutting", Proceeding of Development in Mechanised, Automated, and Robotic Welding Conference, 1980, paper 24, pp. 24/1-24/5.

87 Lim T.G., et al. "Estimation of weld pool sizes in GMA welding process using neural networks", Journal of System and Control Engineering, Vol.27, 1993, pp.15-26.

88 Betz,G. "A general purpose 3D vision system",proceeding of 4th Conference on Robot Vision and Sensory Control, pp.149-154, 1984.

89 Agapakis J.E., et.al. "General visual sensing techniques for automated welding fabrication", 4th International Conference. on Robot Vision and Sensory Control, Oct. 1984, pp 103-114.

90 Richardson R.W. "Coaxial arc weld pool viewing for process monitoring and control". Welding Journal. March 1984, pp..43-50.

91 Neipold R., and Bruemmer F. "Optical sensor system control arc welding process", Proceeding of 2nd Conference on robotic vision and sensory control , USA, 1983, pp.625-633.

92 Zuech N. "Handbook of intelligent sensors for Industrial Automation", Addison-Wesly Inc., 1991, PP203-209.

93 Mccampbell W.M., et.al. "The development of weld intelligence system",Welding Journal, 45 (3), 1966. pp.139-144.

94 Tattam M.J. "Non-contact infra-red temperature measurement handbook", 8th edition, Calex Ltd, 1994, pp.15-16.

95 Loughborough Sound Images Ltd. Loughborough Sound Images Ltd. Catalogue.

96 Nagarajan S., and Chin B.A. "Infrared image analysis for on-line monitoring of arc welding processes", Material Evaluation Dec.(1990) pp.1469-1472.

97 Groom K.N., and Nagarajan S. "Automatic single V-groove welding utilising infrared image for error detection and correction",Welding Journal, , Dec., 1990, pp.441-445.

98 Doumanidis C.C., and Hardt D.E. "Simultaneous in-process control of heat-affected zone and cooling rate during arc welding", Welding Journal, 1990, pp.186-196.

99 Chin B.A., et.al. "Infrared thermography for sensing the arc welding process", Welding Journal, Sept. 1983, pp. 227-233.

100 Chen W., and Chin B.A. "Monitoring joint penetration using infrared sensing techniques", Welding Journal, Apr.1990, pp.181-185.

101 Goldak J., et.al. "Computer modelling of heat flow in welds", Metal. Trans., Vol. 17B, No.9, 1986, pp. 587-600.

102 Hrivnak I "Theory of weldability of metals and alloys", Elsevier Publishing Co., 1992, pp. 18.

103 Banerjee P., et.al "Infrared sensing for on line weld geometry monitoring and control", Journal of Engineering for Industry, August 1995, pp. 323-329.

104 Lancaster,J. F. "Metallurgy of Welding, Brazing and Soldering", Allen and Unwin,1970 , pp.46-47.

105 Christensen N., et. al. "Distribution of temperature in arc welding", British Welding Journal, Feb. 1965, pp.54-75.

107 Bae K.Y, et al. "A study of vision-based measurement of weld joint shap incorporating the neural network",

Journal of Engineering Manufacture, Vol. 208, 1994, pp.61-67.

108 Boillot J.P., et al. "Automatic welding using laser-based 3d vision system", Welding in the World, Vol. 34, 1994, pp.173-182.

109 Roberts D.K., and Wells A.A. "Fusion welding of aluminium alloys", British Welding Journal, Volume 1, 1954 , pp. 553-560.

110 Apps L., and Milner D.R. "Heat flow in argon-arc welding", British Welding Journal, Oct. 1955, pp. 475-848.

111 Eagar T.W., and Tsai N.S. "Temperature fields produced by travelling distributed heat sources", Welding Journal, 62(12), Dec. 1983, pp. 346-355.

112 Weiss.D, et.al. "A model of temperature distribution and weld pool deformation during arc welding ", Mathematical Modelling of Weld Phenomena 2, Edited by Cerjak H., The Institute of Materials, 1995, pp. 23-39.

113 Song J.B., and Hardt D.E. "Multivariable adaptive control of bead geometry in GMA welding", PED-Vol. 51, Welding and Joining Processes, ASME, 1991, pp. 123-134.

114 Kim I.S and Basu A. "A study of influence of welding process variable on GMAW", Transaction of Mechanical Engineering, Australia, Vol. ME20 No. 1, May 1995, pp. 35-41.

115 NeuralWare, Inc. "NeuralWorks professional II/plus and Neural Network explorer", user manual, 1995.

116 Chen S.B., et al. "Self-learning fuzzy neural network for control of uncertain system with time delays", IEEE Transaction on System, Man, and Cybernetics, Vol. 27, No.1 1997, pp. 142-148.

117 Smith D. "Welding skills and technology", McGraw-Hill, 1986, pp.454-455.

118 Hobart Brothers Company Ltd. "Technical guide for gas metal arc welding ", 1980.

119 Fanuc Ltd. "Fanuc robot s-model 100 user manual", Fanuc Ltd. 1986.

120 Aoip Mesures Optical pyrometers TR 7410 - TR7420 instruction manual, June 1989, pp. 7-8.

121 McCulloch W.S., and Pitts W.H., "A logical calculus for the ideas in nervous activity", Bulletins of Mathematical Biophysics, Vol. 5, 1943, 115-133.

122 Rosenblatt F., "Principles of Neurodynamics", Spartan Books, Washington D.C., 1961.

123 Hopfield J.J. "Neural Networks and physical systems with emergent collective computational abilities". Proceedings of the National Academy of Sciences, Vol. 79, 1982, pp. 2554-2558.

124 Rumelhart D.E., and McClelland J.L. "Parallel Distributed Processing: Explorations in the Microstructure of Cognition", Vol. 1-2, 1986, MIT Press, Cambridge, Massachusetts.

125 Naimimohasses, R. "Analysis and modelling of light scattering sensors using neural networks",Ph.D. Thesis - Loughborough University, 1996

126 Limin, Fu. "Neural Network in computer intelligence", MC-Graw_Hill, 1994, pp. 338-339

127 Fahlman S.E., and Lebiere C. "The cascade-correlation learning architecture", report no. CMU-CS-90-100, Carnegie Mellon University, Pittsburgh, PA, 1990, 1-13. (Available via ftp:ernst.mach.cs.cmu.edu).

128 Ash T. "Dynamic node creation", Connection Science, 1989, Vol. 1, no. 4, pp.365-375.

129 Hirose Y., et.al. "Back-propagation algorithm which varies the number of hidden units", Neural Networks, 1991, Vol. 4, pp.61-66.

130 Mozer M.C., "A technique for trimming the fat from a network via relevance "Skeletonization assessment", Advances in Neural Information Processing 1, 1988, San Mateo, Ca, 107-115.

131 Le Cun Y., et.al. "Optimal brain damage", Advances in Neural Information Processing Systems 2, 1990, Morgan and Kaufmann, Inc. pp. 598-605.

132 Lippman, R. P. "An introduction to computing with neural nets", Assp Magazine, A publication of the IEEE Acoustics, Speech, and signal processing society, Vol. 4 No.2, 1987, pp. 2-21.

133 Broomhad D.S., and Lowe D. "Multivariate functional interpolation and adaptive networks", Complex System, Vol. 2, 1988, pp. 321-355.

134 Leonard J.A., et.al. "Using Radial Basis Function to approximate a function and its error bounds", IEEE Transaction on Neural Network, Volume 3, No. 4, 1992, pp. 624-627.

135 Kung S.Y. "Digital Neural Network", Prentic-Hall, Inc.,1993, pp.171-172.

136 Middle J.E., and Khalaf GH. "Neural network modelling of temperature distribution for control of gas metal arc welding", Proceeding of 7th Conference on Modelling Casting and Welding, 1995, pp.397-405.

137 Masters, T. "Practical neural network recipes in C plus plus", Boston: London: Academic Press,1993 pp 197-198

138 Sukhan L.and Rhee M. "Inverse mapping of continuous function using local and global information", IEEE Transactions on Neural Network. Vol. 5.No.3. 1994. pp. 409-422.

139 DTI "Neural computing learning solutions",DTI,1994.

140 Neural Ware Inc. "supplement for neural works professional". Neural Ware, 1995, pp.SU16.

141 Li, Di "Neural network based self-organized fuzzy logic control in arc welding", Proceeding of First International Conference on Knowledge-based Intelligent Electronic System, IEEE, May 1997, pp. 684-690.

142 Boo, K.S., and Cho H.S. "A fuzzy Linguistic control approach to the control of weld pool size in gas metal arc welding processes", PED- vol.51, Welding and Joining Processes, ASME, 1991, pp.73-84.

143 Harris C.J., et.al. "Intelligent Control Aspects of Fuzzy Logic and Neural Nets", World Scientific, 1993, pp. 40.

144 Zadeh L.A. "A fuzzy set-theoretic interpretation of linguistic hedges", Jour. of Cybernetics, vol.2, No.3, 1972, pp 4-34.

145 Jang, R. and Gulley N. "Fuzzy Logic Toolbox", The Matlab Works Inc., 1995 pp. 2-102.

146 Ahmad M. Ibrahim "Introduction to Fuzzy Electronics",Prentice Hall,1997, pp. 83.

147 Tay K.M., and Butler C. "Modelling and optimising of a MIG welding process-a case study using experimental designs

and neural networks", Quality and Reliability Engineering International, Vol. 13, 1997 pp. 61-70..

148 Karsai G., et.al. "Neural network methods for the modelling and control of welding processes", Journal of Intelligent Manufacturing, Vol. 3, 1992, pp. 229-235.

Appendix 1

Welding Exprimental Results

Appendix 1

1.1 experimental data and results for welding achieving 100%-110% depth of penetration

No.	Torch angle deg.	current Amp.	voltage Volt.	speed cm/min	temp T1º C	bead width mm	bead high mm	bead penetration mm	bead penetration %
1.	70	380	37	80	776	8.6	1.5	6.2	103
2.	70	390	37	80	677	9.0	1.5	6.9	115
3.	70	390	37	80	684	9.0	1.5	6.4	107
4.	70	390	37	80	687	9.2	1.9	6.2	103
5.	70	390	37	80	682	8.4	1.7	6.9	115
6.	70	390	37	80	687	8.4	1.9	6.2	103
7.	70	390	37	80	689	9.0	2.4	6.4	107
8.	70	390	37	80	677	9.4	2.1	6.2	103
9.	70	390	37	80	675	8.4	2.1	6.1	102
10.	70	390	37	80	667	9.0	2.1	6.1	102
11.	70	390	37	80	672	9.0	1.1	6.1	102
12.	70	390	42	85	704	8.6	1.1	7.2	120
13.	70	400	37	85	634	8.2	2.3	6.2	103
14.	70	400	37	85	648	7.5	1.9	6.2	103
15.	70	400	37	85	646	7.7	2.1	6.2	103
16.	70	400	37	85	651	7.9	2.4	6.1	102
17.	70	400	37	85	660	7.7	2.3	6.1	102
18.	70	400	37	85	665	7.7	2.3	6.1	102
19.	70	400	37	85	663	8.2	2.4	6.0	100
20.	70	400	37	85	646	8.2	2.6	6.0	100
21.	70	400	37	80	752	9.0	2.0	6.2	103
22.	70	400	37	80	747	9.4	2.1	6.1	102
23.	70	400	37	80	740	9.7	2.0	6.0	100

No.	Torch angle deg.	current Amp.	voltage Volt.	speed cm/min	temp T1 ° C	bead width mm	bead high mm	bead penetration mm	bead penetration %
24.	70	400	37	80	730	9.4	1.7	6.6	110
25.	70	400	37	80	726	8.6	1.7	6.4	107
26.	70	400	37	80	723	8.2	0.9	6.9	115
27.	70	400	37	90	655	7.9	1.7	6.9	115
28.	70	400	37	90	655	7.9	1.7	6.9	115
29.	70	400	37	90	648	8.2	1.7	6.4	107
30.	70	400	37	90	660	8.4	1.7	6.9	115
31.	70	400	37	90	665	8.2	1.5	6.6	110
32.	70	400	37	90	658	8.8	1.7	6.0	100
33.	70	400	37	90	663	9.0	1.7	6.2	103
34.	70	400	37	90	655	8.4	1.7	6.4	107
35.	70	400	37	90	660	7.9	0.6	6.0	100
36.	70	400	42	85	711	9.2	2.0	6.0	100
37.	70	400	42	85	704	9.0	1.1	6.2	103
38.	70	400	42	80	687	8.4	1.7	6.4	107
39.	70	400	42	80	694	9.0	1.8	6.4	107
40.	70	400	42	80	704	9.7	1.9	6.1	102
41.	70	400	42	80	714	9.2	1.9	6.2	103
42.	70	400	42	80	716	9.7	1.9	6.1	102
43.	70	400	47	80	709	8.6	2.3	6.1	102
44.	90	380	37	85	726	6.0	1.2	6.2	103
45.	90	380	37	85	733	6.0	1.5	6.1	102
46.	90	380	37	85	724	6.4	1.5	6.0	100
47.	90	380	37	85	716	6.4	1.6	6.0	100
48.	90	380	37	85	724	6.9	1.5	6.0	100
49.	90	380	37	85	724	6.0	1.4	6.3	105
50.	90	380	37	85	735	6.2	1.5	6.4	107
51.	90	380	37	85	716	6.2	0.4	6.3	105

No.	Torch angle deg.	current Amp.	voltage Volt.	speed cm/min	temp T1 º C	bead width mm	bead high mm	bead penetration mm	bead penetration %
52.	90	390	37	80	721	6.9	2.1	6.4	107
53.	90	390	37	80	723	5.6	1.9	6.6	110
54.	90	390	37	80	726	6.4	2.3	6.2	103
55.	90	390	37	80	721	6.9	2.3	6.0	100
56.	90	390	37	80	726	7.3	2.1	6.2	103
57.	90	390	37	90	718	6.4	1.7	6.4	107
58.	90	390	42	80	960	7.7	2.0	6.3	105
59.	90	390	47	80	856	8.4	2.2	6.1	102
60.	90	390	47	80	815	7.9	2.1	6.0	100
61.	90	390	47	80	806	7.9	1.1	6.1	102
62.	90	400	37	85	733	6.2	2.1	6.3	105
63.	90	400	37	85	736	5.8	2.1	6.4	107
64.	90	400	37	85	731	6.7	-1.7	6.2	103
65.	90	400	37	85	726	6.2	2.4	6.2	103
66.	90	400	37	85	726	6.4	2.4	6.2	103
67.	90	400	37	85	723	6.7	2.4	6.1	102
68.	90	400	37	85	723	6.4	2.4	6.0	100
69.	90	400	37	85	730	6.7	2.6	6.0	100
70.	90	400	37	85	723	6.4	2.6	6.1	102
71.	90	400	37	85	721	7.1	1.3	6.3	105
72.	90	400	37	80	740	7.1	2.3	7.8	130
73.	90	400	37	80	728	5.6	1.5	7.9	132
74.	90	400	37	80	730	5.8	1.7	7.7	128
75.	90	400	37	80	730	5.4	1.8	7.4	123
76.	90	400	37	80	730	6.2	1.9	7.3	122
77.	90	400	37	80	733	6.0	1.9	7.5	125
78.	90	400	37	80	728	5.6	1.7	7.5	125
79.	90	400	37	80	726	5.4	1.7	7.6	127

No.	Torch angle deg.	current Amp.	voltage Volt.	speed cm/min	temp T1 º C	bead width mm	bead high mm	bead penetration mm	bead penetration %
80.	90	400	37	80	716	6.0	1.6	7.9	132
81.	90	400	37	80	713	5.6	0.3	8.1	135
82.	90	400	37	90	721	5.4	1.7	6.3	105
83.	90	400	37	90	723	5.8	1.8	6.3	105
84.	90	400	37	90	726	6.0	2.1	6.2	103
85.	90	400	37	90	726	5.8	2.0	6.2	103
86.	90	400	37	90	726	6.0	2.0	6.2	103
87.	90	400	37	90	723	6.4	2.1	6.2	103
88.	90	400	37	90	726	6.0	2.1	6.2	103
89.	90	400	37	90	718	6.0	2.1	6.2	103
90.	90	400	37	90	716	6.0	1.9	6.3	105
91.	90	400	37	90	711	6.4	1.0	6.1	102
92.	90	400	42	85	936	8.2	1.9	6.1	102
93.	90	400	42	85	910	7.9	2.1	6.0	100
94.	90	400	42	80	895	7.7	1.6	7.5	125
95.	90	400	42	80	909	7.7	1.7	6.6	110
96.	90	400	42	80	919	8.2	1.9	6.6	110
97.	90	400	42	80	878	7.9	1.9	6.7	112
98.	90	400	42	80	837	7.5	1.8	7.0	117
99.	90	400	42	80	810	7.7	2.0	6.2	103
100.	90	400	42	80	793	8.2	2.1	6.0	100
101.	90	400	42	80	779	8.2	2.0	6.1	102
102.	90	400	42	80	791	7.7	1.9	6.2	103
103.	90	400	42	80	788	8.2	1.3	6.2	103
104.	90	400	47	85	873	7.5	2.0	6.0	100
105.	90	400	47	80	871	7.5	1.7	6.4	107
106.	90	400	47	80	878	7.9	1.9	6.4	107
107.	90	400	47	80	924	8.2	1.9	6.7	112

No.	Torch angle deg.	current Amp.	voltage Volt.	speed cm/min	temp T1 ² C	bead width mm	bead high mm	bead penetration mm	bead penetration %
108.	90	400	47	80	912	7.7	1.9	6.6	110
109.	90	400	47	80	885	8.2	2.0	7.1	118
110.	90	400	47	80	861	7.5	2.1	6.4	107
111.	90	400	47	80	849	8.2	1.8	6.6	110
112.	90	400	47	80	854	7.7	1.9	6.6	110
113.	90	400	47	80	871	7.7	2.0	6.2	103
114.	90	400	47	80	871	7.9	1.1	6.4	107
115.	110	380	37	85	815	6.0	1.7	6.0	100
116.	110	380	37	85	815	6.0	1.9	6.0	100
117.	110	380	37	85	805	6.2	1.8	6.0	100
118.	110	390	37	85	779	5.6	2.5	6.0	100
119.	110	390	37	85	769	4.9	2.2	6.0	100
120.	110	390	37	85	781	4.9	0.6	6.1	102
121.	110	390	37	80	796	5.2	1.6	6.6	110
122.	110	390	37	80	777	6.0	1.6	6.9	115
123.	110	390	37	80	770	5.6	2.2	6.6	110
124.	110	390	37	80	774	6.0	2.3	6.0	100
125.	110	390	37	80	772	6.0	2.0	6.4	107
126.	110	390	37	80	767	6.2	2.2	6.4	107
127.	110	390	37	80	757	6.4	2.4	6.2	103
128.	110	390	37	80	747	6.2	2.4	6.3	105
129.	110	390	37	80	750	6.0	2.5	6.6	110
130.	110	390	37	80	747	5.8	1.9	6.6	110
131.	110	400	37	85	796	4.5	1.9	6.4	107
132.	110	400	37	85	767	5.2	2.3	6.0	100
133.	110	400	37	80	759	5.2	1.6	7.5	125
134.	110	400	37	80	745	5.2	1.7	7.3	122
135.	110	400	37	80	733	5.6	2.2	6.6	110

No.	Torch angle deg.	current Amp.	voltage Volt.	speed cm/min	temp T1 º C	bead width mm	bead high mm	bead penetration mm	bead penetration %
136.	110	400	37	80	730	6.0	2.4	6.9	115
137.	110	400	37	80	730	5.6	2.1	7.3	122
138.	110	400	37	80	728	5.8	2.1	6.9	115
139.	110	400	37	80	728	5.8	2.3	7.3	122
140.	110	400	37	80	728	5.4	2.2	6.7	112
141.	110	400	37	80	723	5.6	2.1	7.4	123
142.	110	400	37	80	684	4.9	1.6	7.2	120

1.2 experimental data and results for welding achieving 90%-99% depth of penetration

No.	Torch angle deg.	current Amp.	voltage Volt.	speed cm/min	temp T1 ² C	bead width mm	bead high mm	bead penetration mm	bead penetration %
1.	70	380	37	80	776	8.6	1.5	5.4	90
2.	70	380	37	80	781	9.4	1.7	5.4	90
3.	70	380	37	80	781	9.4	1.7	5.4	90
4.	70	380	37	80	774	9.0	1.7	5.4	90
5.	70	380	37	80	767	9.4	1.9	5.4	90
6.	70	380	37	80	730	9.0	1.5	5.6	93
7.	70	380	37	80	733	9.4	1.7	5.6	93
8.	70	380	37	80	733	9.0	1.1	5.4	90
9.	70	380	37	90	709	7.3	1.3	5.4	90
10.	70	390	37	85	643	7.7	1.9	5.4	90
11.	70	390	37	85	643	7.7	1.9	5.4	90
12.	70	390	42	80	723	8.6	1.8	5.4	90
13.	70	400	37	85	660	8.2	2.4	5.9	98
14.	70	400	37	85	643	8.2	1.5	5.8	97
15.	70	400	37	80	711	9.2	2.1	5.6	93
16.	70	400	37	80	730	9.0	2.2	5.8	97
17.	70	400	37	80	730	9.0	2.0	5.8	97
18.	70	400	37	90	663	9.0	1.8	5.9	98
19.	70	400	42	85	694	7.9	2.3	5.4	90
20.	70	400	42	85	701	7.9	2.1	5.4	90
21.	70	400	42	85	711	9.4	2.1	5.8	97
22.	70	400	42	85	706	9.2	2.3	5.4	90
23.	70	400	42	85	709	9.2	2.1	5.8	97
24.	70	400	42	85	711	9.9	2.1	5.6	93
25.	70	400	42	80	719	9.9	2.2	5.4	90
26.	70	400	42	90	701	8.2	1.9	5.8	97

No.	Torch angle deg.	current Amp.	voltage Volt.	speed cm/min	temp T1 º C	bead width mm	bead high mm	bead penetration mm	bead penetration %
27.	70	400	42	90	704	8.6	1.9	5.6	93
28.	70	400	47	85	701	7.3	1.8	5.8	97
29.	70	400	47	85	697	7.9	1.9	5.6	93
30.	70	400	47	85	689	8.2	2.0	5.8	97
31.	70	400	47	85	687	8.2	1.9	5.4	90
32.	70	400	47	85	699	8.6	1.9	5.4	90
33.	70	400	47	85	699	9.0	1.9	5.4	90
34.	70	400	47	85	682	8.6	1.9	5.4	90
35.	70	400	47	80	723	8.6	1.9	5.4	90
36.	70	400	47	80	733	9.0	2.4	5.4	90
37.	70	400	47	85	682	8.6	1.9	5.4	90
38.	70	400	47	80	723	8.6	1.9	5.4	90
39.	70	400	47	80	733	9.0	2.4	5.4	90
40.	70	400	47	80	728	8.2	2.1	5.6	93
41.	70	400	47	80	738	8.8	2.1	5.4	90
42.	90	380	37	85	731	6.0	1.7	5.9	98
43.	90	380	37	85	738	6.2	1.7	5.4	90
44.	90	380	37	80	750	6.9	2.4	5.6	93
45.	90	380	42	85	929	8.2	1.3	5.6	93
46.	90	380	42	85	963	7.3	1.4	5.4	90
47.	90	380	42	85	900	7.9	1.3	5.4	90
48.	90	390	37	85	713	6.4	1.9	5.8	97
49.	90	390	37	85	718	6.9	2.1	5.4	90
50.	90	390	37	85	718	6.9	2.2	5.4	90
51.	90	390	37	80	723	6.4	0.9	5.6	93
52.	90	390	37	80	726	6.9	2.3	5.6	93
53.	90	390	37	80	726	6.9	2.3	5.5	92
54.	90	390	37	80	726	6.2	2.4	5.6	93

No.	Torch angle deg.	current Amp.	voltage Volt.	speed cm/min	temp T1 º C	bead width mm	bead high mm	bead penetration mm	bead penetration %
55.	90	390	37	80	721	6.2	2.1	5.7	95
56.	90	390	37	90	718	4.9	1.6	5.6	93
57.	90	390	37	90	713	5.6	1.7	5.6	93
58.	90	390	37	90	706	6.0	2.1	5.8	97
59.	90	390	37	90	704	6.0	1.9	5.6	93
60.	90	390	37	90	706	5.6	2.0	5.4	90
61.	90	390	37	90	701	5.6	1.7	5.8	97
62.	90	390	37	90	701	6.0	2.0	5.8	97
63.	90	390	37	90	699	5.6	1.8	5.6	93
64.	90	390	37	90	699	6.2	0.7	5.4	90
65.	90	390	42	80	968	8.2	1.9	5.8	97
66.	90	390	42	80	924	8.2	2.1	5.7	95
67.	90	390	42	80	871	7.7	2.1	5.6	93
68.	90	390	42	80	866	7.9	2.1	5.6	93
69.	90	390	42	80	839	7.9	2.1	5.4	90
70.	90	390	42	80	827	7.7	2.2	5.4	90
71.	90	390	47	85	885	7.9	1.9	5.4	90
72.	90	390	47	80	963	9.0	1.9	5.4	90
73.	90	390	47	80	907	8.2	1.9	5.8	97
74.	90	390	47	80	793	7.7	2.2	5.6	93
75.	90	390	47	80	799	7.7	2.1	5.4	90
76.	90	390	47	80	808	7.7	1.8	5.8	97
77.	90	400	42	85	893	8.8	2.1	5.8	97
78.	90	400	42	85	876	7.9	2.1	5.6	93
79.	90	400	42	85	818	7.7	2.1	5.4	90
80.	90	400	42	85	822	8.2	2.2	5.5	92
81.	90	400	42	85	823	8.2	1.6	5.5	92
82.	90	400	42	90	849	7.7	2.0	5.6	93

No.	Torch angle deg.	current Amp.	voltage Volt.	speed cm/min	temp T1 C	bead width mm	bead high mm	bead penetration mm	bead penetration %
83.	90	400	47	85	905	8.4	2.0	5.6	93
84.	90	400	47	85	931	7.7	2.1	5.5	92
85.	90	400	47	85	919	7.3	2.4	5.8	97
86.	90	400	47	85	888	7.7	2.0	5.8	97
87.	90	400	47	85	856	7.5	2.1	5.4	90
88.	90	400	47	85	842	7.7	2.4	5.4	90
89.	90	400	47	85	856	7.5	2.1	5.4	90
90.	90	400	47	85	876	7.9	1.6	5.5	92
91.	90	400	47	90	914	7.3	1.8	5.4	90
92.	90	400	47	90	931	7.3	1.7	5.4	90
93.	110	380	37	85	868	5.4	1.7	5.6	93
94.	110	380	37	85	801	5.6	1.3	5.6	93
95.	110	380	37	80	830	6.0	2.4	5.4	90
96.	110	390	37	85	786	5.6	1.9	5.4	90
97.	110	390	37	85	786	5.4	2.2	5.6	93
98.	110	390	37	85	781	5.2	1.9	5.8	97
99.	110	390	37	85	774	5.2	2.3	5.5	92
100.	110	390	37	90	805	5.2	1.8	5.4	90
101.	110	390	37	90	757	4.9	2.1	5.4	90
102.	110	390	37	90	752	5.4	2.0	5.4	90
103.	110	390	37	90	740	5.2	1.9	5.7	95
104.	110	390	37	90	745	5.4	2.1	5.7	95
105.	110	390	37	90	742	5.6	1.4	5.4	90
106.	110	400	37	85	793	5.8	2.2	5.4	90
107.	110	400	37	85	759	5.4	2.5	5.8	97
108.	110	400	37	85	759	5.4	2.3	5.6	93
109.	110	400	37	85	759	5.6	2.4	5.4	90
110.	110	400	37	90	798	4.9	2.1	5.9	98

No.	Torch angle deg.	current Amp.	voltage Volt.	speed cm/min	temp T1 º C	bead width mm	bead high mm	bead penetration mm	bead penetration %
111.	110	400	37	90	767	5.4	2.7	5.5	92
112.	110	400	37	90	747	5.2	2.5	5.4	90
113.	110	400	37	90	742	5.6	2.4	5.6	93
114.	110	400	37	90	733	5.6	1.5	5.4	90
115.	110	400	37	90	747	5.2	2.5	5.4	90
116.	110	400	37	90	742	5.6	2.4	5.6	93
117.	110	400	37	90	733	5.6	1.5	5.4	90
118.	110	400	42	90	847	7.1	1.7	5.4	90

1.3 experimental data and results for welding achieving 80%-89% depth of penetration

No.	Torch angle deg.	current Amp.	voltage Volt.	speed cm/min	temp T1 = C	bead width mm	bead high mm	bead penetration mm	bead penetration %
1.	70	380	37	85	697	8.2	1.5	4.9	82
2.	70	380	37	85	701	7.7	1.5	4.9	82
3.	70	380	37	85	665	7.7	1.9	4.9	82
4.	70	380	37	80	740	9.7	1.3	5.1	85
5.	70	380	37	90	728	7.3	2.1	5.1	85
6.	70	380	37	90	735	7.9	1.5	5.1	85
7.	70	380	37	90	733	7.3	1.3	4.9	82
8.	70	380	37	90	730	7.9	1.5	5.1	85
9.	70	380	37	90	747	7.7	1.7	4.9	82
10.	70	380	37	90	730	7.7	1.7	4.9	82
11.	70	380	42	80	750	8.6	- 13.7	5.1	85
12.	70	380	42	80	776	9.4	1.7	4.9	82
13.	70	380	47	80	902	8.6	1.7	4.9	82
14.	70	390	37	85	612	7.3	1.9	5.1	85
15.	70	390	37	85	634	7.9	1.9	5.3	88
16.	70	390	37	85	638	7.9	2.1	5.1	85
17.	70	390	37	85	636	8.4	2.1	5.1	85
18.	70	390	37	85	643	7.7	2.1	4.9	82
19.	70	390	37	85	643	8.2	2.0	4.9	82
20.	70	390	37	85	634	7.7	2.1	5.1	85
21.	70	390	37	85	619	7.7	1.3	4.9	82
22.	70	390	37	90	658	7.7	1.9	5.1	85
23.	70	390	37	90	648	7.7	2.0	5.1	85
24.	70	390	37	90	646	7.9	2.0	5.1	85
25.	70	390	37	90	648	7.9	2.4	5.1	85

No.	Torch angle deg.	current Amp.	voltage Volt.	speed cm/min	temp T1° C	bead width mm	bead high mm	bead penetration mm	bead penetration %
26.	70	390	37	90	651	8.8	1.9	5.1	85
27.	70	390	37	90	634	8.4	1.9	5.1	85
28.	70	390	37	90	629	9.0	1.9	5.1	85
29.	70	390	37	90	626	8.4	1.9	5.1	85
30.	70	390	37	90	634	8.2	1.5	4.9	82
31.	70	390	42	80	721	8.6	2.0	5.1	85
32.	70	390	42	80	728	8.8	1.9	4.9	82
33.	70	390	42	80	730	9.0	1.9	4.9	82
34.	70	390	42	80	728	9.2	1.9	4.9	82
35.	70	390	42	80	723	9.4	2.0	4.8	80
36.	70	390	42	80	728	9.4	1.9	4.8	80
37.	70	390	42	90	709	7.5	1.6	4.9	82
38.	70	390	47	80	740	8.2	2.0	4.8	80
39.	70	390	47	80	772	8.2	2.1	4.9	82
40.	70	390	47	80	774	8.4	2.1	4.9	82
41.	70	400	37	80	682	10.9	24.1	5.1	85
42.	70	400	42	85	723	8.6	6.7	5.1	85
43.	70	400	42	85	711	9.0	2.1	5.1	85
44.	70	400	42	80	719	10.1	2.2	5.1	85
45.	70	400	42	80	716	10.7	2.4	5.1	85
46.	70	400	42	80	714	9.7	2.6	5.1	85
47.	70	400	42	90	694	8.6	1.7	5.1	85
48.	70	400	42	90	706	8.6	1.9	5.1	85
49.	70	400	42	90	706	8.6	2.0	5.1	85
50.	70	400	42	90	706	8.2	1.9	5.1	85
51.	70	400	42	90	704	8.6	1.9	5.1	85
52.	70	400	42	90	706	8.6	1.8	5.1	85
53.	70	400	42	90	706	8.6	2.0	5.1	85
54.	70	400	42	90	701	7.7	1.3	5.1	85

No.	Torch angle deg.	current Amp.	voltage Volt.	speed cm/min	temp T1 º C	bead width mm	bead high mm	bead penetration mm	bead penetration %
55.	70	400	47	85	699	9.0	2.3	5.1	85
56.	70	400	47	85	689	9.4	2.1	5.1	85
57.	70	400	47	85	687	9.0	2.0	5.1	85
58.	70	400	47	80	728	9.0	2.4	5.1	85
59.	70	400	47	80	733	8.6	2.4	5.1	85
60.	70	400	47	80	733	8.8	2.1	4.9	82
61.	70	400	47	80	730	8.8	2.4	4.9	82
62.	70	400	47	80	733	9.0	1.1	4.9	82
63.	70	400	47	90	713	8.2	2.1	5.1	85
64.	70	400	47	90	728	7.7	1.9	4.9	82
65.	70	400	47	90	733	7.9	2.1	5.1	85
66.	70	400	47	90	723	7.7	1.9	5.1	85
67.	70	400	47	90	721	8.2	1.9	4.9	82
68.	70	400	47	90	699	8.2	1.9	4.9	82
69.	70	400	47	90	704	7.9	2.0	4.9	82
70.	90	380	37	80	742	6.4	2.1	5.1	85
71.	90	380	37	80	750	7.3	2.1	4.9	82
72.	90	380	37	80	747	6.4	1.9	4.9	82
73.	90	380	37	80	724	7.3	2.1	4.9	82
74.	90	380	37	80	724	6.4	2.1	4.9	82
75.	90	380	37	80	723	7.5	2.1	4.9	82
76.	90	380	37	80	716	7.7	1.3	5.1	85
77.	90	380	37	90	718	5.6	1.9	4.8	80
78.	90	380	37	90	711	5.4	1.8	4.8	80
79.	90	380	37	90	716	5.6	2.1	4.8	80
80.	90	380	37	90	721	6.0	2.0	4.9	82
81.	90	380	37	90	711	6.2	1.9	4.8	80
82.	90	380	37	90	700	6.0	2.1	4.8	80

No.	Torch angle deg.	current Amp.	voltage Volt.	speed cm/min	temp T1 º C	bead width mm	bead high mm	bead penetration mm	bead penetration %
83.	90	380	37	90	701	6.0	2.1	4.9	82
84.	90	380	37	90	690	5.8	1.8	4.9	82
85.	90	380	37	90	690	5.6	1.0	4.9	82
86.	90	380	42	85	941	7.7	1.5	5.2	87
87.	90	380	42	85	924	7.5	1.5	5.2	87
88.	90	380	42	85	893	7.9	1.4	5.1	85
89.	90	380	42	85	873	7.7	1.5	4.9	82
90.	90	380	42	85	885	7.5	1.5	5.1	85
91.	90	380	42	85	880	7.5	1.5	4.9	82
92.	90	380	42	85	888	7.5	1.3	5.1	85
93.	90	380	42	80	960	7.7	1.9	4.8	80
94.	90	380	42	80	978	8.2	2.0	5.1	85
95.	90	380	42	80	960	7.9	1.9	4.9	82
96.	90	380	42	80	978	8.2	1.7	5.1	85
97.	90	380	42	80	966	8.2	1.7	4.9	82
98.	90	380	42	80	958	8.2	1.8	5.0	83
99.	90	380	42	80	939	8.6	1.9	4.9	82
100.	90	380	42	80	900	8.4	1.8	4.9	82
101.	90	380	47	85	905	8.2	1.6	4.9	82
102.	90	380	47	85	939	8.8	1.7	4.9	82
103.	90	380	47	85	793	7.7	1.5	4.9	82
104.	90	380	47	80	984	8.6	1.8	5.1	85
105.	90	380	47	80	960	8.8	1.8	5.1	85
106.	90	380	47	80	955	8.4	1.7	4.9	82
107.	90	380	47	80	939	8.4	44.8	4.9	82
108.	90	380	47	80	900	7.7	1.9	4.9	82
109.	90	380	47	80	842	7.9	1.7	5.1	85
110.	90	380	47	80	856	8.2	2.1	4.9	82

No.	Torch angle deg.	current Amp.	voltage Volt.	speed cm/min	temp T1 º C	bead width mm	bead high mm	bead penetration mm	bead penetration %
111.	90	380	47	80	834	8.6	1.7	4.9	82
112.	90	390	37	85	721	8.6	2.8	5.2	87
113.	90	390	37	85	721	6.9	2.0	5.2	87
114.	90	390	37	85	716	6.7	2.0	5.1	85
115.	90	390	37	85	716	6.9	2.0	5.2	87
116.	90	390	37	85	713	7.1	2.2	5.1	85
117.	90	390	37	85	709	6.4	2.1	5.1	85
118.	90	390	37	85	709	6.4	2.1	5.1	85
119.	90	390	42	85	790	8.2	2.1	4.8	80
120.	90	390	42	85	801	7.7	2.0	5.0	83
121.	90	390	42	85	805	7.9	1.3	4.9	82
122.	90	390	42	80	902	8.8	1.9	5.2	87
123.	90	390	42	80	830	7.9	2.0	5.1	85
124.	90	390	42	80	827	7.7	1.3	5.2	87
125.	90	390	42	90	833	7.5	1.3	4.9	82
126.	90	390	42	90	836	7.7	1.8	5.1	85
127.	90	390	42	90	835	8.2	1.9	4.9	82
128.	90	390	42	90	805	7.7	1.8	4.9	82
129.	90	390	42	90	805	7.9	1.8	5.1	85
130.	90	390	42	90	790	7.7	1.7	5.1	85
131.	90	390	42	90	791	8.2	1.8	4.9	82
132.	90	390	42	90	790	7.7	1.9	4.9	82
133.	90	390	42	90	790	7.5	1.9	4.9	82
134.	90	390	42	90	785	8.2	1.2	4.9	82
135.	90	390	47	85	863	7.9	1.9	5.1	85
136.	90	390	47	85	866	8.2	2.0	4.9	82
137.	90	390	47	85	849	8.2	2.1	4.9	82
138.	90	390	47	85	834	8.2	1.3	5.1	85

No.	Torch angle deg.	current Amp.	voltage Volt.	speed cm/min	temp T1 º C	bead width mm	bead high mm	bead penetration mm	bead penetration %
139.	90	390	47	85	837	7.7	2.1	4.8	80
140.	90	390	47	85	842	7.7	1.9	5.1	85
141.	90	390	47	85	834	7.5	2.1	4.8	80
142.	90	390	47	85	861	7.3	2.0	4.8	80
143.	90	390	47	80	936	7.5	2.0	4.8	80
144.	90	390	47	80	799	7.5	2.1	5.1	85
145.	90	390	47	90	820	7.7	1.7	4.8	80
146.	90	390	47	90	786	6.9	1.7	4.9	82
147.	90	390	47	90	791	8.2	1.9	4.9	82
148.	90	390	47	90	813	7.7	1.5	4.9	82
149.	90	390	47	90	815	7.7	1.7	5.1	85
150.	90	390	47	90	856	7.7	1.7	4.9	82
151.	90	390	47	90	832	7.3	1.6	4.9	82
152.	90	390	47	90	827	7.7	1.7	4.8	80
153.	90	390	47	90	837	7.9	1.9	4.8	80
154.	90	390	47	90	805	8.2	2.0	4.9	82
155.	90	400	42	85	844	7.7	2.1	5.1	85
156.	90	400	42	85	830	8.2	2.1	5.1	85
157.	90	400	42	85	820	7.9	2.2	5.3	88
158.	90	400	42	90	856	7.7	1.9	5.1	85
159.	90	400	42	90	854	7.5	1.9	5.1	85
160.	90	400	42	90	888	7.7	2.0	5.1	85
161.	90	400	42	90	910	7.7	1.9	5.1	85
162.	90	400	42	90	898	7.3	2.0	4.9	82
163.	90	400	42	90	860	7.7	1.9	4.8	80
164.	90	400	42	90	847	7.7	2.0	4.9	82
165.	90	400	42	90	822	7.7	1.6	4.9	82
166.	90	400	47	85	847	7.7	2.4	5.2	87

No.	Torch angle deg.	current Amp.	voltage Volt.	speed cm/min	temp T1 º C	bead width mm	bead high mm	bead penetration mm	bead penetration %
167.	90	400	47	90	893	7.7	1.9	5.1	85
168.	90	400	47	90	866	7.3	1.8	5.1	85
169.	90	400	47	90	919	7.3	1.8	5.1	85
170.	90	400	47	90	939	7.7	2.0	4.9	82
171.	90	400	47	90	919	7.5	1.9	5.1	85
172.	90	400	47	90	885	7.9	1.9	5.0	83
173.	90	400	47	90	863	7.7	1.5	5.1	85
174.	110	380	37	85	769	4.7	1.5	4.8	80
175.	110	380	37	85	854	5.6	1.8	5.1	85
176.	110	380	37	85	844	5.8	1.8	5.1	85
177.	110	380	37	85	827	5.8	1.6	5.2	87
178.	110	380	37	85	803	5.6	1.6	5.1	85
179.	110	380	37	80	711	5.2	2.2	4.9	82
180.	110	380	37	80	948	6.0	1.9	5.2	87
181.	110	380	37	80	902	6.2	2.2	4.9	82
182.	110	380	37	80	863	6.7	2.4	5.0	83
183.	110	380	37	80	847	6.4	2.3	5.0	83
184.	110	380	37	80	834	6.0	2.3	5.1	85
185.	110	380	37	80	813	5.8	2.4	5.1	85
186.	110	380	37	90	856	5.8	1.8	4.9	82
187.	110	380	37	90	854	6.0	2.0	4.8	80
188.	110	380	37	90	832	6.2	1.8	4.8	80
189.	110	380	37	90	825	5.8	2.1	4.8	80
190.	110	380	37	90	825	5.8	2.1	4.8	80
191.	110	380	37	90	813	5.8	2.1	4.8	80
192.	110	380	37	90	805	5.2	1.8	4.9	82
193.	110	380	37	90	798	5.4	1.2	5.0	83
194.	110	390	37	85	808	5.2	1.9	5.3	88

No.	Torch angle deg.	current Amp.	voltage Volt.	speed cm/min	temp T1 ° C	bead width mm	bead high mm	bead penetration mm	bead penetration %
195.	110	390	37	85	805	5.2	2.3	5.0	83
196.	110	390	37	85	791	5.4	2.4	5.1	85
197.	110	390	37	90	791	4.7	2.1	5.2	87
198.	110	390	37	90	772	5.2	2.2	5.1	85
199.	110	390	37	90	769	5.4	2.0	5.2	87
200.	110	390	37	90	759	5.2	1.9	5.3	88
201.	110	390	42	80	888	7.7	2.1	4.8	80
202.	110	390	42	80	883	7.3	2.0	4.8	80
203.	110	400	37	85	793	5.2	2.5	4.9	82
204.	110	400	37	85	793	5.2	2.3	5.3	88
205.	110	400	37	85	774	6.2	2.4	4.8	80
206.	110	400	37	85	738	6.0	1.8	4.9	82
207.	110	400	37	90	803	4.9	2.2	5.2	87
208.	110	400	37	90	781	5.4	2.6	5.1	85
209.	110	400	37	90	764	5.2	2.5	5.3	88
210.	110	400	37	90	762	4.9	2.4	5.2	87
211.	110	400	37	90	747	5.2	2.6	5.1	85
212.	110	400	42	85	844	7.5	1.8	4.8	80
213.	110	400	42	80	941	7.3	1.9	4.8	80
214.	110	400	42	90	859	7.1	1.8	4.9	82
215.	110	400	42	90	842	7.1	1.7	4.8	80
216.	110	400	42	90	839	7.5	1.9	4.8	80
217.	110	400	47	80	893	7.3	1.7	4.9	82

1.4 experimental data and results for welding achieving 70% - 79% depth of penetration

No.	Torch angle deg.	current Amp.	voltage Volt.	speed cm/min	temp T1 ° C	bead width mm	bead high mm	bead penetration mm	bead penetration %
1.	70	380	37	85	687	7.7	1.7	4.5	75
2.	70	380	37	85	670	7.9	2.4	4.5	75
3.	70	380	37	85	672	8.2	2.1	4.5	75
4.	70	380	37	85	665	7.7	1.9	4.7	78
5.	70	380	37	90	740	8.2	1.7	4.7	78
6.	70	380	37	90	716	7.3	1.7	4.7	78
7.	70	380	37	90	718	6.9	0.4	4.7	78
8.	70	380	42	85	767	7.9	1.7	4.7	78
9.	70	380	42	85	798	9.4	1.7	4.7	78
10.	70	380	42	85	820	9.4	1.7	4.7	78
11.	70	380	42	85	818	9.4	1.7	4.5	75
12.	70	380	42	85	805	9.4	1.7	4.3	72
13.	70	380	42	85	801	9.0	1.7	4.3	72
14.	70	380	42	85	793	9.4	1.7	4.7	78
15.	70	380	42	85	774	9.9	1.7	4.7	78
16.	70	380	42	85	769	9.0	1.7	4.7	78
17.	70	380	42	85	776	9.2	1.3	4.5	75
18.	70	380	42	80	793	9.4	1.7	4.7	78
19.	70	380	42	80	793	9.4	1.7	4.7	78
20.	70	380	42	80	793	9.9	1.9	4.5	75
21.	70	380	42	80	791	9.7	1.9	4.3	72
22.	70	380	42	80	788	9.9	1.9	4.3	72
23.	70	380	42	80	767	9.0	1.9	4.5	75
24.	70	380	42	80	769	9.0	1.9	4.5	75
25.	70	380	42	80	769	9.9	1.1	4.5	75

No.	Torch angle deg.	current Amp.	voltage Volt.	speed cm/min	temp T1 º C	bead width mm	bead high mm	bead penetration mm	bead penetration %
26.	70	380	42	90	774	8.2	1.7	4.7	78
27.	70	380	42	90	788	8.2	1.7	4.5	75
28.	70	380	42	90	798	8.4	1.7	4.3	72
29.	70	380	42	90	803	8.6	1.7	4.7	78
30.	70	380	42	90	801	9.0	1.7	4.5	75
31.	70	380	42	90	791	9.0	1.5	4.5	75
32.	70	380	42	90	781	8.2	1.9	4.3	72
33.	70	380	42	90	796	8.6	1.5	4.5	75
34.	70	380	42	90	796	8.2	1.7	4.5	75
35.	70	380	42	90	781	9.0	1.3	4.3	72
36.	70	380	47	85	837	8.6	1.7	4.5	75
37.	70	380	47	85	854	8.6	1.5	4.7	78
38.	70	380	47	85	863	9.0	1.7	4.3	72
39.	70	380	47	85	866	9.7	1.7	4.3	72
40.	70	380	47	85	856	9.0	1.7	4.3	72
41.	70	380	47	85	842	8.8	1.7	4.3	72
42.	70	380	47	85	851	8.8	1.9	4.3	72
43.	70	380	47	80	842	9.2	1.7	4.7	78
44.	70	380	47	80	895	8.6	1.9	4.7	78
45.	70	380	47	80	907	9.2	1.9	4.5	75
46.	70	380	47	80	890	8.8	1.9	4.3	72
47.	70	380	47	80	900	9.9	1.9	4.7	78
48.	70	380	47	80	885	9.7	2.1	4.3	72
49.	70	380	47	80	851	9.7	2.1	4.5	75
50.	70	380	47	80	851	9.7	1.9	4.5	75
51.	70	380	47	80	844	9.9	1.7	4.3	72
52.	70	380	47	90	847	9.0	1.5	4.5	75
53.	70	380	47	90	878	8.6	1.9	4.5	75

No.	Torch angle deg.	current Amp.	voltage Volt.	speed cm/min	temp T1 º C	bead width mm	bead high mm	bead penetration mm	bead penetration %
54.	70	380	47	90	878	8.8	1.9	4.3	72
55.	70	380	47	90	847	8.2	1.9	4.5	75
56.	70	380	47	90	827	8.6	1.7	4.5	75
57.	70	380	47	90	822	8.8	1.7	4.3	72
58.	70	380	47	90	813	7.5	1.6	4.3	72
59.	70	380	47	90	759	8.6	1.7	4.3	72
60.	70	380	47	90	750	8.4	1.7	4.3	72
61.	70	380	47	90	747	8.4	1.5	4.3	72
62.	70	390	37	90	658	9.4	2.6	4.5	75
63.	70	390	42	85	713	7.9	1.9	4.5	75
64.	70	390	42	85	718	8.6	6.3	4.5	75
65.	70	390	42	85	718	9.0	2.0	4.5	75
66.	70	390	42	85	716	9.0	2.0	4.5	75
67.	70	390	42	85	723	9.2	1.9	4.7	78
68.	70	390	42	85	711	9.2	1.8	4.5	75
69.	70	390	42	85	704	8.8	1.9	4.7	78
70.	70	390	42	85	701	9.7	1.9	4.5	75
71.	70	390	42	80	721	9.9	1.9	4.5	75
72.	70	390	42	80	713	9.9	2.1	4.7	78
73.	70	390	42	80	706	9.7	1.7	4.7	78
74.	70	390	42	90	711	7.7	1.7	4.7	78
75.	70	390	42	90	711	8.2	1.9	4.7	78
76.	70	390	42	90	712	8.2	1.9	4.7	78
77.	70	390	42	90	710	8.2	1.9	4.6	77
78.	70	390	42	90	711	8.6	2.0	4.7	78
79.	70	390	42	90	713	8.6	1.8	4.6	77
80.	70	390	42	90	713	8.6	1.9	4.6	77
81.	70	390	42	90	709	8.2	1.9	4.7	78

No.	Torch angle deg.	current Amp.	voltage Volt.	speed cm/min	temp T1 = C	bead width mm	bead high mm	bead penetration mm	bead penetration %
82.	70	390	42	90	704	8.6	1.5	4.5	75
83.	70	390	47	85	716	8.6	1.6	4.7	78
84.	70	390	47	85	728	8.6	1.8	4.5	75
85.	70	390	47	85	735	9.0	1.7	4.7	78
86.	70	390	47	85	733	9.0	1.9	4.5	75
87.	70	390	47	85	721	9.0	2.1	4.4	73
88.	70	390	47	85	716	9.0	1.9	4.3	72
89.	70	390	47	85	721	8.6	1.9	4.5	75
90.	70	390	47	85	718	9.0	1.7	4.5	75
91.	70	390	47	85	718	8.6	1.9	4.5	75
92.	70	390	47	85	709	9.2	0.9	4.5	75
93.	70	390	47	80	759	8.6	2.3	4.7	78
94.	70	390	47	80	750	8.2	2.1	4.7	78
95.	70	390	47	80	745	8.6	2.4	4.5	75
96.	70	390	47	80	745	8.6	2.4	4.5	75
97.	70	390	47	80	745	8.2	2.1	4.5	75
98.	70	390	47	80	747	8.2	2.1	4.5	75
99.	70	390	47	80	740	7.9	1.3	4.7	78
100.	70	390	47	90	731	8.2	1.7	4.7	78
101.	70	390	47	90	723	8.2	1.7	4.7	78
102.	70	390	47	90	733	8.6	6.2	4.6	77
103.	70	390	47	90	747	8.6	2.0	4.6	77
104.	70	390	47	90	755	8.8	2.0	4.5	75
105.	70	390	47	90	747	8.8	2.0	4.5	75
106.	70	390	47	90	742	9.0	2.3	4.3	72
107.	70	390	47	90	726	8.2	1.3	4.4	73
108.	70	400	42	80	716	10.3	0.9	4.7	78
109.	90	380	37	80	755	6.0	2.2	4.7	78

No.	Torch angle deg.	current Amp.	voltage Volt.	speed cm/min	temp T1 ° C	bead width mm	bead high mm	bead penetration mm	bead penetration %
110.	90	380	37	80	738	7.5	2.1	4.7	78
111.	90	380	37	90	716	6.0	2.1	4.5	75
112.	90	380	42	80	960	8.6	1.8	4.7	78
113.	90	380	42	80	861	8.4	1.5	4.7	78
114.	90	380	42	90	905	7.7	1.4	4.6	77
115.	90	380	42	90	888	7.7	1.3	4.7	78
116.	90	380	42	90	914	7.5	1.7	4.5	75
117.	90	380	42	90	929	7.9	1.5	4.7	78
118.	90	380	42	90	917	7.7	1.5	4.7	78
119.	90	380	42	90	905	7.7	1.7	4.4	73
120.	90	380	42	90	905	7.7	1.5	4.5	75
121.	90	380	42	90	883	7.9	1.6	4.5	75
122.	90	380	42	90	873	7.7	1.5	4.7	78
123.	90	380	42	90	873	7.9	1.8	4.5	75
124.	90	380	47	85	890	8.6	1.8	4.7	78
125.	90	380	47	85	965	8.8	6.2	4.7	78
126.	90	380	47	85	941	8.8	1.7	4.6	77
127.	90	380	47	85	856	9.0	1.8	4.5	75
128.	90	380	47	85	796	8.8	2.0	4.7	78
129.	90	380	47	85	798	7.7	1.7	4.6	77
130.	90	380	47	85	793	8.4	1.9	4.7	78
131.	90	380	47	80	929	8.4	1.9	4.7	78
132.	90	380	47	80	968	8.2	1.7	4.7	78
133.	90	380	47	90	881	7.7	1.5	4.5	75
134.	90	380	47	90	878	7.5	1.6	4.5	75
135.	90	380	47	90	905	8.2	1.6	4.7	78
136.	90	380	47	90	931	7.9	1.7	4.5	75
137.	90	380	47	90	929	8.2	1.7	4.7	78

No.	Torch angle deg.	current Amp.	voltage Volt.	speed cm/min	temp T1 º C	bead width mm	bead high mm	bead penetration mm	bead penetration %
138.	90	380	47	90	912	8.2	1.7	4.5	75
139.	90	380	47	90	900	7.9	1.7	4.5	75
140.	90	380	47	90	866	8.4	1.7	4.4	73
141.	90	380	47	90	844	8.2	1.7	4.5	75
142.	90	380	47	90	830	8.2	1.3	4.7	78
143.	90	390	42	85	878	8.4	1.9	4.7	78
144.	90	390	42	85	893	7.9	1.9	4.7	78
145.	90	390	42	85	842	7.7	2.1	4.7	78
146.	90	390	42	85	815	7.9	2.1	4.7	78
147.	90	390	42	85	805	8.2	2.0	4.7	78
148.	90	390	42	85	805	8.2	2.0	4.7	78
149.	90	390	42	85	793	8.6	2.1	4.5	75
150.	90	390	47	85	853	7.3	2.1	4.7	78
151.	90	400	42	90	830	7.7	1.9	4.7	78
152.	90	400	47	90	878	7.7	1.7	4.7	78
153.	110	380	37	80	815	6.0	2.4	4.7	78
154.	110	380	37	80	793	6.0	1.7	4.7	78
155.	110	380	37	90	842	6.2	2.3	4.7	78
156.	110	380	37	90	839	6.4	2.0	4.6	77
157.	110	380	42	85	917	6.9	2.1	4.3	72
158.	110	380	42	85	893	6.9	2.0	4.3	72
159.	110	380	42	85	893	6.9	2.1	4.3	72
160.	110	380	42	85	926	6.7	2.0	4.2	70
161.	110	380	42	85	946	7.1	1.9	4.2	70
162.	110	380	42	85	972	7.1	1.7	4.2	70
163.	110	380	42	85	968	6.4	1.9	4.3	72
164.	110	380	42	85	984	7.3	1.9	4.5	75
165.	110	380	42	85	965	7.7	2.1	4.6	77

No.	Torch angle deg.	current Amp.	voltage Volt.	speed cm/min	temp T1 º C	bead width mm	bead high mm	bead penetration mm	bead penetration %
166.	110	380	42	85	972	7.7	1.8	4.6	77
167.	110	380	42	80	997	7.3	2.0	4.3	72
168.	110	380	42	80	989	7.3	2.0	4.3	72
169.	110	380	42	80	1009	7.3	2.1	4.3	72
170.	110	380	42	80	1014	7.7	2.1	4.4	73
171.	110	380	42	80	1014	7.5	2.1	4.4	73
172.	110	380	42	80	1014	7.9	2.1	4.5	75
173.	110	380	42	80	1021	7.5	2.1	4.4	73
174.	110	380	42	80	1014	7.7	2.1	4.5	75
175.	110	380	42	80	1023	7.7	2.1	4.5	75
176.	110	380	42	80	989	7.9	1.8	4.4	73
177.	110	380	42	90	970	7.1	1.8	4.2	70
178.	110	380	42	90	941	7.1	1.8	4.2	70
179.	110	380	42	90	924	6.7	1.9	4.3	72
180.	110	380	42	90	926	7.5	1.7	4.2	70
181.	110	380	42	90	946	7.1	2.2	4.2	70
182.	110	380	42	90	953	6.7	1.8	4.4	73
183.	110	380	42	90	953	7.1	2.1	4.4	73
184.	110	380	42	90	943	7.3	1.6	4.4	73
185.	110	380	47	85	851	6.4	1.6	4.2	70
186.	110	380	47	85	837	6.7	1.7	4.5	75
187.	110	380	47	85	839	6.9	1.7	4.3	72
188.	110	380	47	85	859	7.1	1.8	4.5	75
189.	110	380	47	85	861	7.5	2.0	4.4	73
190.	110	380	47	85	861	7.1	2.0	4.2	70
191.	110	380	47	85	866	7.1	1.9	4.3	72
192.	110	380	47	85	849	7.3	2.0	4.5	75
193.	110	380	47	85	847	7.7	2.3	4.5	75

No.	Torch angle deg.	current Amp.	voltage Volt.	speed cm/min	temp T1 ° C	bead width mm	bead high mm	bead penetration mm	bead penetration %
194.	110	380	47	85	813	6.9	1.6	4.3	72
195.	110	380	47	80	861	6.9	2.4	4.3	72
196.	110	380	47	80	849	6.9	1.9	4.5	75
197.	110	380	47	80	849	7.1	2.1	4.5	75
198.	110	380	47	80	839	7.5	2.3	4.2	70
199.	110	380	47	80	832	7.7	2.1	4.2	70
200.	110	380	47	80	832	7.5	2.1	4.3	72
201.	110	380	47	80	830	7.5	2.2	4.3	72
202.	110	380	47	80	842	7.5	2.1	4.5	75
203.	110	380	47	80	825	7.1	1.9	4.3	72
204.	110	380	47	90	861	6.7	1.6	4.3	72
205.	110	380	47	90	844	6.4	1.7	4.2	70
206.	110	380	47	90	849	6.4	1.8	4.3	72
207.	110	380	47	90	830	6.7	2.0	4.5	75
208.	110	380	47	90	818	6.7	2.1	4.5	75
209.	110	380	47	90	813	6.4	2.0	4.4	73
210.	110	380	47	90	805	6.9	1.8	4.5	75
211.	110	380	47	90	798	6.9	1.3	4.4	73
212.	110	380	47	90	791	7.5	2.1	4.5	75
213.	110	380	47	90	784	6.7	1.8	4.3	72
214.	110	390	42	85	890	7.1	2.1	4.5	75
215.	110	390	42	85	871	7.1	2.0	4.6	77
216.	110	390	42	85	868	7.1	1.9	4.5	75
217.	110	390	42	85	871	6.9	2.1	4.3	72
218.	110	390	42	85	859	7.3	2.1	4.3	72
219.	110	390	42	85	847	7.3	2.1	4.5	75
220.	110	390	42	85	842	7.3	2.4	4.5	75
221.	110	390	42	85	830	7.3	2.1	4.4	73

No.	Torch angle deg.	current Amp.	voltage Volt.	speed cm/min	temp T1 ° C	bead width mm	bead high mm	bead penetration mm	bead penetration %
222.	110	390	42	85	842	7.5	2.1	4.5	75
223.	110	390	42	85	830	7.3	1.5	4.5	75
224.	110	390	42	80	895	7.5	2.2	4.5	75
225.	110	390	42	80	876	7.5	2.1	4.5	75
226.	110	390	42	80	888	7.5	1.9	4.7	78
227.	110	390	42	80	900	7.5	2.1	4.7	78
228.	110	390	42	80	900	7.5	2.1	4.7	78
229.	110	390	42	80	876	7.7	1.9	4.5	75
230.	110	390	42	80	871	7.7	2.2	4.7	78
231.	110	390	42	80	863	7.5	1.4	4.6	77
232.	110	390	42	90	851	6.9	1.8	4.4	73
233.	110	390	42	90	827	6.9	1.9	4.3	72
234.	110	390	42	90	827	7.3	1.9	4.3	72
235.	110	390	42	90	827	7.3	1.8	4.3	72
236.	110	390	42	90	815	7.5	1.8	4.5	75
237.	110	390	42	90	815	7.5	1.8	4.6	77
238.	110	390	42	90	818	7.3	1.8	4.6	77
239.	110	390	42	90	834	7.1	1.3	4.2	70
240.	110	390	47	85	868	6.7	1.7	4.3	72
241.	110	390	47	90	859	6.9	1.5	4.5	75
242.	110	390	47	90	856	6.4	1.6	4.4	73
243.	110	390	47	90	859	7.1	1.6	4.2	70
244.	110	390	47	90	844	7.1	1.5	4.3	72
245.	110	390	47	90	839	7.3	1.7	4.2	70
246.	110	390	47	90	830	7.1	1.5	4.5	75
247.	110	390	47	90	825	7.1	1.8	4.2	70
248.	110	390	47	90	820	7.1	1.5	4.5	75
249.	110	400	42	85	866	7.3	1.7	4.4	73

No.	Torch angle deg.	current Amp.	voltage Volt.	speed cm/min	temp T1 ° C	bead width mm	bead high mm	bead penetration mm	bead penetration %
250.	110	400	42	85	856	7.5	1.8	4.3	72
251.	110	400	42	85	856	7.5	1.7	4.5	75
252.	110	400	42	85	856	7.5	1.7	4.7	78
253.	110	400	42	85	830	7.1	1.7	4.5	75
254.	110	400	42	85	827	7.5	1.8	4.5	75
255.	110	400	42	85	825	7.5	1.8	4.4	73
256.	110	400	42	85	822	7.5	1.3	4.2	70
257.	110	400	42	80	953	7.3	2.2	4.5	75
258.	110	400	42	80	943	7.5	2.0	4.6	77
259.	110	400	42	80	948	7.3	2.1	4.5	75
260.	110	400	42	80	948	7.5	2.0	4.6	77
261.	110	400	42	80	939	7.5	1.9	4.3	72
262.	110	400	42	80	939	7.3	2.1	4.2	70
263.	110	400	42	80	934	7.7	1.8	4.2	70
264.	110	400	42	90	883	6.9	1.8	4.7	78
265.	110	400	42	90	861	6.4	1.6	4.7	78
266.	110	400	42	90	849	7.1	2.2	4.5	75
267.	110	400	42	90	847	7.3	1.8	4.7	78
268.	110	400	42	90	839	7.3	1.7	4.7	78
269.	110	400	42	90	837	7.1	1.5	4.5	75
270.	110	400	47	85	907	7.1	1.9	4.5	75
271.	110	400	47	85	907	7.1	2.1	4.3	72
272.	110	400	47	85	892	7.3	1.9	4.2	70
273.	110	400	47	85	892	7.3	2.0	4.2	70
274.	110	400	47	85	885	7.5	2.0	4.4	73
275.	110	400	47	85	870	7.3	1.7	4.3	72
276.	110	400	47	85	865	7.3	2.0	4.3	72
277.	110	400	47	85	860	7.1	1.4	4.3	72

No.	Torch angle deg.	current Amp.	voltage Volt.	speed cm/min	temp T1 º C	bead width mm	bead high mm	bead penetration mm	bead penetration %
278.	110	400	47	80	929	7.5	1.8	4.7	78
279.	110	400	47	80	912	7.3	1.9	4.5	75
280.	110	400	47	80	914	6.9	1.9	4.3	72
281.	110	400	47	80	914	7.5	1.8	4.7	78
282.	110	400	47	80	902	7.7	1.8	4.3	72
283.	110	400	47	80	902	7.5	1.7	4.3	72
284.	110	400	47	80	905	7.3	1.8	4.5	75
285.	110	400	47	80	895	7.5	1.7	4.5	75
286.	110	400	47	90	919	6.7	1.7	4.6	77
287.	110	400	47	90	902	6.7	1.5	4.5	75
288.	110	400	47	90	897	7.1	1.5	4.6	77
289.	110	400	47	90	893	6.7	1.5	4.4	73
290.	110	400	47	90	895	6.9	1.4	4.3	72
291.	110	400	47	90	883	6.9	1.5	4.2	70
292.	110	400	47	90	871	6.9	1.7	4.2	70

1.5experimental data and results for welding achieving 60%-69% depth of penetration

No.	Torch angle deg.	current Amp.	voltage Volt.	speed cm/min	temp T1° C	bead width mm	bead high mm	bead penetration mm	bead penetration %
1.	70	380	37	85	687	7.7	1.7	3.9	65
2.	70	380	37	85	692	7.9	1.7	3.9	65
3.	70	380	37	85	692	7.9	1.9	3.9	65
4.	70	380	47	85	834	9.0	1.7	4.1	68
5.	70	380	47	85	847	9.2	1.9	4.1	68
6.	70	390	47	90	747	8.2	1.9	3.9	65
7.	110	380	42	90	939	7.1	1.9	4.0	67
8.	110	380	42	90	926	7.3	2.0	4.1	68
9.	110	380	47	80	844	7.1	2.3	4.0	67
10.	110	390	42	90	837	7.3	1.3	3.9	65
11.	110	390	42	90	834	6.9	0.9	3.9	65
12.	110	390	47	85	876	7.1	1.8	4.1	68
13.	110	390	47	85	871	6.9	1.7	3.9	65
14.	110	390	47	85	873	6.9	1.8	3.7	62
15.	110	390	47	85	863	7.3	1.9	3.7	62
16.	110	390	47	85	849	7.3	1.8	3.9	65
17.	110	390	47	85	839	7.7	1.8	4.1	68
18.	110	390	47	85	837	7.3	2.0	3.9	65
19.	110	390	47	85	837	7.3	1.8	3.9	65
20.	110	390	47	85	832	7.5	1.5	4.1	68
21.	110	390	47	80	902	6.7	1.9	3.8	63
22.	110	390	47	80	888	6.9	1.7	4.1	68
23.	110	390	47	80	897	6.9	1.9	3.9	65
24.	110	390	47	80	895	6.9	1.9	3.9	65
25.	110	390	47	80	883	6.7	1.8	3.6	60
26.	110	390	47	80	861	6.9	1.7	3.9	65

No.	Torch angle deg.	current Amp.	voltage Volt.	speed cm/min	temp T1 º C	bead width mm	bead high mm	bead penetration mm	bead penetration %
27.	110	390	47	80	849	6.7	1.7	3.8	63
28.	110	390	47	80	856	6.9	1.8	3.9	65
29.	110	390	47	80	861	6.9	1.8	4.1	68
30.	110	390	47	80	859	7.7	1.3	4.0	67
31.	110	390	47	90	856	6.4	2.0	3.9	65
32.	110	390	47	90	866	6.4	1.6	4.1	68
33.	110	400	42	85	834	7.3	1.8	4.1	68
34.	110	400	42	80	946	7.5	1.9	3.8	63
35.	110	400	42	80	934	7.3	1.8	4.1	68
36.	110	400	47	85	924	6.9	1.9	4.1	68
37.	110	400	47	85	909	7.1	1.9	4.1	68
38.	110	400	47	80	888	6.7	0.9	4.1	68
39.	110	400	47	90	868	6.9	1.6	4.1	68
40.	110	400	47	90	859	6.9	1.7	4.1	68
41.	110	400	47	90	854	6.4	1.3	4.1	68

1.6 experimental data and results for welding achieving 100%-110% depth of penetration with 0-1.5mm root gap

No.	T.A	Current	Voltage	Speed cm/min	Temp °C	Root gap mm
1	70	380	37	85	697	0.45
2	70	380	37	85	713	0.37
3	70	380	37	85	718	0.37
4	70	380	37	80	714	0.45
5	70	380	37	80	714	0.37
6	70	380	37	80	726	0.52
7	70	380	37	90	730	0.67
8	70	380	37	90	728	0.52
9	70	380	37	90	728	0.45
10	70	380	37	90	733	0.52
11	70	380	42	85	798	0.52
12	70	380	42	80	801	0.75
13	70	380	42	80	793	0.67
14	70	380	42	80	801	0.52
15	70	380	42	90	796	0.67
16	70	380	47	85	781	0.75
17	70	380	47	85	793	0.67
18	70	380	47	85	788	0.52
19	70	380	47	80	803	0.67
20	70	380	47	80	808	0.52
21	70	380	47	80	808	0.45
22	70	380	47	90	818	0.97
23	70	380	47	90	808	0.82
24	70	380	47	90	801	0.75
25	70	390	37	85	745	0.45
26	70	390	37	85	752	0.37
27	70	390	37	85	747	0.52

No.	T.A	Current	Voltage	Speed cm/min	Temp °C	Root gap mm
28	70	390	37	80	733	0.37
29	70	390	37	80	735	0.52
30	70	390	37	90	745	0.67
31	70	390	37	90	742	0.52
32	70	390	37	90	735	0.45
33	70	390	42	85	803	0.67
34	70	390	42	85	798	0.52
35	70	390	42	85	793	0.45
36	70	390	42	80	803	0.67
37	70	390	42	90	839	0.67
38	70	390	47	85	844	0.52
39	70	390	47	80	849	0.52
40	70	390	47	80	856	0.45
41	70	390	47	80	863	0.37
42	70	390	47	90	730	0.75
43	70	390	47	90	723	0.67
44	70	390	47	90	723	0.52
45	70	400	37	85	631	0.37
46	70	400	37	85	641	0.45
47	70	400	37	80	651	0.37
48	70	400	37	80	651	0.45
49	70	400	37	90	643	0.45
50	70	400	37	90	636	0.37
51	70	400	37	90	634	0.52
52	70	400	42	85	706	0.52
53	70	400	42	85	704	0.45
54	70	400	42	90	711	0.67
55	70	400	42	90	704	0.52
56	70	400	47	85	863	0.75

No.	T.A	Current	Voltage	Speed cm/min	Temp °C	Root gap mm
57	70	400	47	90	856	0.67
58	70	400	47	90	861	0.52
59	70	400	47	90	859	0.45
60	90	380	37	85	607	0.67
61	90	380	37	85	607	0.52
62	90	380	37	85	592	0.45
63	90	380	37	90	592	0.82
64	90	380	37	90	600	0.75
65	90	380	42	85	742	0.67
66	90	380	42	85	769	0.52
67	90	380	42	80	716	0.75
68	90	380	42	80	697	0.67
69	90	380	42	80	689	0.52
70	90	380	42	80	689	0.45
71	90	380	42	80	689	0.37
72	90	380	42	90	682	1.12
73	90	380	42	90	697	1.05
74	90	380	42	90	745	0.97
75	90	380	42	90	747	0.82
76	90	380	47	85	716	0.75
77	90	380	47	85	733	0.67
78	90	380	47	85	701	0.52
79	90	380	47	85	699	0.45
80	90	380	47	80	711	0.75
81	90	380	47	80	714	0.67
82	90	380	47	90	721	0.75
83	90	380	47	90	709	0.67
84	90	380	47	90	699	0.52
85	90	390	37	85	592	0.67

No.	T.A	Current	Voltage	Speed cm/min	Temp °C	Root gap mm
86	90	390	37	85	588	0.52
87	90	390	37	85	595	0.45
88	90	390	37	80	578	0.37
89	90	390	37	90	568	0.45
90	90	390	37	90	563	0.37
91	90	390	37	90	568	0.37
92	90	390	42	85	713	0.52
93	90	390	42	80	723	0.45
94	90	390	42	90	713	0.75
95	90	390	42	90	726	0.67
96	90	390	42	90	726	0.52
97	90	390	42	90	711	0.45
98	90	390	47	85	762	0.75
99	90	390	47	85	750	0.67
100	90	390	47	85	740	0.52
101	90	390	47	85	735	0.45
102	90	390	47	80	706	0.45
103	90	390	47	90	764	0.67
104	90	390	47	90	731	0.52
105	90	390	47	90	709	0.45
108	90	400	37	90	646	0.37
109	90	400	37	90	651	0.37
110	90	400	42	85	755	0.37
112	90	400	42	90	774	0.52
113	90	400	42	90	764	0.45
114	90	400	42	90	755	0.37
116	90	400	47	90	774	0.45
117	90	400	47	90	767	0.37
118	90	400	47	90	759	0.37

No.	T.A	Current	Voltage	Speed cm/min	Temp °C	Root gap mm
119	110	380	37	85	735	0.75
120	110	380	37	85	779	0.67
121	110	380	37	80	769	0.67
122	110	380	37	80	820	0.52
123	110	380	37	90	711	0.82
124	110	380	37	90	713	0.75
125	110	380	37	90	757	0.67
126	110	380	42	85	856	0.97
127	110	380	42	85	871	0.82
128	110	380	42	85	883	0.75
129	110	380	42	80	866	0.75
130	110	380	42	80	876	0.67
131	110	380	42	80	895	0.52
132	110	380	42	90	832	0.67
133	110	380	42	90	859	0.97

Appendix 2

Neural network modelling Results

Appendix 2

2.1.a Neural network training data for 100-110% penetration

No.	Torch angle	current	voltage	speed	temperature
1.	70	380	37	80	776
2.	70	390	37	80	677
3.	70	390	37	80	684
4.	70	390	37	80	687
5.	70	390	37	80	682
6.	70	390	37	80	687
7.	70	390	37	80	677
8.	70	390	37	80	675
9.	70	390	37	80	667
10.	70	390	37	80	672
11.	70	390	42	85	704
12.	70	400	37	85	648
13.	70	400	37	85	646
14.	70	400	37	85	651
15.	70	400	37	85	660
16.	70	400	37	85	665
17.	70	400	37	85	646
18.	70	400	37	80	752
19.	70	400	37	80	747
20.	70	400	37	80	740
21.	70	400	37	80	730
22.	70	400	37	80	723
23.	70	400	37	90	655
24.	70	400	37	90	655
25.	70	400	37	90	648
26.	70	400	37	90	660
27.	70	400	37	90	658
28.	70	400	37	90	663
29.	70	400	37	90	655
30.	70	400	37	90	660
31.	70	400	42	85	711
32.	70	400	42	80	687

No.	Torch angle	current	voltage	speed	temperature
33.	70	400	42	80	694
34.	70	400	42	80	704
35.	70	400	42	80	714
36.	70	400	42	80	716
37.	90	380	37	85	726
38.	90	380	37	85	733
39.	90	380	37	85	724
40.	90	380	37	85	716
41.	90	380	37	85	724
42.	90	380	37	85	735
43.	90	380	37	85	716
44.	90	390	37	80	723
45.	90	390	37	80	726
46.	90	390	37	80	721
47.	90	390	37	80	726
48.	90	390	37	90	718
49.	90	390	42	80	960
50.	90	390	47	80	856
51.	90	390	47	80	815
52.	90	400	37	85	733
53.	90	400	37	85	736
54.	90	400	37	85	731
55.	90	400	37	85	726
56.	90	400	37	85	726
57.	90	400	37	85	723
58.	90	400	37	85	730
59.	90	400	37	85	723
60.	90	400	37	85	721
61.	90	400	37	80	740
62.	90	400	37	80	730
63.	90	400	37	80	730
64.	90	400	37	80	730
65.	90	400	37	80	733
66.	90	400	37	80	728
67.	90	400	37	80	716
68.	90	400	37	80	713
69.	90	400	37	90	721
70.	90	400	37	90	723
71.	90	400	37	90	726
72.	90	400	37	90	726

No.	Torch angle	current	voltage	speed	temperature
73.	90	400	37	90	726
74.	90	400	37	90	723
75.	90	400	37	90	726
76.	90	400	37	90	718
77.	90	400	37	90	716
78.	90	400	42	85	936
79.	90	400	42	85	910
80.	90	400	42	80	895
81.	90	400	42	80	909
82.	90	400	42	80	919
83.	90	400	42	80	837
84.	90	400	42	80	810
85.	90	400	42	80	793
86.	90	400	42	80	779
87.	90	400	42	80	791
88.	90	400	47	85	873
89.	90	400	47	80	871
90.	90	400	47	80	878
91.	90	400	47	80	924
92.	90	400	47	80	912
93.	90	400	47	80	861
94.	90	400	47	80	849
95.	90	400	47	80	854
96.	90	400	47	80	871
97.	90	400	47	80	871
98.	110	380	37	85	805
99.	110	390	37	85	779
100.	110	390	37	85	769
101.	110	390	37	85	781
102.	110	390	37	80	777
103.	110	390	37	80	770
104.	110	390	37	80	774
105.	110	390	37	80	772
106.	110	390	37	80	767
107.	110	390	37	80	747
108.	110	390	37	80	750
109.	110	390	37	80	747
110.	110	400	37	85	796
111.	110	400	37	85	767
112.	110	400	37	80	745

No.	Torch angle	current	voltage	speed	temperature
113.	110	400	37	80	733
114.	110	400	37	80	730
115.	110	400	37	80	730
116.	110	400	37	80	728
117.	110	400	37	80	723
118.	110	400	37	80	684
119.	90	380	37	70	732
120.	90	380	37	70	726
121.	90	380	37	70	736
122.	90	390	37	65	672
123.	90	390	37	65	696
124.	90	390	37	65	708
125.	90	390	37	65	713
126.	90	390	37	65	708
127.	90	390	37	65	700
128.	90	390	37	65	694
129.	90	390	37	65	690
130.	90	390	37	65	698
131.	90	390	42	80	719
132.	90	390	42	80	732
133.	90	390	42	80	728
134.	90	390	42	80	725
135.	90	390	42	80	722
136.	90	390	42	80	848
137.	90	390	42	80	840
138.	90	390	42	80	848
139.	90	390	42	80	826
140.	90	390	42	80	830
141.	90	390	42	80	818
142.	90	390	42	80	814
143.	90	390	42	80	822
144.	90	390	42	80	824
145.	90	390	42	80	830
146.	90	390	47	75	850
147.	90	390	47	75	843
148.	90	390	42	80	846
149.	90	390	47	75	844
150.	90	390	47	75	819
151.	90	390	47	75	813
152.	90	390	47	75	850

No.	Torch angle	current	voltage	speed	temperature
153.	90	390	47	75	856
154.	90	390	47	75	858
155.	90	390	47	70	759
156.	90	390	47	70	763
157.	90	390	47	70	757
158.	90	390	47	70	739
159.	90	390	47	70	745
160.	90	390	47	70	743
161.	90	390	47	70	765
162.	90	400	37	80	696
163.	90	400	37	80	702
164.	90	400	37	80	717
165.	90	400	37	80	708
166.	90	400	37	80	697
167.	90	400	37	80	706
168.	90	400	37	80	687
169.	90	400	37	80	694
170.	90	400	37	80	710
171.	90	400	37	75	702
172.	90	400	37	75	686
173.	90	400	37	75	690
174.	90	400	37	75	700
175.	90	400	37	75	708
176.	90	400	37	75	692
177.	90	400	37	75	697
178.	90	400	37	70	692
179.	90	400	37	70	684
180.	90	400	37	70	678
181.	90	400	37	70	667
182.	90	400	37	70	674
183.	90	400	37	70	682
184.	90	400	37	70	663
185.	90	400	37	70	654
186.	90	400	37	70	657
187.	90	400	37	70	670
188.	90	400	42	80	754
189.	90	400	42	80	763
190.	90	400	42	80	752
191.	90	400	42	80	749
192.	90	400	42	80	742

No.	Torch angle	current	voltage	speed	temperature
193.	90	400	42	80	736
194.	90	400	42	80	730
195.	90	400	42	80	744
196.	90	400	42	80	750
197.	90	400	42	75	795
198.	90	400	42	75	777
199.	90	400	42	75	754
200.	90	400	42	75	749
201.	90	400	42	75	758
202.	90	400	42	75	768
203.	90	400	42	75	757
204.	90	400	42	75	763
205.	90	400	42	75	768
206.	90	400	47	70	769
207.	90	400	47	70	763
208.	90	400	47	70	782
209.	90	400	47	70	792
210.	90	400	47	70	775
211.	90	400	47	70	768
212.	90	400	47	70	771
213.	90	400	47	70	762
214.	90	400	47	70	780
215.	90	410	37	80	636
216.	90	410	37	80	634
217.	90	410	37	80	635
218.	90	410	37	80	646
219.	90	410	37	80	653
220.	90	410	37	80	648
221.	90	410	37	80	644
222.	90	410	37	80	650
223.	90	410	42	85	710
224.	90	410	42	85	718
225.	90	410	42	85	710
226.	90	410	42	85	713
227.	90	410	42	85	702
228.	90	380	42	75	741
229.	90	380	42	75	736
230.	90	380	42	75	742
231.	90	380	42	75	739
232.	90	380	42	75	738

No.	Torch angle	current	voltage	speed	temperature
233.	90	380	42	75	743
234.	90	380	42	75	736
235.	70	390	37	70	619
236.	70	390	37	70	623
237.	70	390	37	70	628
238.	70	390	37	70	612
239.	70	390	37	70	605
240.	70	390	37	70	618
241.	70	390	37	70	607
242.	70	390	37	70	614
243.	70	390	42	75	647
244.	70	390	42	75	663
245.	70	390	42	75	686
246.	70	390	42	75	674
247.	70	390	47	80	696
248.	70	390	47	80	719
249.	70	390	47	80	725
250.	70	390	47	80	720
251.	70	390	47	80	714
252.	70	400	42	80	685
253.	70	400	42	80	711
254.	70	400	42	80	712

2.1.b Neural network evaluation data for 100-110% penetration models

No.	Torch angle	Current	Voltage	Speed	Temperature °C
1	70	390	37	800	689
2	70	400	37	850	634
3	70	400	37	850	663
4	70	400	37	800	726
5	70	400	37	900	665
6	70	400	42	850	704
7	70	400	47	800	709
8	90	380	37	850	724
9	90	390	37	800	721
10	90	390	47	800	806
11	90	400	37	850	723
12	90	400	37	800	728
13	90	400	37	800	726
14	90	400	37	900	726
15	90	400	37	900	711
16	90	400	42	800	878
17	90	400	42	800	788
18	90	400	47	800	885
19	110	380	37	850	815
20	110	390	37	800	796
21	110	390	37	800	757
22	110	400	37	800	759
23	110	400	37	800	728
24	90	390	37	650	693
25	90	390	42	800	846
26	90	390	42	800	846
27	90	390	47	700	754
28	90	400	37	800	699
29	90	400	37	750	687
30	90	400	37	700	675
31	90	400	42	750	790
32	90	400	47	700	775
33	90	410	37	800	642
34	90	380	42	750	733
35	70	390	37	700	625
36	70	390	47	800	707
37	70	400	42	800	697

2.2.a Neural network training data for 90-99% penetration models.

NO.	Torch angle	current	voltage	speed	temperature
1.	70	380	37	80	781
2.	70	380	37	80	781
3.	70	380	37	80	774
4.	70	380	37	80	767
5.	70	380	37	80	730
6.	70	380	37	80	733
7.	70	380	37	80	733
8.	70	380	37	90	709
9.	70	390	37	85	643
10.	70	390	42	80	723
11.	70	400	37	85	660
12.	70	400	37	85	643
13.	70	400	37	80	711
14.	70	400	37	80	730
15.	70	400	37	90	663
16.	70	400	42	85	694
17.	70	400	42	85	701
18.	70	400	42	85	711
19.	70	400	42	85	706
20.	70	400	42	85	709
21.	70	400	42	85	711
22.	70	400	42	80	719
23.	70	400	42	90	704
24.	70	400	47	85	701
25.	70	400	47	85	697
26.	70	400	47	85	689
27.	70	400	47	85	687
28.	70	400	47	85	699
29.	70	400	47	85	699
30.	70	400	47	85	682
31.	70	400	47	80	723
32.	70	400	47	80	733
33.	70	400	47	85	682
34.	70	400	47	80	723
35.	70	400	47	80	733
36.	70	400	47	80	738

NO.	Torch angle	current	voltage	speed	temperature
37.	90	380	37	85	731
38.	90	380	37	85	738
39.	90	380	42	85	929
40.	90	380	42	85	963
41.	90	380	42	85	900
42.	90	390	37	85	713
43.	90	390	37	85	718
44.	90	390	37	85	718
45.	90	390	37	80	723
46.	90	390	37	80	726
47.	90	390	37	80	726
48.	90	390	37	80	726
49.	90	390	37	80	721
50.	90	390	37	90	718
51.	90	390	37	90	713
52.	90	390	37	90	706
53.	90	390	37	90	704
54.	90	390	37	90	706
55.	90	390	37	90	701
56.	90	390	37	90	699
57.	90	390	37	90	699
58.	90	390	42	80	968
59.	90	390	42	80	924
60.	90	390	42	80	871
61.	90	390	42	80	866
62.	90	390	42	80	839
63.	90	390	42	80	827
64.	90	390	47	85	885
65.	90	390	47	80	963
66.	90	390	47	80	907
67.	90	390	47	80	793
68.	90	390	47	80	799
69.	90	390	47	80	808
70.	90	400	42	85	893
71.	90	400	42	85	818
72.	90	400	42	85	822
73.	90	400	42	85	823
74.	90	400	42	90	849
75.	90	400	47	85	905
76.	90	400	47	85	931

NO.	Torch angle	current	voltage	speed	temperature
77.	90	400	47	85	919
78.	90	400	47	85	888
79.	90	400	47	85	856
80.	90	400	47	85	842
81.	90	400	47	85	856
82.	90	400	47	85	876
83.	90	400	47	90	914
84.	90	400	47	90	931
85.	110	380	37	85	868
86.	110	380	37	80	830
87.	110	390	37	85	786
88.	110	390	37	85	786
89.	110	390	37	85	781
90.	110	390	37	85	774
91.	110	390	37	90	805
92.	110	390	37	90	757
93.	110	390	37	90	752
94.	110	390	37	90	740
95.	110	390	37	90	745
96.	110	390	37	90	742
97.	110	400	37	85	759
98.	110	400	37	85	759
99.	110	400	37	85	759
100.	110	400	37	90	798
101.	110	400	37	90	767
102.	110	400	37	90	747
103.	110	400	37	90	742
104.	110	400	37	90	733
105.	110	400	37	90	747
106.	110	400	37	90	742
107.	110	400	37	90	733

2.2.b Neural network validation data for 90-99% penetration models.

NO.	Torch angle	current	voltage	speed	temperature
1.	70	380	37	80	776
2.	70	390	37	85	643
3.	70	400	37	80	730
4.	70	400	42	90	701
5.	70	400	47	80	728
6.	90	380	37	80	750
7.	90	390	37	90	701
8.	90	400	42	85	876
9.	110	380	37	85	801
10.	110	400	37	85	793
11.	110	400	42	90	847

2.3.a Neural network training data for 80-89% penetration models

NO.	Torch angle	current	voltage	speed	temperature
1.	70	380	37	85	697
2.	70	380	37	85	701
3.	70	380	37	85	665
4.	70	380	37	80	740
5.	70	380	37	90	728
6.	70	380	37	90	735
7.	70	380	37	90	733
8.	70	380	37	90	730
9.	70	380	37	90	747
10.	70	380	37	90	730
11.	70	380	42	80	750
12.	70	380	42	80	776
13.	70	380	47	80	902
14.	70	390	37	85	612
15.	70	390	37	85	634
16.	70	390	37	85	638
17.	70	390	37	85	636
18.	70	390	37	85	643
19.	70	390	37	85	643
20.	70	390	37	85	634
21.	70	390	37	85	619
22.	70	390	37	90	658
23.	70	390	37	90	648
24.	70	390	37	90	646
25.	70	390	37	90	648
26.	70	390	37	90	651
27.	70	390	37	90	634
28.	70	390	37	90	629
29.	70	390	37	90	626
30.	70	390	37	90	634
31.	70	390	42	80	721
32.	70	390	42	80	728
33.	70	390	42	80	730
34.	70	390	42	80	728
35.	70	390	42	80	723
36.	70	390	42	80	728

NO.	Torch angle	current	voltage	speed	temperature
37.	70	390	42	90	709
38.	70	390	47	80	740
39.	70	390	47	80	772
40.	70	400	42	85	711
41.	70	400	42	80	719
42.	70	400	42	80	716
43.	70	400	42	80	714
44.	70	400	42	90	694
45.	70	400	42	90	706
46.	70	400	42	90	706
47.	70	400	42	90	704
48.	70	400	42	90	706
49.	70	400	42	90	706
50.	70	400	42	90	701
51.	70	400	47	85	699
52.	70	400	47	85	689
53.	70	400	47	85	687
54.	70	400	47	80	728
55.	70	400	47	80	733
56.	70	400	47	80	733
57.	70	400	47	80	730
58.	70	400	47	80	733
59.	70	400	47	90	713
60.	70	400	47	90	728
61.	70	400	47	90	723
62.	70	400	47	90	721
63.	70	400	47	90	699
64.	70	400	47	90	704
65.	90	380	37	80	742
66.	90	380	37	80	750
67.	90	380	37	80	747
68.	90	380	37	80	724
69.	90	380	37	80	724
70.	90	380	37	80	723
71.	90	380	37	90	718
72.	90	380	37	90	711
73.	90	380	37	90	716
74.	90	380	37	90	721
75.	90	380	37	90	711
76.	90	380	37	90	700

NO.	Torch angle	current	voltage	speed	temperature
77.	90	380	37	90	701
78.	90	380	37	90	69[illegible]
79.	90	380	37	90	69[illegible]
80.	90	380	42	85	893
81.	90	380	42	85	873
82.	90	380	42	85	885
83.	90	380	42	85	88[illegible]
84.	90	380	42	85	888
85.	90	380	42	80	96[illegible]
86.	90	380	42	80	978
87.	90	380	42	80	96[illegible]
88.	90	380	42	80	978
89.	90	380	42	80	966
90.	90	380	42	80	958
91.	90	380	42	80	939
92.	90	380	42	80	90[illegible]
93.	90	380	47	85	905
94.	90	380	47	85	939
95.	90	380	47	85	793
96.	90	380	47	80	984
97.	90	380	47	80	96[illegible]
98.	90	380	47	80	939
99.	90	380	47	80	90[illegible]
100.	90	380	47	80	842
101.	90	380	47	80	856
102.	90	380	47	80	834
103.	90	390	37	85	721
104.	90	390	37	85	716
105.	90	390	37	85	716
106.	90	390	37	85	713
107.	90	390	37	85	709
108.	90	390	37	85	709
109.	90	390	42	85	79[illegible]
110.	90	390	42	85	80[illegible]
111.	90	390	42	85	805
112.	90	390	42	80	83[illegible]
113.	90	390	42	80	827
114.	90	390	42	90	833
115.	90	390	42	90	83[illegible]
116.	90	390	42	90	835

NO.	Torch angle	current	voltage	speed	temperature
117.	90	390	42	90	805
118.	90	390	42	90	805
119.	90	390	42	90	790
120.	90	390	42	90	791
121.	90	390	42	90	790
122.	90	390	42	90	790
123.	90	390	42	90	785
124.	90	390	47	85	863
125.	90	390	47	85	866
126.	90	390	47	85	834
127.	90	390	47	85	837
128.	90	390	47	85	842
129.	90	390	47	85	834
130.	90	390	47	85	861
131.	90	390	47	80	936
132.	90	390	47	80	799
133.	90	390	47	90	820
134.	90	390	47	90	786
135.	90	390	47	90	791
136.	90	390	47	90	813
137.	90	390	47	90	815
138.	90	390	47	90	856
139.	90	390	47	90	832
140.	90	390	47	90	827
141.	90	390	47	90	837
142.	90	390	47	90	805
143.	90	400	42	85	844
144.	90	400	42	85	830
145.	90	400	42	85	820
146.	90	400	42	90	856
147.	90	400	42	90	854
148.	90	400	42	90	888
149.	90	400	42	90	898
150.	90	400	42	90	860
151.	90	400	42	90	847
152.	90	400	42	90	822
153.	90	400	47	85	847
154.	90	400	47	90	893
155.	90	400	47	90	866
156.	90	400	47	90	919

NO.	Torch angle	current	voltage	speed	temperature
157.	90	400	47	90	939
158.	90	400	47	90	919
159.	90	400	47	90	885
160.	90	400	47	90	863
161.	110	380	37	85	854
162.	110	380	37	85	844
163.	110	380	37	85	827
164.	110	380	37	85	803
165.	110	380	37	80	711
166.	110	380	37	80	948
167.	110	380	37	80	902
168.	110	380	37	80	863
169.	110	380	37	80	847
170.	110	380	37	80	834
171.	110	380	37	80	813
172.	110	380	37	90	856
173.	110	380	37	90	854
174.	110	380	37	90	832
175.	110	380	37	90	825
176.	110	380	37	90	825
177.	110	380	37	90	813
178.	110	380	37	90	805
179.	110	390	37	85	791
180.	110	390	37	90	791
181.	110	390	37	90	772
182.	110	390	37	90	769
183.	110	390	37	90	759
184.	110	390	42	80	888
185.	110	390	42	80	883
186.	110	400	37	85	793
187.	110	400	37	85	793
188.	110	400	37	85	774
189.	110	400	37	85	738
190.	110	400	37	90	803
191.	110	400	37	90	781
192.	110	400	37	90	764
193.	110	400	37	90	762
194.	110	400	42	85	844
195.	110	400	42	80	941
196.	110	400	42	90	859

NO.	Torch angle	current	voltage	speed	temperature
197.	11[illegible]	400	42	90	842
198.	11[illegible]	400	42	90	839

2.3.b Neural network validation data for 80-89% penetration models.

NO.	Torch angle	current	voltage	speed	temperature
1.	70	400	42	85	723
2.	70	400	42	90	706
3.	70	390	47	80	774
4.	70	400	37	80	682
5.	70	400	47	90	733
6.	90	380	37	80	716
7.	90	380	42	85	924
8.	90	380	47	80	955
9.	90	390	37	85	721
10.	90	380	42	85	941
11.	90	390	42	80	902
12.	90	390	47	85	849
13.	90	400	42	90	910
14.	110	380	37	90	798
15.	110	390	37	85	805
16.	110	380	37	85	769
17.	110	390	37	85	808
18.	110	400	37	90	747
19.	110	400	47	80	893

2.4.a Neural network training data for 70-79% penetration models.

NO.	Torch angle	current	voltage	speed	temperature
1.	70	380	37	85	687
2.	70	380	37	85	672
3.	70	380	37	85	665
4.	70	380	37	90	740
5.	70	380	37	90	716
6.	70	380	37	90	718
7.	70	380	42	85	767
8.	70	380	42	85	798
9.	70	380	42	85	820
10.	70	380	42	85	805
11.	70	380	42	85	801
12.	70	380	42	85	793
13.	70	380	42	85	774
14.	70	380	42	85	769
15.	70	380	42	85	776
16.	70	380	42	80	793
17.	70	380	42	80	793
18.	70	380	42	80	793
19.	70	380	42	80	791
20.	70	380	42	80	788
21.	70	380	42	80	767
22.	70	380	42	80	769
23.	70	380	42	80	769
24.	70	380	42	90	774
25.	70	380	42	90	788
26.	70	380	42	90	798
27.	70	380	42	90	803
28.	70	380	42	90	801
29.	70	380	42	90	791
30.	70	380	42	90	781
31.	70	380	42	90	796
32.	70	380	42	90	796
33.	70	380	42	90	781

NO.	Torch angle	current	voltage	speed	temperature
34.	70	380	47	85	837
35.	70	380	47	85	854
36.	70	380	47	85	863
37.	70	380	47	85	866
38.	70	380	47	85	856
39.	70	380	47	85	842
40.	70	380	47	85	851
41.	70	380	47	80	842
42.	70	380	47	80	895
43.	70	380	47	80	907
44.	70	380	47	80	890
45.	70	380	47	80	900
46.	70	380	47	80	885
47.	70	380	47	80	851
48.	70	380	47	80	851
49.	70	380	47	80	844
50.	70	380	47	90	847
51.	70	380	47	90	878
52.	70	380	47	90	878
53.	70	380	47	90	847
54.	70	380	47	90	822
55.	70	380	47	90	759
56.	70	380	47	90	750
57.	70	380	47	90	747
58.	70	390	37	90	658
59.	70	390	42	85	713
60.	70	390	42	85	718
61.	70	390	42	85	718
62.	70	390	42	85	716
63.	70	390	42	85	723
64.	70	390	42	85	701
65.	70	390	42	80	721
66.	70	390	42	80	713
67.	70	390	42	80	706
68.	70	390	42	90	711
69.	70	390	42	90	711
70.	70	390	42	90	712
71.	70	390	42	90	710
72.	70	390	42	90	711
73.	70	390	42	90	713

NO.	Torch angle	current	voltage	speed	temperature
74.	70	390	42	90	709
75.	70	390	42	90	704
76.	70	390	47	85	716
77.	70	390	47	85	728
78.	70	390	47	85	735
79.	70	390	47	85	733
80.	70	390	47	85	721
81.	70	390	47	85	716
82.	70	390	47	85	718
83.	70	390	47	85	718
84.	70	390	47	85	709
85.	70	390	47	80	759
86.	70	390	47	80	750
87.	70	390	47	80	745
88.	70	390	47	80	745
89.	70	390	47	80	745
90.	70	390	47	80	747
91.	70	390	47	90	731
92.	70	390	47	90	723
93.	70	390	47	90	733
94.	70	390	47	90	747
95.	70	390	47	90	755
96.	70	390	47	90	747
97.	70	390	47	90	726
98.	70	400	42	80	716
99.	90	380	37	80	755
100.	90	380	37	90	716
101.	90	380	42	80	960
102.	90	380	42	80	861
103.	90	380	42	90	905
104.	90	380	42	90	888
105.	90	380	42	90	914
106.	90	380	42	90	929
107.	90	380	42	90	917
108.	90	380	42	90	905
109.	90	380	42	90	883
110.	90	380	42	90	873
111.	90	380	42	90	873
112.	90	380	47	85	890
113.	90	380	47	85	965

NO.	Torch angle	current	voltage	speed	temperature
114.	90	380	47	85	941
115.	90	380	47	85	856
116.	90	380	47	85	796
117.	90	380	47	85	798
118.	90	380	47	80	929
119.	90	380	47	90	881
120.	90	380	47	90	878
121.	90	380	47	90	905
122.	90	380	47	90	931
123.	90	380	47	90	929
124.	90	380	47	90	912
125.	90	380	47	90	900
126.	90	380	47	90	866
127.	90	380	47	90	830
128.	90	390	42	85	878
129.	90	390	42	85	842
130.	90	390	42	85	815
131.	90	390	42	85	805
132.	90	390	42	85	805
133.	90	390	42	85	793
134.	90	390	47	85	853
135.	90	400	42	90	830
136.	110	380	37	80	815
137.	110	380	37	80	793
138.	110	380	37	90	839
139.	110	380	42	85	917
140.	110	380	42	85	893
141.	110	380	42	85	893
142.	110	380	42	85	926
143.	110	380	42	85	946
144.	110	380	42	85	972
145.	110	380	42	85	968
146.	110	380	42	85	984
147.	110	380	42	85	972
148.	110	380	42	80	997
149.	110	380	42	80	989
150.	110	380	42	80	1009
151.	110	380	42	80	1014
152.	110	380	42	80	1014
153.	110	380	42	80	1014

NO.	Torch angle	current	voltage	speed	temperature
154.	110	380	42	80	1021
155.	110	380	42	80	1014
156.	110	380	42	80	1023
157.	110	380	42	80	989
158.	110	380	42	90	970
159.	110	380	42	90	924
160.	110	380	42	90	926
161.	110	380	42	90	946
162.	110	380	42	90	953
163.	110	380	42	90	953
164.	110	380	42	90	943
165.	110	380	47	85	851
166.	110	380	47	85	837
167.	110	380	47	85	839
168.	110	380	47	85	859
169.	110	380	47	85	861
170.	110	380	47	85	861
171.	110	380	47	85	866
172.	110	380	47	85	849
173.	110	380	47	85	847
174.	110	380	47	85	813
175.	110	380	47	80	861
176.	110	380	47	80	849
177.	110	380	47	80	849
178.	110	380	47	80	839
179.	110	380	47	80	832
180.	110	380	47	80	832
181.	110	380	47	80	830
182.	110	380	47	80	842
183.	110	380	47	80	825
184.	110	380	47	90	861
185.	110	380	47	90	844
186.	110	380	47	90	849
187.	110	380	47	90	830
188.	110	380	47	90	818
189.	110	380	47	90	813
190.	110	380	47	90	805
191.	110	380	47	90	798
192.	110	380	47	90	791
193.	110	380	47	90	784

NO.	Torch angle	current	voltage	speed	temperature
194.	110	390	42	85	890
195.	110	390	42	85	871
196.	110	390	42	85	868
197.	110	390	42	85	871
198.	110	390	42	85	859
199.	110	390	42	85	847
200.	110	390	42	85	842
201.	110	390	42	85	830
202.	110	390	42	85	842
203.	110	390	42	85	830
204.	110	390	42	80	895
205.	110	390	42	80	876
206.	110	390	42	80	888
207.	110	390	42	80	900
208.	110	390	42	80	876
209.	110	390	42	80	871
210.	110	390	42	80	863
211.	110	390	42	90	851
212.	110	390	42	90	827
213.	110	390	42	90	827
214.	110	390	42	90	827
215.	110	390	42	90	815
216.	110	390	42	90	818
217.	110	390	42	90	834
218.	110	390	47	85	868
219.	110	390	47	90	859
220.	110	390	47	90	856
221.	110	390	47	90	859
222.	110	390	47	90	844
223.	110	390	47	90	839
224.	110	390	47	90	830
225.	110	390	47	90	825
226.	110	390	47	90	820
227.	110	400	42	85	866
228.	110	400	42	85	856
229.	110	400	42	85	856
230.	110	400	42	85	830
231.	110	400	42	85	827
232.	110	400	42	85	825
233.	110	400	42	85	822

NO.	Torch angle	current	voltage	speed	temperature
234.	110	400	42	80	953
235.	110	400	42	80	943
236.	110	400	42	80	948
237.	110	400	42	80	948
238.	110	400	42	80	939
239.	110	400	42	80	934
240.	110	400	42	90	883
241.	110	400	42	90	861
242.	110	400	42	90	849
243.	110	400	42	90	847
244.	110	400	42	90	839
245.	110	400	42	90	837
246.	110	400	47	85	907
247.	110	400	47	85	892
248.	110	400	47	85	892
249.	110	400	47	85	885
250.	110	400	47	85	870
251.	110	400	47	85	865
252.	110	400	47	85	860
253.	110	400	47	80	912
254.	110	400	47	80	914
255.	110	400	47	80	914
256.	110	400	47	80	902
257.	110	400	47	80	905
258.	110	400	47	80	895
259.	110	400	47	90	919
260.	110	400	47	90	902
261.	110	400	47	90	897
262.	110	400	47	90	893
263.	110	400	47	90	895
264.	110	400	47	90	883

2.4.b. Neural network validation data for 70-79% penetration models.

NO.	Torch angle	current	voltage	speed	temperature
1.	70	380	37	85	670
2.	70	380	42	85	818
3.	70	380	47	90	827
4.	70	390	42	85	711
5.	70	390	47	80	740
6.	70	390	47	85	721
7.	70	390	42	90	713
8.	70	390	37	80	704
9.	70	390	47	90	742
10.	90	380	47	80	968
11.	90	400	47	90	878
12.	90	380	47	90	844
13.	90	380	42	90	905
14.	90	380	37	80	738
15.	90	390	42	85	893
16.	110	380	37	90	842
17.	110	380	42	85	965
18.	110	380	42	90	941
19.	110	390	42	80	900
20.	110	390	42	90	815
21.	110	400	42	85	856
22.	110	400	47	90	871
23.	110	400	47	80	902
24.	110	400	47	85	907
25.	110	400	42	80	939
26.	110	400	47	80	929

Appendix 3

Fuzzy Logic Rule Base

Appendix 3.

3.1 Fuzzy logic rule base applied in fuzzy logic modelling.

1. If (Temperature is bn) and (Current is L) and (Voltage is M) and (Speed is M) then (cur is VH) (1)

2. If (Temperature is bn) and (Current is L) and (Voltage is M) and (Speed is M) then (vol is VH) (1)

3. If (Temperature is bn) and (Current is L) and (Voltage is M) and (Speed is M) then (sp is L) (1)

4. If (Temperature is bn) and (Current is L) and (Voltage is M) and (Speed is L) then (cur is VH) (1)

5. If (Temperature is bn) and (Current is L) and (Voltage is M) and (Speed is L) then (vol is VH) (1)

6. If (Temperature is bn) and (Current is L) and (Voltage is M) and (Speed is L) then (sp is L) (1)

7. If (Temperature is bn) and (Current is L) and (Voltage is M) and (Speed is H) then (cur is VH) (1)

8. If (Temperature is bn) and (Current is L) and (Voltage is M) and (Speed is H) then (vol is VH) (1)

9. If (Temperature is bn) and (Current is L) and (Voltage is M) and (Speed is H) then (sp is L) (1)

10. If (Temperature is bn) and (Current is L) and (Voltage is L) and (Speed is M) then (cur is VH) (1)

11. If (Temperature is bn) and (Current is L) and (Voltage is L) and (Speed is M) then (vol is VH) (1)

12. If (Temperature is bn) and (Current is L) and (Voltage is L) and (Speed is M) then (sp is L) (1)

13. If (Temperature is bn) and (Current is L) and (Voltage is L) and (Speed is L) then (cur is VH) (1)

14. If (Temperature is bn) and (Current is L) and (Voltage is L) and (Speed is L) then (vol is VH) (1)

15. If (Temperature is bn) and (Current is L) and (Voltage is L) and (Speed is L) then (sp is L) (1)

16. If (Temperature is bn) and (Current is L) and (Voltage is L) and (Speed is H) then (cur is VH) (1)

17. If (Temperature is bn) and (Current is L) and (Voltage is L) and (Speed is H) then (vol is VH) (1)

18. If (Temperature is bn) and (Current is L) and (Voltage is L) and (Speed is H) then (sp is L) (1)

19. If (Temperature is bn) and (Current is L) and (Voltage is H) and (Speed is M) then (cur is VH) (1)

20. If (Temperature is bn) and (Current is L) and (Voltage is H) and (Speed is M) then (vol is VH) (1)

21. If (Temperature is bn) and (Current is L) and (Voltage is H) and (Speed is M) then (sp is L) (1)

22. If (Temperature is bn) and (Current is L) and (Voltage is H) and (Speed is L) then (cur is VH) (1)

23. If (Temperature is bn) and (Current is L) and (Voltage is H) and (Speed is L) then (vol is VH) (1)

24. If (Temperature is bn) and (Current is L) and (Voltage is H) and (Speed is L) then (sp is L) (1)

25. If (Temperature is bn) and (Current is L) and (Voltage is H) and (Speed is H) then (cur is VH) (1)

26. If (Temperature is bn) and (Current is L) and (Voltage is H) and (Speed is H) then (vol is VH) (1)

27. If (Temperature is bn) and (Current is L) and (Voltage is H) and (Speed is H) then (sp is L) (1)

28. If (Temperature is bn) and (Current is M) and (Voltage is M) and (Speed is M) then (cur is VH) (1)

29. If (Temperature is bn) and (Current is M) and (Voltage is M) and (Speed is M) then (vol is VH) (1)

30. If (Temperature is bn) and (Current is M) and (Voltage is M) and (Speed is M) then (sp is L) (1)

31. If (Temperature is bn) and (Current is M) and (Voltage is M) and (Speed is L) then (cur is VH) (1)

32. If (Temperature is bn) and (Current is M) and (Voltage is M) and (Speed is L) then (vol is VH) (1)

33. If (Temperature is bn) and (Current is M) and (Voltage is M) and (Speed is L) then (sp is L) (1)

34. If (Temperature is bn) and (Current is M) and (Voltage is M) and (Speed is H) then (cur is VH) (1)

35. If (Temperature is bn) and (Current is M) and (Voltage is M) and (Speed is H) then (vol is VH) (1)

36. If (Temperature is bn) and (Current is M) and (Voltage is M) and (Speed is H) then (sp is L) (1)

37. If (Temperature is bn) and (Current is M) and (Voltage is L) and (Speed is M) then (cur is VH) (1)

38. If (Temperature is bn) and (Current is M) and (Voltage is L) and (Speed is M) then (vol is VH) (1)

39. If (Temperature is bn) and (Current is M) and (Voltage is L) and (Speed is M) then (sp is L) (1)

40. If (Temperature is bn) and (Current is M) and (Voltage is L) and (Speed is L) then (cur is VH) (1)

41. If (Temperature is bn) and (Current is M) and (Voltage is L) and (Speed is L) then (vol is VH) (1)

42. If (Temperature is bn) and (Current is M) and (Voltage is L) and (Speed is L) then (sp is L) (1)

43. If (Temperature is bn) and (Current is M) and (Voltage is L) and (Speed is H) then (cur is VH) (1)

44. If (Temperature is bn) and (Current is M) and (Voltage is L) and (Speed is H) then (vol is VH) (1)

45. If (Temperature is bn) and (Current is M) and (Voltage is L) and (Speed is H) then (sp is L) (1)

46. If (Temperature is bn) and (Current is M) and (Voltage is H) and (Speed is M) then (cur is VH) (1)

47. If (Temperature is bn) and (Current is M) and (Voltage is H) and (Speed is M) then (vol is VH) (1)

48. If (Temperature is bn) and (Current is M) and (Voltage is H) and (Speed is M) then (sp is L) (1)

49. If (Temperature is bn) and (Current is M) and (Voltage is H) and (Speed is L) then (cur is VH) (1)

50. If (Temperature is bn) and (Current is M) and (Voltage is H) and (Speed is L) then (vol is VH) (1)

51. If (Temperature is bn) and (Current is M) and (Voltage is H) and (Speed is L) then (sp is L) (1)

52. If (Temperature is bn) and (Current is M) and (Voltage is H) and (Speed is H) then (cur is VH) (1)

53. If (Temperature is bn) and (Current is M) and (Voltage is H) and (Speed is H) then (vol is VH) (1)

54. If (Temperature is bn) and (Current is M) and (Voltage is H) and (Speed is H) then (sp is L) (1)

55. If (Temperature is bn) and (Current is H) and (Voltage is M) and (Speed is M) then (cur is VH) (1)

56. If (Temperature is bn) and (Current is H) and (Voltage is M) and (Speed is M) then (vol is VH) (1)

57. If (Temperature is bn) and (Current is H) and (Voltage is M) and (Speed is M) then (sp is L) (1)

58. If (Temperature is bn) and (Current is H) and (Voltage is M) and (Speed is L) then (cur is nc) (1)

59. If (Temperature is bn) and (Current is H) and (Voltage is M) and (Speed is L) then (vol is VH) (1)

60. If (Temperature is bn) and (Current is H) and (Voltage is M) and (Speed is L) then (sp is L) (1)

61. If (Temperature is bn) and (Current is H) and (Voltage is M) and (Speed is H) then (cur is nc) (1)

62. If (Temperature is bn) and (Current is H) and (Voltage is M) and (Speed is H) then (vol is VH) (1)

63. If (Temperature is bn) and (Current is H) and (Voltage is M) and (Speed is H) then (sp is L) (1)

64. If (Temperature is bn) and (Current is H) and (Voltage is L) and (Speed is M) then (cur is nc) (1)

65. If (Temperature is bn) and (Current is H) and (Voltage is L) and (Speed is M) then (vol is VH) (1)

66. If (Temperature is bn) and (Current is H) and (Voltage is L) and (Speed is M) then (sp is L) (1)

67. If (Temperature is bn) and (Current is H) and (Voltage is L) and (Speed is L) then (cur is nc) (1)

68. If (Temperature is bn) and (Current is H) and (Voltage is L) and (Speed is L) then (vol is VH) (1)

69. If (Temperature is bn) and (Current is H) and (Voltage is L) and (Speed is L) then (sp is L) (1)

70. If (Temperature is bn) and (Current is H) and (Voltage is L) and (Speed is H) then (cur is nc) (1)

71. If (Temperature is bn) and (Current is H) and (Voltage is L) and (Speed is H) then (vol is VH) (1)

72. If (Temperature is bn) and (Current is H) and (Voltage is L) and (Speed is H) then (sp is L) (1)

73. If (Temperature is bn) and (Current is H) and (Voltage is H) and (Speed is M) then (cur is nc) (1)

74. If (Temperature is bn) and (Current is H) and (Voltage is H) and (Speed is M) then (cur is nc) (1)

75. If (Temperature is bn) and (Current is H) and (Voltage is H) and (Speed is M) then (sp is L) (1)

76. If (Temperature is bn) and (Current is H) and (Voltage is H) and (Speed is L) then (cur is nc) (1)

77. If (Temperature is bn) and (Current is H) and (Voltage is H) and (Speed is L) then (cur is nc) (1)

78. If (Temperature is bn) and (Current is H) and (Voltage is H) and (Speed is L) then (sp is L) (1)

79. If (Temperature is bn) and (Current is H) and (Voltage is H) and (Speed is H) then (cur is nc) (1)

80. If (Temperature is bn) and (Current is H) and (Voltage is H) and (Speed is H) then (cur is nc) (1)

81. If (Temperature is bn) and (Current is H) and (Voltage is H) and (Speed is H) then (sp is L) (1)

82. If (Temperature is n) and (Current is L) and (Voltage is M) and (Speed is M) then (cur is H) (1)

83. If (Temperature is n) and (Current is L) and (Voltage is M) and (Speed is M) then (vol is VH) (1)

84. If (Temperature is n) and (Current is L) and (Voltage is M) and (Speed is M) then (sp is L) (1)

85. If (Temperature is n) and (Current is L) and (Voltage is M) and (Speed is L) then (cur is H) (1)

86. If (Temperature is n) and (Current is L) and (Voltage is M) and (Speed is L) then (vol is VH) (1)

87. If (Temperature is n) and (Current is L) and (Voltage is M) and (Speed is L) then (sp is L) (1)

88. If (Temperature is n) and (Current is L) and (Voltage is M) and (Speed is H) then (cur is H) (1)

89. If (Temperature is n) and (Current is L) and (Voltage is M) and (Speed is H) then (vol is VH) (1)

90. If (Temperature is n) and (Current is L) and (Voltage is M) and (Speed is H) then (sp is L) (1)

91. If (Temperature is n) and (Current is L) and (Voltage is L) and (Speed is M) then (cur is H) (1)

92. If (Temperature is n) and (Current is L) and (Voltage is L) and (Speed is M) then (vol is VH) (1)

93. If (Temperature is n) and (Current is L) and (Voltage is L) and (Speed is M) then (sp is L) (1)

94. If (Temperature is n) and (Current is L) and (Voltage is L) and (Speed is L) then (cur is H) (1)

95. If (Temperature is n) and (Current is L) and (Voltage is L) and (Speed is L) then (vol is VH) (1)

96. If (Temperature is n) and (Current is L) and (Voltage is L) and (Speed is L) then (sp is L) (1)

97. If (Temperature is n) and (Current is L) and (Voltage is L) and (Speed is H) then (cur is H) (1)

98. If (Temperature is n) and (Current is L) and (Voltage is L) and (Speed is H) then (vol is VH) (1)

99. If (Temperature is n) and (Current is L) and (Voltage is L) and (Speed is H) then (sp is L) (1)

100. If (Temperature is n) and (Current is L) and (Voltage is H) and (Speed is M) then (cur is H) (1)

101. If (Temperature is n) and (Current is L) and (Voltage is H) and (Speed is M) then (vol is VH) (1)

102. If (Temperature is n) and (Current is L) and (Voltage is H) and (Speed is M) then (sp is L) (1)

103. If (Temperature is n) and (Current is L) and (Voltage is H) and (Speed is L) then (cur is H) (1)

104. If (Temperature is n) and (Current is L) and (Voltage is H) and (Speed is L) then (vol is VH) (1)

105. If (Temperature is n) and (Current is L) and (Voltage is H) and (Speed is L) then (sp is L) (1)

106. If (Temperature is n) and (Current is L) and (Voltage is H) and (Speed is H) then (cur is H) (1)

107. If (Temperature is n) and (Current is L) and (Voltage is H) and (Speed is H) then (vol is VH) (1)

108. If (Temperature is n) and (Current is L) and (Voltage is H) and (Speed is H) then (sp is L) (1)

109. If (Temperature is n) and (Current is M) and (Voltage is M) and (Speed is M) then (cur is H) (1)

110. If (Temperature is n) and (Current is M) and (Voltage is M) and (Speed is M) then (vol is VH) (1)

111. If (Temperature is n) and (Current is M) and (Voltage is M) and (Speed is M) then (sp is L) (1)

112. If (Temperature is n) and (Current is M) and (Voltage is M) and (Speed is L) then (cur is H) (1)

113. If (Temperature is n) and (Current is M) and (Voltage is M) and (Speed is L) then (vol is VH) (1)

114. If (Temperature is n) and (Current is M) and (Voltage is M) and (Speed is L) then (sp is L) (1)

115. If (Temperature is n) and (Current is M) and (Voltage is M) and (Speed is H) then (cur is H) (1)

116. If (Temperature is n) and (Current is M) and (Voltage is M) and (Speed is H) then (vol is VH) (1)

117. If (Temperature is n) and (Current is M) and (Voltage is M) and (Speed is H) then (sp is L) (1)

118. If (Temperature is n) and (Current is M) and (Voltage is L) and (Speed is M) then (cur is H) (1)

119. If (Temperature is n) and (Current is M) and (Voltage is L) and (Speed is M) then (vol is VH) (1)

120. If (Temperature is n) and (Current is M) and (Voltage is L) and (Speed is M) then (sp is L) (1)

121. If (Temperature is n) and (Current is M) and (Voltage is L) and (Speed is L) then (cur is H) (1)

122. If (Temperature is n) and (Current is M) and (Voltage is L) and (Speed is L) then (vol is VH) (1)

123. If (Temperature is n) and (Current is M) and (Voltage is L) and (Speed is L) then (sp is L) (1)

124. If (Temperature is n) and (Current is M) and (Voltage is L) and (Speed is H) then (cur is H) (1)

125. If (Temperature is n) and (Current is M) and (Voltage is L) and (Speed is H) then (vol is VH) (1)

126. If (Temperature is n) and (Current is M) and (Voltage is L) and (Speed is H) then (sp is L) (1)

127. If (Temperature is n) and (Current is M) and (Voltage is H) and (Speed is M) then (cur is H) (1)

128. If (Temperature is n) and (Current is M) and (Voltage is H) and (Speed is M) then (vol is H) (1)

129. If (Temperature is n) and (Current is M) and (Voltage is H) and (Speed is M) then (sp is L) (1)

130. If (Temperature is n) and (Current is M) and (Voltage is H) and (Speed is L) then (cur is H) (1)

131. If (Temperature is n) and (Current is M) and (Voltage is H) and (Speed is L) then (vol is H) (1)

132. If (Temperature is n) and (Current is M) and (Voltage is H) and (Speed is L) then (sp is L) (1)

133. If (Temperature is n) and (Current is M) and (Voltage is H) and (Speed is H) then (cur is H) (1)

134. If (Temperature is n) and (Current is M) and (Voltage is H) and (Speed is H) then (vol is H) (1)

135. If (Temperature is n) and (Current is M) and (Voltage is H) and (Speed is H) then (sp is L) (1)

136. If (Temperature is n) and (Current is H) and (Voltage is M) and (Speed is M) then (cur is H) (1)

137. If (Temperature is n) and (Current is H) and (Voltage is M) and (Speed is M) then (vol is H) (1)

138. If (Temperature is n) and (Current is H) and (Voltage is M) and (Speed is M) then (sp is L) (1)

139. If (Temperature is n) and (Current is H) and (Voltage is M) and (Speed is L) then (cur is nc) (1)

140. If (Temperature is n) and (Current is H) and (Voltage is M) and (Speed is L) then (vol is VH) (1)

141. If (Temperature is n) and (Current is H) and (Voltage is M) and (Speed is L) then (sp is L) (1)

142. If (Temperature is n) and (Current is H) and (Voltage is M) and (Speed is H) then (cur is nc) (1)

143. If (Temperature is n) and (Current is H) and (Voltage is M) and (Speed is H) then (vol is H) (1)

144. If (Temperature is n) and (Current is H) and (Voltage is M) and (Speed is H) then (sp is L) (1)

145. If (Temperature is n) and (Current is H) and (Voltage is L) and (Speed is M) then (cur is nc) (1)

146. If (Temperature is n) and (Current is H) and (Voltage is L) and (Speed is M) then (vol is H) (1)

147. If (Temperature is n) and (Current is H) and (Voltage is L) and (Speed is M) then (sp is L) (1)

148. If (Temperature is n) and (Current is H) and (Voltage is L) and (Speed is L) then (cur is nc) (1)

149. If (Temperature is n) and (Current is H) and (Voltage is L) and (Speed is L) then (vol is VH) (1)

150. If (Temperature is n) and (Current is H) and (Voltage is L) and (Speed is L) then (sp is L) (1)

151. If (Temperature is n) and (Current is H) and (Voltage is L) and (Speed is H) then (cur is nc) (1)

152. If (Temperature is n) and (Current is H) and (Voltage is L) and (Speed is H) then (vol is H) (1)

153. If (Temperature is n) and (Current is H) and (Voltage is L) and (Speed is H) then (sp is L) (1)

154. If (Temperature is n) and (Current is H) and (Voltage is H) and (Speed is M) then (cur is nc) (1)

155. If (Temperature is n) and (Current is H) and (Voltage is H) and (Speed is M) then (cur is nc) (1)

156. If (Temperature is n) and (Current is H) and (Voltage is H) and (Speed is M) then (sp is H) (1)

157. If (Temperature is n) and (Current is H) and (Voltage is H) and (Speed is L) then (cur is nc) (1)

158. If (Temperature is n) and (Current is H) and (Voltage is H) and (Speed is L) then (vol is nc) (1)

159. If (Temperature is n) and (Current is H) and (Voltage is H) and (Speed is L) then (sp is L) (1)

160. If (Temperature is n) and (Current is H) and (Voltage is H) and (Speed is H) then (cur is L) (1)

161. If (Temperature is n) and (Current is H) and (Voltage is H) and (Speed is H) then (vol is nc) (1)

162. If (Temperature is n) and (Current is H) and (Voltage is H) and (Speed is H) then (sp is H) (1)

163. If (Temperature is p) and (Current is L) and (Voltage is M) and (Speed is M) then (cur is L) (1)

164. If (Temperature is p) and (Current is L) and (Voltage is M) and (Speed is M) then (vol is L) (1)

165. If (Temperature is p) and (Current is L) and (Voltage is M) and (Speed is M) then (sp is nc) (1)

166. If (Temperature is p) and (Current is L) and (Voltage is M) and (Speed is L) then (cur is L) (1)

167. If (Temperature is p) and (Current is L) and (Voltage is M) and (Speed is L) then (vol is L) (1)

168. If (Temperature is p) and (Current is L) and (Voltage is M) and (Speed is L) then (sp is L) (1)

169. If (Temperature is p) and (Current is L) and (Voltage is M) and (Speed is H) then (cur is L) (1)

170. If (Temperature is p) and (Current is L) and (Voltage is M) and (Speed is H) then (vol is nc) (1)

171. If (Temperature is p) and (Current is L) and (Voltage is M) and (Speed is H) then (sp is L) (1)

172. If (Temperature is p) and (Current is L) and (Voltage is L) and (Speed is M) then (cur is L) (1)

173. If (Temperature is p) and (Current is L) and (Voltage is L) and (Speed is M) then (vol is L) (1)

174. If (Temperature is p) and (Current is L) and (Voltage is L) and (Speed is M) then (sp is L) (1)

175. If (Temperature is p) and (Current is L) and (Voltage is L) and (Speed is L) then (cur is L) (1)

176. If (Temperature is p) and (Current is L) and (Voltage is L) and (Speed is L) then (vol is L) (1)

177. If (Temperature is p) and (Current is L) and (Voltage is L) and (Speed is L) then (sp is L) (1)

178. If (Temperature is p) and (Current is L) and (Voltage is L) and (Speed is H) then (cur is L) (1)

179. If (Temperature is p) and (Current is L) and (Voltage is L) and (Speed is H) then (vol is L) (1)

180. If (Temperature is p) and (Current is L) and (Voltage is L) and (Speed is H) then (sp is L) (1)

181. If (Temperature is p) and (Current is L) and (Voltage is H) and (Speed is M) then (cur is L) (1)

182. If (Temperature is p) and (Current is L) and (Voltage is H) and (Speed is M) then (vol is nc) (1)

183. If (Temperature is p) and (Current is L) and (Voltage is H) and (Speed is M) then (sp is H) (1)

184. If (Temperature is p) and (Current is L) and (Voltage is H) and (Speed is L) then (cur is L) (1)

185. If (Temperature is p) and (Current is L) and (Voltage is H) and (Speed is L) then (vol is H) (1)

186. If (Temperature is p) and (Current is L) and (Voltage is H) and (Speed is L) then (sp is H) (1)

187. If (Temperature is p) and (Current is L) and (Voltage is H) and (Speed is H) then (cur is L) (1)

188. If (Temperature is p) and (Current is L) and (Voltage is H) and (Speed is H) then (vol is H) (1)

189. If (Temperature is p) and (Current is L) and (Voltage is H) and (Speed is H) then (sp is H) (1)

190. If (Temperature is p) and (Current is M) and (Voltage is M) and (Speed is M) then (cur is L) (1)

191. If (Temperature is p) and (Current is M) and (Voltage is M) and (Speed is M) then (vol is L) (1)

192. If (Temperature is p) and (Current is M) and (Voltage is M) and (Speed is M) then (sp is H) (1)

193. If (Temperature is p) and (Current is M) and (Voltage is M) and (Speed is L) then (cur is L) (1)

194. If (Temperature is p) and (Current is M) and (Voltage is M) and (Speed is L) then (vol is nc) (1)

195. If (Temperature is p) and (Current is M) and (Voltage is M) and (Speed is L) then (sp is H) (1)

196. If (Temperature is p) and (Current is M) and (Voltage is M) and (Speed is H) then (cur is nc) (1)

197. If (Temperature is p) and (Current is M) and (Voltage is M) and (Speed is H) then (vol is L) (1)

198. If (Temperature is p) and (Current is M) and (Voltage is M) and (Speed is H) then (sp is H) (1)

199. If (Temperature is p) and (Current is M) and (Voltage is L) and (Speed is M) then (cur is L) (1)

200. If (Temperature is p) and (Current is M) and (Voltage is L) and (Speed is M) then (vol is L) (1)

201. If (Temperature is p) and (Current is M) and (Voltage is L) and (Speed is M) then (sp is nc) (1)

202. If (Temperature is p) and (Current is M) and (Voltage is L) and (Speed is L) then (cur is nc) (1)

203. If (Temperature is p) and (Current is M) and (Voltage is L) and (Speed is L) then (vol is L) (1)

204. If (Temperature is p) and (Current is M) and (Voltage is L) and (Speed is L) then (sp is H) (1)

205. If (Temperature is p) and (Current is M) and (Voltage is L) and (Speed is H) then (cur is L) (1)

206. If (Temperature is p) and (Current is M) and (Voltage is L) and (Speed is H) then (vol is L) (1)

207. If (Temperature is p) and (Current is M) and (Voltage is L) and (Speed is H) then (sp is H) (1)

208. If (Temperature is p) and (Current is M) and (Voltage is H) and (Speed is M) then (cur is nc) (1)

209. If (Temperature is p) and (Current is M) and (Voltage is H) and (Speed is M) then (vol is L) (1)

210. If (Temperature is p) and (Current is M) and (Voltage is H) and (Speed is M) then (sp is H) (1)

211. If (Temperature is p) and (Current is M) and (Voltage is H) and (Speed is L) then (cur is nc) (1)

212. If (Temperature is p) and (Current is M) and (Voltage is H) and (Speed is L) then (vol is nc) (1)

213. If (Temperature is p) and (Current is M) and (Voltage is H) and (Speed is L) then (sp is nc) (1)

214. If (Temperature is p) and (Current is M) and (Voltage is H) and (Speed is H) then (cur is L) (1)

215. If (Temperature is p) and (Current is M) and (Voltage is H) and (Speed is H) then (vol is nc) (1)

216. If (Temperature is p) and (Current is M) and (Voltage is H) and (Speed is H) then (sp is nc) (1)

217. If (Temperature is p) and (Current is H) and (Voltage is M) and (Speed is M) then (cur is L) (1)

218. If (Temperature is p) and (Current is H) and (Voltage is M) and (Speed is M) then (vol is H) (1)

219. If (Temperature is p) and (Current is H) and (Voltage is M) and (Speed is M) then (sp is H) (1)

220. If (Temperature is p) and (Current is H) and (Voltage is M) and (Speed is L) then (cur is nc) (1)

221. If (Temperature is p) and (Current is H) and (Voltage is M) and (Speed is L) then (vol is L) (1)

222. If (Temperature is p) and (Current is H) and (Voltage is M) and (Speed is L) then (sp is nc) (1)

223. If (Temperature is p) and (Current is H) and (Voltage is M) and (Speed is H) then (cur is L) (1)

224. If (Temperature is p) and (Current is H) and (Voltage is M) and (Speed is H) then (vol is nc) (1)

225. If (Temperature is p) and (Current is H) and (Voltage is M) and (Speed is H) then (sp is H) (1)

226. If (Temperature is p) and (Current is H) and (Voltage is L) and (Speed is M) then (cur is nc) (1)

227. If (Temperature is p) and (Current is H) and (Voltage is L) and (Speed is M) then (vol is L) (1)

228. If (Temperature is p) and (Current is H) and (Voltage is L) and (Speed is M) then (sp is H) (1)

229. If (Temperature is p) and (Current is H) and (Voltage is L) and (Speed is L) then (cur is nc) (1)

230. If (Temperature is p) and (Current is H) and (Voltage is L) and (Speed is L) then (vol is L) (1)

231. If (Temperature is p) and (Current is H) and (Voltage is L) and (Speed is L) then (sp is H) (1)

232. If (Temperature is p) and (Current is H) and (Voltage is L) and (Speed is H) then (cur is VL) (1)

233. If (Temperature is p) and (Current is H) and (Voltage is L) and (Speed is H) then (vol is L) (1)

234. If (Temperature is p) and (Current is H) and (Voltage is L) and (Speed is H) then (sp is H) (1)

235. If (Temperature is p) and (Current is H) and (Voltage is H) and (Speed is M) then (cur is L) (1)

236. If (Temperature is p) and (Current is H) and (Voltage is H) and (Speed is M) then (vol is L) (1)

237. If (Temperature is p) and (Current is H) and (Voltage is H) and (Speed is M) then (sp is H) (1)

238. If (Temperature is p) and (Current is H) and (Voltage is H) and (Speed is L) then (cur is L) (1)

239. If (Temperature is p) and (Current is H) and (Voltage is H) and (Speed is L) then (vol is L) (1)

240. If (Temperature is p) and (Current is H) and (Voltage is H) and (Speed is L) then (sp is nc) (1)

241. If (Temperature is p) and (Current is H) and (Voltage is H) and (Speed is H) then (cur is L) (1)

242. If (Temperature is p) and (Current is H) and (Voltage is H) and (Speed is H) then (vol is L) (1)

243. If (Temperature is p) and (Current is H) and (Voltage is H) and (Speed is H) then (sp is H) (1)

244. If (Temperature is bp) and (Current is L) and (Voltage is M) and (Speed is M) then (cur is VL) (1)

245. If (Temperature is bp) and (Current is L) and (Voltage is M) and (Speed is M) then (vol is VL) (1)

246. If (Temperature is bp) and (Current is L) and (Voltage is M) and (Speed is M) then (sp is H) (1)

247. If (Temperature is bp) and (Current is L) and (Voltage is M) and (Speed is L) then (cur is VL) (1)

248. If (Temperature is bp) and (Current is L) and (Voltage is M) and (Speed is L) then (vol is VL) (1)

249. If (Temperature is bp) and (Current is L) and (Voltage is M) and (Speed is L) then (sp is H) (1)

250. If (Temperature is bp) and (Current is L) and (Voltage is M) and (Speed is H) then (cur is VL) (1)

251. If (Temperature is bp) and (Current is L) and (Voltage is M) and (Speed is H) then (vol is VL) (1)

252. If (Temperature is bp) and (Current is L) and (Voltage is M) and (Speed is H) then (sp is H) (1)

253. If (Temperature is bp) and (Current is L) and (Voltage is L) and (Speed is M) then (cur is VL) (1)

254. If (Temperature is bp) and (Current is L) and (Voltage is L) and (Speed is M) then (vol is VL) (1)

255. If (Temperature is bp) and (Current is L) and (Voltage is L) and (Speed is M) then (sp is H) (1)

256. If (Temperature is bp) and (Current is L) and (Voltage is L) and (Speed is L) then (cur is VL) (1)

257. If (Temperature is bp) and (Current is L) and (Voltage is L) and (Speed is L) then (vol is VL) (1)

258. If (Temperature is bp) and (Current is L) and (Voltage is L) and (Speed is L) then (sp is H) (1)

259. If (Temperature is bp) and (Current is L) and (Voltage is L) and (Speed is H) then (cur is VL) (1)

260. If (Temperature is bp) and (Current is L) and (Voltage is L) and (Speed is H) then (vol is VL) (1)

261. If (Temperature is bp) and (Current is L) and (Voltage is L) and (Speed is H) then (sp is H) (1)

262. If (Temperature is bp) and (Current is L) and (Voltage is H) and (Speed is M) then (cur is L) (1)

263. If (Temperature is bp) and (Current is L) and (Voltage is H) and (Speed is M) then (vol is L) (1)

264. If (Temperature is bp) and (Current is L) and (Voltage is H) and (Speed is M) then (sp is H) (1)

265. If (Temperature is bp) and (Current is L) and (Voltage is H) and (Speed is L) then (cur is L) (1)

266. If (Temperature is bp) and (Current is L) and (Voltage is H) and (Speed is L) then (vol is L) (1)

267. If (Temperature is bp) and (Current is L) and (Voltage is H) and (Speed is L) then (sp is H) (1)

268. If (Temperature is bp) and (Current is L) and (Voltage is H) and (Speed is H) then (cur is L) (1)

269. If (Temperature is bp) and (Current is L) and (Voltage is H) and (Speed is H) then (vol is VL) (1)

270. If (Temperature is bp) and (Current is L) and (Voltage is H) and (Speed is H) then (sp is H) (1)

271. If (Temperature is bp) and (Current is M) and (Voltage is M) and (Speed is M) then (cur is L) (1)

272. If (Temperature is bp) and (Current is M) and (Voltage is M) and (Speed is M) then (vol is L) (1)

273. If (Temperature is bp) and (Current is M) and (Voltage is M) and (Speed is M) then (sp is H) (1)

274. If (Temperature is bp) and (Current is M) and (Voltage is M) and (Speed is L) then (cur is L) (1)

275. If (Temperature is bp) and (Current is M) and (Voltage is M) and (Speed is L) then (vol is L) (1)

276. If (Temperature is bp) and (Current is M) and (Voltage is M) and (Speed is L) then (sp is H) (1)

277. If (Temperature is bp) and (Current is M) and (Voltage is M) and (Speed is H) then (cur is L) (1)

278. If (Temperature is bp) and (Current is M) and (Voltage is M) and (Speed is H) then (vol is L) (1)

279. If (Temperature is bp) and (Current is M) and (Voltage is M) and (Speed is H) then (sp is H) (1)

280. If (Temperature is bp) and (Current is M) and (Voltage is L) and (Speed is M) then (cur is L) (1)

281. If (Temperature is bp) and (Current is M) and (Voltage is L) and (Speed is M) then (vol is VL) (1)

282. If (Temperature is bp) and (Current is M) and (Voltage is L) and (Speed is M) then (sp is H) (1)

283. If (Temperature is bp) and (Current is M) and (Voltage is L) and (Speed is L) then (cur is VL) (1)

284. If (Temperature is bp) and (Current is M) and (Voltage is L) and (Speed is L) then (vol is VL) (1)

285. If (Temperature is bp) and (Current is M) and (Voltage is L) and (Speed is L) then (sp is H) (1)

286. If (Temperature is bp) and (Current is M) and (Voltage is L) and (Speed is H) then (cur is VL) (1)

287. If (Temperature is bp) and (Current is M) and (Voltage is L) and (Speed is H) then (vol is VL) (1)

288. If (Temperature is bp) and (Current is M) and (Voltage is L) and (Speed is H) then (sp is H) (1)

289. If (Temperature is bp) and (Current is M) and (Voltage is H) and (Speed is M) then (cur is L) (1)

290. If (Temperature is bp) and (Current is M) and (Voltage is H) and (Speed is M) then (vol is L) (1)

291. If (Temperature is bp) and (Current is M) and (Voltage is H) and (Speed is M) then (sp is H) (1)

292. If (Temperature is bp) and (Current is M) and (Voltage is H) and (Speed is L) then (cur is L) (1)

293. If (Temperature is bp) and (Current is M) and (Voltage is H) and (Speed is L) then (vol is L) (1)

294. If (Temperature is bp) and (Current is M) and (Voltage is H) and (Speed is L) then (sp is nc) (1)

295. If (Temperature is bp) and (Current is M) and (Voltage is H) and (Speed is H) then (cur is VL) (1)

296. If (Temperature is bp) and (Current is M) and (Voltage is H) and (Speed is H) then (vol is VL) (1)

297. If (Temperature is bp) and (Current is M) and (Voltage is H) and (Speed is H) then (sp is H) (1)

298. If (Temperature is bp) and (Current is H) and (Voltage is M) and (Speed is M) then (cur is L) (1)

299. If (Temperature is bp) and (Current is H) and (Voltage is M) and (Speed is M) then (vol is L) (1)

300. If (Temperature is bp) and (Current is H) and (Voltage is M) and (Speed is M) then (sp is H) (1)

301. If (Temperature is bp) and (Current is H) and (Voltage is M) and (Speed is L) then (cur is L) (1)

302. If (Temperature is bp) and (Current is H) and (Voltage is M) and (Speed is L) then (vol is L) (1)

303. If (Temperature is bp) and (Current is H) and (Voltage is M) and (Speed is L) then (sp is H) (1)

304. If (Temperature is bp) and (Current is H) and (Voltage is M) and (Speed is H) then (cur is L) (1)

305. If (Temperature is bp) and (Current is H) and (Voltage is M) and (Speed is H) then (vol is nc) (1)

306. If (Temperature is bp) and (Current is H) and (Voltage is M) and (Speed is H) then (sp is H) (1)

307. If (Temperature is bp) and (Current is H) and (Voltage is L) and (Speed is M) then (cur is VL) (1)

308. If (Temperature is bp) and (Current is H) and (Voltage is L) and (Speed is M) then (vol is L) (1)

309. If (Temperature is bp) and (Current is H) and (Voltage is L) and (Speed is M) then (sp is H) (1)

310. If (Temperature is bp) and (Current is H) and (Voltage is L) and (Speed is L) then (cur is L) (1)

311. If (Temperature is bp) and (Current is H) and (Voltage is L) and (Speed is L) then (vol is L) (1)

312. If (Temperature is bp) and (Current is H) and (Voltage is L) and (Speed is L) then (sp is H) (1)

313. If (Temperature is bp) and (Current is H) and (Voltage is L) and (Speed is H) then (cur is VL) (1)

314. If (Temperature is bp) and (Current is H) and (Voltage is L) and (Speed is H) then (vol is L) (1)

315. If (Temperature is bp) and (Current is H) and (Voltage is L) and (Speed is H) then (sp is H) (1)

316. If (Temperature is bp) and (Current is H) and (Voltage is H) and (Speed is M) then (cur is L) (1)

317. If (Temperature is bp) and (Current is H) and (Voltage is H) and (Speed is M) then (vol is L) (1)

318. If (Temperature is bp) and (Current is H) and (Voltage is H) and (Speed is M) then (sp is H) (1)

319. If (Temperature is bp) and (Current is H) and (Voltage is H) and (Speed is L) then (cur is L) (1)

320. If (Temperature is bp) and (Current is H) and (Voltage is H) and (Speed is L) then (vol is L) (1)

321. If (Temperature is bp) and (Current is H) and (Voltage is H) and (Speed is L) then (sp is H) (1)

322. If (Temperature is bp) and (Current is H) and (Voltage is H) and (Speed is H) then (cur is L) (1)

323. If (Temperature is bp) and (Current is H) and (Voltage is H) and (Speed is H) then (vol is L) (1)

324. If (Temperature is bp) and (Current is H) and (Voltage is H) and (Speed is H) then (sp is H) (1)

325. If (angle is l) then (an is N) (1)

326. If (angle is m) then (an is nc) (1)

327. If (angle is h) then (an is P) (1)